5-2013

The Role of Nucleolin in B-cell Lymphomas and Fas-Mediated Apoptotic Signaling

Jillian F. Wise

The Role of Nucleolin in B-cell Lymphomas and Fas-Mediated Apoptotic Signaling

by

Jillian F Wise, BS

Approved:

_____
Felipe Samaniego, MD, Supervisory Professor

_____
David McConkey, PhD

_____
Joya Chandra, PhD

_____
Timothy McDonnell, MD, PhD

_____
Varsha Gandhi, PhD

Approved:

_____
Dean, The University of Texas
Graduate School of Biomedical Sciences at Houston

THE ROLE OF NUCLEOLIN IN B-CELL LYMPHOMAS AND FAS-MEDIATED APOPTOTIC SIGNALING

A

DISSERTATION

Presented to the Faculty of
The University of Texas
Health Science Center at Houston
and
The University of Texas
M. D. Anderson Cancer Center
Graduate School of Biomedical Sciences
in Partial Fulfillment

of the Requirements

for the Degree of

DOCTOR OF PHILOSOPHY

By
Jillian F. Wise, BS

Houston, Texas

May 2013

Dedication

I dedicate this dissertation to my loving family; my husband Kevin McGoff, my parents Diane and David Wise, my siblings, especially Stephanie Wise, and to my extended family that have provided unconditional love and support through all my aspirations.

Acknowledgements

First and Foremost, I would like to thank my family and friends for their constant encouragement and optimism throughout my educational quests. I would like to thank my parents, David and Diane Wise for their lifelong dedication to my continued growth into an intelligent and mature woman. To Kevin McGoff, although his contributions have come later in my career, I have been illuminatingly happy from the time he has been here to support, encourage, and laugh with me during all of my endeavors and I know that he will be a blessing to my career and life going forward. To my siblings, thank you for supporting me and contributing to the person I am today. I would also like to show my gratitude to my extended family that helped raise and support me through all roads of life, especially my Aunt Paula Mogan for helping me with applications throughout my educational career. Also, I would like to thank my friends and loved ones with a special extension of gratitude to Rebecca Bloomer, Kalin Cogar, Megan Van Der Kloot, Tarra Epstein, Rachel Pennellatore, Valerie Hoover, Anthony Connor and Cassie Buck, with all sincerity, for the inspiration and joy to continue life with the utmost happiness in- and out- side of science.

I would like to express my sincere gratitude to Dr. Samaniego, his continual support and advice has been irreplaceable to my success as a scientist and within this project. He has been an excellent guide and resource in my discoveries and development as a researcher. He also provides an unmatched dispersal of pride in my work to others in the field and networking opportunities that most young scientists do not experience. He also provides an unmatched desire to succeed in creating new therapies to help his patients in their quest to cure lymphomas, and has adamantly shared his patient experiences with me, which has provided constant strength to continue in the field. I would also like to thank all the members of my committees, throughout my experience at the GSBS, for their contributions to my educational success. Dr. Sastry, Dr. Butel, Dr. Cooper, Dr. Watowich, Dr. Grimm, Dr. McConkey, Dr. Chandra, Dr. McDonnell and Dr. Gandhi. All of my advisors have continually pushed me to go beyond my own expectations of scientific endeavors, without which my career would not be nearly as successful. Dr. Sastry has provided continued support on and off my committees and as the advisor to the Virology program. Dr. Cooper has continued to allow scientific support past his scientific advice on my committee for my project, especially with the utilization of his Biostation system with the help of Janos Roszik and Drew Deniger. Dr. McConkey and Dr. Chandra have made themselves constantly available for advice, support, and reagents for apoptotic signaling.

Additionally, I would like to thank previous mentors for guiding me to my current journey at MD Anderson Cancer Center. To Dr. Cheryl Baker, my first scientific advisor and mentor, for

helping me complete my senior thesis in pancreatic cancer, and instilling within me the desire to complete a career in cancer research. Without her guidance I would not have applied to MD Anderson Cancer Center or the University of Texas Graduate School of Biomedical Sciences. I would also like to extend gratitude to my first mathematical and scientific inspiration Dr. Watkins, for making education in these fields challenging and enjoyable.

I would like to thank the friends I have made here at the University of Texas GSBS and MD Anderson Cancer Center for their friendships and continued advice and scientific contribution to my project: Omid Tavana, Krista Swanson, Hillary Gibbons, Danielle Fontenot, Amy Courtney and Laura Amendola. Also to my lab members for their contributions to my project: Xue Ao for her expertise in PCR work, Dr. Berkova for her writing and intellectual contributions and emotional support, Dr. Daniluk for her continued experimental contributions, Dr. Tao, Dr. Kerros, Dr. Wang, Dr. Maeng, Dr. Zhu, Dr. Braun, Dr. Mathur and Dr. Lee for helping me with experimental methods and support throughout my time in the Samaniego lab. Also, an extremely large thank you to Dr. Keyur Patel and Dr. Timothy McDonnell for analyzing and being the main contributors to the ImmunoHistoChemical analysis of B-cell neoplasm samples, and Rashmi Mishra for organizing samples with me. Also, to the South Campus flow core lab for their nonstop support, expertise, and personal dealings with my project. Lastly, I send a sincere thank you to the GSBS staff, including Dr. Goka and Dr. Stancel, for helping with scholarship opportunities and the intellectual support of my project.

The work in my dissertation would not have been completed without the support, advice and inspiration from all of these people.

The Role of Nucleolin in B-cell Lymphomas and Fas-Mediated Apoptotic Signaling

Publication No. _____

Jillian F. Wise, BS

Supervisory Professor: Felipe Samaniego, MD

The death receptor Fas has a key role in mediating homeostasis, elimination of defective cells and more recently implicated in cancer promotion. Many effective anti-cancer therapies depend on Fas-mediated apoptosis to eradicate tumor cells and ineffective Fas-apoptotic signaling is a basis for primary as well as acquired resistance to chemotherapy. We hypothesized that Fas is subjected to direct regulation by inhibitory proteins attained by cancer cells. To screen for potential binding modulators of Fas, we analyzed lymphoma cells for Fas binding proteins. This purification scheme identified high scoring peptides derived from nucleolin, a nuclear protein known to be overexpressed in cancer.

We confirmed binding of nucleolin to Fas and the presence of nucleolin-Fas complexes on the surface of lymphoma cells. Using deletion mutants of nucleolin, we identified RBD 4 and glycine/arginine rich region of nucleolin to be required for the binding to Fas. BJAB cells, a Burkitts lymphoma cell line, with partial knockdown of nucleolin showed significantly higher rates of apoptosis in response to Fas agonists and increased ligand binding when compared to non-target controls. Transfection of mice with nucleolin-expressing plasmids showed significantly higher survival rates in nucleolin-transfected mice than vector control- and non-Fas-binding nucleolin mutant- transfected mice after lethal Fas agonist challenge. We next examined the expression of nucleolin in human B-cell lymphomas. We observed that nucleolin is overexpressed in multiple B-cell lymphomas and its localization changes in transformed cells. In a tissue microarray analysis we showed that although total nucleolin levels did not correlate with patient outcome, including progression free survival and overall survival, the nucleolin levels did correlate with proliferative staining. We developed a method for detecting nucleolin surface expression levels and showed that surface nucleolin expression is increased in aggressive B-cell lymphoma subtypes including MCL and DLBCL yet is low in healthy B cells and chronic lymphocytic leukemia, a low grade cancer. We also determined that nucleolin surface expression correlates with a worsening prognostic index.

Results from this investigation provide the first evidence of nucleolin overexpression as a clinical correlate for worsening prognosis of lymphomas. The potential underlying mechanism

involves blocking of Fas-mediated apoptotic death pathway through direct binding of nucleolin to the Fas receptor on the extracellular surface of cancer cells.

Contents

List of Figures

List of Tables

Abbreviations

5-FU……...…….……5-fluorouracil

AgNOR……..……...Silver stained nucleolar organizer regions

ALG-2……..…...……Asparagine-linked glycosylation 2

ALPS…….……..Autoimmune lymphoproliferative syndrome

APL....……...……Acute promyelocytic leukemia

ATP…….Adenosine triphosphate

Bcl-2……..…….B-cell lymphoma 2

Bcl-XL……..…..…….B-cell lymphoma extra-large

CD……circular dichroism

CI…….Confidence Intervals

cIAP……..……Cellular inhibitor of apoptosis

CID……Collision-induced dissociation

c-FLIP…….Cellular homologue of FLICE inhibitory proteins
or cellular FADD-like interleukin 1β converting enzyme inhibitory protein

CHOP……Cyclophosphamide, doxorubicin, vincristine, and prednisone

CKII…….Casein kinase II

CLL..…….Chronic lymphocytic leukemia

coIP……...…….…..Coimmunoprecipitation

C-terminal……..……Carboxy-terminus end

DAPI…….4',6-diamidino-2-phenylindole

dATP……...Deoxyadenosine triphosphate

DcR3…….……..…Decoy receptor 3

DD……...Death domain

DED……..……...…...Death effector domain

dGTP……...……Deoxyguanosine triphosphate

DISC……..…….Death-inducing signaling complex

DLBCL…….Diffuse large B-cell lymphoma

DNA……..……Deoxyribonucleic acid

EBNA-1……...…….…...Epstein-Barr virus nuclear antigen-1

EBV……..Epstein-Barr virus

ELISA……..……Enzyme-linked immuno sorbent assay

ER…….Endoplasmic reticulum

ErbB…….epidermal growth factor receptor

FADD…….…….Fas-associated death domain

FADD-DN…….…….…..FADD dominant negative

Fas...……...……..FS-7 associated surface antigen or TNF receptor superfamily member 6

FasL……...……Fas ligand

FITC……Fluorescein isothiocyanate

FL……..……...…….Follicular lymphoma

GAPDH…….Glyceraldehyde 3-phosphate dehydrogenase

GAR……..……..Glycine/arginine rich domain

GFP……Green fluorescent protein

Gld…….Fas ligand deficient mice

GRO……...……...…G-rich oligonucleotides

GPI……...……...Glycosylphosphatidylinositol

GTP……..……Guanosine triphosphate

H&E…….……...Haematoxylin and eosin

HB-19…….Anti-HIV psuedopentameric peptide

HdM2……..…….Human homolog of mouse double minute 2

HIV……...Human immunodeficiency virus

HGFR…….Hepatocyte growth factor receptor

HMGB1……...High mobility group box 1 protein

HPV……...……Human papilloma virus

HRP……..Horseradish peroxidase

IAP……...Inhibitor of apoptosis

IB…….…….Immunoblotting

ICAD……..…..Inhibitory unit of the caspase-activated DNase

Ig……..Immunoglobulin

IHC……...Immunohistochemistry

IL-2……...…….Interleukin 2

IP……...…..……...Immunoprecipitation

IPI……...International prognostic index

kDa……...…….Kilo dalton

LDH……...……Lactate dehydrogenase

LDLRP-1……Low density lipoprotein receptor related protein-1

Lpr……..……..Fas deficient mice

LR1……..…..Lipopolysaccharide responsive factor 1

MCL……...Mantle cell lymphoma

MDC1……...…..……Mediator of DNA damage checkpoint protein1

MFI…….....Median fluorescence intensity

miR……micro ribonucleic acid

MMP-9……..…….Metalloproteinase-9

mRNA……..…….Messenger ribonucleic acid

MS……..……..……..……Mass spectroscopy

MyH9…….....Non-muscle myosin heavy chain 9

MZL……..Marginal zone lymphoma

NCL……Nucleolin

NHL……Non-Hodgkin's lymphoma

N-terminal……...……..Amino-terminus end

OS…….Overall survival

PARP……...……..……Poly(ADP-ribose) polymerase

PBMC……..peripheral blood mononuclear cell

PCNA……..……...Proliferating cell nuclear antigen

PFS……...…..Progression free survival

PI3K…….……..……..Phosphatidylinositide 3 kinases

pKO……..…..partial knockout/down

PLAD…….pre-ligand binding assembly domain

PNGase……peptide-N4-(N-acetyl-beta-glucosaminyl)asparagine amidase

PTN……...…….Pleiotrophin

Rb…….…….Retinoblastoma

RBD……...…..RNA binding domain

RFP……...Red fluorescent protein

rRNA……..……...…….Ribosomal ribonucleic acid

RT……..……..…….Room temperature

SAPK……..……...……Stress activated protein kinase

SELEX……..……...Systematic evolution of ligands by exponential enrichment

SDS-PAGE……...……Sodium dodecyl sulfate – polyacrylamide gel electrophoresis

SEM…….Standard error of the mean

sFas……...…..……..Soluble Fas

shRNA……small/short hairpin RNA

SLE……..……..…….……..Systemic lupus erythematosus

SLL……...…….Small cell lymphocytic lymphomas

SPION……...……..…..Superparamagnetic iron oxide nanoparticle

tBID…….……....Truncated BH3 interacting-domain death agonist

TEM……..……..……..……..Transmission electron microscopy

TGF-β…….…Transforming growth factor beta

Tipα……...……TNF-alpha inducing protein

TMA……..…….……..…Tissue microarray

TNF……Tumor necrosis factor

TNFR……...……Tumor necrosis factor receptor

TNFR1……..…….Tumor necrosis factor receptor 1

TRAIL-R1…….…..……Tumor necrosis factor related inducing ligand receptor 1

TRAIL-R2…….....……Tumor necrosis factor related inducing ligand receptor 2

TUNEL.....Terminal deoxy-nucleotidyl transferase-mediated Z'-deoxyuridine S'-triphosphate nick end labeling

uPAR…….Urokinase specific receptor

UV…….....Ultraviolet

VCN……Vibrio cholerae neuraminidase

VEGF……Vascular endothelial growth factor

VM-26……...……...Teniposide

VTLM…….…...Video time-lapse microscopy

WGA……Wheat germ agglutinin

XIAP……...…..X-chromosome-linked inhibitor of apoptosis

YB-1…….……Y box-binding protein

Chapter 1: Review of the Relevant Literature

B-cell Non-Hodgkin's Lymphomas

B-cell lymphomas are malignant neoplasms stemming from the B cells of the immune system.(3) B cells undergo multiple differentiation and activation steps throughout development and therefore malignant transformations can occur at varying stages producing lymphomas of over 30 categories.(3, 4) Currently, the World Health Organization (WHO) recognizes 34 subtypes of B-cell lymphomas, although the classification system is dynamic and constantly evolving.(5) The subtypes are divided into two major groups, non-Hodgkin's lymphomas (NHL) and Hodgkin's lymphomas, the difference is based on the presence of characteristic large malignant Reed-Sternberg cells in Hodgkin's lymphoma.(4) Given the existence of so many diverse conditions within this one immune cell type in the body, successful treatments have to be based on extensive basic and clinical research employing multiple strategies.

In 2011, there were approximately 500,000 people living with NHL, with approximately 70,130 new cases per year.(6, 7) The incidence of NHL in North America, Western Europe, and Australia increased by 3-4% per year throughout the 1970's and 1980's and has continued to increase since, albeit at a slower rate.(8-11) Between 1978-1995, the rates of high grade NHL tripled among males and doubled among females.(10, 11) This increase remains unexplained, yet based on the increase of new cases NHL ranks fifth among increasingly common cancers.(11, 12) The mortality rate of NHL is 30%, making it the sixth most common cause of cancer death in males and seventh in females.(6) To achieve better outcomes for lymphoma patients, the development of scientifically sound treatment approaches for the diverse spectra of NHL malignancies will be a major step in the eradication of lymphoma and increasing patient's quality of life.

To aid in predicting the prognosis of NHL patients, a clinical tool called the International Prognostic Index (IPI) was developed. To calculate IPI, points are assigned to different risk factors: age greater than 60, Ann Arbor stage III or IV disease, elevated serum lactate dehydrogenase (LDH) above 618 UI/L, Zubrod performance status of above 1, and more than one extranodal site. Based on the sum of the risk factor score (points) the patients are divided into groups: low risk (0-1 points), with 5-year survival of 73%; low-intermediate risk (2 points), with 5-year survival of 51%; high-intermediate risk (3 points), with 5-year survival of 43%; and high risk (4-5 points), with 5-year survival of 26%.(13)

The most common NHL subtypes in developed countries are diffuse large B-cell lymphoma (DLBCL) (20-30%) and follicular lymphoma (FL) (20-30%), with the other subtypes representing less than 10% of NHL cases.(14, 15) Our research focused on four of the NHL subtypes: DLBCL, Burkitts lymphoma, mantle cell lymphoma (MCL) and small lymphocytic lymphoma/chronic lymphocytic leukemia (SLL/CLL). Diffuse large B-cell lymphoma is the most common and the most aggressive form of NHL. The median age at presentation of DLBCL is in the mid-60s, and most patients present with advanced-stage disease. Diffuse large B-cell lymphoma accounts for almost half of NHLs that involve extranodal sites: stomach, small intestine, colon, soft tissue, and thyroid gland.(10) The disease is more frequent among males than females of middle ages and more common among whites than blacks at older age groups.(10) There are two distinctive types of DLBCL, germinal center B-cell like (GCB) and activated B-cell like (ABC). These two subgroups share marker expression patterns with normal germinal center B cells and mitogenically activated B cells, respectively. Diffuse large B-cell lymphomas often show altered expression of B-cell lymphoma 6 (bcl-6), caused by a rearrangement of chromosome 3q27.(16)

Burkitts lymphoma is an extremely aggressive form of DLBCL associated with a c-myc translocation. Burkitts lymphoma accounts for only 1-5% of all NHL in adults.(17) The c-myc expression is dysregulated by a balanced recombination event between chromosome 8 at breakpoint q24 and either chromosomes 14, 2, or 22.(18) Combination chemotherapy treatments for Burkitts have shown up to an 8-year survival rate of 91% in low risk, 90% in low-intermediate risk, 67% in high-intermediate risk, and 31% in high risk cases.(19)

The MCL subgroup is defined as a moderately aggressive lymphoma with over 99% of cases carrying the t(11;14) rearrangement responsible for overexpression of cyclin D1.(20) The overexpression of cyclin D1 results in a pathogenesis of constitutive cell cycle dysregulation.(21) Originally, MCL's were classified as a small cleaved cell lymphoma, however after the identification of the t(11;14) rearrangement in 1979 and its resulting oncogene, MCLs became a separate histology in 1991.(22) Although generally categorized as an aggressive lymphoma, indolent subtypes have been identified based on non-nodal disease.(21) The overall 5-year survival rate for MCL is generally 50% for advanced stage MCL and 70% for limited-stage MCL.(23, 24)

Chronic lymphocytic leukemia is an indolent form associated with increasing age, affecting mainly adults around 70. Chronic lymphocytic leukemia rates are higher in people of Jewish, Russian, and eastern European background. While CLL is often asymptomatic, with diagnosis made through routine blood counts, late stages can be very symptomatic including; fatigue, weight loss and large tumor burden. Poor risk features for CLL include expression of ZAP70,

CD38, non-mutated immunoglobulin heavy chain gene, and chromosome 17p (p53) deletion.(25) There were approximately 16,060 new cases diagnosed in 2012 and the estimated deaths are 4,580 per year with an 81% 5-year survival rate.(7)

Despite the numerous diagnostic and treatment advances, innate and de novo acquired resistance to current chemotherapies remains one of the biggest obstacles to the successful treatment of patients with lymphoma.(26) An estimated 27% of patients will die because of resistance to chemotherapy.(7) Therefore, elucidating and targeting mechanisms of chemoresistance remains a key strategy for the successful eradication of NHL.

Recent Advancements in Treatments of B-cell Non-Hodgkin's Lymphoma

Recent advances in the treatment strategies for NHL have resulted in enhanced cure rates and a correspondingly increased group of long-term survivors.(27) Therefore, despite the increased incidence, lymphoma related deaths have been steadily declining.(11) Although treatment strategies vary by subtype, many chemotherapy regimens utilize similar basic combinations. The most common combination, CHOP, consists of cyclophosphamide, doxorubicin, vincristine, and prednisone. The introduction of novel biological therapies for NHL, such as the monoclonal chimeric anti-CD20 IgG1 antibody, rituximab, approved in 1997, have significantly reduced mortality of NHL patients.(28-30) Rituximab has been added to a score of standard therapies, in particular CHOP, now referred to as R-CHOP. In a 2-year analysis, R-CHOP had shown a 19% absolute improvement in event free survival rates and a 13% improvement in over-all survival rates when compared to CHOP alone.(29)

Multiple long-term complications of NHL treatment have been identified, providing a need to scan for therapies with less toxicity. The major long-term complications identified thus far in NHL patients post- irradiation and treatment with alkylating agents, especially cyclophosphamide, are an increased risk for myelodysplasia, acute myelogenous leukemia (alkylating and irradiation of bone marrow), and other types of cancer, including bladder (cyclophosphamide and irradiation), lung (CHOP), GI tract (CHOP), head and neck, thyroid gland, central nervous system, sarcoma, melanoma, and mesothelioma.(31) Beyond secondary tumors, cardiac disease and gonadal dysfunction have been observed as the most common delayed complications of NHL therapies.(31) Doxorubicin, a key component of NHL treatment regimens, is associated with cardiomyopathy and congestive heart disease with an incidence of 208 per 10,000 NHL patient-years.(31) One NHL study reported doxorubicin is associated with a 28% chance of ventricular dysfunction. Specifically in patients treated for DLBCL, the risk of congestive heart failure increased to 29%.(31) Gonadal

dysfunction seems to be more relevant in men, as women often resume their menstrual cycle.(31) With the growing number of survivors, these long-term complications will continue to rise, making clear the need for less toxic therapies for NHL patients to avoid long-term complications and to increase the quality of life post-NHL.

Although there have been improvements in the effectiveness of current treatments, patients still suffer from early deaths with lymphoma, making it necessary to identify novel therapeutic approaches. Therefore, we are focused on finding new treatment targets in B-cell lymphoma to enhance the ability to cure patients and to overcome the major hindrances to survival, chemotherapeutic resistance and relapse, without adverse side effects. Chemoresistance of tumor cells to current clinical treatments may represent an extensive network of responses and mechanisms. Current research on chemoresistance mechanisms have focused on a diverse number of mechanisms such as decreased efficacy of drug efflux, downregulation of tumor suppressor genes, overexpression of oncogene and anti-apoptotic proteins, and modification of the DNA damage response elements.(32-36) The working hypothesis in our laboratory is that inhibition of a natural form of cell death, apoptosis, is a major reason for the chemotherapeutic resistance of B-cell lymphomas. Our group is actively seeking a basic understanding of the underlying mechanisms and pursuing strategies to overcome this inhibition of cell death in B-cell lymphomas.

Apoptosis

The elimination of unwanted cells has been observed as having an important role in multiple biological processes including embryogenesis, immune monitoring, clonal deletion of autoreactive T-cells, tissue remodeling, viral clearance, and even tumor regression.(37, 38) Therefore, the process of the host eliminating unwanted cells is a pivotal factor in maintaining homeostasis and development of organisms. This process of programmed cell death was termed apoptosis by Kerr et al., in 1972, as derived from the Greek term for falling of petals from trees.(39) Apoptosis differs from other forms of cell death as it results in multiple morphological changes that have been clearly characterized. Necrosis, another form of cell death, is a chaotic process resulting in swelling, disorganized breakdown of organelles, and membrane rupture.(40) In contrast, apoptosis is a biochemically distinct mode of cell death characterized by cell shrinkage, membrane blebbing, apoptotic body formation, and deoxyribonucleic acid (DNA) fragmentation, often followed by phagocystosis by other cells, including neighboring cells and macrophages.(39) Apoptosis can be monitored independently of other cell death types by measuring the extent of

phosphatidylserine flipping from the inner membrane of cells to their outer surface, a biochemical change specific to apoptotic cell death.(41) The DNA fragmentation during the late stages of apoptosis is also specific, producing DNA fragments of about 180 base pairs, and is another method for monitoring apoptosis.(38)

One highly studied method of initiating apoptosis occurs through the signaling of death receptors. The most well characterized family of death receptors, the tumor necrosis factor (TNF) receptor superfamily, is highly regulated and many of the receptors also function in cell survival, proliferation, and immune regulation. The TNF receptor with a clear role in apoptosis regulation identified as TNF receptor superfamily member 6 or FS-7 associated surface antigen, Fas, is the focus of this project.(38)

Fas

In 1985 Aggarwal et al. discovered the first death receptor termed tumor necrosis factor receptor (TNFR).(42) This discovery led to the identification of the entire new super family of death receptors, TNF receptor superfamily, and eventually to the discovery of one of the most well characterized receptors, Fas. Nagata et al. were the first to clone Fas and map the essential cysteine-rich domains of the transmembrane protein necessary for apoptosis initiation by Fas.(38)

Fas is naturally expressed in the thymus, liver, heart, and ovaries.(43) Fas messenger ribonucleic acid (mRNA) transcripts exist as 6 splice variants.(44) However, Fas protein exists in 2 forms, a membrane-bound form and soluble Fas (sFas).(44) The membrane-bound form contains 3 extracellular cysteine-rich domains (CRDs) approximately 40 amino acids in length with 6 conserved cysteine residues, a transmembrane domain, and a 70-amino acid intracellular death domain (DD) necessary for transmission of the extracellular death signal into the cells.(45) The soluble forms, produced by 5 of the alternative mRNA splicing variants, consist only of portions of the extracellular domain.(44) It has been shown that the soluble form of Fas can be released to compete with Fas receptors for its ligand, thereby acting as an inhibitor of activation.(46)

In addition to splice variants, Fas also undergoes multiple post-translational modifications. Fas has two N-glycosylation sites within the extracellular domain of Fas at N118 and N136.(47) It has been shown that there is about a 3 kilo Dalton (kDa)-size difference between glycosylated and unglycosylated Fas, as represented by a double band of 45kDa and 48kDa found by SDS-PAGE separation (sodium dodecyl sulfate-polyacrylamide gel electrophoresis), however this size can vary between cell types.(47, 48) In addition to glycosylation modifications, Fas is reported to be sialylated on the N-linked oligosaccharide chains. The multiple sialylation events can account for

up to an 8-kDa change in Fas' molecular mass.(49) It has been determined that both glycosylated and non-glycosylated Fas can be presented on the surface and that both forms of Fas can be excreted in vesicles from colorectal carcinoma cells. However, mutation of the glycosylation sites does not affect either transport to the cell surface (47, 48) or sensitivity to apoptosis and downstream signaling events.(47, 50) Moreover, despite total removal of all glycosylated residues of Fas, Fas-mediated apoptosis remains intact.(47, 51) Overall, the literature suggests that the glycosylation of Fas affects neither its transportation nor its ability to signal apoptosis.

Fas Apoptotic Signaling

In 1993 the corresponding ligand for the Fas death receptor was cloned (52) and eventually the remaining family member ligands were discovered. The TNF superfamily ligands share multiple structural elements including (β-sheets) and transmembrane domains, and mechanisms of receptor activation through oligomerization. Fas is activated by two methods; either receptor binding, through a trimeric association of receptor and trimeric binding of the ligand subunits of FasL (Fas ligand), and receptor aggregation in lipid rafts.(53) The carboxy-terminal domain of FasL has been determined to bind the Fas receptor; a deletion of only 3 amino acids can interfere with Fas receptor binding.(54)

Fas trimerizes through interaction of the amino-terminus end (N-terminal) pre-ligand assembly domains (PLAD).(44) Preassembled trimers bind FasL and the activation continues with the opening of the hydrophobic core of Fas by the fusing of helices 5 and 6 of the DD, a region essential for signaling apoptosis.(38, 55, 56) Similar domains are found in multiple death receptors including TNFR1, Tumor necrosis factor related inducing ligand receptor 1 (TRAILR1), TRAILR2, and TNF receptor-related apoptosis-mediating protein (TRAMP).(55, 57) This DD binds similar DDs, including death domain adaptor proteins containing homologous DD's to TNF receptors.(58) The adaptor protein involved in Fas signaling is referred to as FADD (Fas-associated death domain) and can also act as an adaptor protein for TNFR-1, TRAIL-R1, and TRAIL-R2. FADD's DD is composed of 6 helices at the carboxy-terminus end (C-terminal) domain and binds receptors when phosphorylated.(58-61)

After forming a complex with Fas, FADD uses its additional 6 helices in the N-terminal domain, termed the DED (death effector domain), for recruitment of cysteine proteases crucial for apoptotic signaling.(56) Cysteine-dependent aspartate-directed proteases, termed caspases, known for cleaving substrates after the P1 aspartic acid residue, include two initiator caspases, caspase-8 and caspase-10.(59, 60, 62, 63) The caspases' resting state or zymogen state is termed procaspases.

Caspase-8, a ubiquitously expressed protein except in fetal brain, binds to FADD through its N-terminal pro-domain DED.(61, 62) The formation of the death-inducing signaling complex (DISC) consisting of Fas, FADD, and caspase-8 is necessary for the induction of apoptosis (Figure 1). After formation of the DISC complex, a conformational change in caspase-8 allows for the autoproteolytic cleavage at three aspartate residues, allowing for a heterotetrameric formation of caspase-8 into its effector subunits, p10 and p18.(64) Caspase-10 is the only other cysteine protease known to have a DED homologous to caspase-8 and is found on the same region of chromosome 2q33-34, suggesting a shared ancestry.(65) Caspase-10 also has the ability to bind FADD and induce apoptosis through Fas and TNF signaling, however caspases-8 and -10 do have biochemically distinct cleavage and inhibition specificities.(63, 65) At this point, based on cell predisposition, apoptosis in the cell can proceed via two distinct signaling cascades.

Figure 1:

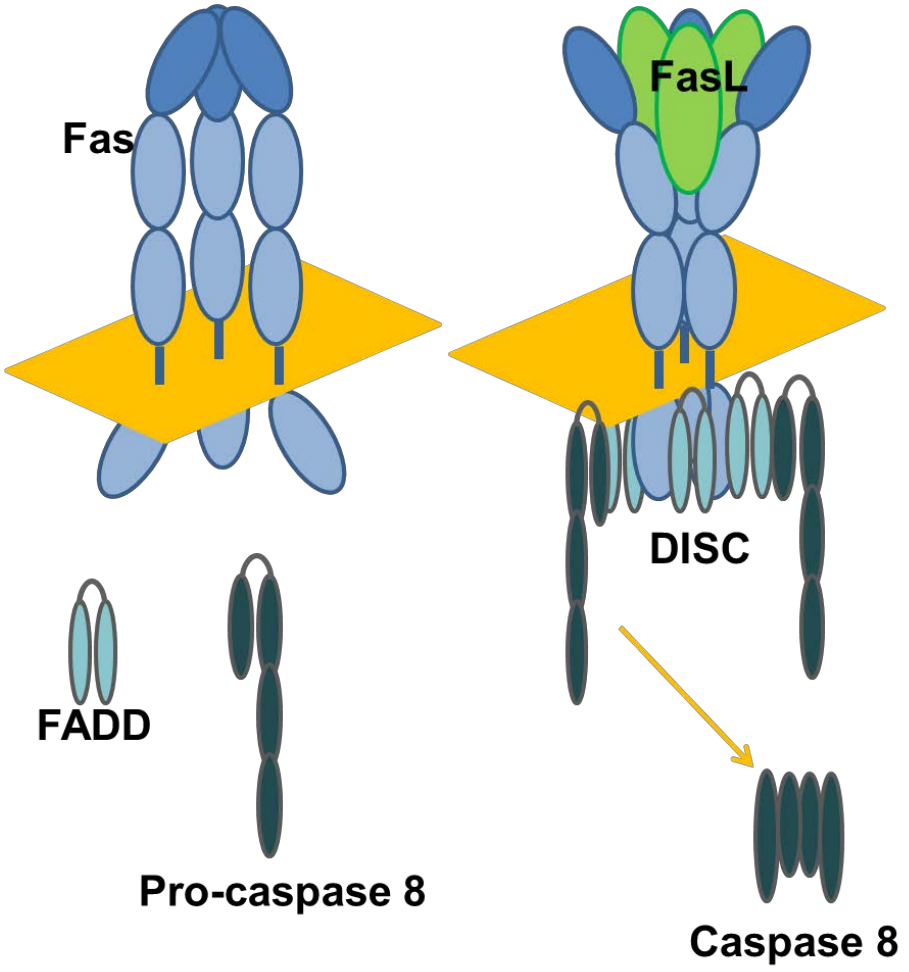

Figure 1: Death-inducing signaling complex (DISC).
Schematic of the Fas death receptor and the Fas ligand induced activation/assembly of the DISC.

In the type I signaling cascade, initial cleavage of caspase-8 is followed by receptor internalization and more robust caspase-8 activation at the endosomal membranes.(66) The p18 and p10 subunits directly activate additional caspases, known as effector caspases, and bypass the cells mitochondria.(67) The executioner or effector caspases include caspases-3,-6,-7,-4 and -9. After activation by proteolytic cleavage, the zymogen forms into a heterotetrameric complex of two large subunits.(62) Activation of caspases leads to the cleavage and proteolysis of many protein substrates resulting in apoptotic dissolution of a cell.(68) The substrates of caspases include proteins involved with genomic function, cell-cycle regulators, and structural proteins.(68) One of the first substrates known to be cleaved by caspases, therefore making its cleavage useful as a marker of cell death, is PARP (DNA repair enzyme poly(ADP-ribose) polymerase).(68) Another important cleavage substrate is the inhibitory unit of the caspase-activated DNase (ICAD); by removing the inhibitory unit the DNase, the CAD translocates to the nucleus to degrade DNA, eventually culminating in the death of the cell.(69)

In type II signaling, the cleavage of caspase-8 at the DISC is limited but sufficient to cleave Bid into tBID (truncated BH3-interacting-domain death agonist) which activates mitochondrial amplification of the death signal.(66, 67) Then, tBID triggers oligomerization of B-cell lymphoma 2 associated X protein (Bax) and B-cell lymphoma 2 homologous antagonist/killer (Bak) to form pores in the mitochondrial membrane in order to release cytochrome c into the cytosol.(70) Cytochrome c along with apoptotic protease activating factor one (apaf-1) and deoxyadenosine triphosphate (dATP) form an apoptosome that is responsible for the proteolytic cleavage and activation of caspase-9.(71, 72) Caspase-9 than in turn activates effector caspases-3 and -7, merging with the type I apoptotic signaling cascade to complete cell death.(66, 68) Monitoring the mitochondrial membrane potential is an effective way of determining apoptosis induction in type II signaling.(73) B cells are known to signal primarily through type I signaling.(74)

Although clearly defined as an apoptotic initiator, Fas has more recently been implicated in non-apoptotic signaling. Overwhelming evidence now suggests that Fas and FasL can promote cell survival in cancer cells. Activation of Fas can produce survival signals through activation of nuclear factor kappa-light-chain-enhancers of activated B cells (NF-kB).(75) However, a switch between apoptotic and survival Fas signaling has yet to be elucidated and remains a key to our understanding of the Fas receptor role in health and disease.(76)

Fas-mediated Apoptosis in Disease

Programmed cell death is a selective process aimed at eliminating defective cells; therefore, in order to avoid inappropriate apoptosis, the Fas-mediated apoptotic system has to be tightly regulated. Logically, the imbalance of this tightly controlled system contributes to the development of multiple diseases.

Fas-deficient (lpr) and FasL-deficient (gld) mice develop lymphoproliferative disorder characterized by the accumulation of activated lymphocytes, mainly T cells, in the spleen and lymph nodes, accompanied by autoimmune diseases.(43) The lpr defect also presents with large amounts of Immunoglobulin (Ig)G and IgM autoantibodies, including anti-DNA antibodies. Additionally, lpr mice produce rheumatoid (Rh) factor and present with a phenotype resembling the human autoimmune disease, systemic lupus erythematosus (SLE), suggesting that Fas is necessary for the negative selection of autoantigen-targeting T cells.(77) The gld defect, caused by a missense point mutation in *fasl*, changing phenylalanine to leucine at position 273 of the FasL C-terminal domain, abolishes FasL's ability to induce apoptosis.(43, 78)

Mutations of Fas identified in humans result in autoimmune lymphoproliferative syndrome (ALPS) characterized by lymphadenopathy, hepatosplenomegaly, autoimmunity, and altered T-cell populations.(79) ALPS also encompass' human lymphoproliferative diseases resulting from mutations within the Fas-apoptotic pathway including caspases-8 and -10.(79) The Fas mutations causing ALPS include a deletion of the DD, lack of Fas on the cell surface, and a frame-shift mutation rendering the protein unable to signal.(45) The phenotypes of these mutations suggest a critical role of Fas in immune system homeostasis.(45, 80)

In addition to ALPS, Fas signaling defects have been implicated in cancer formation and progression. Although Fas mutations are not extremely common in cancer, multiple abnormal modulations of Fas-mediated signaling are implicated in the development of cancer.(81) It has been reported that multiple cancers upregulate FasL, sFas, and multiple inhibitors of the Fas signaling cascade. Although the physiological functions have not been completely defined, it is hypothesized that FasL upregulation and release may contribute to the protection of cancer cells from T cells in the tumor microenvironment.(82)

Fas Receptor-Targeting Inhibition Mechanisms

One of the six hallmarks of cancer, defined by Robert Weinberg, include the adaptation of cancer cells to evade apoptosis, a key regulatory mechanism that allows the cells to become oncogenic.(83) However, only some cancers have mutations in the Fas alleles and Fas surface

expression does not always correlate with susceptibility to FasL-induced apoptosis, raising the question of how Fas is dysregulated in cancers and how cells circumvent self-destruction.(81) One potential mechanism is the presence of inhibitors of the apoptosis-signaling cascade; thus the overexpression of inhibitors of Fas-mediated apoptosis represents one of the escape mechanisms employed by cancer cells.

The first and most proximal step of apoptosis can be targeted by cancer cells through interference with ligand binding to the Fas receptor. Tumor cells can avoid detection and cytotoxicity of the immune system by releasing sFas, which blocks the killing effects of FasL.(84) The release of sFas was shown to correlate with a worse prognosis of multiple cancers, including lymphomas and leukemias.(46, 85) Increased sFas levels, as compared with those of healthy donors, were seen in patients with T-cell acute lymphoblastic leukemia, hairy cell leukemia, and CLL. Additionally, high sFas levels are associated with poor prognosis in aggressive NHL, particularly in the IPI's high-intermediate and high risk groups.(85, 86) In one particular study, it was concluded that the sFas levels were significantly higher in those who failed to respond to therapy, suggesting that high serum sFas levels could, in fact, offer chemoresistance.(86) The correlation of sFas release with the inhibition of Fas-mediated apoptosis and chemoresistance further underscores the importance of determining the mechanism(s) of Fas regulation in cancer cells.

Other known competitors for ligand binding are the membrane-bound decoy receptors, such as Decoy receptor 3 (DcR3), which lack the DDs necessary for signaling. These inactive receptors bind and sequester ligands and desensitize cells to Fas-mediated apoptosis.(87-89) Decoy receptor 3 is upregulated in B- and T- cell lymphomas, and the overexpression of DcR3 in B-cell lymphomas correlates with an overall decreased survival.(90) The decrease in overall survival in DcR3-positive lymphomas also correlates with a poor response to CHOP chemotherapy and further delineates the desensitization to anthracyclines (e.g., doxorubicin).(90) The upregulation of DcR3 also correlates with virus-positive lymphomas including Epstein-Barr virus (EBV) and Human T-lymphotropic virus (HTLV).(91) The correlation between the escape of Fas in cancer and viruses is intriguing, as there may be additional undiscovered mechanisms of Fas signaling regulation.

Moreover, the last 15 amino acids of Fas protein have been shown to interact with an inhibitory protein called Fas-associated phosphatase-1 (FAP-1), which has been shown to inhibit trafficking of Fas to the surface of cells, thereby preventing its activation.(92) Many of the Fas receptor-targeting inhibitory mechanisms clearly affect prognosis and outcome in lymphoma, leaving a clear target for therapy that remains mostly unexplored.

Downstream Inhibitors of Fas-mediated Apoptosis

In addition to regulation of Fas-mediated apoptosis by receptor-targeting mechanisms, cells have multiple mechanisms to interfere with the downstream steps of the apoptotic cascade, such as inhibition of the assembly of the DISC complex and activation of the caspase cascade. In order to prevent cellular apoptosis during normal B cell maturation in the lymphoid germinal centers, B cells upregulate cellular homologue of FLICE inhibitory proteins (c-FLIP) which bind to the DISC and prevent Fas signaling.(81, 93) The c-FLIP protein contains two N-terminal DEDs that act in a dominant negative fashion, competing for caspase-8 recruitment to the DISC, and c-FLIP can also bind pro-caspase-3 and prevent its activation and thus apoptosis. An additional inhibition of Fas signaling stems from the alternative caspase-8 splicing into caspase-8L, which is missing the key catalytic sites for activation and thereby acts as an inhibitor of DISC activation.(94) PED/PEA-15 is a DED containing multifunctional cytosolic protein which, when biphosphorylated, binds to FADD and caspase-8 preventing DISC formation and thereby preventing apoptosis.(95, 96)

The function of the key DISC adaptor protein, FADD, can also be regulated via post-translational modifications. Protein kinase C phosphorylation of FADD can reduce its ability to form the DISC complex.(81, 97) Sentrin and ALG-2 (asparagine-linked glycosylation 2) are two other DD interacting proteins with opposite effects on signaling. Sentrin inhibits Fas- and TNFR1-mediated apoptosis and ALG-2 is necessary for successful signaling, yet their exact mechanistic roles have yet to be elucidated.(98, 99)

The B-cell lymphoma 2 (Bcl-2) superfamily oncogenes are inner mitochondrial membrane proteins that block programmed cell death through inhibition of the mitochondrial-mediated arm of signaling. This superfamily includes Bcl-2, B-cell lymphoma extra-large (Bcl-xl), Mcl-1, Boo, A1, Bfl-1, Brag-1, and Bcl-w.(100, 101) B cells exhibit an inverse expression of Fas and Bcl-2 throughout B-cell developmental stages and maturation, such as the upregulation of Fas and concerted downregulation of Bcl-2 in germinal centers during the antigen-dependent selection process.(102)

Inhibitors of apoptosis proteins (IAPs), which interact with and inhibit caspases, include X-chromosome-linked IAP (XIAP), survivin, cellular IAP1 (cIAP1), cIAP2, neuronal apoptosis inhibitory protein (NAIP), IAP-like protein 2, apollon, and melanoma IAP (livin).(103) XIAP, cIAP1, cIAP2, and IAP-like protein 2 inhibit caspase-8 activation. Caspase-3 and caspase-7 are inhibited by NAIP, XIAP, c-IAP1, c-IAP2, survivin, livin.(100, 101) Interestingly XIAP is the only IAP able to bind and inhibit active caspases.(70)

Heat shock proteins 27 and 70 can inhibit apoptosis inducing factor (AIF) and the apoptosome formation.(100) ICAD, which is constitutively expressed in cells, prevents cleavage of

DNA by forming complexes with the endonuclease CAD. The localization of the ICAD/CAD complex is altered in various cancers and within lymphoma subtypes, with mainly a nuclear localization in normal B cells.(69, 104)

Presently, we have very superficial knowledge of how cancers inhibit and escape antitumor apoptosis and chemotherapy-induced Fas activation. Although it appears to be a multistep event, a complete description of Fas regulation and its effects on chemoresistance will provide the potential to create and design novel therapies to enhance our ability to eradicate lymphoma.

Fas and Chemoresistance

Fas is implicated as a factor contributing to the success of many cancer treatment regimens, yet we know little about how to utilize this observation for a successful eradication of disease (Table 1). Resistance to genotoxic drugs can occur when Fas is inactive and unable to signal. Thymocytes of lpr mice are resistant to multiple chemotherapeutic agents including 5-fluorouracil (5-FU).(105) FasL-deficient gld-mice resist doxorubicin clearance of various tumors, implicating a role of Fas/FasL in doxorubicin cell death.(106) Blocking antibodies against the Fas receptor have been shown to markedly reduce the effectiveness of multiple chemotherapeutic agents including doxorubicin and bleomycin.(67, 107-109) Herr et al showed that transfection of antisense FasL protects against doxorubicin-induced cell death.(110) Doxorubicin-induced cell death is also diminished by overexpression of the dominant negative form of FADD (FADD-DN) in type I cells, specifically.(67, 111) Etoposide also shows decreased activity in type I cancer cells overexpressing FADD-DN, and concurring experiments have shown that both etoposide and doxorubicin induce DISC formation.(67)

The inability of chemotherapeutic regimens to eliminate Fas-defective cells suggests the utilization of the Fas-/FasL system by our current chemotherapies (Table 1). Although many studies have found the role of the Fas pathway in chemotherapy-induced apoptosis as controversial, most authors agree that many therapeutic agents have sensitizing effects on Fas-mediated signaling.(112) Multiple therapies including cisplatin, mitomycin, methotrexate, mitoxantrone, doxorubicin, rituximab and bleomycin upregulate Fas (Table 2).(109, 113-115) The up-regulation of Fas occurs in response to therapeutic agents through a variety of mechanisms. A large number of our therapeutic agents work through inducing DNA damage, the resulting breaks in DNA are identified by ataxia telangiectasia mutated protein (ATM) or similar genes sensing DNA damage.(36) These response proteins subsequently modify p53 which results in its activation and transcriptional activation of Fas's intronic p53 response element.(116, 117) The upregulation of Fas

can also occur independent of p53 response to chemotherapeutics. Interferon and tumor necrosis factor alpha are two cytokines that are often released by cells post-chemotherapeutic influx and are also responsible for the upregulation of Fas. Interferon's activate Stat1 phosphorylation which increases the transcriptional activation of the Fas promoter (118), while tumor necrosis factor alpha activates NF-κB signaling resulting in the upregulation of Fas expression.(119) Histone deactelyase inhibitors have recently been introduced as a clinical treatment for cancer patients, and can induce transcriptional regulator sp3 activation.(120) Sp3 has been identified as an activator of Fas transcription.(121) In response to irradiation and other cell stressors the c-jun N-terminal kinases (JNK) pathway is activated which results in the activation and transcriptional activation of c-jun, a potent activator of Fas expression.(122) Thus, cells can use an extensive network of response elements to activate Fas expression post-chemotherapeutic treatment.

Additional modulation of the Fas receptor system occurs through the upregulation of FasL by multiple therapies including doxorubicin, cytarabine, etoposide, teniposide (VM-26), cisplatin, bleomycin, irradiation, paclitaxel, thiadiazolide derivatives, ABT-510, and antimetabolites such as methotrexate and 5-FU (Table 2).(109, 114, 123-131) FasL upregulation is independent of the p53 DNA damaging response pathway, and can occur through the activation of NF-κB and sp1 transcriptional elements.(113, 132)

Additionally, chemotherapeutic agents modulate signaling events further downstream within the Fas apoptotic cascade including upregulation of FADD and caspase-8. FADD and caspase-8 overexpression occurs during treatment with theaflavins, doxorubicin, cisplatin and mitomycin C.(133, 134) Chemotherapeutic drugs, including rituximab and doxorubicin, have also been reported to increase recruitment of DISC proteins.(67, 115) Curcumin, a potent cancer prevention method and treatment used in melanoma, activates the Fas pathway by inducing Fas expression and aggregation, in addition to down regulating XIAP.(135)

Several reports disagreeing with Fas' role in chemotherapeutic responses have concluded that drug-induced apoptosis does not rely on Fas, although their use of CD95 blocking antibodies and caspase inhibitors did decrease efficacy of current chemotherapies.(136-140) However, all of these reports used type II signaling cells (136-138), which have been shown to be less reliant on the Fas/FasL system for genotoxic drug-induced cell death.(67) These results suggest that the reliance on Fas-mediated apoptosis in genotoxic cell death varies between cell types. However, many of these studies did reveal utilization if not dependency on the Fas/FasL system or a synergy between chemotherapeutic drugs and the Fas system. Overall the data does not undermine the importance of Fas in chemotherapy responses.(137-139)

The knowledge that the Fas/FasL system is not fully functional in all cancers and that there is a clear resistance of cells deficient in Fas signaling to multiple chemotherapies indicates that elucidation of modulators responsible for Fas resistance would have great potential to restore Fas signaling and possibly enhance current treatment strategies and outcomes.

Table 1: Fas and FasL's Roles in Chemotherapy-induced Cell Elimination.

Evidence for FasL/Fas Modulation by Chemotherapy Induced Apoptosis
Chemotherapies upregulate FasL (109, 114, 123-131)
Chemotherapies upregulate Fas (109, 113-115)
Upregulation of Fas is functional (chemotherapy sensitizes cells to Fas-crosslinking) (67)
Fas-resistant clones are resistant to anticancer therapies (105)
FasL-negative clones are resistant to chemotherapeutics (106)
FasL is necessary for caspase-8 activation in doxorubicin treated cells (114)

Recent findings suggest that genotoxic drugs and other chemotherapies utilize various steps of Fas-mediated apoptosis for functional cell killing.

Table 2: Chemotherapies that Regulate Fas-mediated Apoptotic Factors.

Chemotherapy	Fas Upregulation	FasL Upregulation	Fas-FasL Dependency
Doxorubicin (106, 114, 141)	+	+	+
Cisplatin (136, 142, 143)	+	+	
Mitomycin (113, 133)	+		
Methotrexate (113, 143, 144)	+		
Mitoxantrone (113)	+		
Bleomycin (109, 113, 145)	+	+	+
Cytarabine (111, 123, 144, 146, 147)		+	
Etoposide (123, 126, 147)		+	+
VM-26 (123)		+	
5-FU (105, 130)		+	
Thiadiazolidine (129) **Derivatives** (129)		+	
Paclitaxel (130)		+	
ABT-510 (123)		+	
λ- irradiation (123, 127)		+	
Betulinic Acid (123)	–	–	
Fludarabine (123, 137)		+	

Chemotherapies that upregulate Fas and or FasL and their receptive dependencies on the Fas/FasL system, as determined by blocking antibodies.

Fas in Non-Hodgkin's Lymphomas

Although Fas is often expressed normally in B-cell lymphomas, certain changes in Fas were found to be associated with each diagnosis. In a study of 150 NHL patients, the nine exons of the *Fas* gene were sequenced, and it was determined that 11% of sporadic NHL's harbor *Fas* mutations. Of the sixteen identified mutations, six were missense variations in exon 9, encoding the DD. The Fas mutations were identified in a CLL, two FL's, three low-grade mucosa-associated lymphoid tissue (MALT) lymphomas, nine DLBCLs, and one anaplastic large cell lymphoma. Of these patients, 94% showed extranodal involvement, and 37% presented with recurrences, suggesting that *Fas* mutations in NHL patients correlate with extranodal disease presentation.(148)

Diffuse large B-cell lymphomas have been shown to express a wide range of Fas expression levels on the cell surface. Mantle cell lymphoma and SLL express little Fas.(149) Large cell lymphoma and FL cells are known to express high Fas levels.(148, 149) Nonetheless, while these cancers are resistant to Fas agonists, they are sensitive to the activation of perforin/granzyme B pathways, (148) suggesting a non-functional Fas signaling.

Mantle cell lymphomas often show abnormal expression of Fas and its signaling cascade components. First, it has been determined that there is a significant downregulation of Fas expression in MCLs.(148) An MD Anderson study showed that while 29% of normal cells expressed Fas only 2.1% of MCL cells had Fas expression.(20) Furthermore, it has been determined that FADD, caspase 2, and other apoptosis-related genes, are substantially downregulated in mantle cell lymphoma tumor samples.(150) The biological consequence of a disrupted Fas-apoptotic pathway is decreased Fas sensitivity and Fas-apoptotic impairment in MCLs.(20, 148)

A resistance to Fas-mediated apoptosis could be one mechanism involved in the development of B-cell malignancies and a potential escape mechanism of the tumor's B cells from the immune regulatory system. However, the mechanisms behind Fas evasion differ among lymphomas and individual patients and thus, are responsible for our lack of clear knowledge of all the mechanisms for Fas inhibition.

Nucleolin

Nucleolin is a ubiquitously expressed multifunctional protein of 713 amino acids with a predicted molecular mass of 77kDa. It was originally identified as a nucleolar protein that can account for up to 10% of the total nucleolar region.(151, 152) The nucleolin gene consists of 14 exons and 13 introns located on chromosome 2q12-qter.(153) It has a characteristic GC-rich

promoter sequence often found in housekeeping genes.(152) Interestingly, three small nucleolar RNAs (snoRNAs: U20,U23, and U82) are encoded in introns 11, 12, and 5, respectively.(154, 155) The nucleolin protein consists of three different structural domains consisting of a highly acidic and highly phosphorylated N-terminal domain (151), four central RNA-binding domains (RBDs), and a glycine/arginine rich C-terminal domain (GAR) with high levels of N^G, N^G-dimethylarginines.(151)

The negatively charged amino acids within nucleolin's N-terminal domain are responsible for nucleolin's apparent 105kDa molecular weight by SDS-PAGE separation.(152) This region also contains a nuclear localization signal and multiple modification sites, including self-proteolytic sites that control many of nucleolin's functions throughout the cell. The N-terminal domain has also been implicated in interactions with chromatin and nucleic acids.(152)

Figure 1:

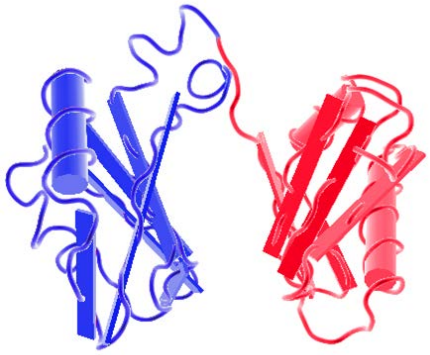

Figure 2: Ribbon Representation of Nucleolin's RBD1 and 2. Analyzed from NCBI molecular modeling database. (1, 2).

Table 3: Binding Proteins of Nucleolin's GAR Domain.

C-terminal GAR Binding Partners
ErbB receptors (156)
p53 (157)
Nucleic acids (158)
G-G paired DNAs (159)
ssDNA (151)
RNA helices (160)
Urokinase (161)
Ribosomal proteins (162, 163)
HIV (164)
hTERT (165)
PRMT5 (166)

Published results reveal multiple binding proteins to the GAR domain of nucleolin.

Human nucleolin consists of 4 central globular RBDs that contain alternating hydrophobic and hydrophilic stretches with a suggested pocket structure (Figure 2).(167) The first two RBDs constitute the recognition sites of a small RNA stem loop structures present in ribosomal ribonucleic acid (rRNA) and the 5'UTR and 3'UTR of the 18S and 28S RNA sequences.(163) RBD's 3 and 4 are involved in nucleolin's association with G-rich DNA, adenosine triphosphate (ATP), guanosine triphosphate (GTP), deoxyadenosine triphosphate (dATP), deoxyguanosine triphosphate (dGTP), telomerase, and human homolog of mouse double minute 2 (HdM2).(152, 162, 165, 168)

The GAR of nucleolin consists of repeated type I ß-turns that are known to facilitate interactions with proteins.(158, 160) This domain is interspersed with

dimethylarginine and phenylalanine residues.(160) Multiple heterogeneous nuclear ribonucleoproteins (hnRNPs), pre-mRNA processing and pre-mRNA nucleocytoplasmic transport proteins, have similar C-terminal GAR domains.(169) The GAR domain contributes to DNA interactions, localization to the nucleoli, and unwinding of RNA for recognition and accessibility.(158, 160, 162, 170) The GAR domain has also been shown to dissipate from the essential role of rRNA processing, and is additionally used for multiple protein-protein interactions, including viral proteins (Table 3).(156, 157, 163, 164, 166, 168, 171) Additionally, the autocatalytic protease activity of nucleolin has been mapped to its GAR domain.(152)

There is an emerging pattern of stimulations and modifications that control the multifunctional aspects of nucleolin's actions throughout the cell. Nucleolin's modifications include phosphorylation, glycosylation, ADP ribosylation, arginine methylation, and proteolytic cleavage.(166, 172) Nucleolin is phosphorylated on serine and threonine residues within its N-terminal domain.(173) Nucleolin glycosylation involves both N- and O- linked sugars. Two N-glycosylation sites have been identified at N317 and N492. Five potential O-glycosylation sites are predicted at T84, T92, T2105, T106, and T113.(174, 175) Additionally, the premature termination of glycosylation, a cancer-related occurrence, results in the incomplete O-glycosylations termed T and Tn antigens and have been identified specifically on surface- and cytoplasm- expressed nucleolin.(174)

Moreover, nucleolin is a self-proteolytic protein, which autocatalyzes its own degradation; the degradation product bands of 95, 76, 70, 60, and 50 kDa are readily visible on immunoblots.(176, 177) The cleavage products of 60 and 50 kDa cannot be detected with nucleolin's N-terminus targeting antibodies, suggesting that these products correspond to the C-terminal portions of nucleolin.(178) The full-size 105kDa nucleolin protein is stable and increased in proliferating and activated cells, versus resting and non-dividing cells.(176, 179-181). The cleavage products increase with decreased proliferation and are intricately regulated with preribosome maturation.(177) Therefore, it is not surprising that nucleolin's synthesis is in parallel with the increased rates of cell division and ribosomal gene activity.(152, 177, 181) Nucleolin's expression is stimulated in multiple cells during the G_0-G_1 transition and mitosis.(152, 181) On the other hand, its expression is low in non-dividing and serum-deprived cells.(152)

Nucleolin has also been identified as the substrate for several kinases including casein kinase II (CKII), $p34^{cdc2}$, protein kinase C-ζ, and potentially cyclic-AMP kinases, all of which have been implicated in cell cycle-specific interactions with nucleolin.(152, 173, 182, 183) Specifically, cdc2 kinase phosphorylates nucleolin at a threonine residue during mitosis and stimulates nucleolin mitotic reorganization as well as controls its helicase activity.(152, 170, 173, 184) Serine

phosphorylation of nucleolin by CKII during interphase is necessary for transcription of rDNA genes and for nuclear-to-cytoplasmic translocation of nucleolin, which is enhanced in tumor and embryonic cells (Table 4).(152, 170, 171, 184)

The diverse roles of nucleolin throughout the cell have been extensively studied; however, the most pivotal role remains its essential function in the regulation of rRNA and ribogenesis.(151, 152, 163, 180, 185, 186) In addition to nucleolin's role in rRNA biogenesis, recent evidence suggests a role in micro ribonucleic acid (miRNA) processing and stabilization through interaction with Drosha.(187) Some of the most studied aspects of nucleolin's functions, outside its nucleolar roles, are processes involved in DNA repair and recombination. These include DNA decondensation/chromatin formations through inhibitory interactions with histone H1 and H2AX (151, 188, 189), nucleogenesis, DNA/RNA helicase activity (although there are some discrepancies and controversies regarding this activity) (170, 190), ssDNA annealing (162), DNA-dependent ATPase (170), telomerase localization (165), transcriptional regulation (191-194), interaction with DNA repair proteins p53, Y Box-binding protein 1 (YB-1), Rad51, proliferating cell nuclear antigen (PCNA), mediator of DNA damage checkpoint protein 1(MDC1), replication protein A (RPA), (157, 189, 190, 193, 195-200) and class switching recombination in B-cells.(201, 202) For simplicity, these functions are summarized in Table 5. The relationship between nucleolin's nucleolar activities, DNA repair, recombination, and transcription suggests that nucleolin is intricately involved in the fundamental aspects of cell proliferation and growth.(152)

Localization of Nucleolin

The localization of nucleolin has been avidly pursued in the last 10 years as multiple functions have been attributed to nucleolin based on its various positions within the cell, yet its translocation mechanism remains elusive. As mentioned above, nucleolin is mainly localized to the nucleolus of eukaryotic cells.(177, 203) Its position within the nucleus during the cell cycle has been well characterized.(185, 204-206) During interphase, nucleolin is localized in the nucleoli.(207) During mitosis, nucleolin's localization changes with the progression of the cell cycle; it is seen at discrete sites on metaphase chromosomes and is relocated to the cytoplasm after nucleolar disintegration. During mitotic disassembly, nucleolin redistributes to the perichromosomal sheath and the cytoplasm.(207) In telophase, nucleolin accumulates in prenucleolar bodies and in the reforming nucleoli.(206) Many of the localization changes throughout mitosis are linked to modifications by V-src, cdc2 kinase, p38α (Table 4).(208) During S phase, nucleolin's DNA binding activity becomes more prominent.(162, 209)

Beyond cell cycle regulation of nucleolin's localization, nucleolin has been implicated in responses to trauma and environmental stressors, resulting in further changes to nucleolin's location in the cell. Heat shock can very quickly (5-15minutes) cause a redistribution of nucleolin from the nucleolus to the nucleoplasm in a p53 dependent manner.(190, 196, 199) This phenomenon has also been shown with other stress inducers including gamma-irradiation, camptothecin treatment, and topoisomerase I inhibition, with a p53 dependency (Table 4).(157, 190)

Table 4: Cell Treatments Effects on Translocation of Nucleolin.

	Translocation	Response Function
Heat shock (210)	Nucleolar →Nucleoplasm	Inhibition of chromosomal and DNA replication
γ-irradiation (172)	Nucleolar →Nucleoplasm	
Camptothecin (211)	Nucleolar →Nucleoplasm	
Topoisomerase I inhibitor (212)	Nucleolar →Nucleoplasm	
Protein kinase C-ζ (183)	Nucleolar→ Nucleoplasm	
Mitotic disassembly (207)	Perichromosomal Sheath → Cytoplasm	
Inhibition of rRNA synthesis (212)	Nucleus → Cytoplasm	
CKII serine phosphorylation (213)	Nuclear → Cytoplasmic	During Interphase, increase in ribosome biogenesis
PI3K/c-src phosphorylation (214)	Cytoplasm → Surface	
PTN (215)	Cytoplasm → Surface	
VEGF (216)	Cytoplasm → Surface	
Serum addition (217)	Cytoplasm → Surface	
Laminin-1 (208)	Cytoplasm → Surface	
LDLRP-1 (218)	Cytoplasm → Surface	
Actinomycin D (175, 219)	Cytoplasmic → Nuclear	
High salt concentration (190)	Surface → Medium	
Cyclophosphamide (175, 219)	Surface → Nuclear	
Tunicamycin (219)	Surface → Cytoplasmic	
SAPK p38 activation (208)		Increased RNA binding activity
Cdc2 kinase threonine phosphorylation (173)		During mitosis, Enhances helicase activity
UV irradiation (220)		Increased RNA binding activity, binding of PCNA and Inhibition of NER, bcl-xl stabilization
Fibroblast growth factor-2 (213)		Stimulates CKII phosphorylation of nucleolin, inducing proliferation and mitogenic responses
IL-2 (221, 222)		Increased nucleolin mRNA expression
Dexamethasone (223)		Decreases CKII phosphorylation of nucleolin and rRNA synthesis

Various biological and chemical treatments can cause redistribution of nucleolin throughout the cell. The treatments, location changes and the resulting regulation on nucleolin are presented.

Adding another layer of complexity to nucleolin's localization, nucleolin has been identified in the cytoplasm and on the cell surface. In intestinal cells and granulocytes, translocation of nucleolin from the nucleus into the cytoplasm occurs concomitantly with differentiation, implicating a role of nucleolin translocated-associated inhibition of rRNA synthesis during differentiation.(208, 224) Nucleolin's nucleolar-to-cytoplasmic translocation is also associated with inhibition of DNA synthesis (Table 4).(196, 199) The nucleo-cytoplasmic trafficking of nucleolin has been confirmed by identification of nucleolin as a cytoplasmic-to-nuclear shuttling protein for the pro-survival proteins midkine and transforming growth factor beta (TGF-β) receptor 1.(152, 218, 224-226) Beyond shuttling capacities, cytoplasmic nucleolin is associated with the stabilization of multiple mRNA's including those of amyloid precursor protein, bcl-2, bcl-XL, and interleukin 2 (IL-2), resulting in additional survival mechanisms of the cell.(192, 220, 221, 227) There is a clear difference between isoelectric points of cytoplasmic and nuclear nucleolin suggesting that posttranslational modifications affect nucleolin's cytoplasmic localization.(178) Phosphorylation and arginine methylation have been implicated in nucleolin's shuttling abilities and potential contribution to the observed isoelectric point changes.(151, 169) Cytoplasmic nucleolin is reduced by inhibitors of protein synthesis, cyclophosphamide and actinomycin D, but not by glycosylation inhibitor tunicamycin, suggesting that newly transcribed and translated nucleolin carries out cytoplasmic functions independently of glycosylations.(175, 228)

The localization of nucleolin on the cell surface is intricately associated with cell growth conditions and the proliferation status.(178) The molecular mechanism underlying the translocation of nucleolin to the plasma membrane is not fully understood. Nucleolin lacks a transmembrane domain or a glycosylphosphatidylinositol (GPI) anchor and is predicated to be held to the plasma membrane through an association with an unknown protein.(178, 216) Additionally, nucleolin does not translocate to the cell surface through the classical biosynthetic pathway involving the endoplasmic reticulum (ER) and Golgi, as inhibitors of this pathway do not affect nucleolin cell-surface localization.(178) However, nucleolin has been identified in intracytoplasmic vesicles.(178) Cross-linking of surface nucleolin with nucleolin antibodies induces clustering, which resembles capping, typically observed in membrane-anchored antigens.(178) However, high salt concentrations dissociate nucleolin from the cell surface, suggesting that nucleolin associates with an integral membrane or GPI-anchored protein through isoelectrostatic interactions.(190) Moreover, it has been observed that tunicamycin and cyclophosphamide can inhibit surface nucleolin, suggesting that newly translated and glycosylated nucleolin is transported to the cell surface.(175, 219) On the other hand, nuclear nucleolin was unaffected by those inhibitors,

confirming that other modifications, listed above, control nucleolin trafficking to the nucleus and nucleolus.(210) Recent studies have shown that in endothelial cells, glioblastomas, and other integrin $\alpha_v\beta_3$ expressing cells, integrin $\alpha_v\beta_3$ and phosphatidylinositide 3 kinases (PI3K)/c-src signaling are necessary for the translocation of nucleolin to the cell surface.(214) Several molecules including vascular endothelial growth factor (VEGF), serum, laminin-1, low density lipoprotein receptor related protein-1(LDLRP-1), and pleiotrophin (PTN) have been reported to increase cell surface nucleolin (Table 4).(178, 208, 214, 216, 218, 229)

Nucleolin's localization at the cell surface is frequently followed by internalization (171), or it can eventually be released from the extracellular membrane.(178) Surface-localized nucleolin's degradation half-life is estimated between 45 minutes and one hour, while nuclear nucleolin's half-life is estimated to be up to twenty-four hours, suggesting that nucleolin's surface localization is tightly regulated.(210) Internalization of nucleolin occurs only at 37°C and higher temperatures and is abolished at lower temperatures, implying an active internalization process.(178, 229, 230) Nucleolin's entrance into the cell from the surface was determined to be a calcium-dependent entry.(210) One report suggests that nucleolin is closely associated with the globular actin within the cytoskeleton, and this can be a potential link between its surface localization and entry to the cell, as well as being a modulator of its receptor functions (described in the next section).(178) In angiogenic cells, non-muscle myosin heavy chain 9 (MyH9) was identified as a key player in the organization of nucleolin on the cell-surface.(216) The selective cell-surface expression of nucleolin in multiple types of cancer cells implies nucleolin as a potential therapeutic target.

Nucleolin as a Receptor

Although the mechanism of nucleolin's delivery to the cell surface remains poorly understood, multiple interactions and functions within its surface expression have been identified. Nucleolin's recent identification on the surface of cells was facilitated by the discovery of nucleolin as a docking protein or entry point for multiple viruses: coxsackie B viruses, hepatitis C, human immunodeficiency virus (HIV), and adeno-associated virus type-2 (AAV-2).(164, 231)

The importance of nucleolin receptor functions in cancer biology was highlighted by identification of its ligands, which play a critical role in tumorigenesis and angiogenesis, and by relevant transport of multiple pro-survival factors by nucleolin. Nucleolin was identified as the receptor for PTN, an angiogenic and mitogenic growth factor,(215, 232); apoB- and apoE-containing lipoproteins; and laminin-1 neurite-promoting IKVAV site, a neurite growth and

maintenance factor.(233, 234) Nucleolin is also a receptor for the *helicobacter pylori* TNF-α inducing protein (Tipα), and translocates Tipα into the cell where it engages in the carcinogenic process.(235) Lastly, nucleolin mediates the internalization of endostatin, a proteolytic fragment of collagen XVIII and potent inhibitor of angiogenesis.(236, 237) However, nucleolin-mediated endostatin internalization is restricted to endothelial cells, suggesting that nucleolin signaling varies with cell type.(237) In summary, numerous pro-survival functions attributed to nucleolin are associated with its selective extra-nuclear/cell surface localization.

Pro-Survival Functions of Nucleolin

Nucleolin's roles in the nucleolar region, its function as a transcriptional regulator, and its receptor functions suggest nucleolin serves as a growth enhancing and pro-survival molecule. Furthermore, overexpression of nucleolin decreases p53 translation in response to DNA damage, suggesting a role in preventing growth arrest and apoptosis in cells.(168, 195) Multiple pro-survival molecules and cytokines, including IL-2, fibroblast growth factor -2 (FGF-2), and VEGF (213) (216) upregulate and modify nucleolin and enhances nucleolin's pro-survival functions.(222)

Nucleolin has been identified as a binding partner and potential regulator of many pro-survival proteins including, insulin receptor substrate-1, -2, uPAR (urokinase specific receptor) (171, 238), laminin-1(234), L-selectin (239), and epidermal growth factor receptor (ErbB).(240) The growth factor, midkine, PTN, and heparin binding growth-associated nucleolin-interacting molecules are involved in mitogenic, angiogenic, and anti-apoptotic effects in transformed cells.(218, 241)

Nucleolin has been extensively studied within the angiogenic system, because angiogenesis-specific cell-surface localization of nucleolin was observed.(216) It is reported that nucleolin's interacts with PTN and stimulates angiogenesis.(232) Additionally, nucleolin binds the G-quadruplex-forming region of the VEGF gene promoter *cis*-element acting as transcriptional activator of VEGF, and is a transcriptional promoter of krüppel-like factor-2 during flow-specific stress.(242, 243) Anti-nucleolin polyclonal antibodies (pAbs) are able to prevent cell migration and tubule formation by angiogenic endothelial cells, (216) and nucleolin is also necessary for integrin $\alpha_v\beta_3$-stimulated migration.(214)

Many of the mRNAs stabilized by cytoplasmic nucleolin are necessary for cell survival and oncogenesis, including bcl-2, bcl-xl, and metalloproteinase-9 (MMP-9).(220, 244, 245) Lastly, nucleolin's role in oncogenesis has been characterized: it cooperates with the Ras oncogene in transforming rat fibroblasts, associates and blocks the tumor suppressor retinoblastoma protein (Rb)

to trigger human papilloma virus (HPV)-18 positive cervical carcinomas(246), and transcriptionally activates B-cell transformation genes c-myc and Epstein-Barr virus nuclear antigen-1(EBNA-1) as a part of the lipopolysaccharide-responsive factor 1(LR1) complex.(195, 201, 229, 247) Deregulated nucleolin expression is associated with hypertrophy of the nucleolus, a distinct cytological feature of cancer cells.(190) Proteomics analysis of etoposide, Adriamycin or mitoxantrone-resistant cell lines identified nucleolin overexpression associated with chemoresistance (248), suggesting an oncogenic and chemoresistant role of nucleolin in cancers.

Nucleolin and the Apoptotic Pathway

Nucleolin's localization during apoptosis has been extensively studied, as it was assumed to be a contributing factor to the distinctive morphological and biochemical events that determine cell death pathways. Nucleolin is clearly redistributed rapidly after apoptosis induction, leaving the nucleus to be relocated throughout the cell.(172) However, a fraction of nucleolin remains in micronuclei bodies referred to as HERDS (heterogeneous ectopic RNP-derived structures) that are enriched in nuclear matrix proteins and nucleolar proteins. Nucleolin is also released in apoptotic bodies during leukemia cell apoptosis, which leads to production of nucleolin autoantibodies if the apoptotic bodies are not efficiently cleared and autophagocytosed.(249) The nucleolin autoantibodies are the first autoantibodies that appear in the sera of SLE patients, as they are the earliest autoantibodies made.(250, 251) Interestingly, the model used to study SLE and autoantibodies production is a Fas-defective lpr mouse model. In a multiple sclerosis disease model, decreased nucleolin levels in the sera are a potential prognostic marker for a relapse.(252) Therefore, nucleolin's localization and secretion during apoptosis is clinically important, yet its functions remain to be elucidated.

In Burkitts lymphoma cell line BL60, nucleolin is cleaved after apoptosis induction, and caspase-3 inhibition prevents nucleolin's cleavage.(253) Nucleolin's cleavage has also been identified in association with another form of cell death, cytotoxic T-cell mediated granzyme degradation, in which nucleolin was identified as a substrate for granzyme A.(254) In this instance, cleaved nucleolin is utilized to activate autolytic endonucleases for DNA fragmentation. However, in a different study, ultraviolet radiation (UV) and camptothecin-induced apoptosis triggered nucleolin's translocation into the nucleus, release in apoptotic bodies, and overall decrease in protein, without cleavage.(172, 211) Therefore, the cleavage of nucleolin may be cell type- and cell death pathway-specific, or the 76kDa nucleolin fragment observed in the former studies may be one of the cell cycle-specific, self-proteolytic sites of nucleolin and may not be representative of a

caspase-3-specific cleavage product. Nucleolin was also shown to increase its RNA-binding activity during genotoxic stress induced by ionizing or UV radiation through SAPK (stress activated protein kinase) p38 phosphorylation.(255) Therefore, nucleolin's behavior during apoptosis in response to various stimuli and in different cell types needs to be clarified.

In addition to changes in localization and potential modifications of nucleolin during apoptosis, nucleolin associates with and regulates multiple apoptotic proteins, including PARP.(172) Its association with PARP is hypothesized to be involved in translocation of PARP and nucleolin into apoptotic bodies and poly ADP-ribosylation of nucleolin.(172) In a search for the receptor of sialoglycoprotein CD43 on monocytes and macrophages responsible for capping, an early apoptotic step for cells undergoing oxidized cell death, a nucleolin 50kDa fragment was discovered as the receptor for phosphatidylserine and CD43. The amino acids 295-302 were necessary for this recognition.(256) Also, Factor J, a cationic glycoprotein acting as an inhibitor of the complement activation, was identified as a ligand for surface nucleolin.(230, 257)

Lastly, nucleolin is also an important stabilizer of anti-apoptotic mRNAs, binding the AU-rich element (ARE) in bcl-2 mRNA and competing for binding of ARE binding/degradation factor (AUF1), thus preventing bcl-2 mRNA degradation.(258) Nucleolin also stabilizes anti-apoptotic bcl-xl mRNA.(220) These interactions, although they appear to be multifactorial, may expose nucleolin as a key regulator of the apoptotic pathway.

Table 5: Nucleolin Interacting Proteins and their Functions.

Location	Interaction	Proposed Function
Surface	Phosphatidylserine (256)	Macrophage receptor
	CD43 (256)	Macrophage receptor
	Factor J (230)	Inhibition of complement activation
	uPAR (161)	Induce translocation of receptor/ligand and stimulate mitogenic response
	MyH9 (216)	Translocation of nucleolin within surface and cytoplasm with VEGF stimulation
	Endostatin (237)	Receptor and surface → cytoplasmic → nuclear shuttling
	Laminin-1 (234)	Neurite growth and maintenance
	Tipα (259)	Receptor and surface → cytoplasmic → nuclear shuttling
	Viral receptor (231, 260, 261)	Coxsackie B, Hepatitis, HIV, AVV-2
	PTN (232)	Angiogenesis stimulation
	ErbB (240)	Receptor dimerization and phosphorylation
	Integrin $\alpha_v\beta_3$ (214)	Migration stimulation
	Hepatocyte growth factor (262)	Receptor and inducer of proliferation stimulation
	LDL receptor (263)	Low affinity receptor of HepG2 cells
	L-Selectin (239)	Receptor and adhesion of leucocytes
Cytoplasm	bcl-2 ARE (258)	mRNA stabilization
	bcl-xl ARE (220)	mRNA stabilization
	MMP-9 (244)	mRNA stabilization
	APP 3'UTR (192)	Cytoplasmic RNA stability
	Granzyme A (254)	Degradation protein of Granzyme A
	YB-1 (221)	IL-2 mRNA stabilization
	Midkine (241)	Anti-apoptotic cytoplasm → nuclear transport
	PRMT5 (166)	Nucleolin methylation
	TGF-β receptor 1(226)	Cytoplasmic → nuclear transport
	HdM2 (264)	Inhibition of p53 ubiquitination
Nucleus	LR1 complex (201)	Immunoglobulin switch recombination, c-myc and EBNA-1 transcription
	Histone H1 and H2AX (188)	Chromatin decondensation
	Factor B B-motif (191)	Transcriptional repression of AGP
	RPL26 (193)	Repression of p53 translation
	p53(195)	Inhibition of DNA replication and repair during stress
	Rad51 (197)	Recombinational DNA repair
	MDC1 (189)	Accumulation at DSB in DNA repair

	hRPA (196)	Inhibition of chromosomal replication during stress
	Viral proteins (246)	Transcription factor
	VEGF promoter (242)	Transcriptional activator
	Krüppel-like-factor-2 (243)	Transcriptional promoter
	Rb (247)	G_1 phase transcriptional repressor of HPV18 oncogenes
	Insulin-receptor substrate- 1 (238)	Nuclear → cytoplasmic shuttling during differentiation
	A- and C- Myb (194)	Repressor of Myb transcriptional regulation
	YB-1 (198)	DNA repair
	Telomerase (165)	Telomerase nucleolar localization
	PCNA (200)	During stress inhibits NER
	PRMT5 (166)	Nucleolin methylation
	Drosha (187)	MicroRNA biogenesis

Nucleolin is a multifunctional protein that interacts with various molecules throughout the cell. Described are nucleolin binding partners by location within the cell and the various roles of the interactions.

Nucleolin as a Prognostic Indicator of Neoplasms

Nucleolin's association and accumulation with silver-stained nucleolar organizer regions (AgNORs) correlates with cell proliferation in human cancers.(181) Since this initial finding, nucleolin has been assigned as a prognostic marker for a growing number of cancers. The Children's Cancer and Leukaemia Group Biological Studies Committee was one of the first to report that high nucleolin levels were the single most important biological predictor of a worsening outcome in pediatric intracranial ependymomas.(265) A secondary study of childhood ependymomas by the Associazione Italiana Ematologia Oncologia Pediatrica, also determined that nucleolin protein expression was a credible prognostic marker for both worsened overall survival and decreased relapse-free survival rates.(266) Most recently, another group further substantiated surface and cytoplasmic localization of the glycosylated form of nucleolin as a prognostic marker in gliomas. The antibody gp273 against the glycosylated form of nucleolin was able to decipher nucleolin's localization throughout tumor cells.(267) Results obtained consistently showed an increase of glycosylated nucleolin in the cytoplasm and cell surface in high grade gliomas, suggesting that nucleolin's deregulation and glycosylation-related changes in localization are a major contributing factor to poor outcomes in patients with gliomas.

In a study designed to compare various stages of melanoma, it was shown that malignant and atypical lesions have abnormal nucleolin staining, but that abnormal staining appears during early melanogenesis, accumulates during melanoma progression, and presents a worse prognosis.(268) Furthermore, a significantly higher nucleolin nuclear expression was found in pancreatic ductal adenocarcinoma than in non-neoplastic pancreatic ductal epithelial cells with the significant correlation with prognosis in stage II disease.(269)

Nucleolin may also serve as a peripheral blood biomarker indicating the presence of early stage of cervical cancer.(270) Collectively, these studies suggest that nucleolin could serve as a prognostic and diagnostic marker for other cancers such as lymphomas, and suggest that the nucleolin levels may represent a diverse and important diagnostic tool.

Targeting Nucleolin as a Cancer Therapy

The anti-cancer agent dexamethasone has been shown to decrease phosphorylation of nucleolin by CKII, resulting in a loss of RNA polymerase activity, and suggesting that nucleolin has been unknowingly targeted in cancer therapeutics for a long time.(271) Inhibition of RNA polymerase has induced tumor regression.(272) In recent years nucleolin has been selected as a target in multiple therapeutic strategies. Nucleolin was targeted by anti-HIV pentameric

pseudopeptide HB-19, which binds irreversibly to the RGG C-terminal domain of nucleolin and is currently being tested as a potential therapeutic in cancer beyond its original purpose in HIV infection. The HB-19 pseudopeptide and derived pseudopeptide targeting nucleolin-termed nucants (nucleolin antagonists) showed varying effects depending upon tumor type.(273) In leukemia and lymphoma models, the nucants induced cell death and proliferation inhibition, while in the adherent cell type cancers including breast, colon, cervical, and melanoma they induced little cell death but marked growth inhibition.(229, 273, 274)

In addition to the HB-19 pseudopeptide, additional peptides targeting nucleolin have moved into pre-clinical testing. During the screening of tumor blood vessels for specific markers, tumor homing peptide F3, a nucleolin ligand, was identified.(275) Interestingly, F3 is selectively internalized by tumor and angiogenic cells, which led to the use of the F3 peptide in multiple successful and specifically targeted therapeutic delivery systems. The F3 peptide was modified into a F3 peptide-targeted sterically stabilized pH-sensitive liposomes for delivery of doxorubicin to breast tumor cells and angiogenic vesicles.(276) The treatment proved effective in delivery of the chemotherapeutic agent to the tumor microenvironment with significantly decreased uptake in non-specific cells and tissues, as compared to other commercially available liposomes.(276) The F3 targeting moiety was also conjugated to single-walled carbon nanotubes (SWNT), which when targeted with near-infrared light therapy cause thermal ablation of nearby cells with a polyethylene glycol-linker.(277) In an in vitro model in which cells were killed with F3-SWNT followed by laser treatment, 99.8% of angiogenic cells were killed while there was no uptake of the F3-SWNT in non-angiogenic endothelial cells. ^{213}Bi-DTPA (an alpha-emitter radionuclide which causes induction of double stranded breaks in cells) conjugated F3 was used as a delivery method in peritoneal carcinomatosis breast cancer models.(278) The homing radionuclide was taken up in a breast cancer cell in vitro model 200 times more than ^{213}Bi-DTPA used alone, showed decreased formation of peritoneal carcinomatosis, and increased survival of mice by 80%.(278) Lastly, PEG-PLA nanoparticles loaded with paclitaxel with surface-functionalized F3 peptide and co-administered with tLyP-1 to gliomas showed improved penetration and increased survival of mice in a glioma model.(279) These results prove that nucleolin is a high-quality therapeutic target for endothelial cells and cancers.

Beyond peptides, nucleolin antibodies have also been tested for their ability to prevent allograft failure in organ transplants. Antibodies against endothelial cells were found in transplant patients that failed allografts, and many of these antibodies targeted nucleolin. It was determined that nucleolin antibodies from transplant patients' sera and a crosslinked commercial anti-nucleolin antibody inhibited growth of endothelial cells and induced apoptosis.(280) Although the focus of

this study was to determine reasons for allograft failure, it revealed the potential of anti-nucleolin antibodies as a potential therapeutic.

Aptamers, ssDNA/RNA molecules, targeting nucleolin have recently come to the forefront in the translational and clinical search for potential therapeutics in neoplasms. A novel class of aptamers called GROs, G-rich oligonucleotides, with a strong secondary structure, binds nucleolin and inhibits growth of tumors in prostate, breast, and cervical carcinoma models.(209) The most successful nucleolin, GRO, AS1411, has shown anti-proliferative activity in almost every cancer cell type tested, and thus appears to have a broad therapeutic potential (281); AS1411 moved from Phase I clinical trials, in a variety of advanced solid tumors, into two Phase II clinical trials for acute myeloid leukemia and renal cell carcinoma. It is also interesting to note that in breast cancer cells, AS1411 destabilizes *bcl-2* mRNA by interfering with nucleolin *bcl2* mRNA binding.(282) Recently, AS1411 was attached to a nanoparticle for delivery of the anti-miRNA 221 and miR-221MB in a rat glioma tumor burden model where it successfully reduced tumor volume.(283) Also, the nucleolin-targeting aptamer, LNA-aptamer, obtained from the cell-SELEX (systematic evolution of ligands by exponential enrichment) technology(284), was developed into a SPION (superparamagnetic iron oxide nanoparticle)(285) called LNA-aptamer, which is currently showing potential against cancer cells in cell culture models.(286)

The successful elimination and inhibition of tumor growth by direct nucleolin targeting or through the use of nucleolin ligand-linked drug delivery systems further underscores nucleolin's potential as a cancer therapy. Advancements in our understanding of nucleolin's role and its localization in tumor cell survival and apoptosis will greatly improve the effectiveness and specificity of interventions using this promising target in cancer therapy. In this regard, the current investigation focused on characterizing nucleolin's expression in B-cell lymphomas and showed that nucleolin is directed to the extracellular cell surface specifically in oncogenic B cells.

Chapter 2: Background, Rationale and Research Plans

Background

Progress in the management and understanding of NHL, the fifth leading incidence of cancer in North America, has made it clear that there are multiple clinical characteristics, gene profiles, expression patterns, and chemotherapeutic responses among patients beyond the defined NHL subtypes. These differing characteristics, particularly chemotherapeutic responses, have a major role in the 27% death rate for NHL.(7, 26) This clearly points to the need for further advancements in the screening and identification of possible diagnostic and therapeutic targets for the multiple profiles of NHL in order to more effectively stratify patients into varying risk and treatment groups.(6, 7)

The largest hindrance to effective elimination of cancer cells is chemoresistance resulting in chemotherapy-refractory disease and minimal residual disease. Defining the attributes that cause chemoresistance would be a major step toward eradicating NHL. Some of the chemoresistance of cancer cells can be based on the decreased ability of tumor cells to undergo apoptosis. In multiple cancers the inhibition of the death receptor Fas results in a decrease in chemotherapeutic sensitivity.(82, 105, 287-289) Moreover, several forms of chemotherapy induce higher expression levels of Fas and/or FasL in order to effectively eliminate tumor cells.(109, 130, 143, 290) Despite often adequate levels of Fas expression, NHL cells are commonly resistant to Fas-mediated apoptosis.(102, 149) Investigations into the defects of Fas-mediated apoptosis show there are multiple layers of controls affecting Fas signaling. However, for the vast majority of lymphomas a complete explanation of Fas obstruction remains elusive.(291) Therefore, clarification of Fas inhibition and subsequent restoration of Fas signaling in B-cell lymphomas will allow efficient chemotherapy induced cell death.(101)

Rationale

We set out to identify novel modulators of Fas-mediated apoptosis whose expression may correlate with chemoresistance in B-cell lymphomas. The idea to look for Fas-associated regulators came from our previous work that revealed the oncogene K1of human herpesvirus-8 binds to Fas, inhibits FasL binding, and subsequently blocks apoptosis.(292-294) We also discovered that PML-RARα, an oncogenic fusion protein, binds Fas and recruits c-FLIP to the DISC and ultimately prevents Fas-mediated apoptosis in acute promyelocytic leukemias (APL).(295) Moreover, we showed that these interactions can be targeted and modified in order to sensitize cells to apoptosis.(292) Based on these findings, we hypothesized the existence of potential endogenous

and analogous Fas binding partners to K1 in lymphomas. The main aim of this thesis is the characterization of nucleolin, one of the Fas-binding proteins identified through a screening process isolating binding partners of inactive/activation-resistant Fas.

Nucleolin was selected for extensive study as a potential novel modulator of Fas-mediated apoptosis. At the time nucleolin was known mainly as a nuclear protein associated with rRNA and ribosome modulation. However, nucleolin is a strongly multifunctional protein and its roles change depending on its location, post-translation modifications, cell cycle status, and proliferative capacity of the cell. The localization of nucleolin is altered in highly proliferating cells, where it has been shown to translocate out of the nucleus into the cytoplasm and on to the plasma membrane.(172, 178, 256, 260, 273, 275) In recent years, nucleolin has been found upregulated in cancer and cancer-associated endothelial cells, and in certain cases its upregulation correlates with clinically worse outcomes.(163, 245, 265, 267-269, 275, 281, 296, 297) The functions and roles of nucleolin within the cancer cell all indicate that nucleolin serves as a pro-survival protein. However, nucleolin's localization, expression levels, and functions in B-cell lymphomas remain elusive.(152, 275) Based on previously described roles of nucleolin in the survival of cancer cells, its selective surface expression, and our identification of nucleolin as a Fas-binding partner, we investigated nucleolin's effect on Fas-mediated apoptosis.

Research Plan

Based on previous findings, we hypothesized that nucleolin is overexpressed in lymphomas where it acts as an inhibitor of apoptosis signaling through direct interaction with Fas on the cell surface. In order to investigate this hypothesis I have set out to characterize nucleolin's expression and role in Fas-mediated apoptosis in B-cell lymphomas, with intent to complete the following aims:

AIM 1: To characterize nucleolin's binding of Fas in B-cell lymphomas

We set out to identify potential binding partners of Fas by isolating complexes associated with activation-sensitive and activation-resistant Fas. Through a screening process, we identified nucleolin as a binding partner and potential modulator of Fas in B-cell lymphomas. Our objective in this aim was to confirm the ability of nucleolin to form complexes with Fas in B-cell lymphomas and characterize the nucleolin-Fas complex by studying formation of the complex, specifically through investigations of the binding sites and localization of the complex within the cell. I

anticipated that nucleolin-Fas complexes would exist selectively on the extracellular surface in lymphoma tissues.

AIM 2: To characterize the effect of the nucleolin-Fas complex on Fas-mediated apoptosis

The objective of this aim was to determine if nucleolin or nucleolin-Fas complexes modulate Fas-mediated apoptosis. We set out to determine the effects of nucleolin levels and the presence of nucleolin-Fas complexes on Fas signaling and to clarify a potential mechanism of modulation through investigations with nucleolin knockdown cells and an in vivo mouse overexpression model. I anticipated that nucleolin would act as an inhibitor of Fas-mediated apoptosis and thus, decreased nucleolin in B-cell lymphomas would sensitize cells to Fas-mediated apoptosis. The overexpression of nucleolin in B-cell lymphoma cells would be anticipated to inhibit Fas receptor activation and thus desensitize cells to Fas-mediated apoptosis.

AIM 3: To characterize the expression and localization of nucleolin in B-cell lymphomas

The objective of this aim was to characterize nucleolin's expression in B-cell lymphomas through investigations of protein levels, protein localization, mRNA levels, transcriptional rates, and correlation with diagnosis, prognosis, and outcome of B-cell lymphomas. I anticipated that in comparison to healthy donor B cells, nucleolin protein and mRNA will be overexpressed in both lymphoma cell lines and primary lymphoma tissue.

Significance

Targeted therapeutics aimed to cancer-specific surface molecules show much promise and may help improve the treatment efficacy of many medical conditions especially cancer. Nucleolin's selective surface localization in highly proliferating cancer and cancer-associated cells makes it an ideal target for cancer therapeutics, which should theoretically have low cytotoxic effects on normal cells. In this project, we studied nucleolin's expression and localization patterns in B-cell lymphomas in relation to clinical outcomes, thereby extending nucleolin's suggested oncogenic role to NHL. Characterization of nucleolin expression in B-cell lymphomas underscores nucleolin's potential as a feasible prognostic marker and therapeutic target in NHL.

In addition, we focused on defining nucleolin's potential to interfere with Fas-mediated apoptosis and subsequently induce chemoresistance. Failure to induce apoptosis and eliminate damaged cells is thought to permit gene abnormalities and promote genetic instability. Thus, an inability to activate Fas can contribute to the generation of viable but genetically altered cells that

can undergo malignant transformation. Resistance to chemotherapies and Fas-mediated apoptosis may have multiple causes. Thus, an understanding of the mechanism of nucleolin's interference with Fas signaling will contribute to the development of novel therapeutic strategies for B-cell lymphomas.

Chapter 3: Nucleolin Interacts with Fas

Rationale

Our previous work characterized two Fas binding and modulatory proteins, K1 and PMLRARα, which are key to the pathogenesis of human herpesvirus-8 infected Kaposi's sarcoma and APL, respectively.(293, 295) Based on the viral mimicry theory, we hypothesized the existence of endogenous proteins that are similar to the viral protein. In order to identify these potential binding partners of Fas we developed a screening process for proteins associated with activation-resistant Fas. In this chapter we identified, through our screening process, that nucleolin is a Fas interacting protein. We pursued confirmation of nucleolin as a potential Fas-binding partner and characterization of the interaction. By defining and characterizing the interaction of nucleolin and Fas in B-cell lymphomas, we are further expanding our ability to create a therapeutic concept for targeting the nucleolin-Fas complex for a clinical application.

Results

Identification of Nucleolin in Fas-resistant Complexes

To identify potential binding partners of Fas contributing to the inhibition of Fas signaling, we analyzed activation-resistant Fas complexes from interacting proteins. We subjected the EBV negative human Burkitts lymphoma line BJAB, which expresses Fas but shows low response to Fas activation, and cells from a human primary NHL tissue to Fas activation and immunodepletion by agonistic Fas antibody, CH-11. The remaining supernatants, harboring any inactive/activation-resistant/inaccessible Fas, were subjected to a second Fas IP with a B-10 antibody directed to an intracellular Fas epitope. The precipitated proteins were separated by gel electrophoresis and visualized by silver stain. Any protein band found selectively in the activation-resistant lane was destained, excised, trypsin digested, and analyzed by nanoflow-LC-mass spectroscopy (MS)/MS (298) (Figure 3a-b).(295) The resulting collision-induced dissociation (CID) fragmentation spectra results were searched against the National Center for Biotechnology Information (NCBI) non-redundant protein database with MASCOT. Six of the peptide spectra found in the Fas-resistant specific 100-kDa-excised band (Figure 3b, asterisk) matched nucleolin with a rank 1 (Figure 3c-m), suggesting that nucleolin is part of an activation-resistant Fas complex.

Figure 3

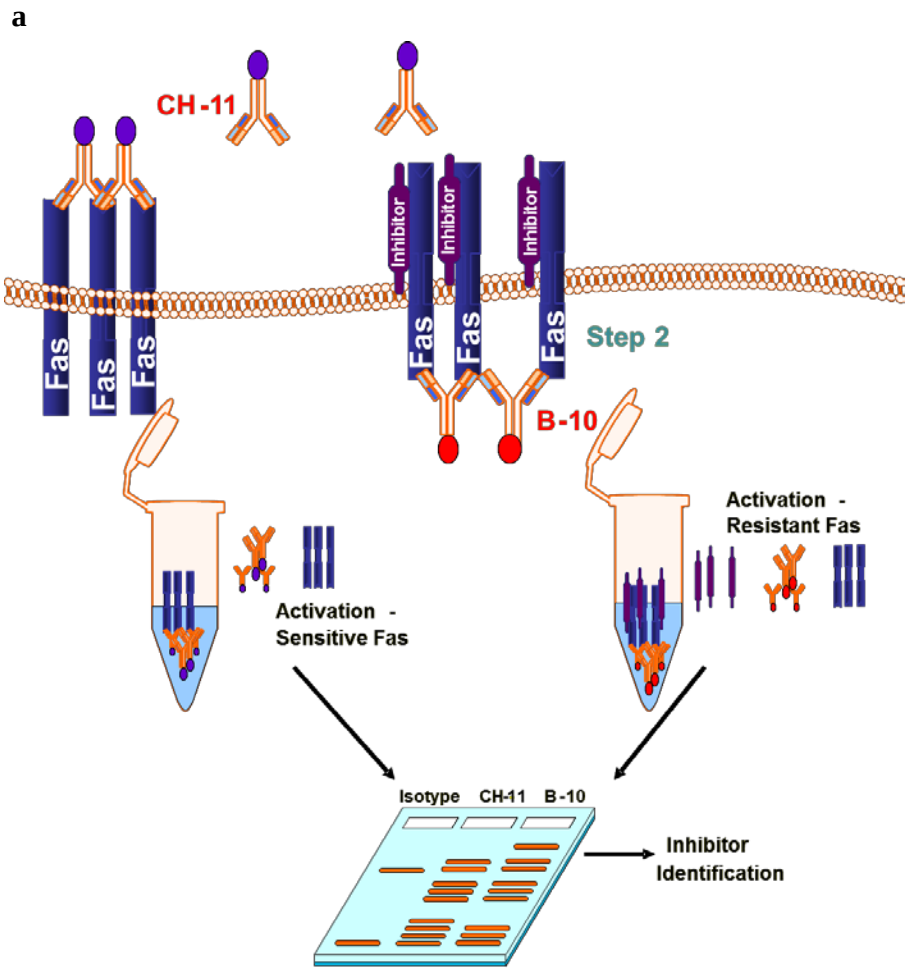
a
CH-11
Inhibitor
Inhibitor
Inhibitor
Fas
Fas
Fas
Fas
Fas
Fas
Step 2
B-10
Activation -
Resistant Fas
Activation -
Sensitive Fas
Isotype
CH-11
B-10
Inhibitor
Identification

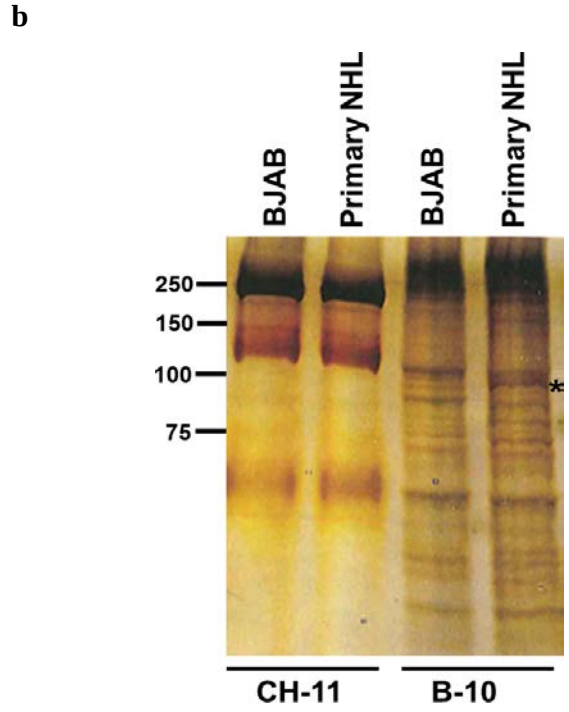
b
BJAB
Primary NHL
BJAB
Primary NHL
250
150
100
75
*
CH-11
B-10

c **Peptide: EVFEDAAEIR** **Found In: NUCL_HUMAN, Nucleolin OS=Homo sapiens GN=NCL**

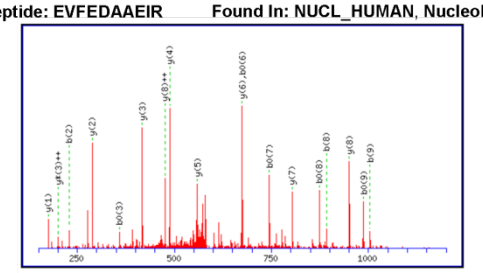

Average mass of neutral peptide Mr(calc): 1178.2487
Ions Score: 65 **Expect:** 0.00011
Matches : 18/86 fragment ions using 30 most intense peaks (help)

#	b	b^{++}	b^{0}	b^{0++}	Seq.	y	y^{++}	y^{*}	y^{*++}	y^{0}	y^{0++}	#
1	130.1214	65.5644	112.1061	56.5568	E							10
2	229.2525	115.1299	211.2372	106.1223	V	1050.1422	525.5748	1033.1117	517.0595	1032.1269	516.5671	9
3	376.4264	188.7169	358.4111	179.7093	F	***951.0111***	476.0092	933.9806	467.4940	932.9958	467.0016	8
4	505.5404	253.2739	487.5251	244.2663	E	***803.8372***	402.4223	786.8067	393.9070	785.8219	393.4146	7
5	620.6278	310.8176	602.6125	301.8100	D	***674.7232***	337.8653	657.6927	329.3500	656.7079	328.8576	6
6	691.7057	346.3565	673.6904	337.3489	A	***559.6358***	280.3216	542.6053	271.8063	541.6205	271.3139	5
7	762.7836	381.8955	744.7683	372.8879	A	***488.5579***	244.7826	471.5274	236.2674	470.5426	235.7750	4
8	891.8976	446.4525	873.8823	437.4449	E	***417.4800***	209.2437	400.4495	200.7284	399.4647	200.2360	3
9	1005.0552	503.0313	987.0399	494.0237	I	***288.3660***	144.6867	271.3355	136.1714			2
10					R	***175.2084***	88.1079	158.1779	79.5926			1

d **Peptide: EVFEDAAEIR** **Found In: NUCL_HUMAN, Nucleolin OS=Homo sapiens GN=NCL**

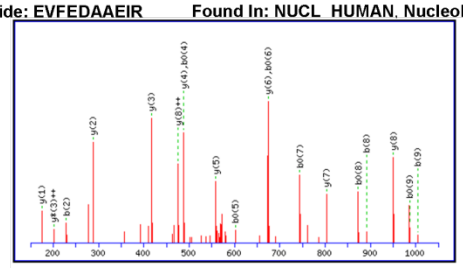

Average mass of neutral peptide Mr(calc): 1178.2487
Ions Score: 70 **Expect:** 3.7e-005
Matches : 19/86 fragment ions using 27 most intense peaks (help)

#	b	b^{++}	b^{0}	b^{0++}	Seq.	y	y^{++}	y^{*}	y^{*++}	y^{0}	y^{0++}	#
1	130.1214	65.5644	112.1061	56.5568	E							10
2	229.2525	115.1299	211.2372	106.1223	V	1050.1422	525.5748	1033.1117	517.0595	1032.1269	516.5671	9
3	376.4264	188.7169	358.4111	179.7093	F	***951.0111***	476.0092	933.9806	467.4940	932.9958	467.0016	8
4	505.5404	253.2739	487.5251	244.2663	E	***803.8372***	402.4223	786.8067	393.9070	785.8219	393.4146	7
5	620.6278	310.8176	602.6125	301.8100	D	***674.7232***	337.8653	657.6927	329.3500	656.7079	328.8576	6
6	691.7057	346.3565	673.6904	337.3489	A	***559.6358***	280.3216	542.6053	271.8063	541.6205	271.3139	5
7	762.7836	381.8955	744.7683	372.8879	A	***488.5579***	244.7826	471.5274	236.2674	470.5426	235.7750	4
8	891.8976	446.4525	873.8823	437.4449	E	***417.4800***	209.2437	400.4495	200.7284	399.4647	200.2360	3
9	1005.0552	503.0313	987.0399	494.0237	I	***288.3660***	144.6867	271.3355	136.1714			2
10					R	***175.2084***	88.1079	158.1779	79.5926			1

e **Peptide: EVFEDAAEIR** **Found In: NUCL_HUMAN, Nucleolin OS=Homo sapiens GN=NCL**

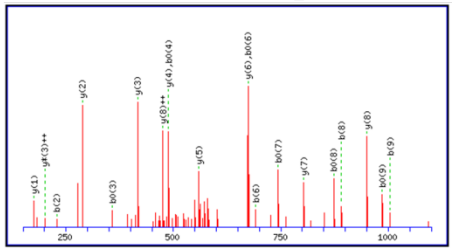

Average mass of neutral peptide Mr(calc): 1178.2487
Ions Score: 61 **Expect:** 0.00024
Matches : 20/86 fragment ions using 37 most intense peaks (help)

#	b	b^{++}	b^{0}	b^{0++}	Seq.	y	y^{++}	y^{*}	y^{*++}	y^{0}	y^{0++}	#
1	130.1214	65.5644	112.1061	56.5568	E							10
2	229.2525	115.1299	211.2372	106.1223	V	1050.1422	525.5748	1033.1117	517.0595	1032.1269	516.5671	9
3	376.4264	188.7169	358.4111	179.7093	F	***951.0111***	476.0092	933.9806	467.4940	932.9958	467.0016	8
4	505.5404	253.2739	487.5251	244.2663	E	***803.8372***	402.4223	786.8067	393.9070	785.8219	393.4146	7
5	620.6278	310.8176	602.6125	301.8100	D	***674.7232***	337.8653	657.6927	329.3500	656.7079	328.8576	6
6	691.7057	346.3565	673.6904	337.3489	A	***559.6358***	280.3216	542.6053	271.8063	541.6205	271.3139	5
7	762.7836	381.8955	744.7683	372.8879	A	***488.5579***	244.7826	471.5274	236.2674	470.5426	235.7750	4
8	891.8976	446.4525	873.8823	437.4449	E	***417.4800***	209.2437	400.4495	200.7284	399.4647	200.2360	3
9	1005.0552	503.0313	987.0399	494.0237	I	***288.3660***	144.6867	271.3355	136.1714			2
10					R	***175.2084***	88.1079	158.1779	79.5926			1

f **Peptide:VTQDELKEVFEDAAEIR Found In: NUCL_HUMAN, Nucleolin OS=Homo sapiens GN=NCL**

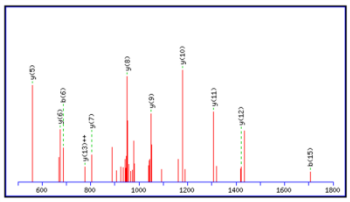

Average mass of neutral peptide Mr(calc): 1992.1442
Ions Score: 58 **Expect:** 0.00049
Matches : 11/182 fragment ions using 18 most intense peaks (help)

#	b	b^{++}	b^*	b^{*++}	b^0	b^{0++}	Seq.	y	y^{++}	y^*	y^{*++}	y^0	y^{0++}	#
1	100.1385	50.5729					V							17
2	201.2424	101.1249			183.2271	92.1173	T	1894.0206	947.5140	1876.9901	938.9987	1876.0053	938.5063	16
3	329.3716	165.1895	312.3411	156.6742	311.3563	156.1819	Q	1792.9167	896.9620	1775.8862	888.4468	1774.9014	887.9544	15
4	444.4590	222.7332	427.4285	214.2179	426.4437	213.7256	D	1664.7875	832.8974	1647.7570	824.3822	1646.7722	823.8898	14
5	573.5730	287.2902	556.5425	278.7749	555.5577	278.2826	E	1549.7001	775.3537	1532.6696	766.8385	1531.6848	766.3461	13
6	686.7306	343.8690	669.7001	335.3537	668.7153	334.8614	L	*1420.5861*	710.7967	1403.5556	702.2815	1402.5708	701.7891	12
7	814.9029	407.9551	797.8724	399.4399	796.8876	398.9475	K	*1307.4285*	654.2179	1290.3980	645.7027	1289.4132	645.2103	11
8	944.0169	472.5121	926.9864	463.9969	926.0016	463.5045	E	*1179.2562*	590.1318	1162.2257	581.6165	1161.2409	581.1241	10
9	1043.1480	522.0777	1026.1175	513.5624	1025.1327	513.0701	V	*1050.1422*	525.5748	1033.1117	517.0595	1032.1269	516.5671	9
10	1190.3219	595.6646	1173.2914	587.1494	1172.3066	586.6570	F	*951.0111*	476.0092	933.9806	467.4940	932.9958	467.0016	8
11	1319.4359	660.2216	1302.4054	651.7064	1301.4206	651.2140	E	*803.8372*	402.4223	786.8067	393.9070	785.8219	393.4146	7
12	1434.5233	717.7653	1417.4928	709.2501	1416.5080	708.7577	D	*674.7212*	337.8653	657.6927	329.3500	656.7079	328.8576	6
13	1505.6012	753.3043	1488.5707	744.7890	1487.5859	744.2967	A	*559.6358*	280.3216	542.6053	271.8063	541.6205	271.3139	5
14	1576.6791	788.8432	1559.6486	780.3280	1558.6638	779.8356	A	488.5579	244.7826	471.5274	236.2674	470.5426	235.7750	4
15	1705.7931	853.4002	1688.7626	844.8850	1687.7778	844.3926	E	417.4800	209.2437	400.4495	200.7284	399.4647	200.2360	3
16	1818.9507	909.9790	1801.9202	901.4638	1800.9354	900.9714	I	288.3660	144.6867	271.3355	136.1714			2
17							R	175.2084	88.1079	158.1779	79.5926			1

g **Peptide: ALELTGLK Found In: NUCL HUMAN, Nucleolin OS=Homo sapiens GN=NCL**

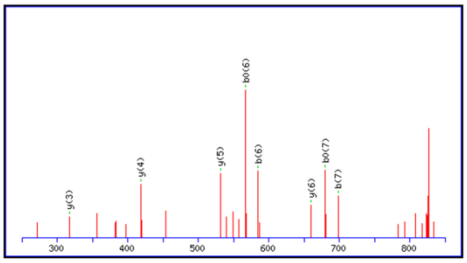

Average mass of neutral peptide Mr(calc): 844.0074
Ions Score: 34 **Expect:** 0.15
Matches : 8/30 fragment ions using 12 most intense peaks (help)

#	b	b^0	Seq.	y	y^*	y^0	#
1	72.0853		A				8
2	185.2429		L	773.9370	756.9065	755.9217	7
3	314.3569	296.3416	E	*660.7794*	643.7489	642.7641	6
4	427.5145	409.4992	L	*531.6654*	514.6349	513.6501	5
5	528.6184	510.6031	T	*418.5078*	401.4773	400.4925	4
6	*585.6697*	567.6544	G	*317.4039*	300.3734		3
7	*698.8273*	680.8120	L	260.3526	243.3221		2
8			K	147.1950	130.1645		1

h **Peptide: ATFIKVPQNQNGK Found In: NUCL HUMAN, Nucleolin OS=Homo sapiens GN=NCL**

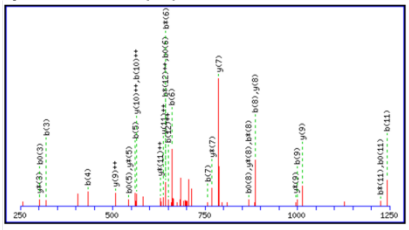

Average mass of neutral peptide Mr(calc): 1444.6344
Ions Score: 50 **Expect:** 0.0035
Matches : 31/112 fragment ions using 49 most intense peaks (help)

#	b	b^{++}	b^*	b^{*++}	b^0	b^{0++}	Seq.	y	y^{++}	y^*	y^{*++}	y^0	y^{0++}	#
1	72.0853	36.5463					A							13
2	173.1892	87.0983			155.1739	78.0907	T	1374.5639	687.7856	1357.5334	679.2704	1356.5486	678.7780	12
3	*320.3631*	160.6852			302.3478	151.6776	F	1273.4600	637.2337	1256.4295	628.7184			11
4	*433.5207*	217.2640			415.5054	208.2564	I	1126.2861	563.6467	1109.2556	555.1315			10
5	*561.6930*	281.3502	544.6625	272.8349	543.6777	272.3426	K	1013.1285	507.0679	996.0980	498.5527			9
6	*660.8241*	330.9157	643.7936	322.4005	642.8088	321.9081	V	884.9562	442.9818	867.9257	434.4665			8
7	*757.9393*	379.4733	740.9088	370.9581	739.9240	370.4657	P	785.8251	393.4162	768.7946	384.9010			7
8	*886.0685*	443.5379	869.0380	435.0227	868.0532	434.5303	Q	688.7099	344.8586	671.6794	336.3434			6
9	*1000.1711*	500.5892	983.1406	492.0740	982.1558	491.5816	N	560.5807	280.7940	543.5502	272.2788			5
10	1128.3003	564.6538	1111.2698	556.1386	1110.2850	555.6462	Q	446.4781	223.7427	429.4476	215.2275			4
11	*1242.4029*	621.7051	1225.3724	613.1899	1224.3876	612.6975	N	318.3489	159.6781	301.3184	151.1629			3
12	1299.4542	650.2308	1282.4237	641.7155	1281.4389	641.2232	G	204.2463	102.6268	187.2158	94.1116			2
13							K	147.1950	74.1012	130.1645	65.5859			1

i

Peptide: ATFIKVPQNQNGK Found In: NUCL_HUMAN, Nucleolin OS=Homo sapiens GN=NCL

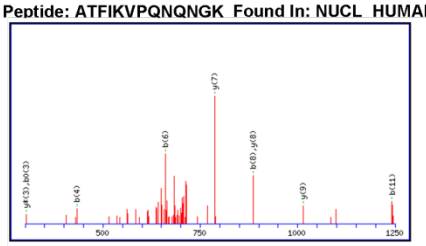

Average mass of neutral peptide Mr(calc): 1444.6344
Ions Score: 29 **Expect:** 0.45
Matches : 9/112 fragment ions using 8 most intense peaks (help)

#	b	b++	b*	b*++	b0	b0++	Seq.	y	y++	y*	y*++	y0	y0++	#
1	72.0853	36.5463					A							13
2	173.1892	87.0983			155.1739	78.0907	T	1374.5639	687.7856	1357.5334	679.2704	1356.5486	678.7780	12
3	320.3631	160.6852			302.3478	151.6776	F	1273.4600	637.2337	1256.4295	628.7184			11
4	*433.5207*	217.2640			415.5054	208.2564	I	1126.2861	563.6467	1109.2556	555.1315			10
5	561.6930	281.3502	544.6625	272.8349	543.6777	272.3426	K	1013.1285	507.0679	996.0980	498.5527			9
6	*660.8241*	330.9157	643.7936	322.4005	642.8088	321.9081	V	884.9562	442.9818	867.9257	434.4665			8
7	757.9393	379.4733	740.9088	370.9581	739.9240	370.4657	P	785.8251	393.4162	768.7946	384.9010			7
8	*886.0685*	443.5379	869.0380	435.0227	868.0532	434.5303	Q	688.7099	344.8586	671.6794	336.3434			6
9	1000.1711	500.5892	983.1406	492.0740	982.1558	491.5816	N	560.5807	280.7940	543.5502	272.2788			5
10	1128.3003	564.6538	1111.2698	556.1386	1110.2850	555.6462	Q	446.4781	223.7427	429.4476	215.2275			4
11	*1242.4029*	621.7051	1225.3724	613.1899	1224.3876	612.6975	N	318.3489	159.6781	301.3184	151.1629			3
12	1299.4542	650.2308	1282.4237	641.7155	1281.4389	641.2232	G	204.2463	102.6268	187.2158	94.1116			2
13							K	147.1950	74.1012	130.1645	65.5859			1

Peptide:GFGFVDFNSEEDAK Found In: NUCL_HUMAN, Nucleolin OS=Homo sapiens GN=NCL

j.

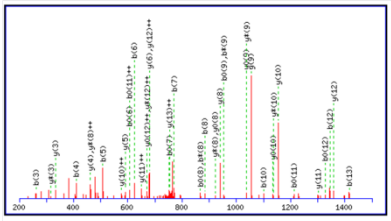

Average mass of neutral peptide Mr(calc): 1561.6036
Ions Score: 64 **Expect:** 0.00012
Matches : 41/128 fragment ions using 78 most intense peaks (help)

#	b	b++	b*	b*++	b0	b0++	Seq.	y	y++	y*	y*++	y0	y0++	#
1	58.0587	29.5330					G							14
2	205.2326	103.1200					F	1505.5597	753.2835	1488.5292	744.7683	1487.5444	744.2759	13
3	*262.2839*	131.6456					G	*1358.3858*	679.6966	1341.3553	671.1813	1340.3705	670.6889	12
4	*409.4578*	205.2326					F	*1301.3345*	651.1709	1284.3040	642.6557	1283.3192	642.1633	11
5	*508.5889*	254.7981					V	*1154.1606*	577.5840	1137.1301	569.0687	1136.1453	568.5763	10
6	*623.6763*	312.3418			605.6610	303.3342	D	*1055.0295*	528.0184	1037.9990	519.5032	1037.0142	519.0108	9
7	*770.8502*	385.9288			752.8349	376.9212	F	*939.9421*	470.4747	922.9116	461.9595	921.9268	461.4671	8
8	*884.9528*	442.9801	867.9223	434.4648	866.9375	433.9725	N	792.7682	396.8878	775.7377	388.3725	774.7529	387.8801	7
9	972.0301	486.5187	954.9996	478.0035	954.0148	477.5111	S	*678.6656*	339.8365	661.6351	331.3212	660.6503	330.8288	6
10	*1101.1441*	551.0757	1084.1136	542.5605	1083.1288	542.0681	E	*591.5883*	296.2978	574.5578	287.7826	573.5730	287.2902	5
11	1230.2581	615.6327	1213.2276	607.1175	1212.2428	606.6251	E	*462.4743*	231.7408	445.4438	223.2256	444.4590	222.7332	4
12	*1345.3455*	673.1764	1328.3150	664.6612	1327.3302	664.1688	D	*333.3603*	167.1838	316.3298	158.6686	315.3450	158.1762	3
13	*1416.4234*	708.7154	1399.3929	700.2001	1398.4081	699.7078	A	218.2729	109.6401	201.2424	101.1249			2
14							K	147.1950	74.1012	130.1645	65.5859			1

k

Peptide:GLSEDTTEETLKESFDGSVR Found In: NUCL_HUMAN, Nucleolin OS=Homo sapiens GN=NCL

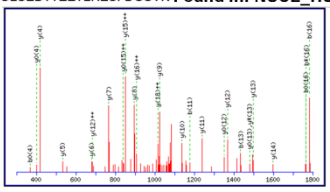

Average mass of neutral peptide Mr(calc): 2200.2704
Ions Score: 70 **Expect:** 2.8e-005
Matches : 26/198 fragment ions using 50 most intense peaks (help)

#	b	b++	b*	b*++	b0	b0++	Seq.	y	y++	y*	y*++	y0	y0++	#
1	58.0587	29.5330					G							20
2	171.2163	86.1118					L	2144.2266	1072.6170	2127.1961	1064.1017	2126.2113	1063.6093	19
3	258.2936	129.6505			240.2783	120.6429	S	2031.0690	1016.0382	2014.0385	1007.5229	2013.0537	1007.0305	18
4	387.4076	194.2075			369.3923	185.1999	E	1943.9917	972.4995	1926.9612	963.9843	1925.9764	963.4919	17
5	502.4950	251.7512			484.4797	242.7436	D	1814.8777	907.9425	1797.8472	899.4273	1796.8624	898.9349	16
6	603.5989	302.3031			585.5836	293.2955	T	1699.7903	850.3988	1682.7598	841.8836	1681.7750	841.3912	15
7	704.7028	352.8551			686.6875	343.8475	T	*1598.6864*	799.8469	1581.6559	791.3316	1580.6711	790.8392	14
8	833.8168	417.4121			815.8015	408.4045	E	*1497.5825*	749.2949	1480.5520	740.7797	1479.5672	740.2873	13
9	962.9308	481.9691			944.9155	472.9615	E	*1368.4685*	684.7379	1351.4380	676.2227	1350.4532	675.7303	12
10	1064.0347	532.5210			1046.0194	523.5134	T	*1239.3545*	620.1809	1222.3240	611.6657	1221.3392	611.1733	11
11	*1177.1923*	589.0998			1159.1770	580.0922	L	*1138.2506*	569.6290	1121.2201	561.1137	1120.2353	560.6213	10
12	1305.3646	653.1860	1288.3341	644.6707	1287.3493	644.1784	K	*1025.0930*	513.0502	1008.0625	504.5349	1007.0777	504.0425	9
13	*1434.4786*	717.7430	1417.4481	709.2277	1416.4633	708.7354	F	*896.9207*	448.9640	879.8902	440.4488	878.9054	439.9564	8
14	1521.5559	761.2816	1504.5254	752.7664	1503.5406	752.2740	S	*767.8067*	384.4070	750.7762	375.8918	749.7914	375.3994	7
15	1668.7298	834.8686	1651.6993	826.3533	1650.7145	825.8610	F	*680.7294*	340.8684	663.6989	332.3531	662.7141	331.8607	6
16	*1783.8172*	892.4123	*1766.7867*	883.8970	*1765.8019*	883.4047	D	*533.5553*	267.2814	516.5250	258.7662	515.5402	258.2738	5
17	1840.8685	920.9379	1823.8380	912.4227	1822.8532	911.9303	G	*418.4681*	209.7377	401.4376	201.2225	400.4528	200.7301	4
18	1927.9458	964.4766	1910.9153	955.9613	1909.9305	955.4690	S	361.4168	181.2121	344.3863	172.6968	343.4015	172.2044	3
19	2027.0769	1014.0421	2010.0464	1005.5269	2009.0616	1005.0345	V	274.3395	137.6734	257.3090	129.1582			2
20							R	175.2084	88.1079	158.1779	79.5926			1

l Peptide: SISLYYTGEK Found In: NUCL_HUMAN, Nucleolin OS=Homo sapiens GN=NCL

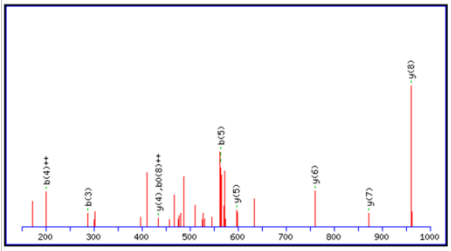

Average mass of neutral peptide Mr(calc): 1160.2731
Ions Score: 26 **Expect:** 0.9
Matches : 10/88 fragment ions using 26 most intense peaks (help)

#	b	b^{++}	b^0	b^{0++}	Seq.	y	y^{++}	y^*	y^{*++}	y^0	y^{0++}	#
1	88.0847	44.5460	70.0694	35.5384	S							10
2	201.2423	101.1248	183.2270	92.1172	I	1074.2033	537.6053	1057.1728	529.0901	1056.1880	528.5977	9
3	288.3196	144.6635	270.3043	135.6559	S	961.0457	481.0265	944.0152	472.5113	943.0304	472.0189	8
4	401.4772	201.2423	383.4619	192.2347	L	873.9684	437.4879	856.9379	428.9726	855.9531	428.4802	7
5	564.6505	282.8289	546.6352	273.8213	Y	760.8108	380.9091	743.7803	372.3938	742.7955	371.9014	6
6	727.8238	364.4156	709.8085	355.4080	Y	597.6375	299.3224	580.6070	290.8072	579.6222	290.3148	5
7	828.9277	414.9675	810.9124	405.9599	T	434.4642	217.7358	417.4337	209.2205	416.4489	208.7281	4
8	885.9790	443.4932	867.9637	434.4856	G	333.3603	167.1838	316.3298	158.6686	315.3450	158.1762	3
9	1015.0930	508.0502	997.0777	499.0426	E	276.3090	138.6582	259.2785	130.1429	258.2937	129.6505	2
10					K	147.1950	74.1012	130.1645	65.5859			1

m Peptide: SISLYYTGEK Found In: NUCL_HUMAN, Nucleolin OS=Homo sapiens GN=NCL

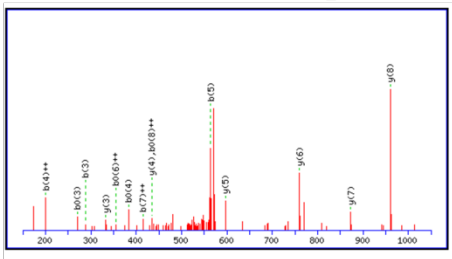

Average mass of neutral peptide Mr(calc): 1160.2731
Ions Score: 43 **Expect:** 0.018
Matches : 15/88 fragment ions using 25 most intense peaks (help)

#	b	b^{++}	b^0	b^{0++}	Seq.	y	y^{++}	y^*	y^{*++}	y^0	y^{0++}	#
1	88.0847	44.5460	70.0694	35.5384	S							10
2	201.2423	101.1248	183.2270	92.1172	I	1074.2033	537.6053	1057.1728	529.0901	1056.1880	528.5977	9
3	288.3196	144.6635	270.3043	135.6559	S	961.0457	481.0265	944.0152	472.5113	943.0304	472.0189	8
4	401.4772	201.2423	383.4619	192.2347	L	873.9684	437.4879	856.9379	428.9726	855.9531	428.4802	7
5	564.6505	282.8289	546.6352	273.8213	Y	760.8108	380.9091	743.7803	372.3938	742.7955	371.9014	6
6	727.8238	364.4156	709.8085	355.4080	Y	597.6375	299.3224	580.6070	290.8072	579.6222	290.3148	5
7	828.9277	414.9675	810.9124	405.9599	T	434.4642	217.7358	417.4337	209.2205	416.4489	208.7281	4
8	885.9790	443.4932	867.9637	434.4856	G	333.3603	167.1838	316.3298	158.6686	315.3450	158.1762	3
9	1015.0930	508.0502	997.0777	499.0426	E	276.3090	138.6582	259.2785	130.1429	258.2937	129.6505	2
10					K	147.1950	74.1012	130.1645	65.5859			1

n

Nucleolin protein sequence: Peptides in **red** found in Fas inhibitor screen in primary tissue

```
  1 MVKLAKAGKN QGDPKKMAPP PKEVEEDSED EEMSEDEEDD SSGEEVVIPQ
 51 KKGKKAAATS AKKVVVSPTK KVAVATPAKK AAVTPGKKAA ATPAKKTVTP
101 AKAVTTPGKK GATPGKALVA TPGKKGAAIP AKGAKNGKNA KKEDSDEEED
151 DDSEEDEEDD EDEDEDEDEI EPAAMKAAAA APASEDEDDE DDEDDEDDDD
201 DEEDDSEEEA METTPAKGKK AAKVVPVKAK NVAEDEDEEE DDEDEDDDDD
251 EDDEDDDDED DEEEEEEEEE EPVKEAPGKR KKEMAKQKAA PEAKKQKVEG
301 TEPTTAFNLF VGNLNFNKSA PELKTGISDV FAKNDLAVVD VRIGMTRKFG
351 YVDFESAEDL EKALELTGLK VFGNEIKLEK PKGKDSKKER DARTLLAKNL
401 PYKVTQDELK EVFEDAAEIR LVSKDGKSKG IAYIEFKTEA DAEKTFEEKQ
451 GTEIDGRSIS LYYTGEKGQN QDYRGGKNST WSGESKTLVL SNLSYSATEE
501 TLQEVFEKAT FIKVPQNQNG KSKGYAFIEF ASFEDAKEAL NSCNKREIEG
551 RAIRLELQGP RGSPNARSQP SKTLFVKGLS EDTTEETLKE SFDGSVRARI
601 VTDRETGSSK GFGFVDFNSE EDAKAAKEAM EDGEIDGNKV TLDWAKPKGE
651 GGFGGRGGGR GGFGGRGGGR GGRGGFGGRG RGGFGGRGGF RGGRGGGGDH
701 KPQGKKTKFE
```

Figure 3: Nucleolin Binds Activation-Resistant Fas.

(a) Schematic of activation-resistant Fas isolation process. (b) Silver-stained gel separating primary NHL and BJAB samples subjected to Fas activation with subsequent IP with agonistic antibody CH-11 (CH-11 Lanes). The remaining lysates were subjected to a second Fas IP (B-10) of any remaining activation-resistant Fas. (B-10 Lane) (b) Specific activation-resistant Fas bands from a silver stain gel were excised, trypsin digested, and analyzed by nanoflow-LC-MS/MS fragmentation by a CID spectra profiling. A 100 kDa band of interest (asterisk) represents the protein that is the focus of the current study. (c-m) Eleven fragmentation spectra profiles and the fragmentation ions of the peptides produced by the tryptic digestion and CID of the 100 kDa band; the spectra profiles match to known nucleolin peptides through MASCOT. (n) The protein sequence of nucleolin. The peptides in red font represent peptides from the 100 kDa band identified by nanoflow-LC-MS/MS. The peptides map to the RBD's in the C-terminal region of nucleolin.

Nucleolin Forms a Complex with Fas in B-cell Lymphomas

To confirm the formation of nucleolin-Fas complexes in B-cell lymphomas, we subjected lymphoma cell lines, a monocytic-like histocytic lymphoma line and two healthy B-cell samples (CD19-positive isolated cells from healthy donors) to Fas IP and detection of nucleolin (coimmunoprecipitation (coIP)) (Figure 4a). The U937 cell line was used because of previous work showing expression of surface nucleolin. Nucleolin represents 5% of non-DNA-associated protein in the nucleus (296), therefore, we hypothesized that Fas is the limiting factor in our assay, which is implicated by of our analysis of a Fas IP followed by nucleolin immunoblotting (IB) versus the reciprocal. The nucleolin-Fas complex was detected in all B-cell lymphoma cell lines, but was absent in the histocytic lymphoma and B lymphocytes. Detection of nucleolin results in a 105, 80, 70 kDa pattern due to autodegradation of the N-terminal domain. (176, 179) Fas protein is detected in a double or triple staining pattern due to protein glycosylation and sialylation. A repeated IP with increased numbers of healthy B lymphocytes, to increase Fas IP, confirmed a lack of nucleolin-Fas association in B lymphocytes (Figure 4b). Next, to confirm the complex formation exists in primary B-cell lymphomas, we performed a Fas-nucleolin coIP analysis on ten primary samples to test for presence of the complex. Two primary lymphoma samples, a DLBCL and MCL, yielded a nucleolin-Fas complex (Figure 4c-d).

Figure 4

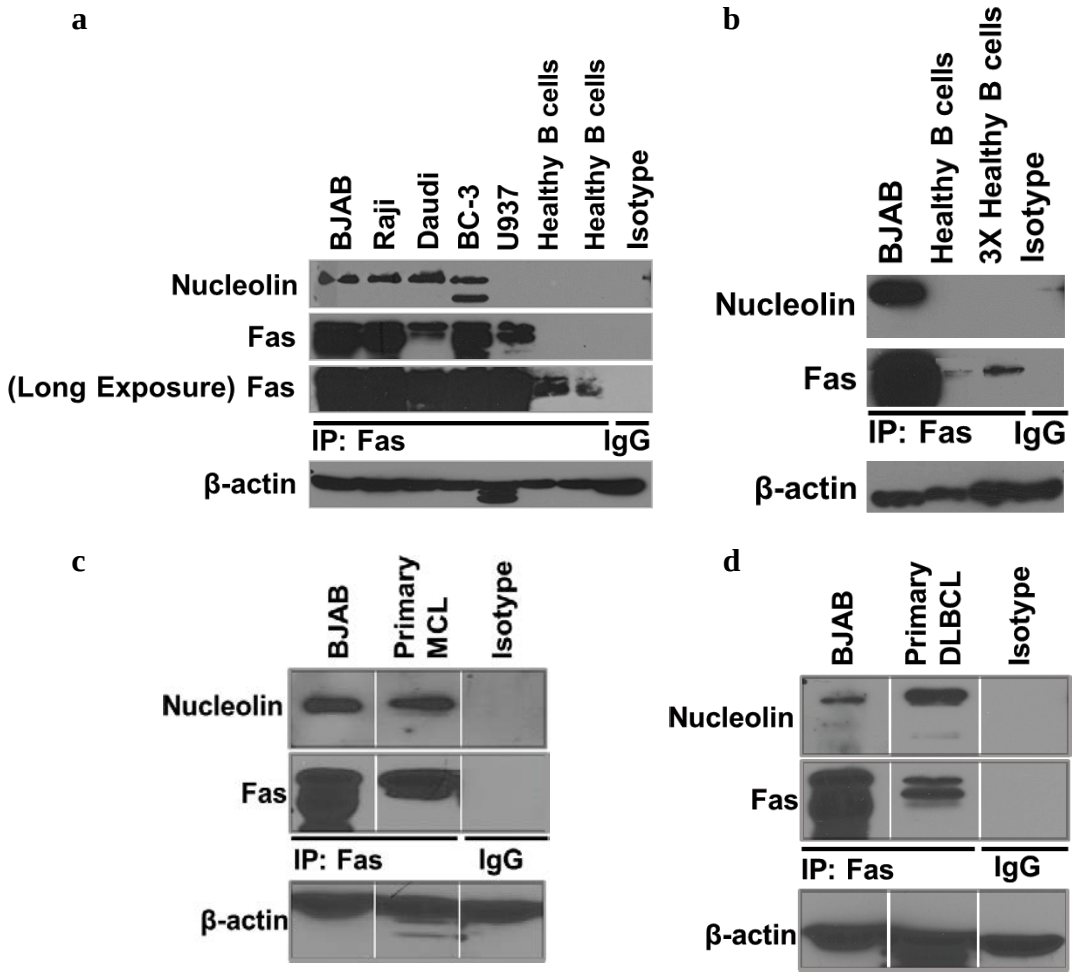
a
BJAB
Raji
Daudi
BC-3
U937
Healthy B cells
Healthy B cells
Isotype
Nucleolin
Fas
(Long Exposure) Fas
IP: Fas
IgG
β-actin
b
BJAB
Healthy B cells
3X Healthy B cells
Isotype
Nucleolin
Fas
IP: Fas
IgG
β-actin
c
BJAB
Primary MCL
Isotype
Nucleolin
Fas
IP: Fas
IgG
β-actin
d
BJAB
Primary DLBCL
Isotype
Nucleolin
Fas
IP: Fas
IgG
β-actin

Figure 4: Nucleolin Interacts with Fas in B-cell lymphoma Cell Lines and B-cell Lymphoma Primary Samples.

(a) Whole-cell extracts from BJAB, Raji, Daudi, BC-3, and U937 cell lines and two B-lymphocyte isolations from healthy donors were subjected to IP with anti-Fas agarose and analyzed by IB for the presence of nucleolin. Representative data from three different experiments are shown. (b) Healthy donor B cells, with an increased cell number and protein loading, were re-subjected to Fas IP followed by Fas and nucleolin IB. The expression level of nucleolin and β-actin in whole-cell extracts are shown by western blot in the lower panels-input control. (c-d) Shown is analysis of two primary lymphoma samples (MCL and DLBCL) demonstrating nucleolin-Fas complex from a screen of four DLBCL and six MCL primary samples. Extracts were immunoprecipitated with Fas agarose and analyzed by IB for the presence of nucleolin in precipitated complexes. BJAB cells and isotype IP were used as positive and negative controls, respectively; β-actin was used as a loading control.

The RNA-binding Domain 4 and Glycine/arginine Rich Domain of Nucleolin are Required for Fas Binding

Nucleolin consists of 6 domains, the N-terminal domain, 4 RBDs, and a GAR domain (Figure 5a). To identify the domain responsible for interaction with Fas, we created various single- and multi-domain DDK-tagged deletion constructs of nucleolin (Figure 5b and Appendix A Figure 26). DDK-tagged mutants, transiently expressed in human embryonic kidney (HEK) cells, subjected to coIP of Fas and nucleolin (Figure 5c) showed that the interaction of nucleolin with Fas was ablated with the deletion of the GAR domain (as represented by the lack of detection in the NR1234 lane). Binding of full-length nucleolin and nucleolin domains R34GAR and R4GAR was detected, yet absent in all other nucleolin domain proteins. The shortest nucleolin mutant protein capable of binding to Fas consisted of the R4 and GAR domains. However, neither GAR alone nor domains consisting of R4 without GAR were found in complex with Fas, suggesting that both the GAR and RBD 4 are necessary for the interaction.

The Nucleolin-Fas Complex Exists Selectively on the Surface of B-cell Lymphomas

To assess the localization of the nucleolin-Fas complex within the cell, we analyzed BJAB cells, NHL tissue, and healthy donor peripheral blood mononuclear cells (PBMCs) by confocal fluorescence microscopy. Fas and nucleolin co-localized on the surface of BJAB cells and NHL cells (Figure 6a-b), whereas intracellular staining revealed no complex inside the cells (Figure 7a-b). PBMCs showed no detectable Fas-nucleolin complex formation (Figure 6c, Figure 7c). Results suggest that the nucleolin-Fas complex exists selectively on the surface of B-cell lymphomas. To confirm their surface interaction, we incubated recombinant nucleolin with the extracellular portion of Fas fused to a chimeric Fc fragment. An IP of the Fc fragment showed a dose-dependent binding of nucleolin (Figure 8), confirming a direct interaction between nucleolin and the extracellular domain of Fas.

Figure 5

a

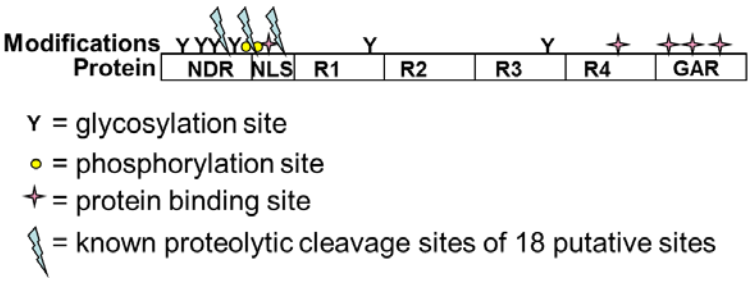
Modifications
Protein
NDR
NLS
R1
R2
R3
R4
GAR
Y = glycosylation site
= phosphorylation site
= protein binding site
= known proteolytic cleavage sites of 18 putative sites

b

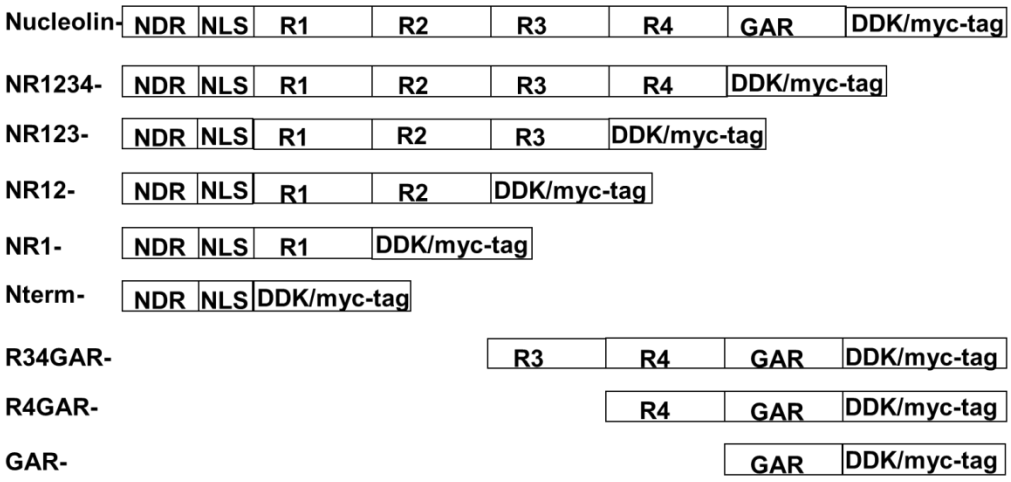
DDK-myc tagged PCMV-ENTRY Nucleolin Domain Constructs
Nucleolin-
NR1234-
NR123-
NR12-
NR1-
Nterm-
R34GAR-
R4GAR-
GAR-
NDR
NLS
R1
R2
R3
R4
GAR
DDK/myc-tag

c

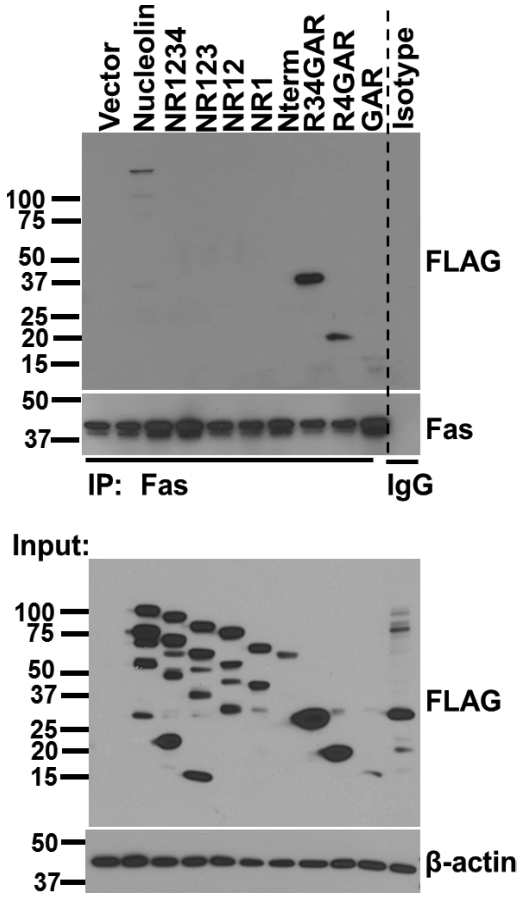
Vector
Nucleolin
NR1234
NR123
NR12
NR1
Nterm
R34GAR
R4GAR
GAR
Isotype
100
75
50
37
25
20
15
FLAG
Fas
IP: Fas
IgG
Input:
β-actin

Figure 5: Nucleolin's R4 and GAR Domains are Necessary for its Interaction with Fas.

(a) Schematic of the nucleolin domains and their known modifications: NDR (N-terminal domain region), NLS (nuclear localization signal), R 1-4 (RBD's 1-4), and GAR (glycine/arginine rich C-terminal domain). Glycosylation sites are represented by Y, phosphorylation sites by yellow circles, protein-binding sites by stars, and 3 defined proteolytic cleavage sites (of a potential 18 putative sites) by a blue lightning bolt. (b) Domain deletions were created by using the Stratagene Quick Change II XL mutagenesis kit using C-terminal DDK/myc-tagged PCMV-ENTRY construct of full-length nucleolin (Origene) as a template. (c) 293T HEK cells were transfected with the indicated nucleolin domain deletion mutants and lysed for IP/IB analysis. Whole-cell lysates were subjected to Fas IP with anti-Fas agarose. Proteins were separated and immunoblotted for detection of co-precipitated domain mutants with an anti-DDK- horseradish peroxidase (HRP) antibody. A mixture of all domain mutants was precipitated with mouse IgG and protein G agarose as a negative control. Whole-cell lysate samples prior to IP were immunoblotted with anti-DDK-HRP to reveal expression levels of the transfected constructs -input control. Representative data from three different experiments are shown.

Figure 6

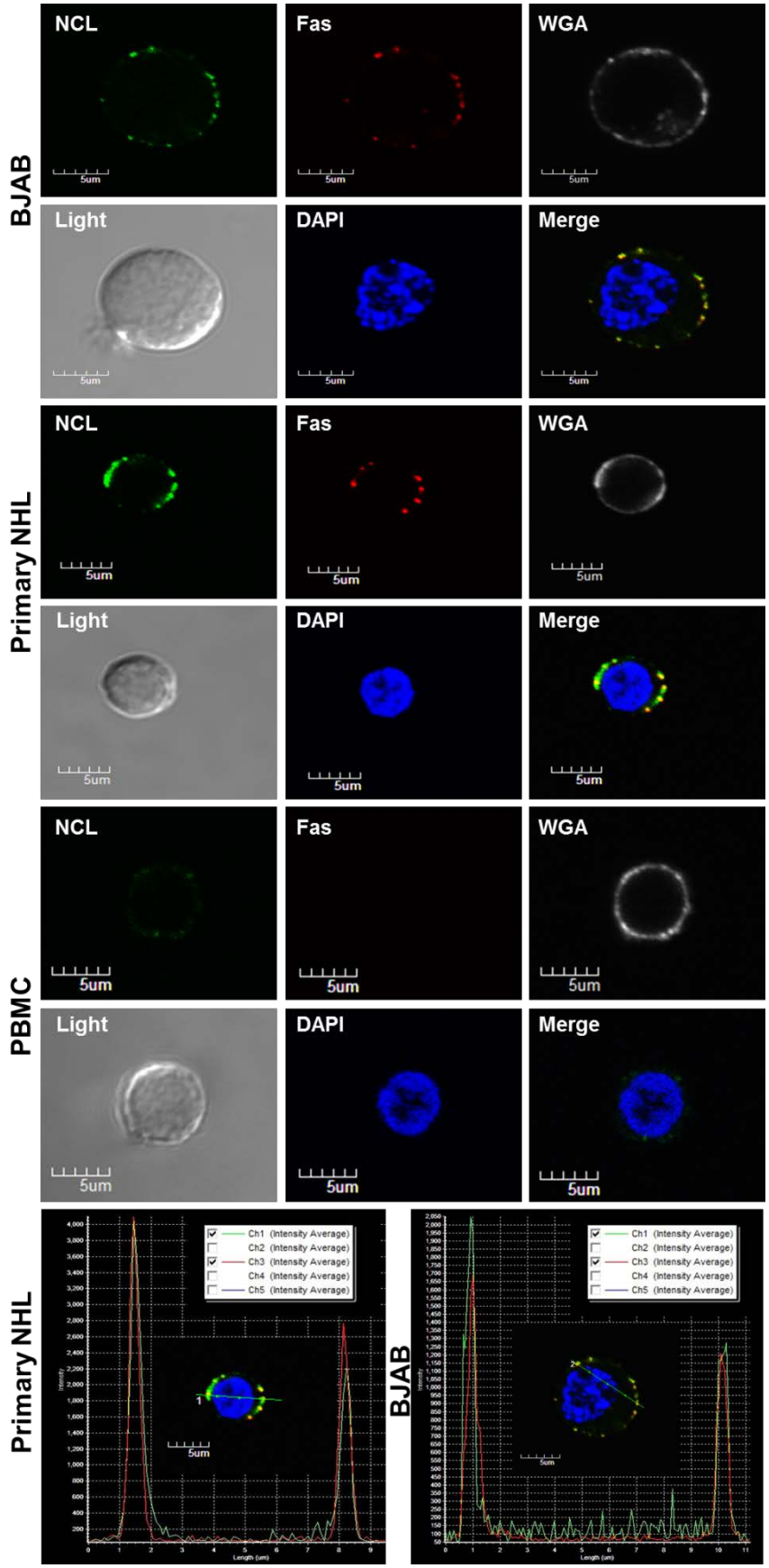
a
BJAB
NCL
Fas
WGA
Light
DAPI
Merge
b
Primary NHL
NCL
Fas
WGA
Light
DAPI
Merge
c
PBMC
NCL
Fas
WGA
Light
DAPI
Merge
d
Primary NHL
BJAB
Ch1 (Intensity Average)
Ch2 (Intensity Average)
Ch3 (Intensity Average)
Ch4 (Intensity Average)
Ch5 (Intensity Average)
5um

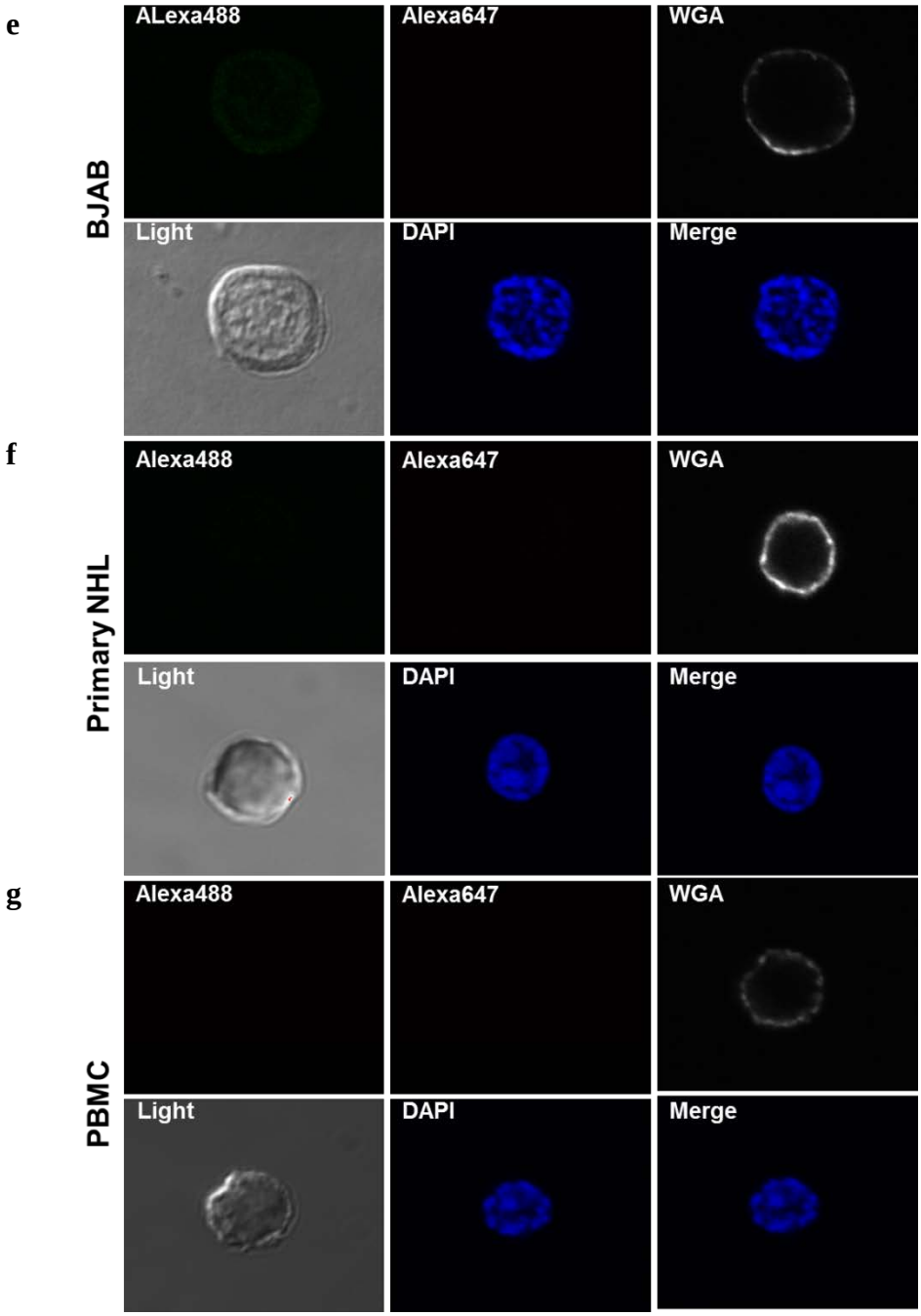
e
ALexa488
Alexa647
WGA
BJAB
Light
DAPI
Merge
f
Alexa488
Alexa647
WGA
Primary NHL
Light
DAPI
Merge
g
Alexa488
Alexa647
WGA
PBMC
Light
DAPI
Merge

Figure 6: Nucleolin Associates with Fas on the Surface of B-cell Lymphoma Cells.

BJAB cells (a), NHL primary tissue (b) and PBMCs (c) were incubated with an anti-nucleolin antibody (MS-3), anti-Fas antibody (Abcam), and respective secondary antibodies stepwise at 4°C. Subsequent incubation with wheat germ agglutinin (WGA) alexa555 was followed by mounting with prolong gold anti-fade reagent containing 4',6-diamidino-2-phenylindole (DAPI) and examination by confocal microscopy. The images were captured by the Nikon A1R confocal laser microscope system (Nikon Instruments). All images were acquired at similar voltages for Channel 1 (488nm) 620V and Channel 3 (647nm) 510V. An aberration corrected objective (Paplon 1:40) and Nomarski prism for Brightfield DIC image was used for acquiring images. Original image size 1024×1024 with clip size of 302×280. Powerpoint was used for further image processing; all panels were adjusted for brightness at correction 44. Top panels (left to right): nucleolin staining on the surface of BJAB cells (green), Fas staining on the surface of BJAB cells (red), WGA revealing surface sialic acid-modified proteins (white) as a control for extracellular membrane localization. Bottom panels (left to right): Brightfield image revealing whole cell structure, DAPI nuclear stain (blue), merged/overlaid images of nucleolin, Fas and DAPI. Note an almost a complete colocalization of Fas and nucleolin throughout the surface of BJAB and primary NHL cells (yellow) and no co-localization on the surface of a healthy lymphocyte largely because of a lack of surface Fas and low levels of nucleolin. We selected a healthy PBMC that had some positive nucleolin staining as an example. Two of 15 B lymphocytes from healthy donors, scanned by flow cytometry for surface nucleolin, identified a small shift in staining median fluorescence intensity (MFI) (data not shown) (d) Intensity profile and Pearson coefficient analysis for colocalization, revealing positive co-localized staining of Fas and nucleolin in BJAB cells (merged image from A). (e-g) Isotype staining of BJABs, NHL primary tissue, and PBMCs following the same procedure showed little to no non-specific staining.

Figure 7

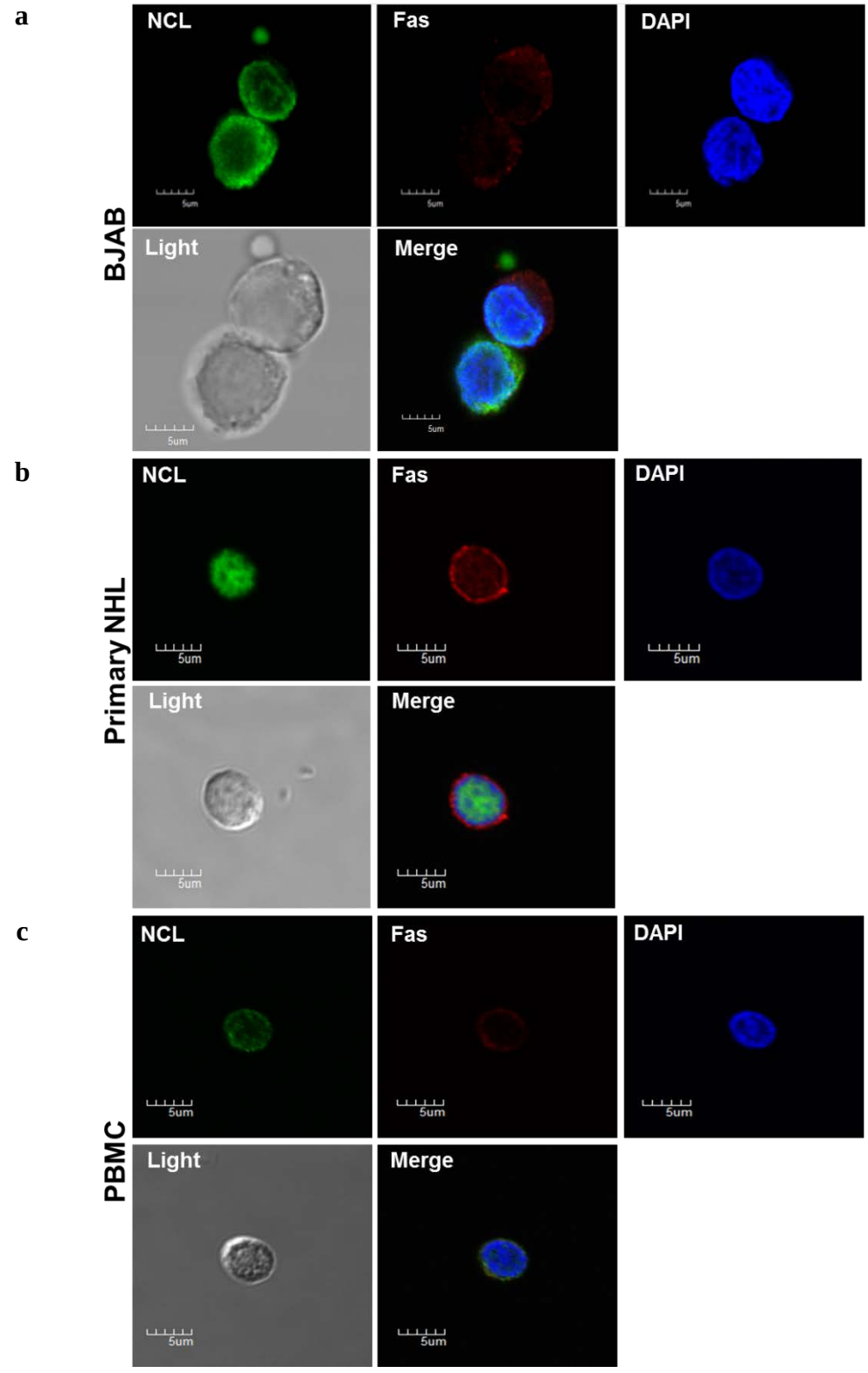
a
BJAB
NCL
Fas
DAPI
Light
Merge
b
Primary NHL
NCL
Fas
DAPI
Light
Merge
c
PBMC
NCL
Fas
DAPI
Light
Merge
5um

Figure 7: Nucleolin and Fas do not Colocalize in the Intracellular Compartments in B cells.

Fixed and permeabilized BJAB cells (a), primary NHL tissue (b) and PBMCs (c) were incubated with an anti-nucleolin antibody (MS-3), anti-Fas antibody (Abcam), and respective secondary antibodies stepwise at 4°C. Subsequent mounting with prolong gold anti-fade reagent containing DAPI was followed by examination by confocal microscopy. BJAB cells, top panels (left to right): nucleolin staining (green), Fas staining (red), DAPI nuclear stain (blue). Bottom panels (left to right): Brightfield image revealing whole cell structure, merged/overlaid images of nucleolin, Fas, and DAPI; note a faint Fas cytoplasmic staining and nucleolin nuclear and nuclear/cytoplasmic staining in the two BJAB cells yet a lack of co-localization. Overall, there was a much lower signal of Fas (cytoplasmic) and nucleolin (nuclear) in PBMCs than primary NHL and BJAB cells.

Figure 8

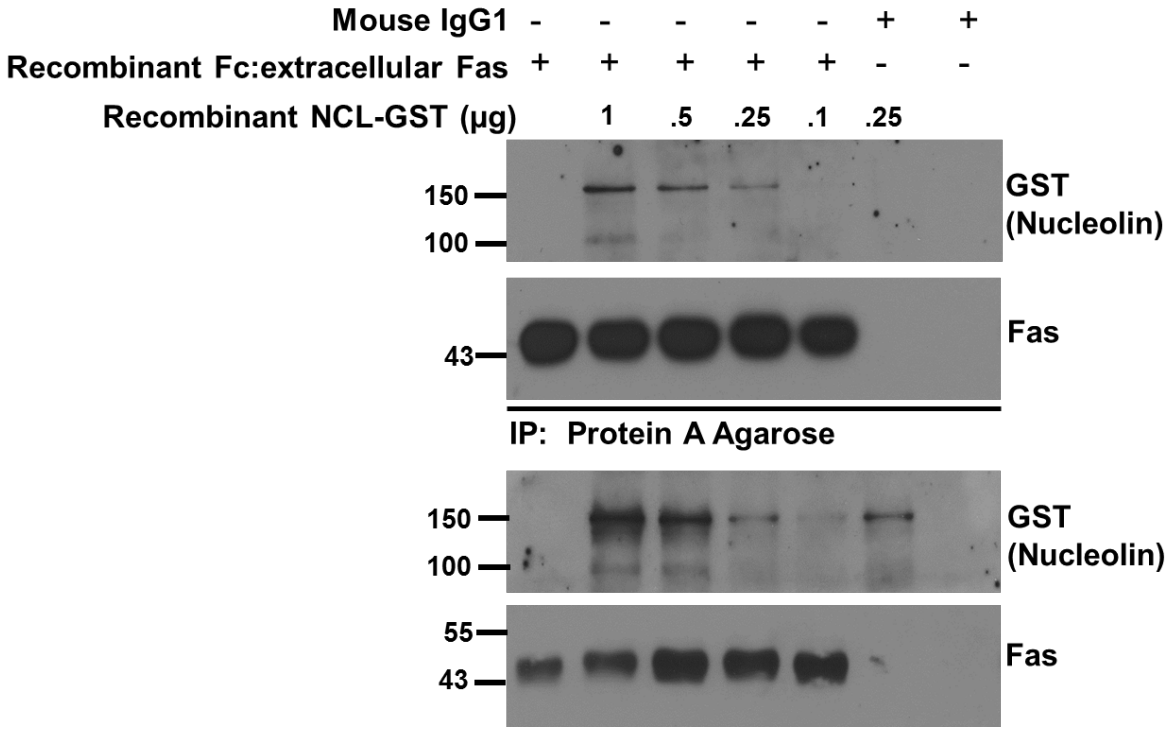

Figure 8: Nucleolin Binds to the Extracellular Portion of Fas Directly.

A chimeric Fc:Fas (extracellular domain of Fas fused to the two heavy domains of the constant region of an antibody) was incubated with varying concentrations of recombinant nucleolin-GST for 1.5 hours at 4°C. Fc:Fas was immunoprecipitated with protein A overnight and precipitates were separated by SDS-PAGE gel electrophoresis. In Western blots nucleolin (NCL)-GST was found in Fas-precipitated complexes in a dose-dependent manner. Lower panels of GST and Fas IP represent input controls.

Summary

In this study, we designed and performed a screening process for the identification of novel activation-resistant Fas binding partners (Figure 3a) and identified nucleolin as found in complex with activation-resistant Fas. We were able to confirm the presence of nucleolin-Fas complexes in B-cell lymphomas and a lack of the complex in healthy donor B cells (Figure 4a-d). Our initial analyses deserved further investigation due to the low Fas expression in the healthy donor B cells. In order to confirm that healthy B cells are void of nucleolin-Fas complex, the coIP of nucleolin-Fas was repeated with increased protein amounts. Analysis showed that even with the increase of Fas utilized for coIP, there was an absence of nucleolin-Fas complex, thereby confirming that the nucleolin-Fas complex is a complex of lymphoma cells (Figure 4b). We further examined the presence of nucleolin-Fas complexes by screening multiple primary lymphoma samples by coIP. We were able to detect a nucleolin-Fas interaction in four of ten primary samples tested (Figure 4c-d). The absence of nucleolin-Fas complex in the remaining samples may be explained by either low Fas expression, sensitivity of the assay, the heterogeneity of tumors, or potentially a lack of utilizing nucleolin for Fas inhibition in a particular tumor, as this may be an adapted phenotype of tumors that may not be used consistently. As not all properties of cells that are observed in cell culture, will be observed in the clinical or in vivo setting, we examined human tissue and the nucleolin-Fas complex is present in primary lymphomas. These results suggest that the nucleolin-Fas complex formation is present in B-cell lymphomas, confirming and expanding the results from our initial Fas inhibitor screening process.

We further clarified the nucleolin-Fas association by mapping the Fas interacting domain of nucleolin to the R4-GAR domain (Figure 5c). Signaling through Fas, in type I cells, is initiated at the plasma membrane, and it depends on lipid raft formation and receptor internalization. Fas is transported to the surface through the classical secretory pathway involving the ER and the Golgi apparatus. Trafficking of nucleolin is still elusive; it by-passes the classical pathway and seems to involve an actin-dependent trafficking mechanism.(178, 299) The different mechanisms of cell surface transport of nucleolin and Fas should limit their interaction within the cell, and most cell complexes should reflect cell surface nucleolin-Fas complexes. Thus, we used confocal microscopy and an in vitro binding assay with the extracellular portion of Fas to detect nucleolin-Fas complexes (Figure 6, Figure 7, Figure 8). We observed that the nucleolin-Fas complexes exist on the extracellular surface of B-cell lymphomas and are absent in healthy donor PBMC's, as determined by confocal microscopy of BJAB cells, primary NHL tissue, and healthy donor PBMCs. CoIP of recombinant extracellular Fas protein and recombinant nucleolin in solution determined that

nucleolin interacts with the extracellular Fas protein and showed a direct binding of Fas and nucleolin (Figure 8). In conclusion, we determined that nucleolin binds Fas through its R4-GAR domain on the extracellular surface of B-cell lymphomas but not in healthy donor PBMC.

Limitations and Future Directions

Our results could be further strengthened by the selective overexpression of surface nucleolin as a tool to study nucleolin's surface function in B-cell lymphomas. For over 20 years we have known that nucleolin is transported to the surfaces of tumor cells. Yet, the mechanism of transporting and tethering nucleolin on the cell surface still remains elusive. In order to perform functional studies of nucleolin interactions on cell surface, we will first need to know more about its transport and adhesion to cell surface. After this information becomes available, studies can be done to map interactions with properly delivered mutants to the cells surface and better characterize its interactions with Fas.(178, 216)

Despite the limitations, taken together, the provided experimental evidences indicate nucleolin as a novel surface binding partner of Fas in B-cell lymphomas. The specificity of surface nucleolin and nucleolin-Fas complex formation in B-cell lymphomas compared to healthy B cells suggests an acquired function of nucleolin in the survival of lymphomas, and led us to investigate its role in protection against Fas-mediated apoptosis.

Chapter 4: Nucleolin's Regulation of Fas-mediated Apoptosis

Rationale

Fas is present on the surface of multiple B-cell lymphomas, often without mutations, yet unable to signal, suggesting it is subjected to regulation. The formation of Fas-nucleolin complexes selectively in B-cell lymphomas suggests an acquired/adapted regulation in cancer cells. In order to determine if nucleolin-Fas complexes modulate Fas-mediated apoptosis, we set out to determine the effects of nucleolin levels and the presence of nucleolin-Fas complexes on Fas signaling and to clarify a potential mechanism of Fas modulation by creating nucleolin partial knockdown B-cell lymphoma cell lines. BJAB's were selected for these experiments because they exhibited overexpression of nucleolin compared to healthy donor B cells, surface nucleolin expression, decreased Fas sensitivity, absence of Fas mutations, and nucleolin-Fas complex formation without an EBV infection.(300) Also, BJABs undergo mainly type I Fas signaling (67), are Bcl-2, Bcl-xl, Mcl-1, and *bcl-2, bcl-xl and mcl-1* negative, making them an applicable model for studying nucleolin and Fas interaction for B-cell lymphomas (300) (Figure 9e), as nucleolin has been reported to stabilize bcl-2 mRNA.(227, 245) Through the use of nucleolin partial knockdowns and an in vivo mouse overexpression model we pursued the elucidation of the molecular mechanism behind Fas's inability to signal, despite adequate expression levels, with the motivation of contributing to a more complete understanding of the mechanisms of chemoresistance in lymphomas.

Results

Partial Knockdown of Nucleolin Expression Results in Ablation of Surface Expression and Nucleolin-Fas Complex Formation

We used a small/short hairpin RNA (shRNA) micro ribonucleic acid (miR)30 construct to stably reduce the level of nucleolin in BJAB cells. We created a pooled partial knock-down (pKO) BJAB cell line (906P1) and four single-cell clones (906S1, -S2, -S4 and -S5) (Figure 9a-b). We observed at least a 50% suppression of nucleolin compared with the parental and non-silencing BJAB cells (controls) by IB and mRNA analysis (Figure 9b-d). We confirmed the lack of Bcl-2 expression in parental BJAB and shRNAmiR30 transfected BJAB cells (Figure 9e). Biotinylation of surface proteins showed an absence of surface nucleolin in pKO clones compared with controls (Figure 9f).

Further analysis confirmed ablation of the nucleolin-Fas complex formation in the nucleolin pKOs (Figure 9g).

Figure 9

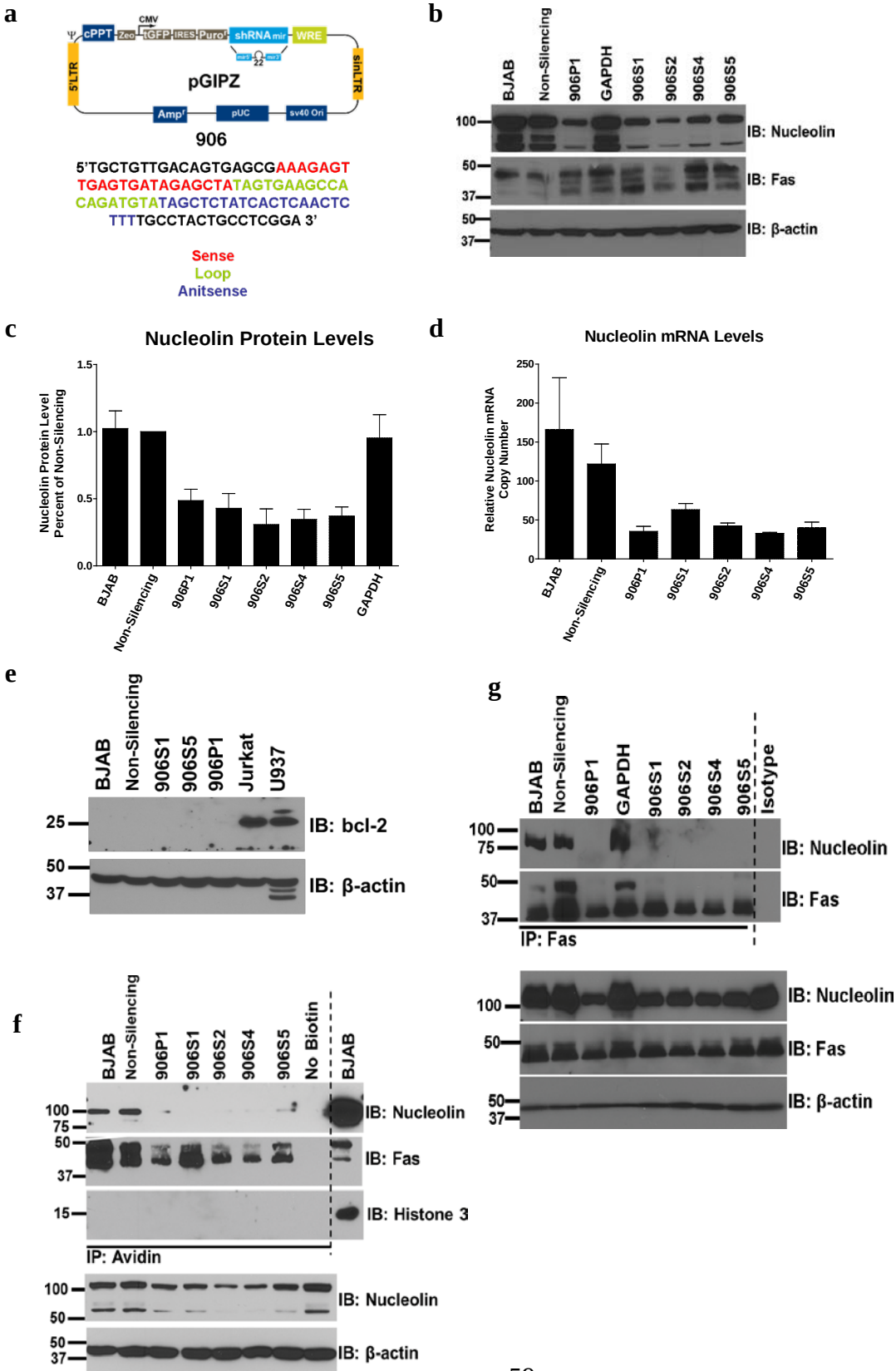
a
cPPT
CMV
Zeo
GFP
IRES
Puro
shRNA mir
WRE
5'LTR
3'sinLTR
pGIPZ
Amp
pUC
sv40 Ori
906
5'TGCTGTTGACAGTGAGCGAAAGAGT
TGAGTGATAGAGCTATAGTGAAGCCA
CAGATGTATAGCTCTATCACTCAACTC
TTTTGCCTACTGCCTCGGA 3'
Sense
Loop
Anitsense
b
BJAB
Non-Silencing
906P1
GAPDH
906S1
906S2
906S4
906S5
IB: Nucleolin
IB: Fas
IB: β-actin
c
Nucleolin Protein Levels
Nucleolin Protein Level
Percent of Non-Silencing
d
Nucleolin mRNA Levels
Relative Nucleolin mRNA
Copy Number
e
IB: bcl-2
IB: β-actin
Jurkat
U937
f
No Biotin
IB: Histone 3
IP: Avidin
g
Isotype
IP: Fas

Figure 9: Creation and Characterization of Nucleolin Partial Knockdown BJAB Cells.

(a) Nucleolin-specific (906), control non-targeting (non-silencing), and a glyceraldehyde 3-phosphate dehydrogenase (GAPDH) targeting shRNAmiR30 constructs were used for transfection of BJAB cells to create a pooled non-silencing (NS) control, GAPDH control, and nucleolin pKO (906P1) cell line. Four single-cell clones (906S1, -S2, -S4, -S5) were derived from the original pooled cell line 906P1. (b) Whole-cell lysates were analyzed by IB for nucleolin and Fas protein expression. β-actin was used as a loading control. (c) Densitometry analysis showed a minimum of 50% knock-down of nucleolin in the pKO cells compared with parental BJAB cells, non-silencing and GAPDH controls (906P1: $P< .026$; 906S1: $P< 035$; 906S2: $P< 027$; 906S4: $P< .013$; 906S5: $P< .0114$) Mean data and standard error of the mean (SEM) of three independent experiments are shown. (d) Nucleolin pKO cells, BJAB, and non-silencing controls were analyzed for nucleolin mRNA levels and normalized to GAPDH (906P1: $P<.031$, 906S1: $P< .095$, 906S2: $P< .038$, 906S4: $P< .026$, 906S5: $P<.038$). (e) Whole-cell lysates were analyzed by IB for Bcl-2 to confirm the absence of protein. β-actin was used as a loading control. (f) Surface levels of nucleolin and Fas were analyzed in the parental BJAB, non-silencing control, and nucleolin pKOs by biotinylation followed with strepavidin agarose IP. Histone 3 IB was used as a control for purity of the surface fraction. BJAB whole cell extracts were used as a positive control for antibody specificity. Input levels of nucleolin and β-actin were used as a loading control. Representative data from three different experiments are shown. (g) Association of nucleolin and Fas was analyzed in parental BJAB cells, non-silencing control, a GAPDH control, and pKOs by IP with Fas agarose. Nucleolin was detected by IB. Mouse isotype-matched IgG and protein G agarose were used as a negative control for non-specific binding. BJAB whole-cell extracts were used as a positive protein control. Expression levels of nucleolin and β-actin in whole-cell extracts were determined by IB analysis and used as input and loading controls. Representative data from three different experiments are shown.

Partial Knockdown of Nucleolin Expression Results in Decreased Proliferation, Dysregulated Centromere Formation and Multinucleation

Previous reports on nucleolin observed that decreasing nucleolin levels in cancer cells resulted in a decrease in proliferation, dysregulated centromere formation, and multi-nucleated cells.(301) Thus, our next step was to prove the functional reproducibility of previous work with our B-cell nucleolin pKO model. As expected, we observed similar effects on proliferation (Figure 10a). Multinucleation of nucleolin pKOs was also confirmed by TEM (transmission electron microscopy), DRAQ5 nuclear staining, and phalloidin/DAPI confocal microscopy (Figure 10b-d). Transduction of pKOs, BJABs and non-silencing controls with red fluorescent protein (RFP)-tubulin confirmed observations of centromere formation increases resulting in dysregulated cell division by video time lapse microscopy (VTLM) imaging (Video 1.1).(301) The dysregulated centromere formation and cell division resulted in division of pKO cells into three or four daughter cells followed by a fusion back together, resulting in the previously characterized multinucleated cells (Video 1.2). These results confirm research by previous investigators on the induction of nucleolin knockdown in cells and further expand the observations to B-cell lymphomas.

Ablation of the Nucleolin-Fas Complex by Nucleolin Suppression Enhances Fas Sensitivity

To assess whether the pKO of nucleolin affects Fas signaling, we incubated cells with FasL or Fas-agonistic antibody (Figure 11a-b). Cell death was significantly increased in nucleolin pKOs after either stimulation. Detailed analysis of the Fas signaling cascade by coIP showed increased DISC formation in the pKO cells compared to non-silencing controls (Figure 11c-d), thus revealing the increase in proximal Fas signaling events in nucleolin pKOs. We observed a similar increase in the caspase 8 cleavage, by IB of caspase-8 in the pKO cells compared to non-silencing controls (Figure 11e-g). The dependency of increased apoptosis susceptibility on caspase-8 cleavage was confirmed by treatment with Z-IETD-FMK caspase-8 inhibitor prior to CH-11 challenge. (Figure 11h) To determine whether the sensitivity to Fas-mediated apoptosis was specific, we challenged pKO and control cells with the closely related tumor necrosis factor related inducing ligand (TRAIL). There was no significant change in sensitivity to TRAIL (Figure 12a) and there was no physical interaction between nucleolin and TRAIL-R1 (Figure 12b), indicating a Fas-specific effect of nucleolin.

Figure 10

a

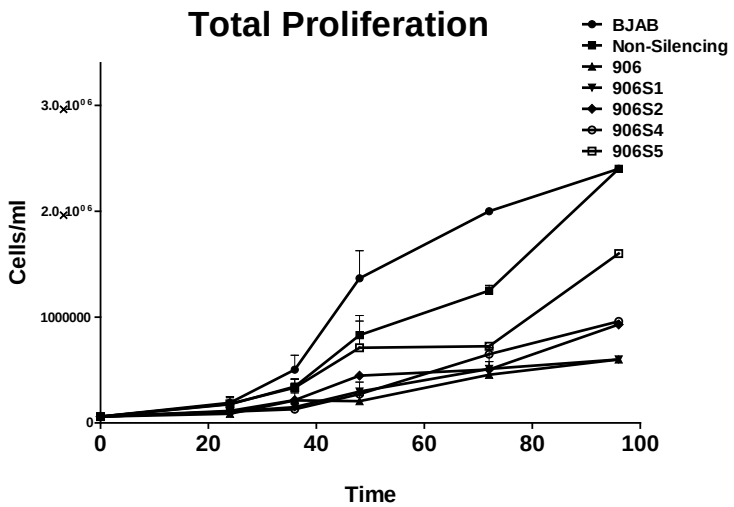

b

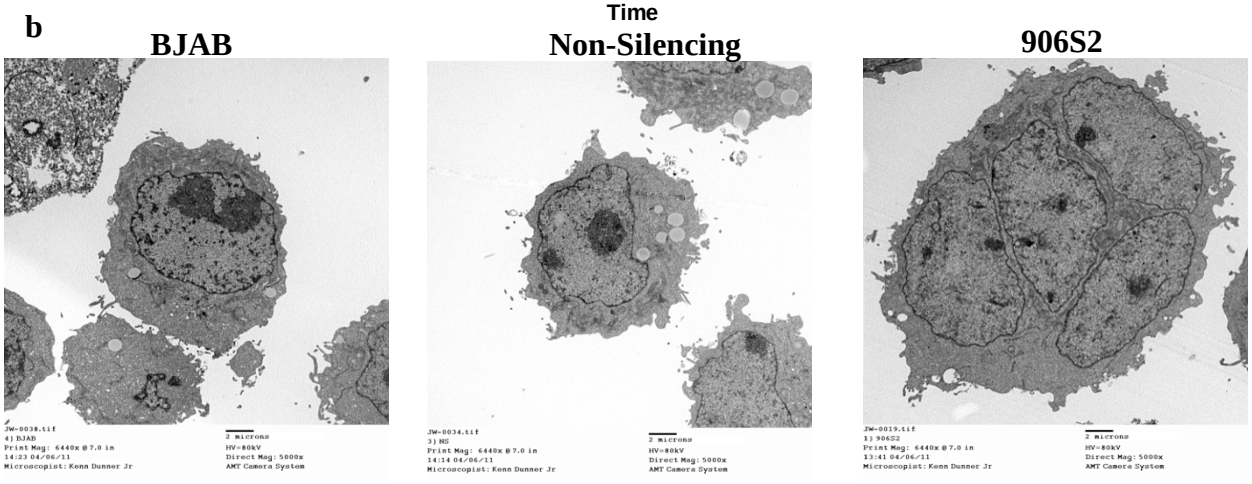

c

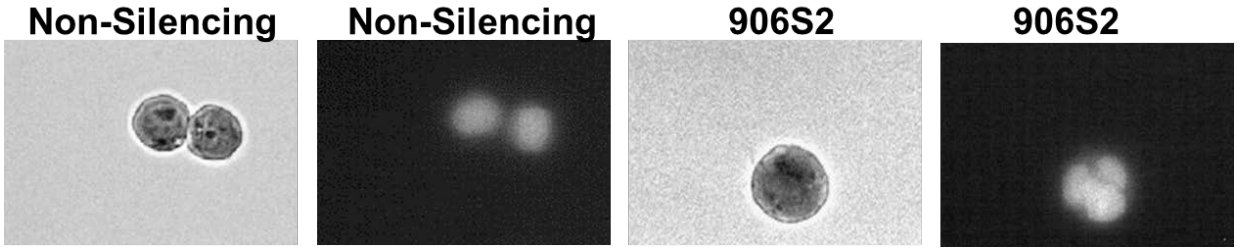

d

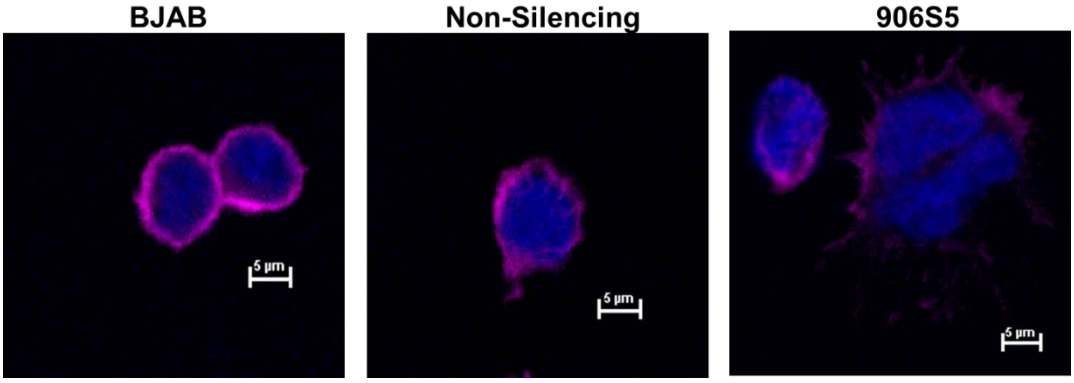

Figure 10: Characterization of the Physiological Effects of the Down-regulation of Nucleolin in BJAB Cells.

(a) Trypan blue live cell stain was used to determine BJAB, non-silencing, 906P1, 906S1-S5 cell counts every twenty-four hours for 100 hours. Proliferative calculations identified a trend of decreased proliferation in nucleolin pKOs to control BJAB and non-silencing cells. (b) Transmission electron microscopy was used to capture images of fixed BJAB, non-silencing and 906S2 cells. The images were captured by the JEM 1010 transmission electron microscope (JEOL USA, Inc.) equipped with a digital camera (AMT). All images were acquired at a 5000 magnification. Original image size at 6440X at 7 inches. Multinucleation was observed in 906S2 cells in comparison to BJAB and non-silencing controls. (c) DRAQ5 staining was used on live non-silencing and 906S2 cells. Whole cell and nuclear images were captured with the Nikon VTLM Biostation (Nikon). All images were acquired using NIS-Elements AR software (Nikon). Multinucleation of up to five nuclei in nucleolin pKO's 906S2 was observed (d) Fixed and permeabilized 906S2 cells were incubated with a dilute phalloidin-568 methanolic solution for 20 minutes at room temperature (RT). Subsequent mounting with prolong gold antifade reagent with DAPI was followed by examination by confocal microscopy. The images were captured by the Nikon A1R microscope (Nikon) and NIS Elements software. Merge/overlaid images of F-actin phalloidin-568 (pink) and DAPI nuclear stain (blue) revealed that downregulation of nucleolin in 906S2 increased the number of self-contained nuclear structures.

Video 1.1:

See attached CD for Video1.1

Video 1.1: Centromere Formation Deregulation in Nucleolin Partial Knockdown Cells. Non-silencing control and 906S2 cells were transduced at a MOI of 1 with a Tubulin-RFP containing virus. Live cell imaging using VTLM with an RFP fluorescence filter was used for visualization of centromere formation and cell division. The 906S2 transduction of tubulin-RFP showed the malfunctional division of multiple cells; in the displayed video a cell shows formation of three centromeres. Each image was recorded at 1600×1200 pixels via a 20X objective using phase contrast and fluorescent channels with an exposure time of 1 minute for twenty-four hours.

Video 1.2:

See attached CD for Video 1.2

Video 1.2: Dysregulated Cell Division with the Downregulation of Nucleolin Results in Large Multinucleated Cells. VTLM was used to observe non-silencing and 906S2 nucleolin pKO cells for twenty-four hours. The 906S2 nucleolin pKO cells were observed undergoing irregular cell division, specifically with division into three/four cells that eventually fuse back together to form 1 large multinucleated cell. Each image was recorded at 1600×1200 pixels via a 20X objective using phase contrast and fluorescent channels with an exposure time of 1 minute for twenty-four hours.

Figure 11

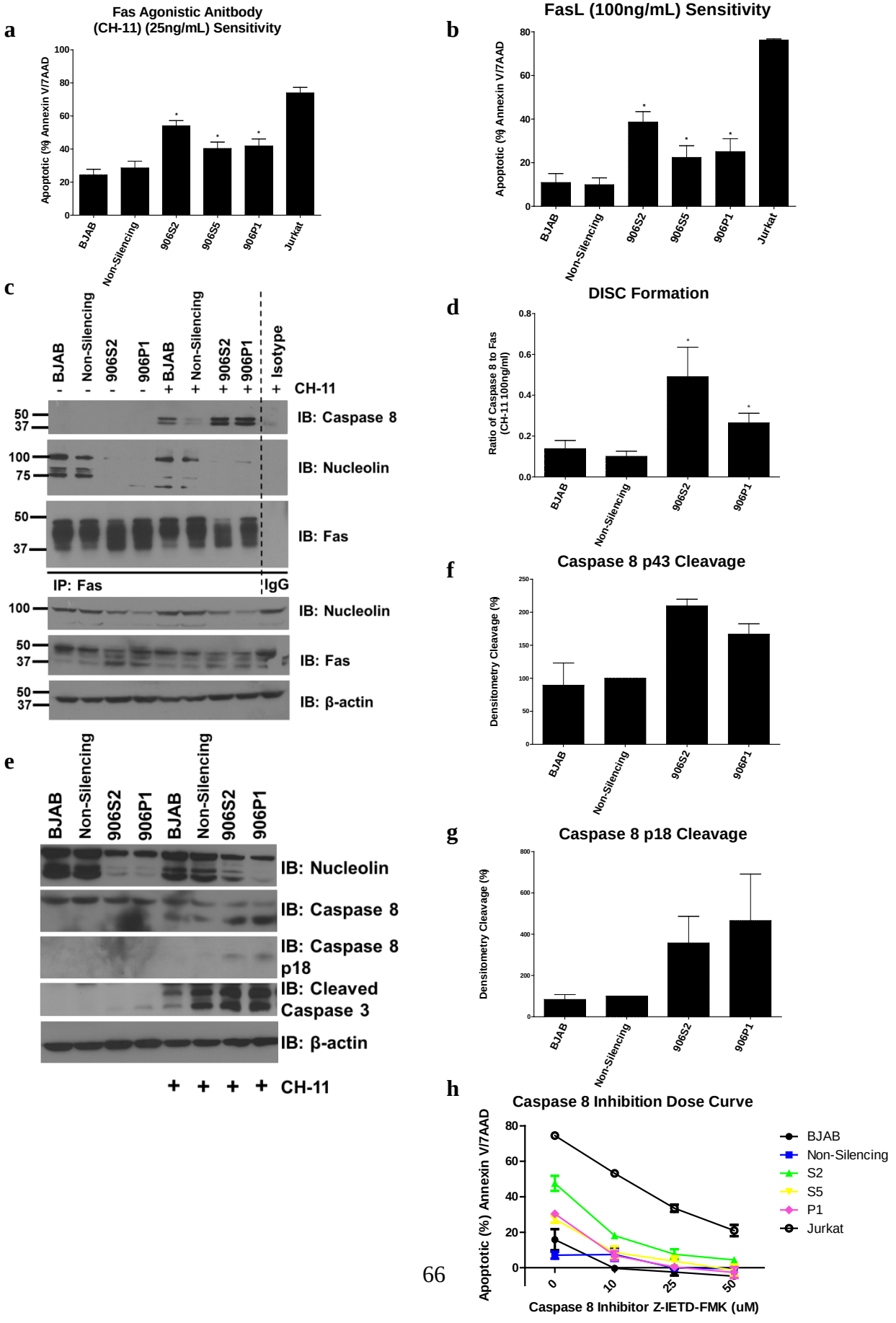
a
Fas Agonistic Anitbody (CH-11) (25ng/mL) Sensitivity
Apoptotic (%) Annexin V/7AAD
BJAB
Non-Silencing
906S2
906S5
906P1
Jurkat
b
FasL (100ng/mL) Sensitivity
c
CH-11
IB: Caspase 8
IB: Nucleolin
IB: Fas
IP: Fas
IgG
IB: β-actin
d
DISC Formation
Ratio of Caspase 8 to Fas (CH-11 100ng/ml)
e
IB: Caspase 8 p18
IB: Cleaved Caspase 3
f
Caspase 8 p43 Cleavage
Densitometry Cleavage (%)
g
Caspase 8 p18 Cleavage
h
Caspase 8 Inhibition Dose Curve
Caspase 8 Inhibitor Z-IETD-FMK (uM)
S2
S5
P1

Figure 11: Loss of Surface Nucleolin and Nucleolin-Fas Complex Sensitizes B-cell Lymphomas to Fas-mediated Apoptosis.

(a) Indicated cells were challenged with FasL (100ng/mL) overnight and analyzed for apoptosis levels by Annexin V/7AAD staining and flow cytometry. The nucleolin pKO cells 906S2, 906S5, and 906P1 showed significant increases in FasL sensitivity compared to non-silencing control cells (906S2: $P<.001$, 906S5: $P<.02$, 906P1: $P<.01$). A Fas-sensitive T-cell line, Jurkat, was used as a positive control for Fas activation. Mean data and SEM of three or more independent experiments each with three replicates are shown. (b) Cells were challenged with the agonistic Fas antibody CH-11 (25ng/mL) overnight and analyzed for apoptosis levels as in (a). The nucleolin pKO cells showed significant increases in apoptosis compared to non-silencing control cells (906S2: $P<.001$, 906S5: $P<.001$, 906P1: $P<.02$). Mean data and SEM of three independent experiments each with three replicates are shown. (c) Parental BJAB, non-silencing control, 906P1, and -S2 cells were subjected to IP of Fas pre- and 1 hr post- CH-11 (25ng/mL) challenge. The immunoprecipitated proteins were analyzed for Fas, caspase-8, and nucleolin by IB. Note a lack of nucleolin binding to Fas in 906 -P1 and -S2 cells. Lower panels of nucleolin, Fas and β-actin expression levels in whole-cell extracts as determined by IB analysis were used as input and loading controls. Representative data from three different experiments are shown. (d) Densitometry analysis of the caspase-8 levels co-precipitated with Fas. The results are shown as a ratio of caspase-8 to Fas band intensity levels. Mean data and SEM of three independent experiments are shown (906P1: $P< .02$, 906S2: $P<.038$). (e) Parental BJAB, non-silencing control, and nucleolin pKO's 906P1 and 906S2, were treated with 25ng/ml of CH-11. Cells were analyzed for caspase-8 and caspase-3 cleavage by IB. Expression levels of nucleolin and β-actin in whole-cell extracts were used as loading controls. Representative data from three different experiments are shown. (f-g) Subsequent densitometry for caspase-8 cleavage products. Increased levels of p43 and p18 caspase cleavage products were observed in 906P1 and 906S2 nucleolin knockdowns as compared to parental BJAB and non-silencing clones. ($P=.008, .05$, respectively) (h) Parental BJAB, non-silencing control, 906P1, and -S2 cells were subjected Z-IETD-FMK caspase-8 inhibitor at the indicated doses one hour prior and eighteen hours post CH-11 (25ng/mL) challenge. Cells were subsequently analyzed for apoptosis levels by Annexin V/7AAD staining and flow cytometry. Note the dependency of apoptosis sensitization on caspase-8 cleavage.

Figure 12

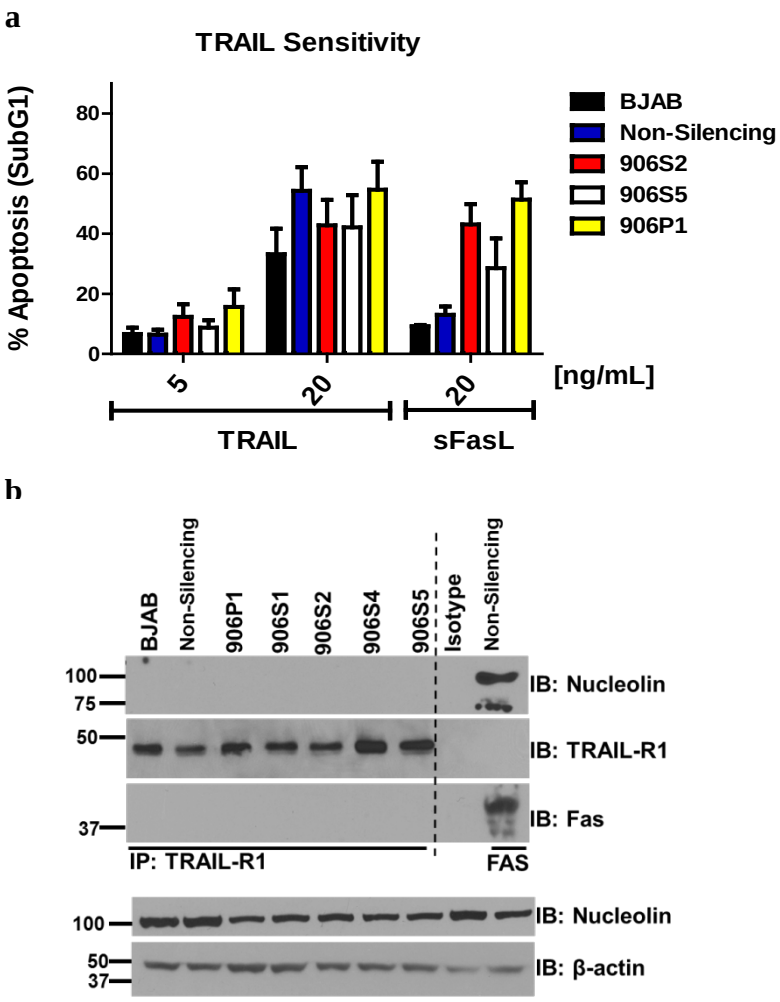

Figure 12: Nucleolin's Effect on Apoptosis is Fas Specific.

(a) Parental BJAB, non-silencing control, and partial knockdowns of nucleolin 906P1, 906S2, and 906S5 were treated with indicated doses of killerTRAIL or superFasL. There were no significant differences between control BJAB/non-silencing clones and nucleolin pKOs 906P1, 906S2, and 906S5 as measured by frequency of hypodiploid cells. (b) Parental BJAB, non-silencing control, and nucleolin pKO's 906P1, 906S2 were subjected to TRAIL-R1 IP. A Fas IP of non-silencing lysates was used as a positive control. Although TRAIL-R1 was efficiently precipitated (Middle panel), IB analysis showed a lack of nucleolin co-IP with TRAIL-R1 (Top panel). Nucleolin was efficiently co-precipitated with Fas from non-silencing cells. Lower Panels: IB analysis of nucleolin and β-actin levels in whole cell lysates prior to IP –loading control.

Downregulation of Nucleolin Increases Fas-FasL Interaction

Thus far, we determined that nucleolin interacts with Fas on the surface of B-cell lymphomas and interferes with Fas-meditated apoptosis at the most proximal signaling steps. To determine whether the observed sensitization is due to modulation of receptor-agonist interaction, we used flow cytometry to evaluate the ability of the nucleolin pKOs to bind Fas agonists (FasL and CH-11). The nucleolin pKOs bound significantly higher levels of both agonists than did controls (Figure 13c-d), confirming that the lack of nucleolin-Fas complexes (Figure 9g) is associated with intensity of the Fas receptor-ligand interaction.

To exclude the possibility that increased agonist binding results from increased surface Fas, we analyzed the levels of surface Fas in pKOs in comparison with controls and surface-Fas negative Daudi cells. No significant increase or decrease in surface Fas levels was observed (Figure 13e). It is noticeable that the higher molecular weight Fas was not immunoprecipitated nor biotinylated in the nucleolin partial knockdown cell lines (Figure 9f-g). However, the total levels of higher-molecular-weight Fas remained unchanged, thereby indicating the possibility that the absence of nucleolin has changed the accessibility or ability to immunoprecipitate the higher molecular weight Fas (Figure 9b). Further analysis determined that the higher-molecular-weight bands represent sialylated and glycosylated Fas (Figure 14) as reported previously.(47, 49) Fas glycosylation does not alter apoptosis sensitivity suggesting that the observed changes do not interfere with our functional studies. (28, 30) Thus, as clearly indicated by the increase in ligand binding to the receptor, nucleolin acts to hinder FasL binding to Fas receptor in B-cell lymphomas.

Figure 13

a

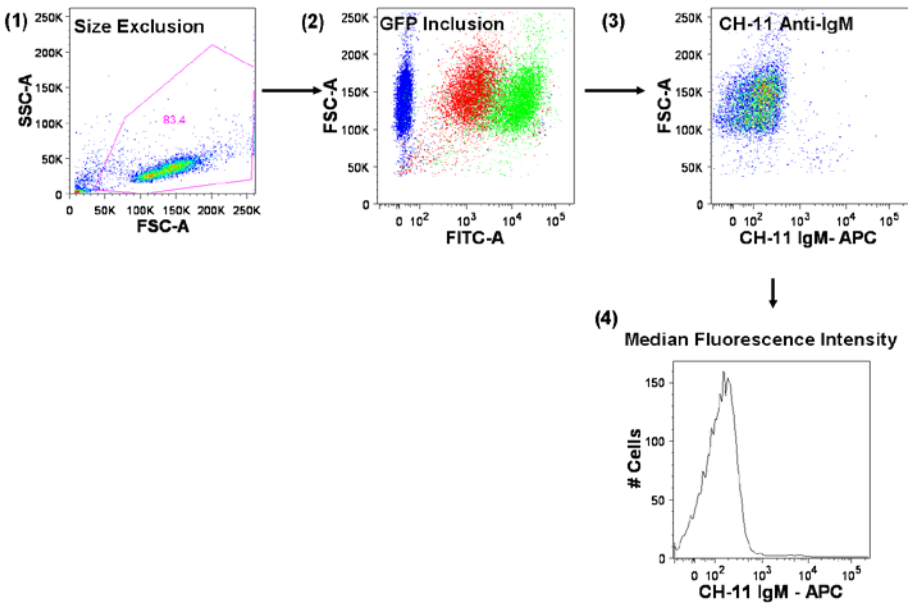
(1) Size Exclusion
SSC-A
FSC-A
83.4
(2) GFP Inclusion
FSC-A
FITC-A
(3) CH-11 Anti-IgM
FSC-A
CH-11 IgM- APC
(4)
Median Fluorescence Intensity
Cells
CH-11 IgM - APC

b

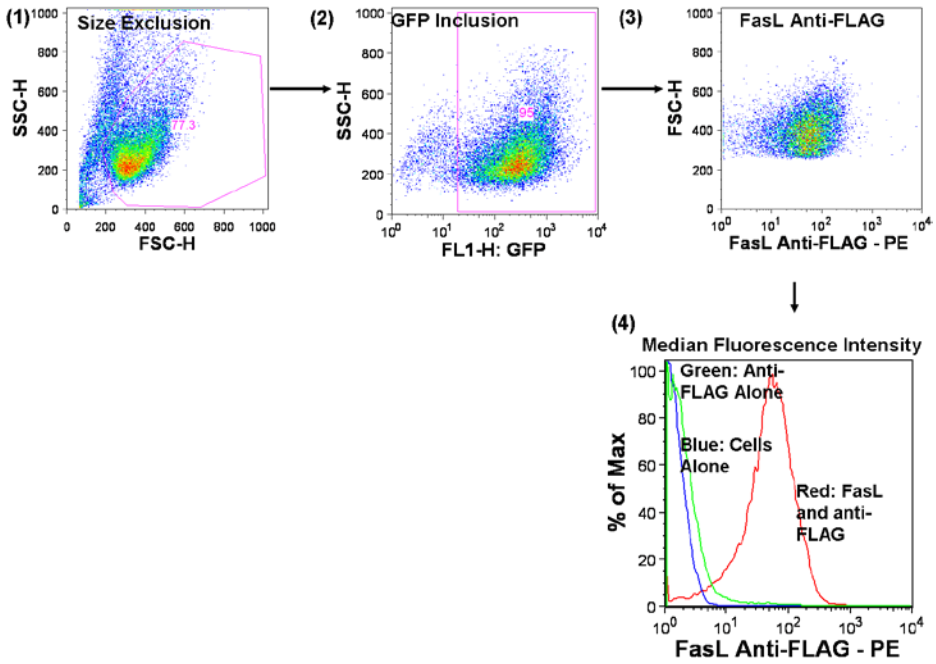
(1) Size Exclusion
SSC-H
FSC-H
77.3
(2) GFP Inclusion
SSC-H
FL1-H: GFP
95
(3) FasL Anti-FLAG
FSC-H
FasL Anti-FLAG - PE
(4)
Median Fluorescence Intensity
Green: Anti-FLAG Alone
Blue: Cells Alone
Red: FasL and anti-FLAG
% of Max
FasL Anti-FLAG - PE

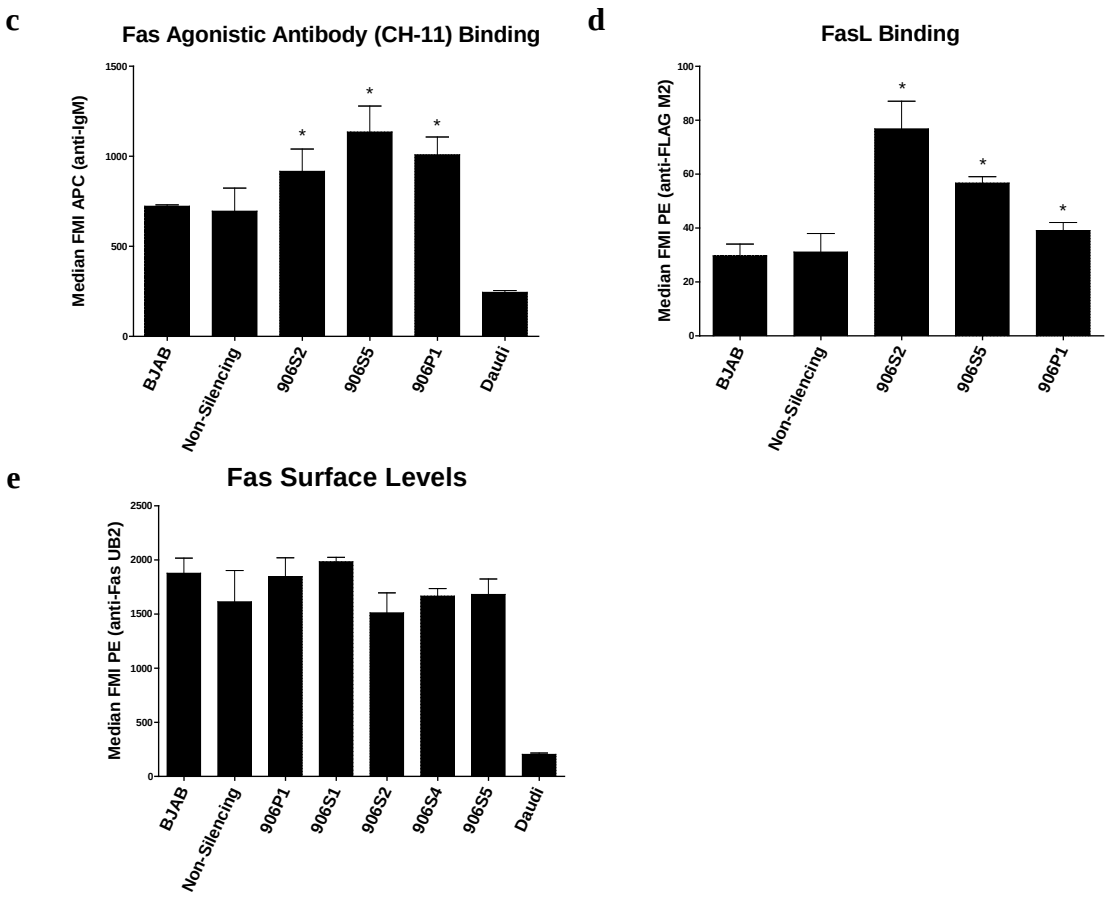

Figure 13: Absence of Nucleolin-Fas Complex Enhances FasL Binding.

(a) Flow cytometric analysis and gating strategy for CH-11 binding in BJAB cells. (b) Flow cytometric analysis and gating strategy for FasL binding in BJAB cells. (c) Indicated cell lines were incubated with CH-11 (Ig-M subclass) for 20 minutes and the amount of bound antibody was analyzed by flow cytometry by measuring an anti-IgM-APC secondary antibody signal. The nucleolin pKO cells showed a significant increase in CH-11 signal from non-silencing controls (906S2: $P<.001$, 906S5: $P< .03$, 906P1: $P< .04$). Mean data and SEM of three independent experiments each with three replicates are shown. (d) Cells were incubated with FasL (FLAG-tagged) for 20 minutes and cells were analyzed for the presence of ligand with an anti-FLAG-PE secondary antibody by flow cytometry. The nucleolin pKO cells showed significantly increased FasL signal compared to non-silencing controls (906S2: $P<.01$, 906S5: $P< .01$, 906P1: $P< .03$). Mean data and SEM of three independent experiments each with three replicates are shown. (e) Surface levels of Fas in parental BJAB, non-silencing control, 906P1, -S1,-S2, -S4,-S5, and a surface-Fas negative control Daudi cells were measured by flow cytometry using the UB2 extracellular anti-Fas antibody conjugated to PE. Note the absence of significant alterations in Fas surface levels in the nucleolin partial knock-down cells compared with non-silencing cells. Mean data and SEM of three independent experiments each with three replicates are shown.

Figure 14

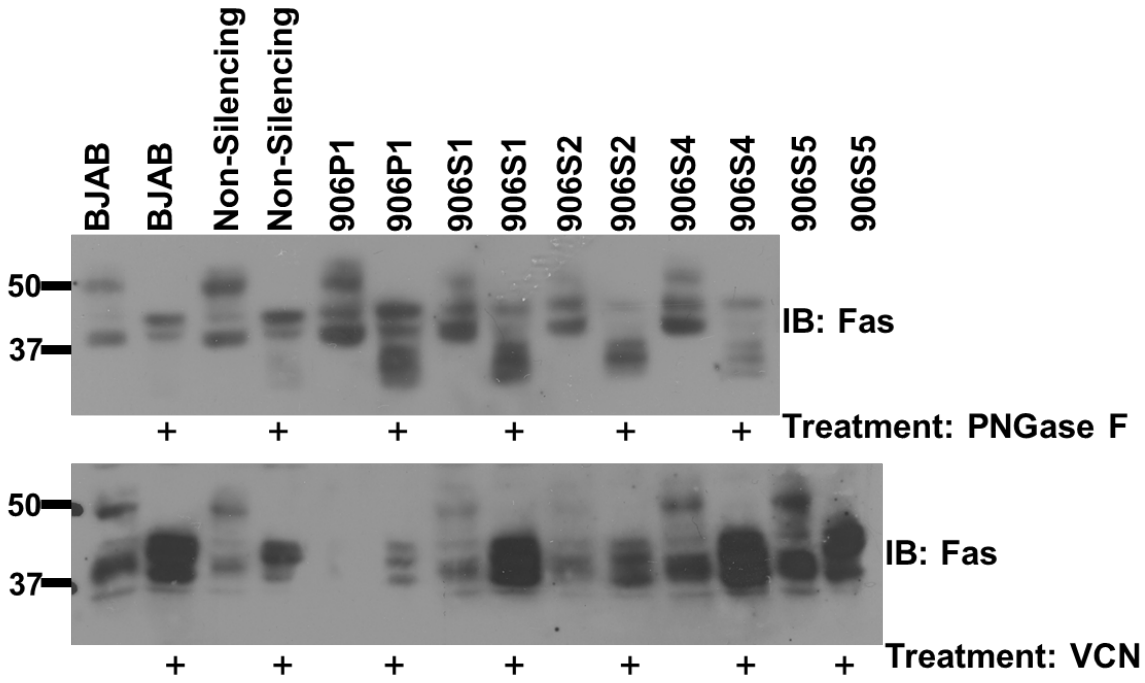

Figure 14: High Molecular Weight Fas is not Affected in the Downregulation of Nucleolin.

Parental BJAB, non-silencing control, and nucleolin pKO's 906P1, 906S1, 906S2, 906S4 lysates were treated with peptide-N4-(N-acetyl-beta-glucosaminyl)asparagine amidase (PNGase) F, a deglycosylase, following the manufacturers' protocol. Non-treated and treated whole cell lysates were separated on a 7% SDS-PAGE gel and analyzed for Fas levels. Deglycosylation ablated the high molecular weight Fas band, leaving the two lower molecular weight bands intact and produced a third lower molecular weight band, suggesting that the highest molecular weight band is a glycosylated form of Fas (upper panel). Parental BJAB, non-silencing control, and nucleolin pKO's 906P1, 906S1, 906S2, 906S4 and 906S5 cells were pretreated with a de-sialylase, vibrio cholerae neuraminidase (VCN), and analyzed by IB for Fas levels. The banding of Fas appears to shift down, suggesting that the upper molecular weight band of Fas had sialylation modifications, yet contained an additional modification.

Nucleolin Overexpression and Nucleolin-Fas Complexes Protect Mice from a Lethal Fas-Agonist Challenge

To further confirm the ability of nucleolin to block Fas signaling, we used a mouse liver overexpression model (Figure 15a) to determine whether nucleolin expression affects Fas-mediated apoptosis in vivo, as interaction in cell culture may not have relevance to interactions in an in vivo setting. We transfected mice with plasmid expressing full-length nucleolin and empty vector (302, 303), and evaluated their ability to protect the mice from a lethal challenge with Fas agonistic antibody (Jo2). Eight hours after the challenge, nucleolin-transfected mice showed a significantly increased survival rate ($P < .006$) (Figure 15b). Gross examination of the livers showed extensive hemorrhaging in vector-transfected livers, which was confined to segregated areas in nucleolin-transfected livers (Figure 15c). H&E staining confirmed massive hemorrhaging, extravasations, and dead cells in livers transfected with vector alone, whereas these effects were less dramatic in nucleolin-expressing livers (Figure 15d). Apoptosis analysis by terminal deoxy-nucleotidyl transferase-mediated Z'-deoxyuridine S'-triphosphate nick end labeling (TUNEL), cleaved caspase-3, and cleaved PARP staining showed increased numbers of apoptotic cells in vector- compared to nucleolin-transfected livers (Figure 15d). Analysis of liver tissues by IB (Figure 15e) further confirmed decreased levels of PARP, caspase-3, and caspase-8 cleavage in nucleolin-transfected livers. Note that one nucleolin-transfected mouse that did not survive the Jo2 agonistic Fas challenge, included in the immunoblot analysis, showed increased expression of the downstream mediators of Fas, yet did not show overexpression of nucleolin. Nucleolin overexpression did not correlate directly with bcl-2 overexpression, suggesting nucleolin's protection was not conferred through enhanced bcl-2 mRNA stabilization (Figure 15e). The presence of nucleolin was confirmed by FLAG staining in vector- and nucleolin-transfected livers (Figure 15f). These results show that nucleolin overexpression confers resistance to Fas-mediated apoptosis in vivo.

Our tissue culture results indicate the need for nucleolin-Fas interaction to block Fas. To test for this requirement, we transfected mice with plasmids expressing the full-length nucleolin, Fas-non-binding nucleolin construct NR123, and empty vector to evaluate the respective constructs ability to protect the mice from a lethal Jo2 challenge. Eight hours after the challenge, none of the seventeen NR123 mice, and only one of thirteen vector-transfected mice survived, whereas seven of the eleven nucleolin-transfected mice remained alive ($P < .003$) (Figure 16a). Gross examination of the livers showed extensive hemorrhaging in vector- and NR123-transfected livers. In contrast, hemorrhaging was confined to small segregated areas in nucleolin-transfected livers (Figure 16b). Apoptosis analysis by TUNEL, cleaved caspase-3, and cleaved PARP staining showed increased

numbers of apoptotic cells in vector- and NR123- compared to nucleolin-transfected livers (Figure 16c). We confirmed expression of nucleolin and NR123 by IB of anti-FLAG and anti-nucleolin in liver tissue (Figure 16d). Additional analysis of liver tissues by IB (Figure 16d) confirmed decreased levels of PARP and caspase-8 cleavage in nucleolin-transfected livers compared to vector- and NR123- transfected livers. These results support our finding that nucleolin-Fas interaction is necessary for nucleolin-mediated inhibition of Fas signaling.

Figure 15

a

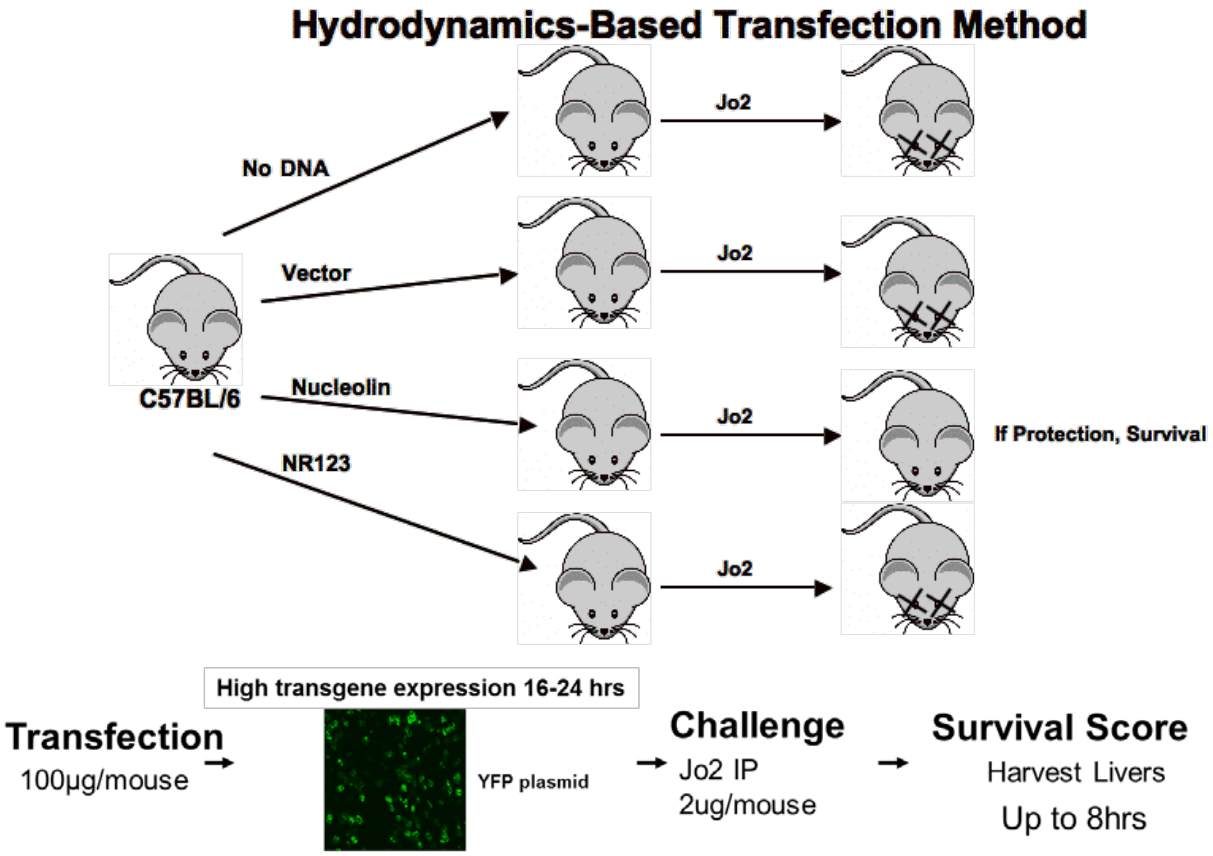

b

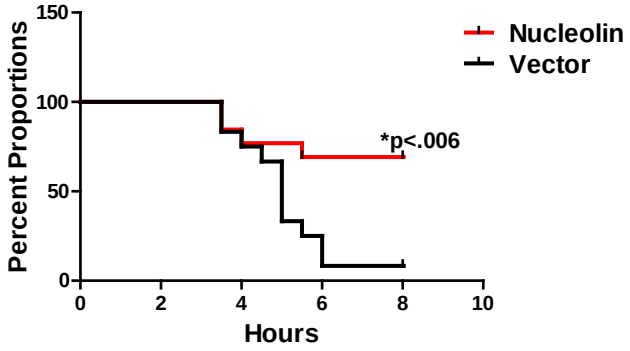

c

d

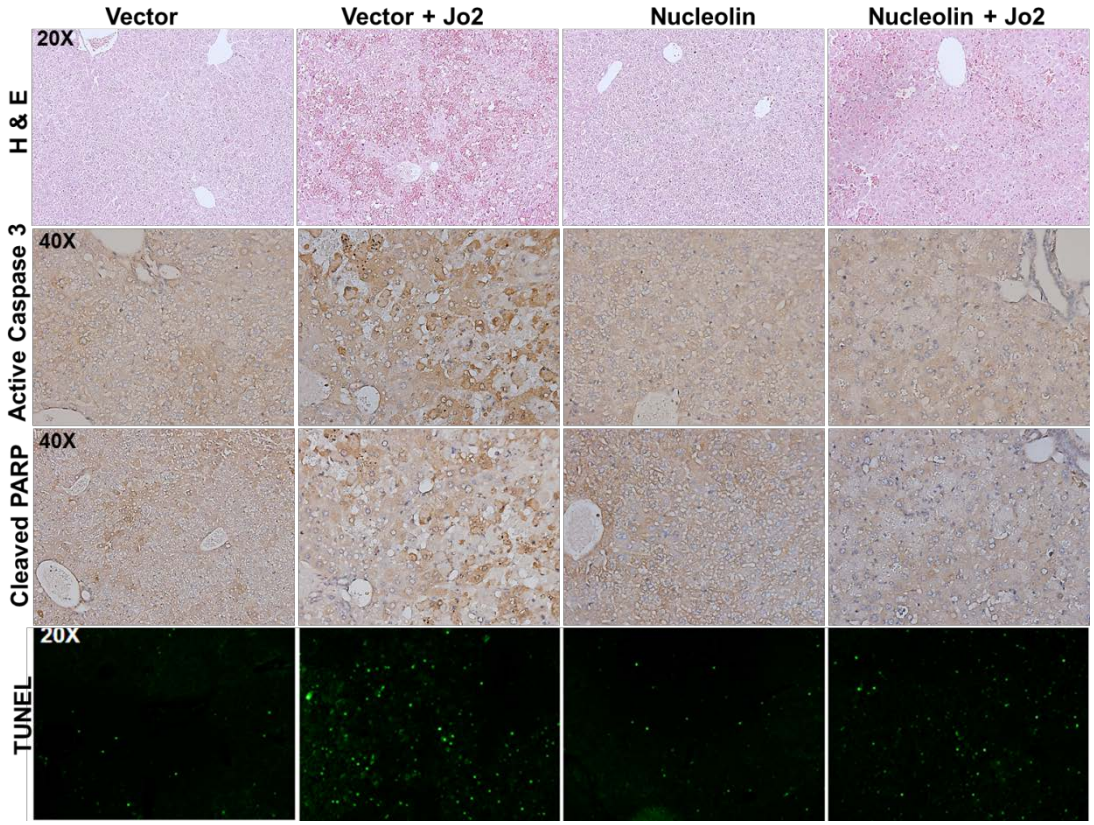
Vector
Vector + Jo2
Nucleolin
Nucleolin + Jo2
H & E
20X
Active Caspase 3
40X
Cleaved PARP
40X
TUNEL
20X

e

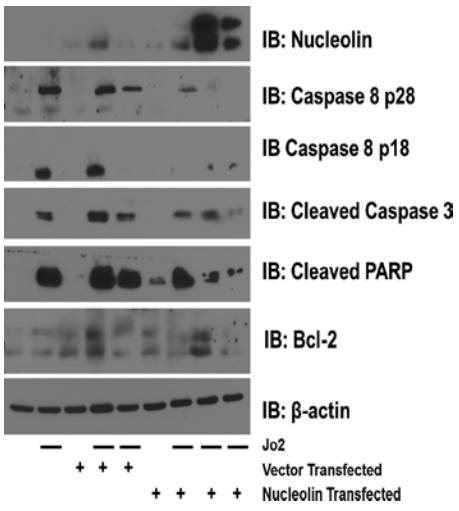
IB: Nucleolin
IB: Caspase 8 p28
IB Caspase 8 p18
IB: Cleaved Caspase 3
IB: Cleaved PARP
IB: Bcl-2
IB: β-actin
Jo2
Vector Transfected
Nucleolin Transfected

f

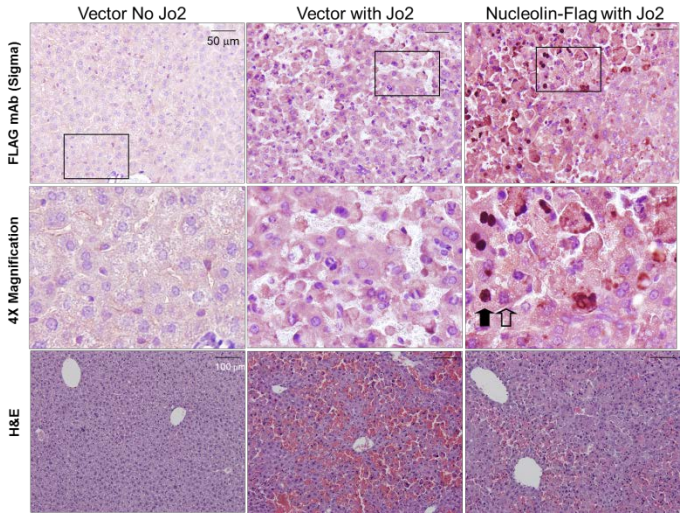
Vector No Jo2
Vector with Jo2
Nucleolin-Flag with Jo2
FLAG mAb (Sigma)
50 μm
4X Magnification
H&E

Figure 15: Overexpression of Nucleolin Protects Mice from a Lethal Fas Activation.

(a) A schematic of the hydrodynamics-based transfection mouse model used to analyze inhibitors of Fas-mediated apoptosis. We evaluated nucleolin's effect on Fas apoptosis by intravenous transfection of a large injection volume of plasmids expressing indicated proteins into the tail veins of C57B6 mice. Twenty-four hours post-injection and plasmid uptake into the liver, mice were challenged with a lethal dose Jo2. Mice were monitored for up to eight hours and scored for survival, as Jo2 injections kill mice by liver hemorrhaging and damage (63). Shown is the expression of an YFP plasmid in whole liver as representative transgene expression twenty-four hrs post transfection. (b) Mice were hydrodynamically transfected with a vector control or a plasmid expressing DDK-tagged full-length nucleolin. Twenty-four hours later, the mice were challenged with a lethal dose of Jo2 agonistic anti-Fas antibody (2 μg/g weight) and monitored for survival for up to eight hours post-challenge. The survival rate of nucleolin-transfected mice was significantly higher than mice transfected with vector alone ($P < .006$; log rank (mantel-cox) test). Representative data from three different experiments are shown. (c) Gross examination of vector and non-transfected livers challenged with Jo2 revealed massive hemorrhaging as indicated by darkening and swelling. Nucleolin expressing livers challenged with Jo2 showed decreased hemorrhaging as indicated by less darkened portions. (d) Livers were harvested, resected, and stained with haematoxylin and eosin (H&E) (upper panel), were analyzed using cleaved caspase-3, cleaved PARP antibody or TUNEL assay to evaluate apoptosis. The images were captured by the Olympus BX41 (Olympus) UPlan FL N 40X/0.75 objective. Images were acquired with DP Controller (Olympus) with a -2 exposure adjustment for TUNEL staining with a Fluorescein isothiocyanate (FITC) filter (Olympus). Adobe Photoshop PS2 was used for further image enhancement of FITC with+30 brightness for all 4 panels equally. (e) Homogenized vector-, nucleolin- and non-transfected Jo2 challenged and unchallenged liver samples were subjected to lysis, SDS-PAGE and IB analysis of nucleolin, caspase-8, caspase-3, PARP, Bcl-2, and β-actin. (f) Livers were harvested, resected, and stained with H&E (lower panel), or were analyzed using FLAG antibody to evaluate nucleolin expression. (upper panel). Boxes represent the area used for 40X magnification in the middle panel. A black arrow reveals positive nuclear nucleolin staining and outlined arrow reveals a negative nuclei. The images were captured by the Olympus BX41 (Olympus) UPlan FL N 40X/0.75 objective. Images were acquired with DP Controller (Olympus).

Figure 16

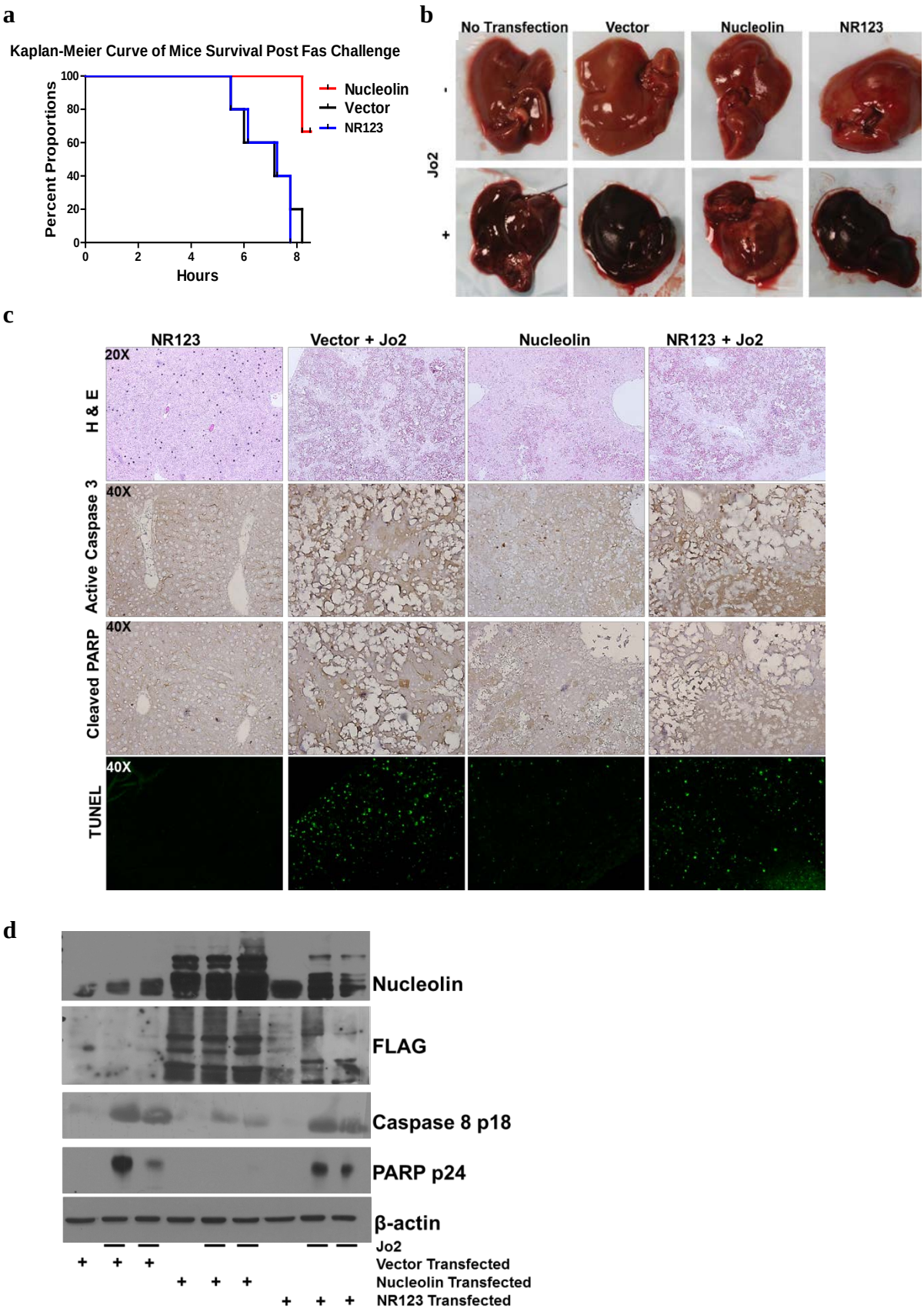
a
Kaplan-Meier Curve of Mice Survival Post Fas Challenge
Percent Proportions
Hours
Nucleolin
Vector
NR123
b
No Transfection
Vector
Nucleolin
NR123
Jo2
c
NR123
Vector + Jo2
Nucleolin
NR123 + Jo2
H & E
Active Caspase 3
Cleaved PARP
TUNEL
20X
40X
d
Nucleolin
FLAG
Caspase 8 p18
PARP p24
β-actin
Jo2
Vector Transfected
Nucleolin Transfected
NR123 Transfected

Figure 16: Nucleolin Protects Mice from a Lethal Fas Activation through Nucleolin-Fas Complex.

(a) Mice were transfected with vector control, DDK-tagged full-length nucleolin, or DDK-tagged mutant, lacking the Fas-nucleolin binding domain, NR123 plasmids. Mice were challenged with a lethal dose of Jo2 antibody (.5 μg/g weight) and monitored for survival for up to eight hours post-challenge. The survival rate was significantly higher for nucleolin-transfected mice than for mice transfected with vector alone or non-binding mutant NR123 ($P < .003$; log rank (mantel-cox) test). Mean data and SEM of 2 independent experiments are shown.(b) On gross examination, non-transfected, vector- and NR123-transfected livers challenged with Jo2 exhibited massive hemorrhaging as shown by darkening and swelling. Nucleolin livers challenged with Jo2 showed decreased hemorrhaging as shown by lighter liver portions. (c) Livers were harvested, resected, and stained with H&E (upper panel), or were analyzed using cleaved caspase-3, cleaved PARP antibody or TUNEL assay to evaluate apoptosis. The images were captured by the Olympus BX41 (Olympus) UPlan FL N 40X/0.75 objective. Images were acquired with DP Controller (Olympus) with a -2 exposure adjustment and 4.01 level adjustment for TUNEL staining with a FITC filter (Olympus). (d) Homogenized vector-, nucleolin- and NR123- Jo2 challenged and unchallenged liver samples were subjected to lysis, SDS-PAGE and IB analysis of nucleolin, FLAG, caspase-8, PARP, and β-actin.

Summary

To determine nucleolin's role in Fas-mediated apoptosis, we created nucleolin pKOs in BJAB cells, which lost the Fas-nucleolin complex and surface nucleolin expression (Figure 9). Characterization of nucleolin pKOs by confocal microscopy, TEM, and VTLM determined that defects in proliferation and centrosome formation resulting in the accumulation of multi-nucleated cells as previously described existed (Figure 10).(301) All of these results confirm that nucleolin's down-regulation in B cells mimics previously described roles of nucleolin in cell biology, and it confirms the specificity of the knockdown. Analysis of Fas-mediated apoptotic response in nucleolin pKOs revealed a sensitization to Fas agonists (CH-11 and FasL) in comparison to parental and non-silencing BJAB controls (Figure 11). Further analysis of downstream signaling events revealed increased DISC formation and caspase cleavage in pKO cells (Figure 11). These results suggest a sensitization to Fas agonists at proximal signaling events. Binding experiments revealed that FasL and CH-11 bound to nucleolin pKO cells more efficiently than to control BJABs without an increase in levels of surface Fas (Figure 13). A lack of enhanced TRAIL sensitivity and binding in nucleolin pKO cells suggests that nucleolin's inhibition of apoptosis may be Fas specific (Figure 12).

We further elucidated nucleolin's regulation of Fas-mediated apoptosis by overexpression of nucleolin and a nucleolin non-Fas binding mutant NR123 in vivo (Figure 15, Figure 16). Challenge of mice with an intraperitoneal injection of Fas agonist Jo2 results in apoptosis and massive hemorrhaging in mice livers and eventual death. This hydrodynamic based transfection model is an accepted model for expressing proteins of choice in mouse liver and for study of cell signaling, including Fas-mediated signaling.(302) Analysis of mice challenged with Jo2 revealed a protection against death and apoptosis in nucleolin-transfected mice in comparison to vector- and NR123-transfected mice (Figure 15, Figure 16). Taken together, these results reveal that nucleolin confers resistance to Fas-mediated apoptosis when in complex with Fas.

Limitations and Future Directions

The study of nucleolin knockout cells has been impractical. Nucleolin is essential for cell survival, and thus most cell culture knockouts last less than a week and no nucleolin knockdown mice have been successfully generated.(159, 301) The creation of an inducible system could overcome some these issues. Thus, it would be intriguing to create a Tet-on/off shRNA system to study the effects of gradual nucleolin downregulation.(304) Additionally, by creating an inducible knockdown system, we would be able to achieve an acute nucleolin protein decrease and potentially see more dramatic responses to Fas signaling. A creation of a Tet-on/off shRNA system would also

allow for investigations with an in vivo tumor growth model. However, due to nucleolin's diverse and ubiquitous interactions in oncogenesis and proliferation, it would be difficult to confirm nucleolin's regulation of Fas as a key step to chemotherapeutic resistance in such in vivo tumor growth studies.

Our results show that cell surface nucleolin binds Fas, inhibits ligand binding, and thus prevents induction of Fas-mediated apoptosis in B-cell lymphomas. The regulation of apoptosis is a key step in malignant transformation as well as in response to chemotherapy. Our novel findings support the importance of nucleolin in blocking Fas-mediated apoptosis, which could contribute to cancer immune evasion as well as cancer chemoresistance. In addition, nucleolin surface expression in cancer could serve as a therapeutic target in B-cell lymphomas and many other cancers that overexpress nucleolin.

Chapter 5: Nucleolin Expression in B-cell Lymphomas

Rationale

The failure of chemotherapy and the resulting 27% death rate in NHL underscores the necessity to be able to stratifying patients according to prognostic risk analysis and to prospectively identify chemosensitive and chemoresistant lymphomas.(7) The comparison of cancer and healthy tissue proteomes has revealed important cancer-specific targets for the treatment of NHL.(305) Nucleolin has recently been identified as a pro-survival protein that is frequently up-regulated in cancer and cancer-associated endothelial cells.(163, 267-269, 275, 281, 296, 297) Furthermore, nucleolin's localization is often altered in highly proliferating cells, where it translocates out of the nucleus into the cytoplasm and exterior surfaces of cells.(172, 178, 256, 260, 273, 275) The selective surface expression of nucleolin further underscores its potential as a therapeutic target.

Nucleolin's role in promoting the survival of cancer cells may affect the clinical outcome of patients with B-cell lymphomas. This had been an unexplored topic, so we aimed to investigate nucleolin's expression and localization patterns in B-cell lymphomas and examine whether nucleolin expression correlates with clinical outcomes. We aimed to define whether or not nucleolin's expression and localization could serve as a novel biomarker and target in B-cell lymphomas.

Results

Nucleolin Expression and Localization in Human B-cell Lymphoma Tissues

To identify potential nucleolin alterations in B-cell lymphomas, we performed IB of nucleolin in two cell lines each of Burkitts lymphoma, MCL, DLBCL cell lines; five primary DLBCL tissues; nine primary MCL tissues, and compared them with healthy donor B cells (Figure 17a-c). Densitometry of nucleolin bands revealed elevation of nucleolin levels in B-cell lymphoma cell lines when compared to that of corresponding normal tissues (Figure 17a). As seen in Figure 17b-c, nucleolin expression in DLBCL and MCL primary tissues was also elevated from normal B-cell tissues, suggesting that increased nucleolin expression may be a consistent property of B-cell lymphomas.

In order to identify changes in location of nucleolin, the extracts of cell lines were subjected to subcellular fractionation. The cell extracts were separated into nuclear and cytosolic protein fractions by partial hypotonic lysis (Figure 17d). A comparison of the densitometry readings of

bands from cytosolic fraction of B-cell lymphoma cell lines and that in normal B cells (Figure 17d) showed an increase in cytosolic nucleolin fraction as a percentage of total nucleolin in B-cell lymphomas compared with B cells. Thus, a shift in nucleolin's localization to the cytoplasm/surface occurs in B-cell malignancies. This is in agreement with features of transforming and aggressive properties of cancer cells.(247, 306)

Nucleolin mRNA Expression in Human B-cell Lymphoma Tissues

To determine whether the increase in nucleolin protein expression was caused by an increase in its mRNA levels, we analyzed nucleolin mRNA levels in healthy B cells, B-cell lymphoma cell lines, primary MCL, primary DLBCL and primary CLL tissues. Nucleolin mRNA levels in MCL subjects were significantly elevated from normal B cells (P = .013); however, no such effects were identified in the B-cell lymphoma cell lines, DLBCL and CLL subjects (Figure 17f). Thus, nucleolin mRNA should not be regarded as a driving force for high levels of nucleolin proteins.

Nucleolin Surface Expression in Human B-cell Lymphoma Tissues

To further delineate the cellular localization changes of nucleolin in B-cell lymphomas, we developed a flow cytometry staining protocol to measure surface nucleolin levels in primary tissues. The gating strategy for primary lymphoma cell (source cells were collected from apheresis, fluid, and leukemic blood) samples is demonstrated in Figure 18a. The shift in the intensity of nucleolin staining is highly specific yet not intense enough to produce two distinct populations. It displays a small shift of the entire population instead, suggesting the amount of nucleolin molecules on the surface is detectable but rather low (Figure 18a). Similar shifts of the entire nucleolin surface population have been reported previously.(275)

Comparison of the surface expression of nucleolin in B-cell lymphomas with healthy individuals' B cells reveals a significantly higher level in B-cell lymphomas (P-value=.001) (Figure 18b-c). However, the nucleolin levels in CLL samples were similar to those in healthy B cells, suggesting that nucleolin surface levels are increased in aggressive B-cell lymphomas and lower in indolent B-cell lymphomas (Figure 18b). The latter lymphomas are known to have lower cell proliferation rates, which may account for this difference.

Previous findings have indicated that the deregulation and overexpression of nucleolin correlated to a worse prognosis in ependymomas, stage II pancreatic ductal adenocarcinomas, and

relapsed acute leukemias (265, 269, 297). Here we examine whether nucleolin surface levels correlate with prognosis in lymphomas. We compared nucleolin surface levels with the IPI lymphoma risk groups. For MCL patients, IPI calculations were adjusted for the Mantle Cell Lymphoma International Prognostic Index (MIPI) (Figure 18c).(307) The CLL patients were applied to the IPI (which is typically used for DLBCL) in order to have a common stratification in these patients. The nucleolin levels among IPI groups were significantly different (P-value=0.0137), with high risk IPI groups having increased surface levels of nucleolin (Figure 18c). Taken together, B-cell lymphomas elevate nucleolin protein levels, correlating with a worsening prognosis as determined by the relationship between surface nucleolin and IPI.

Figure 17

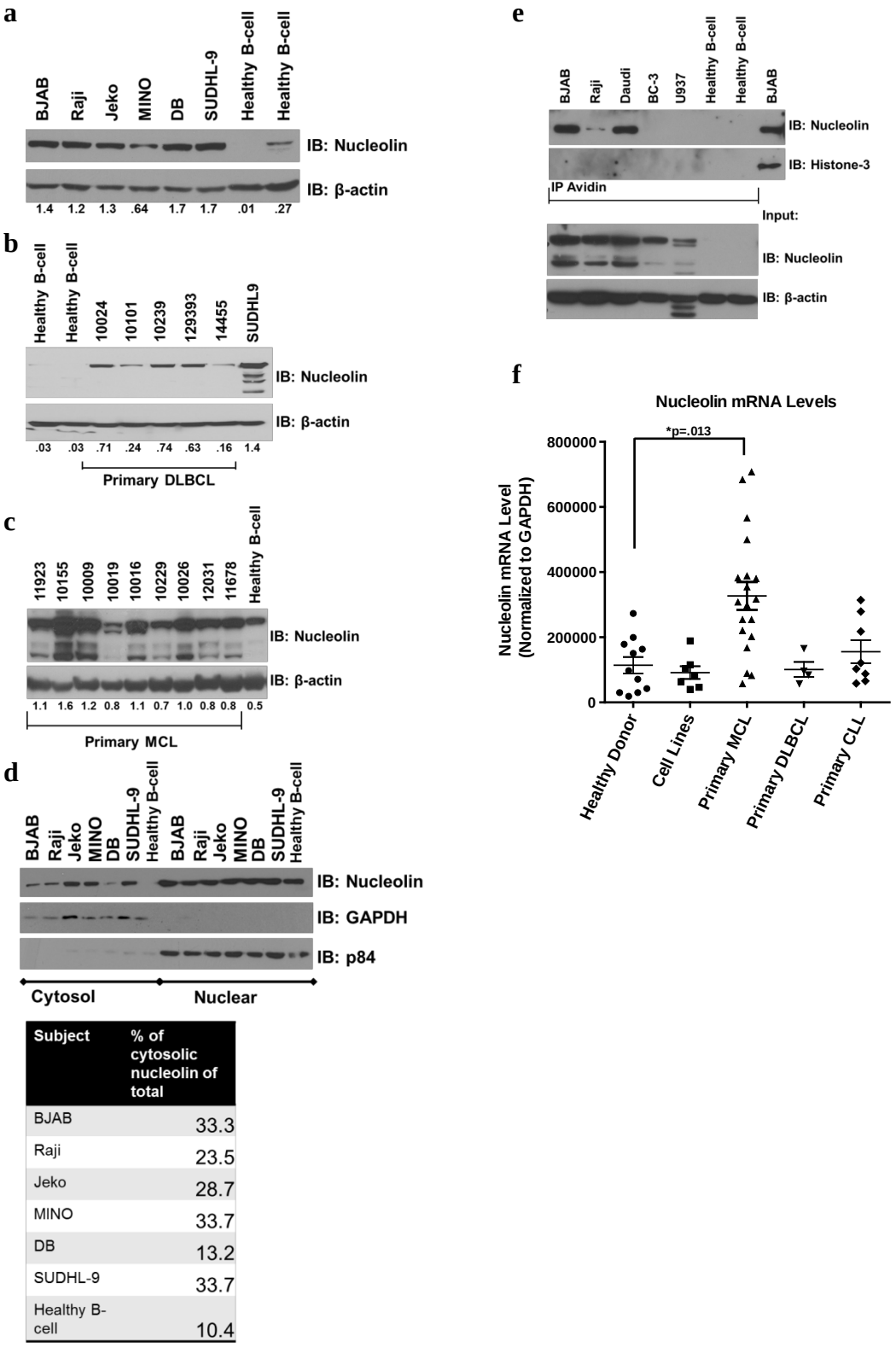

Subject	% of cytosolic nucleolin of total
BJAB	33.3
Raji	23.5
Jeko	28.7
MINO	33.7
DB	13.2
SUDHL-9	33.7
Healthy B-cell	10.4

Figure 17: B-cell Lymphomas Express Higher Levels of Nucleolin Compared to Healthy B cells.

(a) A representative immunoblot of nucleolin levels in paired cell lines: BJAB, Raji (Burkitts lymphoma); Jeko, MINO (MCL); DB, SU-DHL-9 (DLBCL); and two healthy donor CD19-positive B-cell populations. Densitometric analysis of IB of nucleolin protein expression levels normalized to β-actin loading control. (b) A representative IB of nucleolin levels in DLBCL primary tissues and two healthy donor CD19 positive B-cell populations. Densitometric analysis of IB of nucleolin protein expression levels normalized to β-actin loading control. (c) A representative IB of nucleolin levels in MCL primary tissues and one healthy donor CD19 positive B-cell population. Densitometric analysis of IB of nucleolin protein expression levels normalized to β-actin loading control. The multiple bands of nucleolin match the nucleolin 105, 80, 70 kDa pattern that has been attributed to autodegradation of its N-terminal domain. (d) A representative immunoblot of nucleolin levels from a cytosolic/nuclear fractionation assay with the paired cell lines: BJAB, Raji, Jeko, MINO, DB, SU-DHL-9, and a healthy donor CD19 positive B-cell population. GAPDH and p84 were used to test the purity of fractions. (e) Surface levels of nucleolin was analyzed in BJAB, Raji, Daudi, BC-3(a primary effusion lymphoma), U937 (histocytic lymphoma) and a two healthy donor CD19 positive B-cell populations by intact cell biotinylation followed with streptavidin-agarose IP. Histone 3 was used as a control for purity of the surface fraction. BJAB whole-cell extracts were used as a positive control for antibody specificity. Input levels of nucleolin and β-actin were used as loading controls. Representative data from three different experiments are shown. (f) Dot-plot of nucleolin mRNA expression levels in healthy donor B cell, MCL, DLBCL, and CLL tissues normalized to GAPDH as the internal control. The horizontal bar represents the means with the vertical bars representing the SEM.

Figure 18

a

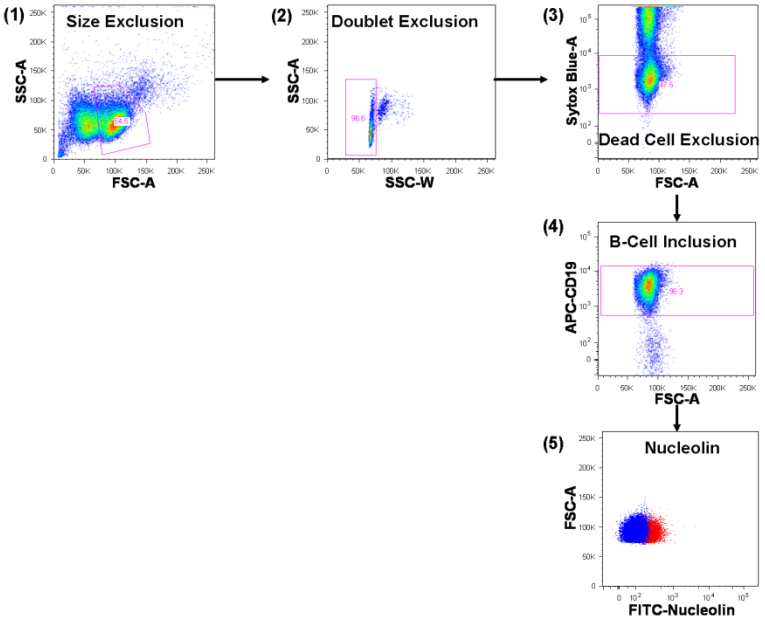

b

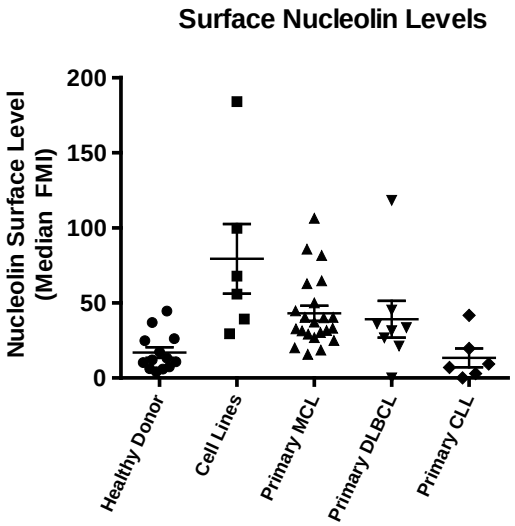

c

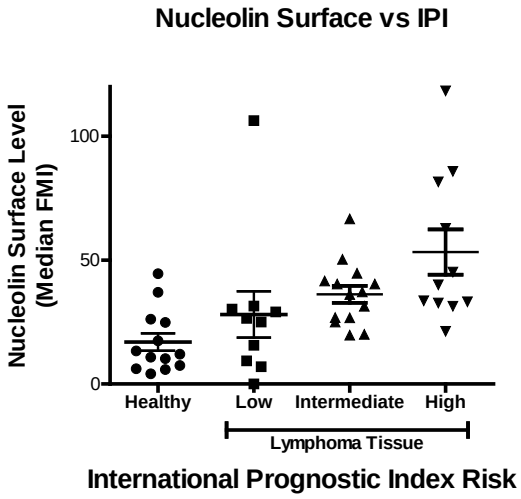

Figure 18: Differential Expression of Surface Nucleolin in Lymphoma Primary Samples.

(a) Gating strategy to analyze nucleolin levels in B-cell populations. Initial gating for normal forward (size) and side (granulation) scatter populations (1). Doublet cells were excluded by gating on single cell populations through side scatter area and side scatter wide (2). Live cells were next gated by live cell staining through negative exclusion of sytox blue positive cells. Our results with Sytox staining also eliminate the possibility that antibodies entered the cell through permeabilized membranes (3). This was followed by separation of live singlet cells, which were gated for CD19-positive population representing B cells (4). Finally, the detected nucleolin levels were analyzed on FlowJo using a log scale of FITC median fluorescent intensity (5). (b) Dot-plot of surface nucleolin levels in healthy donor B cells and MCL, DLBCL, and CLL tissues as determined by flow cytometry. The horizontal bars represent the means with the vertical bars representing the SEM. A P-value of 0.001 from Wilcoxon rank sum test indicates that the difference in nucleolin levels between the healthy patients and patients with tumor is statistically significant. (c) Dot-plot of surface nucleolin levels in healthy donor B cells and MCL, DLBCL, and CLL tissues stratified into low, intermediate, or high risk populations by IPI or MIPI, depending on diagnosis. A P-value of 0.0137 from Kruskal-Wallis test indicates that the difference in nucleolin levels among the IPI groups is statistically significant.

Patients' Characteristics and Outcome

To further demonstrate the biological relevance of nucleolin deregulation in B-cell malignancies, we created a retrospective tissue microarray (TMA) from 119 patients with B-cell lymphoma. The median age of the patients at biopsy was 56 years (range, 24 - 84). Their clinical characteristics are reported in Table 6. Overall survival (OS) time was calculated from biopsy date to death date. Patients were censored at last follow-up date if death had not occurred. The median OS time was 102 months (95% confidence interval (CI): 52.1, 147). The median follow-up time for the censored observations was 137.98 months (range: 0.39 – 212.62). The 5-year OS rate of the 119 patients from this study cohort was 58% (95%CI: 0.5, .68), and the 5-year progression free survival (PFS) rate was 41% (95%CI: .33, .51). (Figure 20) (Table 11, Table 10). Of the known associated clinically relevant prognostic variables, the performance score was significantly associated with best complete response status (p-value=0.0072), PFS (p-value=0.0006), and OS (p-value=0.0247) (Table 7, Table 8, Table 9, Table 10, Table 11). The Ann Arbor Stage was significantly associated with histology (p-value=0.0289) (Table 8). The diagnosis was also significantly associated with PFS (p-value=0.047) (Figure 20b) (Table 10).

Marker Expression

Three markers were evaluated for association with response status, patient demographics, clinical characteristics, PFS, and OS: Ki-67 intensity, average number of nucleolin positive cells, and nucleolin intensity. Zero (0), low (1), intermediate (2) and high (3) nucleolin-positive cell populations were defined as 0=no zero staining, 1= 1-25% cut point, 2=25-75% cut point, 3= >75% cut point (Figure 19a). Low (1) and high (2) nucleolin intensity scores were defined by pathologists (Figure 19b). Low (1) intermediate (2) and high (3) Ki-67 intensity scores were defined by pathologists (Figure 19c).

Figure 19

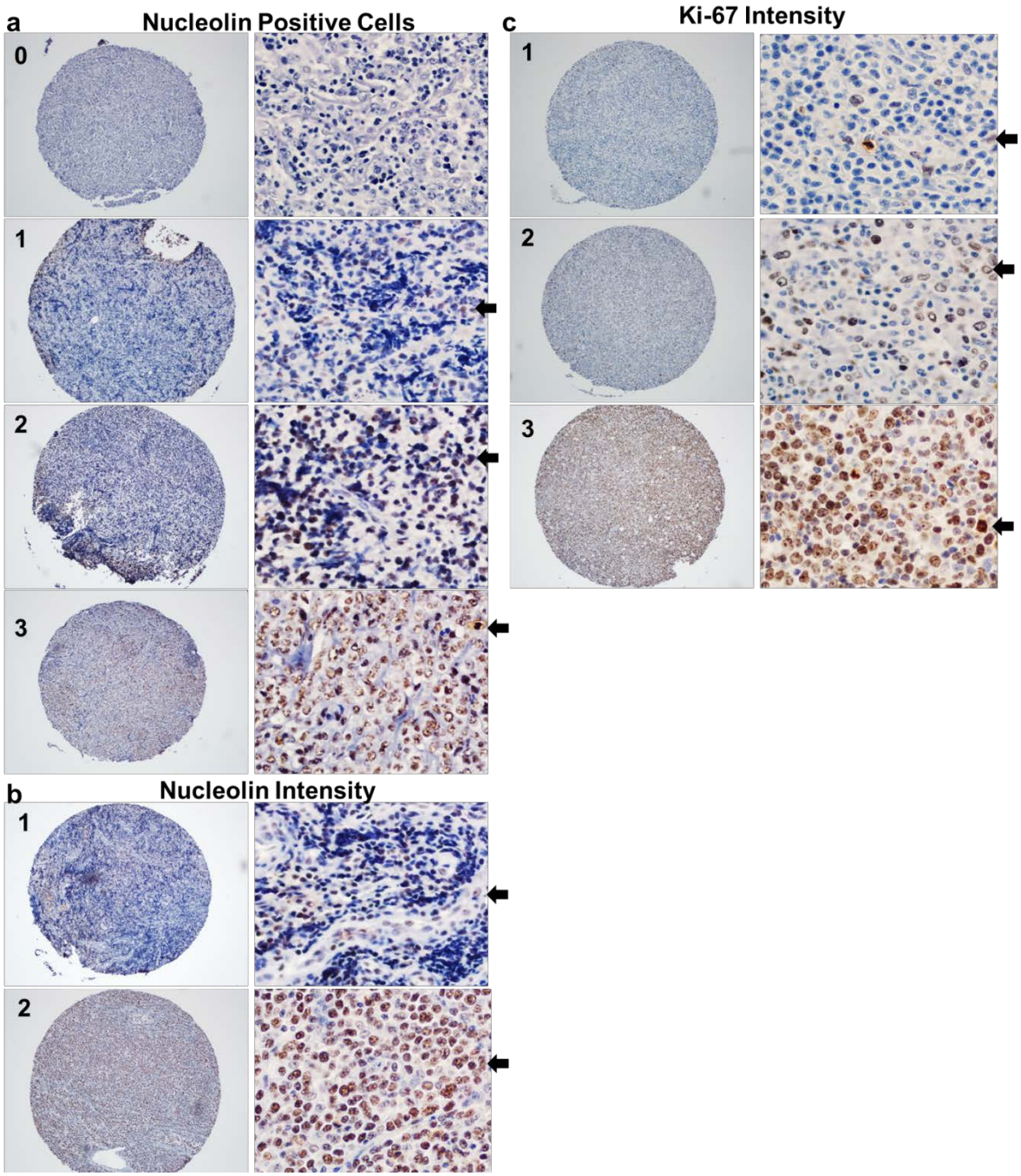

Figure 19: Nucleolin and Ki-67 Marker Expression.

Representative immunohistochemistry cases from the TMA to assess nucleolin expression. (a) Representative DLBCL with nucleolin positive cell scores of 0-3. (b) Representative DLBCL with nucleolin intensity scores of 1-2. (c) Representative DLBCL with Ki-67 intensity scores of 1-2. The images were captured by the Olympus BX41 microscope system. An Olympus Model DP72 camera and cellSens Standard 1.6 software (Olympus Corporation) was used for acquiring images. Each case is shown as acquired under 10X and 60X magnifications.

Nucleolin Protein Expression and Clinical Characteristics

The number/percentage of nucleolin-positive cells associated significantly with both histology (P<0.0001) and patients Zubrod performance score (P-value=0.0096) at the time of biopsy (Table 8, Table 9). The number of positive cells in patients with DLBCL was distinctly higher (range 0 % to <75%, median <75%) than that in the indolent lymphoma CLL/SLL (range 0 % to <75%, median 1-25%) (Table 8). The average intensity score of nucleolin also correlated significantly with histology (P-value=0.0015) but less significantly with the patient's Zubrod performance score (P-value=0.0585) at the time of biopsy. Neither the average percentage of nucleolin-positive cells nor the average nucleolin intensity score was significantly associated with PFS and OS (Figure 20f-g, Figure 21f-g). Multivariable analysis confirmed that the markers are not significant with the adjustment of age and performance scores in the model.

Ki-67 Intensity and Clinical Characteristics

The proliferative marker, Ki-67, is often used to determine treatment strategies for patients with B-cell lymphomas. At the time of biopsy the average intensity of Ki-67 associated significantly with histology (P-value=0.0003) (Table 8). The average intensity in patients with DLBCL was distinctly higher (range 1-3, median 3) than that in the indolent lymphoma SLL (range1-3, median 2) (Table 8). The average Ki-67 intensity score was not significantly associated with PFS and OS (Figure 20h, Figure 21h).

Interestingly, Ki-67 intensity score was significantly associated with the average number of nucleolin-positive cells (p-value<0.0001) and the average intensity score of nucleolin-positive cells (P-value<0.0001) (Table 12) (Figure 22).

Table 6 : Clinical Characteristics of the 119 B-cell Lymphoma Patients.

Variable	Category	Frequency count (Percentage)
Gender	F	53 (44.54%)
	M	66 (55.46%)
Diagnosis	DLBCL	67 (56.3%)
	FL	34 (28.57%)
	MCL	4 (3.36%)
	MZL	3 (2.52%)
	SLL	11 (9.24%)
Initial or Relapsed Patients	I	81 (68.90%)
	R	37 (31.09%)
Performance Score	0	50 (43.86%)
	1	44 (38.6%)
	2	16 (14.04%)
	3	4 (3.51%)
Ann Arbor Stage	1	7 (6.19%)
	2	13 (11.5%)
	3	35 (30.97%)
	4	58 (51.33%)
First Rx After Biopsy	A: CHOP Therapy	45 (43.69%)
	B: Combination Therapy	37 (35.92%)
	C: Fludarabine Therapy	16 (15.53%)
	D: Other	5 (4.85%)
Response to First Rx	CR	75 (72.12%)
	PR	10 (9.62%)
	Progression	17 (16.35%)
	Stable	2 (1.92%)
Total Treatments	0	1 (0.89%)
	1	49 (43.75%)
	2	15 (13.39%)
	3	18 (16.07%)
	4	21 (18.75%)
	5	2 (1.79%)
	6	4 (3.57%)
	10	1 (0.89%)
	12	1 (0.89%)
Average Number NCL Positive	0	5 (4.2%)
	1	20 (16.81%)
	2	29 (24.37%)
	3	65 (54.62%)
Average Intensity of NCL	0	5 (4.2%)
	1	59 (49.58%)
	2	55 (46.22%)
Average Intensity of Ki67	1	19 (18.27%)
	2	35 (33.65%)
	3	50 (48.08%)
Last Follow-up Status	Deceased	69 (57.98%)
	Lost	6 (5.04%)
	Remission	44 (36.97%)
Cause of Death	Remission	13 (20.97%)
	Unknown	1 (1.61%)
	With Lymphoma	48 (77.42%)

Analysis Variable : Age							
N	Mean	Std Dev	Minimum	Lower Quartile	Median	Upper Quartile	Maximum
119	55.48	14.58	0.00	45.40	56.27	66.76	84.50

Data regarding performance status (n=114), Ann Arbor score (n=113), first reaction after biopsy (n=103), response to first treatment (n=104), total treatments (n=112), Ki-67 staining (n=104) and cause of death (n=62) were not available for all patients. The average number of nucleolin stained cells was coded as follows: no staining of nucleolin = 0, 1-25% = 1, 25-75% = 2, >75% = 3. Nucleolin intensity was scored as low or high correlating to 1 and 2, respectively. Ki-67 intensity was scored as 1, 2 or 3 from the lowest to the highest intensity.

Table 7: Response Status to the First Treatment after Biopsy and by Patients Characteristics.

Variable	Levels	0: not CR	1: CR	p-value
Gender	F	16(34%)	31(66%)	.2035
	M	13(22.8%)	44(77.2%)	.
Diagnosis	DLBCL	20(35.1%)	37(64.9%)	.4672
	FL	7(21.9%)	25(78.1%)	.
	MCL	.(.%)	3(100%)	.
	MZL	.(.%)	3(100%)	.
	SLL	2(22.2%)	7(77.8%)	.
Performance Score	0	5(11.4%)	39(88.6%)	.0072**
	1	16(41%)	23(59%)	.
	2	5(38.5%)	8(61.5%)	.
	3	1(33.3%)	2(66.7%)	.
Ann Arbor Stage	1	.(.%)	5(100%)	.1724
	2	3(25%)	9(75%)	.
	3	6(18.8%)	26(81.3%)	.
	4	18(36.7%)	31(63.3%)	.
First Rx After Biopsy	A:CHOPTher	11(24.4%)	34(75.6%)	.7097
	B:CombTher	13(36.1%)	23(63.9%)	.
	C:FludTher	4(26.7%)	11(73.3%)	.
	D:Other	1(20%)	4(80%)	.
Average Number NCL Positive	0	.(.%)	4(100%)	.1777
	1	5(27.8%)	13(72.2%)	.
	2	4(15.4%)	22(84.6%)	.
	3	20(35.7%)	36(64.3%)	.
Average Intensity of NCL	0	.(.%)	4(100%)	.5585
	1	14(26.9%)	38(73.1%)	.
	2	15(31.3%)	33(68.8%)	.
Average Intensity of Ki67	1	5(27.8%)	13(72.2%)	.1945
	2	6(18.8%)	26(81.3%)	.
	3	16(38.1%)	26(61.9%)	.

Variable	CR to First Rx	n	mean	std	min	q1	median	q3	max	p-value
Age	0: not CR	29	57.714	15.856	27.748	45.402	62.552	70.335	84.498	0.14916
	1: CR	75	53.198	14.062	0.000	44.099	54.472	61.782	76.468	.

*Data regarding performance status (n=114), Ann Arbor score (n=113), first treatment after biopsy (n=103) for initial or relapsed presentation of lymphoma, and Ki-67 staining (n=104) were not available for all patients; the patients were stratified according to their response status. Fisher's exact test or Chi-square test was used to evaluate the difference in complete response rate between/among patient groups. ** The association between performance score and best complete response status was significant (P-value=0.0072). The difference in age between the groups of patients who achieved CR and the group of patients who did not achieved CR was not significant (P-value=0.15, Wilcoxon rank sum test).*

Table 8: Clinical Characteristics of 119 B-cell Lymphoma Patients Grouped According to Histology.

Variable	Levels	DLBCL	FL	MCL	MZL	SLL	p-value
Gender	F	33(49.3%)	12(35.3%)	.(.%)	2(66.7%)	6(54.5%)	.1964
	M	34(50.7%)	22(64.7%)	4(100%)	1(33.3%)	5(45.5%)	.
Performance Score	0	22(34.9%)	16(48.5%)	2(50%)	3(100%)	7(63.6%)	.4872
	1	26(41.3%)	12(36.4%)	2(50%)	.(.%)	4(36.4%)	.
	2	13(20.6%)	3(9.1%)	.(.%)	.(.%)	.(.%)	.
	3	2(3.2%)	2(6.1%)	.(.%)	.(.%)	.(.%)	.
Ann Arbor Stage	1	6(9.4%)	.(.%)	.(.%)	1(33.3%)	.(.%)	.0289**
	2	7(10.9%)	5(15.6%)	.(.%)	1(33.3%)	.(.%)	.
	3	22(34.4%)	10(31.3%)	2(50%)	1(33.3%)	.(.%)	.
	4	29(45.3%)	17(53.1%)	2(50%)	.(.%)	10(100%)	.
First Rx After Biopsy	A:CHOPTher	33(57.9%)	10(31.3%)	.(.%)	1(50%)	1(11.1%)	<.0001**
	B:CombTher	23(40.4%)	11(34.4%)	3(100%)	.(.%)	.(.%)	.
	C:FludTher	.(.%)	9(28.1%)	.(.%)	.(.%)	7(77.8%)	.
	D:Other	1(1.8%)	2(6.3%)	.(.%)	1(50%)	1(11.1%)	.
Average Number NCL Positive	0	2(3%)	2(5.9%)	.(.%)	1(33.3%)	.(.%)	<.0001**
	1	7(10.4%)	4(11.8%)	1(25%)	.(.%)	8(72.7%)	.
	2	9(13.4%)	15(44.1%)	2(50%)	1(33.3%)	2(18.2%)	.
	3	49(73.1%)	13(38.2%)	1(25%)	1(33.3%)	1(9.1%)	.
Average Intensity of NCL	0	2(3%)	2(5.9%)	.(.%)	1(33.3%)	.(.%)	.0015**
	1	24(35.8%)	20(58.8%)	3(75%)	2(66.7%)	10(90.9%)	.
	2	41(61.2%)	12(35.3%)	1(25%)	.(.%)	1(9.1%)	.
Average Intensity of Ki67	1	9(15%)	6(21.4%)	1(25%)	.(.%)	3(33.3%)	.0003**
	2	12(20%)	12(42.9%)	2(50%)	3(100%)	6(66.7%)	.
	3	39(65%)	10(35.7%)	1(25%)	.(.%)	.(.%)	.

*Data regarding performance status (n=114), Ann Arbor score (n=113), first treatment after biopsy (n=103), and Ki-67 staining (n=104) were not available for all patients; the patients were stratified according to their diagnosis. Fisher's exact test was used to evaluate the associations between histology and other patient characteristics. ** The associations between diagnosis and the following variables were significant: Ann Arbor stage, first treatment after biopsy, the average number of nucleolin-positive cells, the intensity of nucleolin staining and the intensity of Ki-67 staining (P-values=0.0289, <.0001, <.0001, .0015, and .0003, respectively).*

Table 9: Clinical Characteristics of 119 B-cell Lymphoma Patients Grouped According to Performance Score.

Variable	Levels	PS=0	PS=1	PS=2	PS=3	p-value
Gender	F	20(39.2%)	21(41.2%)	10(19.6%)	.(.%)	.1274
	M	30(47.6%)	23(36.5%)	6(9.5%)	4(6.3%)	.
Diagnosis	DLBCL	22(34.9%)	26(41.3%)	13(20.6%)	2(3.2%)	.4872
	FL	16(48.5%)	12(36.4%)	3(9.1%)	2(6.1%)	.
	MCL	2(50%)	2(50%)	.(.%)	.(.%)	.
	MZL	3(100%)	.(.%)	.(.%)	.(.%)	.
	SLL	7(63.6%)	4(36.4%)	.(.%)	.(.%)	.
First Rx After Biopsy	A:CHOPTher	21(46.7%)	16(35.6%)	6(13.3%)	2(4.4%)	.0467**
	B:CombTher	8(25%)	18(56.3%)	6(18.8%)	.(.%)	.
	C:FludTher	9(56.3%)	5(31.3%)	1(6.3%)	1(6.3%)	.
	D:Other	4(80%)	.(.%)	.(.%)	1(20%)	.
Average Number NCL Positive	0	4(80%)	.(.%)	.(.%)	1(20%)	.0096**
	1	8(40%)	11(55%)	1(5%)	.(.%)	.
	2	15(55.6%)	4(14.8%)	7(25.9%)	1(3.7%)	.
	3	23(37.1%)	29(46.8%)	8(12.9%)	2(3.2%)	.
Average Intensity of NCL	0	4(80%)	.(.%)	.(.%)	1(20%)	.0585
	1	27(47.4%)	21(36.8%)	9(15.8%)	.(.%)	.
	2	19(36.5%)	23(44.2%)	7(13.5%)	3(5.8%)	.
Average Intensity of Ki67	1	8(44.4%)	8(44.4%)	1(5.6%)	1(5.6%)	.0938
	2	21(60%)	12(34.3%)	2(5.7%)	.(.%)	.
	3	15(32.6%)	19(41.3%)	10(21.7%)	2(4.3%)	.

*Data regarding Ann Arbor score (n=113), first treatment after biopsy (n=103), and Ki-67 staining (n=104) were not available for all patients; the patients were stratified according to their performance score. Fisher's exact test was used to evaluate the associations between performance score and other patient characteristics. ** The associations between performance score and the following variables were significant or marginally significant: first treatment after biopsy and the average number of nucleolin positive cells and the intensity of nucleolin staining (P-values= .0467, .0096, and 0.0585, respectively).*

Figure 20

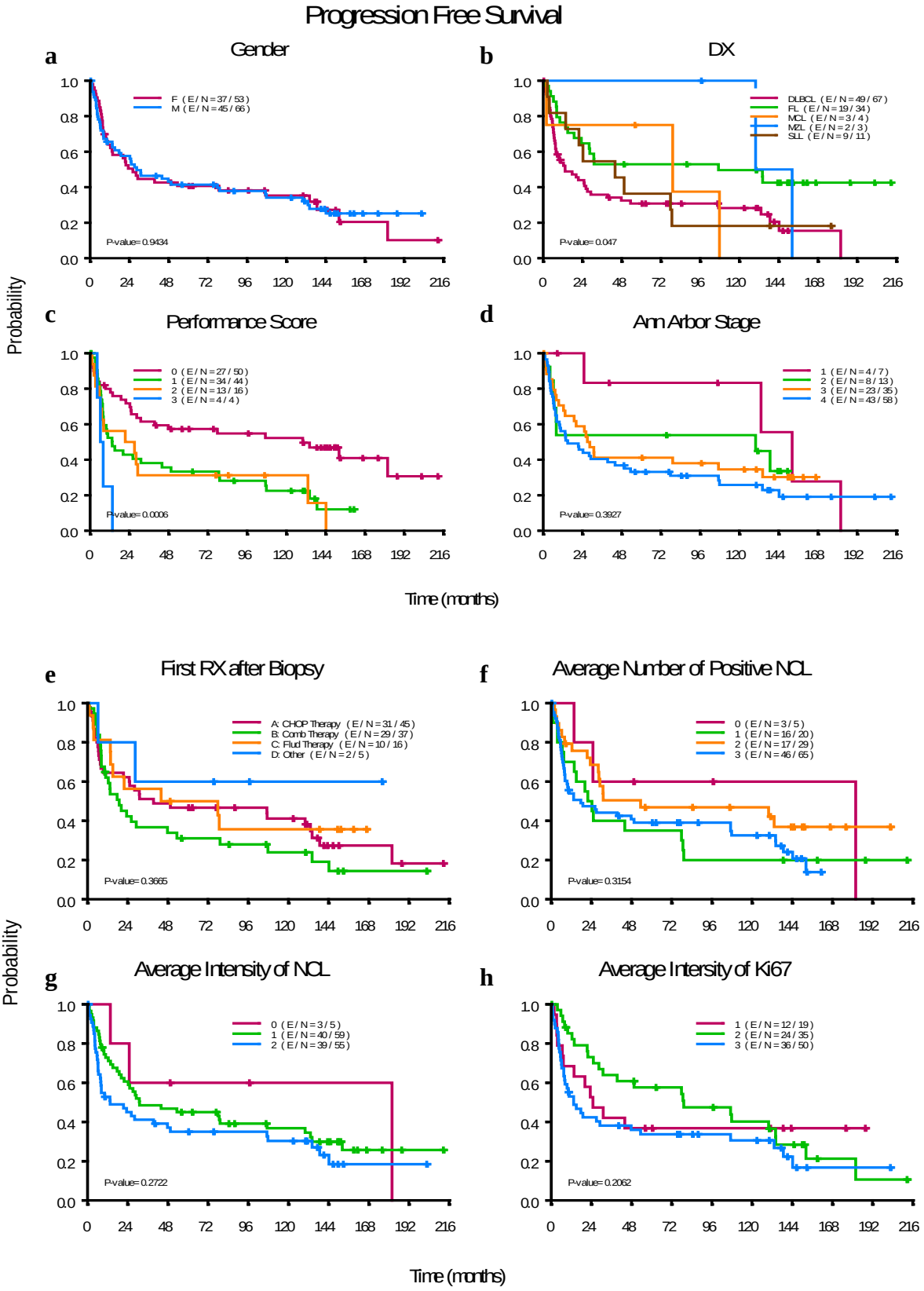
Progression Free Survival
a
Gender
F (E/N=37/53)
M (E/N=45/66)
P-value=0.9434
b
DX
DLBCL (E/N=49/67)
FL (E/N=19/34)
MCL (E/N=3/4)
MZL (E/N=2/3)
SLL (E/N=9/11)
P-value=0.047
c
Performance Score
0 (E/N=27/50)
1 (E/N=34/44)
2 (E/N=13/16)
3 (E/N=4/4)
P-value=0.0006
d
Ann Arbor Stage
1 (E/N=4/7)
2 (E/N=8/13)
3 (E/N=23/35)
4 (E/N=43/58)
P-value=0.3927
Probability
Time (months)
e
First RX after Biopsy
A: CHOP Therapy (E/N=31/45)
B: Comb Therapy (E/N=29/37)
C: Flud Therapy (E/N=10/16)
D: Other (E/N=2/5)
P-value=0.3665
f
Average Number of Positive NCL
0 (E/N=3/5)
1 (E/N=16/20)
2 (E/N=17/29)
3 (E/N=46/65)
P-value=0.3154
g
Average Intensity of NCL
0 (E/N=3/5)
1 (E/N=40/59)
2 (E/N=39/55)
P-value=0.2722
h
Average Intensity of Ki67
1 (E/N=12/19)
2 (E/N=24/35)
3 (E/N=36/50)
P-value=0.2062
Probability
Time (months)

Figure 20: Progression Free Survival of Patients with B-cell Lymphomas.

According to (a) gender stratified by male and female; (b) diagnosis stratified by DLBCL, FL, MCL, marginal zone lymphoma (MZL) and SLL; (c) performance score stratified by 0-3 scoring; (d) Ann Arbor staging stratified by 0-4 staging; (e) first treatment after biopsy stratified by CHOP, combination, Fludarabine, or other treatment regimens; (f) average number of nucleolin positive cells stratified by 0-3 scoring; (g) average intensity of nucleolin staining stratified by 0-2 scoring; (h) average intensity of Ki-67 staining stratified by 1-3 scoring. Time was calculated from biopsy date to progression date or death date, whichever occurred first. Patients were censored at the last follow-up date if progression or death had not occurred. The median PFS time was 27.1 months (95% CI: 18.9, 78.8). The difference in PFS among performance score and diagnosis groups were significant (P-values=.0006 and .047, respectively)

Table 10: The Progression Free Survival Rates at Years 1, 3, and 5 along with the 95% Confidence Intervals.

Variable	Level	N	Event	Median PFS time in months (95%CI)	PFS Rate at 1 Year (95%CI)	PFS Rate at 3 Years (95%CI)	PFS Rate at 5 Years (95%CI)	p-value
	All patients	119	82	27.1 (18.89 , 78.75)	0.65 (0.57 , 0.74)	0.46 (0.37 , 0.56)	0.41 (0.33 , 0.51)	
Gender	F	53	37	26.22 (13.44 , 134.1)	0.64 (0.52 , 0.78)	0.45 (0.33 , 0.6)	0.41 (0.29 , 0.56)	0.9434
	M	66	45	28.55 (15.08 , 107.79)	0.66 (0.55 , 0.78)	0.46 (0.36 , 0.61)	0.41 (0.31 , 0.56)	
Diagnosis	DLBCL	67	49	13.47 (7.88 , 29.17)	0.54 (0.43 , 0.67)	0.36 (0.26 , 0.5)	0.31 (0.21 , 0.45)	0.047**
	FL	34	19	107.23 (28.12 , NA)	0.76 (0.63 , 0.92)	0.53 (0.39 , 0.73)	0.53 (0.39 , 0.73)	
	MCL	4	3	79.24 (2.07 , NA)	0.75 (0.43 , 1)	0.75 (0.43 , 1)	0.75 (0.43 , 1)	
	MZL	3	2	141.08 (129.93 , NA)	1 (1 , 1)	1 (1 , 1)	1 (1 , 1)	
	SLL	11	9	43.92 (21.91 , NA)	0.82 (0.62 , 1)	0.55 (0.32 , 0.94)	0.36 (0.17 , 0.79)	
Performance Score	0	50	27	129.93 (30.91 , NA)	0.8 (0.7 , 0.92)	0.62 (0.49 , 0.77)	0.57 (0.45 , 0.73)	0.0006**
	1	44	34	13.45 (8.08 , 78.75)	0.52 (0.39 , 0.7)	0.38 (0.26 , 0.56)	0.33 (0.22 , 0.51)	
	2	16	13	24.31 (6.34 , NA)	0.56 (0.37 , 0.87)	0.31 (0.15 , 0.65)	0.31 (0.15 , 0.65)	
	3	4	4	7.15 (4.37 , NA)	0.25 (0.05 , 1)			
Ann Arbor Stage	1	7	4	152.23 (133.18 , NA)	1 (1 , 1)	0.83 (0.58 , 1)	0.83 (0.58 , 1)	0.3927
	2	13	8	129.93 (6.64 , NA)	0.54 (0.33 , 0.89)	0.54 (0.33 , 0.89)	0.54 (0.33 , 0.89)	
	3	35	23	27.83 (18.89 , NA)	0.71 (0.57 , 0.88)	0.41 (0.28 , 0.62)	0.41 (0.28 , 0.62)	
	4	58	43	15.08 (9.82 , 49.47)	0.56 (0.45 , 0.71)	0.4 (0.29 , 0.55)	0.33 (0.23 , 0.48)	
First Rx After Biopsy	A: CHOP Therapy	45	31	39.39 (21.52 , 138.7)	0.64 (0.52 , 0.8)	0.51 (0.38 , 0.68)	0.47 (0.34 , 0.64)	0.3665
	B: Comb Therapy	37	29	18.89 (10.78 , 79.24)	0.62 (0.48 , 0.8)	0.37 (0.24 , 0.56)	0.31 (0.19 , 0.51)	
	C: Flud Therapy	16	10	60.87 (13.83 , NA)	0.81 (0.64 , 1)	0.56 (0.37 , 0.87)	0.5 (0.31 , 0.82)	
	D: Other	5	2	NA (28.55 , NA)	0.8 (0.52 , 1)	0.6 (0.29 , 1)	0.6 (0.29 , 1)	
Average Number NCL Positive	0	5	3	181.87 (24.93 , NA)	1 (1 , 1)	0.6 (0.29 , 1)	0.6 (0.29 , 1)	0.3154
	1	20	16	23.14 (13.83 , 79.24)	0.7 (0.53 , 0.93)	0.4 (0.23 , 0.68)	0.35 (0.19 , 0.64)	
	2	29	17	53.45 (28.12 , NA)	0.79 (0.66 , 0.96)	0.5 (0.35 , 0.73)	0.47 (0.32 , 0.7)	
	3	65	46	17.67 (8.21 , 107.23)	0.54 (0.43 , 0.68)	0.44 (0.33 , 0.58)	0.39 (0.29 , 0.53)	
Average Intensity of NCL	0	5	3	181.87 (24.93 , NA)	1 (1 , 1)	0.6 (0.29 , 1)	0.6 (0.29 , 1)	0.2722
	1	59	40	31.04 (21.91 , 129.93)	0.73 (0.62 , 0.85)	0.49 (0.37 , 0.63)	0.45 (0.34 , 0.6)	
	2	55	39	13.47 (7.88 , 107.13)	0.53 (0.41 , 0.68)	0.41 (0.3 , 0.57)	0.35 (0.24 , 0.51)	
Average Intensity of Ki67	1	19	12	24.93 (13.67 , NA)	0.68 (0.5 , 0.93)	0.42 (0.25 , 0.71)	0.37 (0.2 , 0.66)	0.2062
	2	35	24	79.24 (30.91 , 152.23)	0.85 (0.74 , 0.98)	0.64 (0.49 , 0.83)	0.58 (0.43 , 0.77)	
	3	50	36	13.47 (8.02 , 107.13)	0.53 (0.41 , 0.69)	0.38 (0.27 , 0.55)	0.34 (0.23 , 0.5)	

*Performance status (n=114), Ann Arbor score (n=113), first treatment after biopsy (n=103), and Ki-67 staining (n=104) were not available for all patients. PFS rates at years 1, 3, and 5 along with the 95% confidence intervals and the P-values from the log-rank test (univariable analysis) are provided. ** The difference in PFS among the five histology groups was significant (P-value=0.047). The difference in PFS among the 4 performance score groups was also significant (P-value=0.0006).*

Figure 21

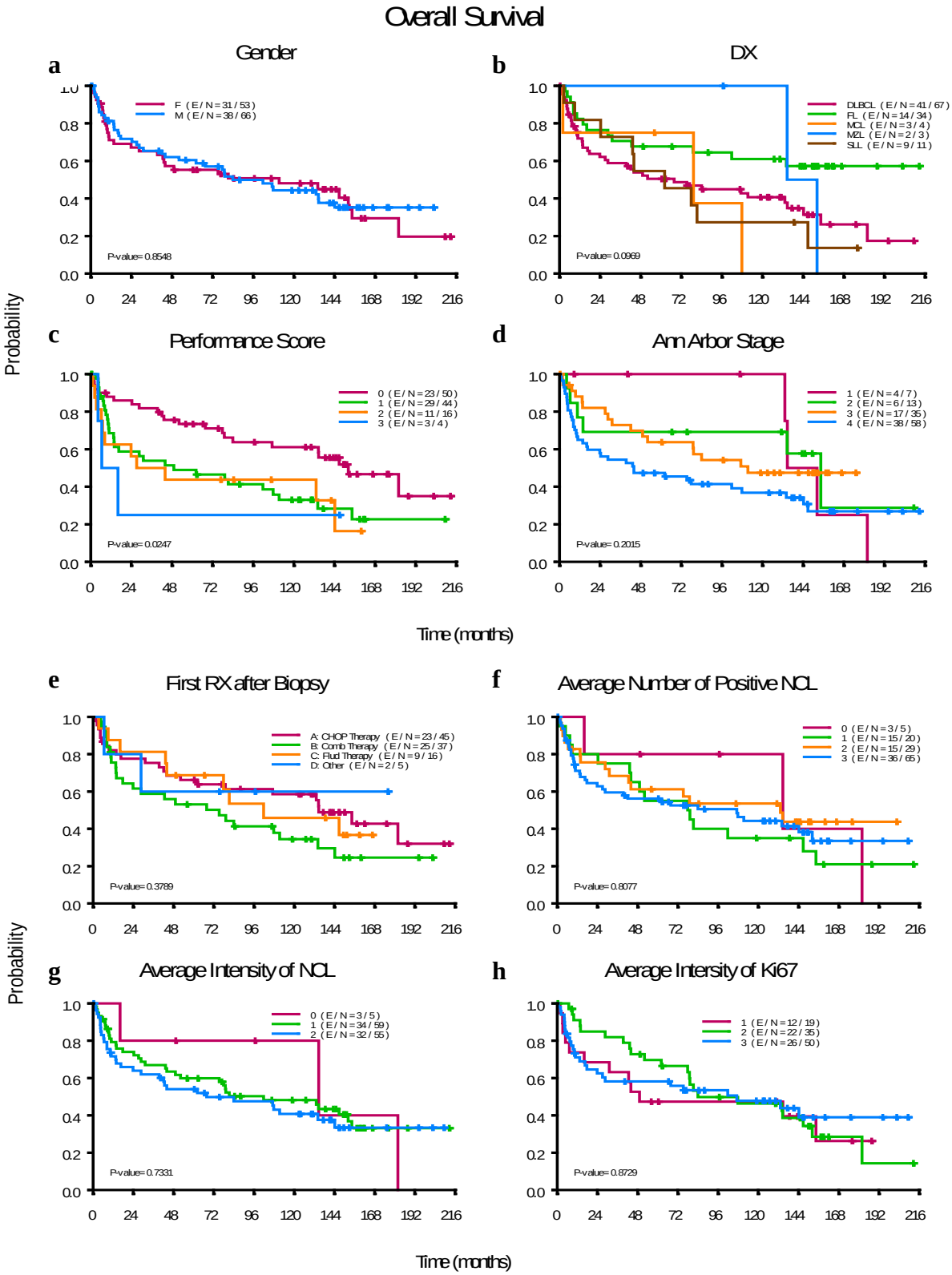
Overall Survival
a
Gender
F (E/N=31/53)
M (E/N=38/66)
P-value=0.8548
b
DX
DLBCL (E/N=41/67)
FL (E/N=14/34)
MCL (E/N=3/4)
MZL (E/N=2/3)
SLL (E/N=9/11)
P-value=0.0969
c
Performance Score
0 (E/N=23/50)
1 (E/N=29/44)
2 (E/N=11/16)
3 (E/N=3/4)
P-value=0.0247
d
Ann Arbor Stage
1 (E/N=4/7)
2 (E/N=6/13)
3 (E/N=17/35)
4 (E/N=38/58)
P-value=0.2015
Probability
Time (months)
e
First RX after Biopsy
A: CHOP Therapy (E/N=23/45)
B: Comb Therapy (E/N=25/37)
C: Fludarabine Therapy (E/N=9/16)
D: Other (E/N=2/5)
P-value=0.3789
f
Average Number of Positive NCL
0 (E/N=3/5)
1 (E/N=15/20)
2 (E/N=15/29)
3 (E/N=36/65)
P-value=0.8077
g
Average Intensity of NCL
0 (E/N=3/5)
1 (E/N=34/59)
2 (E/N=32/55)
P-value=0.7331
h
Average Intersity of Ki67
1 (E/N=12/19)
2 (E/N=22/35)
3 (E/N=26/50)
P-value=0.8729
Probability
Time (months)

Figure 21: Overall Survival of Patients with B-cell Lymphomas.

According to (a) gender stratified by male and female; (b) diagnosis stratified by DLBCL, FL, MCL, MZL and SLL; (c) performance score stratified by 0-3 scoring; (d) Ann Arbor staging stratified by 0-4 staging; (e) first treatment after biopsy stratified by CHOP, combination, fludarabine, or other treatment regimens; (f) average number of nucleolin positive cells stratified by 0-3 scoring; (g) average intensity of nucleolin staining stratified by 0-2 scoring; (h) average intensity of Ki-67 staining stratified by 1-3 scoring. OS time was calculated from biopsy date to death date. Patients were censored at the last follow-up date if death had not occurred. The median overall survival time was 102 months (95% CI: 52.1, 147). The median follow-up time for the censored observations was 137.98 months (range: 0.39 – 212.62). The difference in OS among performance scores was significant (P-value=.0247)

Table 11: The Overall Survival (OS) Rates at Years 1, 3, and 5 along with the 95% Confidence Intervals.

Variable	Level	N	Event	Median OS time in months (95%CI)	OS Rate at 1 Year (95%CI)	OS Rate at 3 Years (95%CI)	OS Rate at 5 Years (95%CI)	p-value
	All patients	119	69	101.77 (52.14 , 146.81)	0.77 (0.69 , 0.85)	0.65 (0.57 , 0.75)	0.58 (0.5 , 0.68)	
Gender	F	53	31	111.3 (42.61 , NA)	0.71 (0.6 , 0.85)	0.65 (0.53 , 0.8)	0.55 (0.43 , 0.71)	0.8548
	M	66	38	84 (52.14 , NA)	0.81 (0.72 , 0.91)	0.65 (0.55 , 0.78)	0.6 (0.49 , 0.74)	
Diagnosis	DLBCL	67	41	67.74 (27.1 , 144.28)	0.72 (0.62 , 0.84)	0.59 (0.48 , 0.72)	0.5 (0.39 , 0.65)	0.0969
	FL	34	14	NA (101.77 , NA)	0.82 (0.7 , 0.96)	0.71 (0.57 , 0.88)	0.68 (0.54 , 0.85)	
	MCL	4	3	79.24 (2.07 , NA)	0.75 (0.43 , 1)	0.75 (0.43 , 1)	0.75 (0.43 , 1)	
	MZL	3	2	143.36 (134.49 , NA)	1 (1 , 1)	1 (1 , 1)	1 (1 , 1)	
	SLL	11	9	62.19 (43.2 , NA)	0.82 (0.62 , 1)	0.73 (0.51 , 1)	0.55 (0.32 , 0.94)	
Performance Score	0	50	23	152.23 (107.13 , NA)	0.88 (0.79 , 0.97)	0.82 (0.72 , 0.93)	0.73 (0.62 , 0.87)	0.0247**
	1	44	29	49.11 (13.86 , 134.1)	0.69 (0.56 , 0.84)	0.54 (0.41 , 0.71)	0.49 (0.36 , 0.67)	
	2	16	11	35.56 (6.96 , NA)	0.62 (0.43 , 0.91)	0.5 (0.31 , 0.82)	0.44 (0.25 , 0.76)	
	3	4	3	11.32 (4.37 , NA)	0.5 (0.19 , 1)	0.25 (0.05 , 1)	0.25 (0.05 , 1)	
Ann Arbor Stage	1	7	4	143.45 (133.18 , NA)	1 (1 , 1)	1 (1 , 1)	1 (1 , 1)	0.2015
	2	13	6	154.4 (13.86 , NA)	0.77 (0.57 , 1)	0.69 (0.48 , 0.99)	0.69 (0.48 , 0.99)	
	3	35	17	111.3 (52.14 , NA)	0.88 (0.78 , 1)	0.73 (0.59 , 0.9)	0.64 (0.49 , 0.82)	
	4	58	38	43.92 (16.59 , 144.28)	0.65 (0.54 , 0.79)	0.54 (0.43 , 0.69)	0.47 (0.36 , 0.62)	
First Rx After Biopsy	A: CHOP Therapy	45	23	134.66 (78.98 , NA)	0.82 (0.72 , 0.94)	0.75 (0.64 , 0.89)	0.66 (0.54 , 0.82)	0.3789
	B: Comb Therapy	37	25	75.3 (23.82 , 144.28)	0.75 (0.63 , 0.91)	0.59 (0.45 , 0.77)	0.53 (0.39 , 0.72)	
	C: Flud Therapy	16	9	101.77 (43.92 , NA)	0.88 (0.73 , 1)	0.81 (0.64 , 1)	0.69 (0.49 , 0.96)	
	D: Other	5	2	NA (28.58 , NA)	0.8 (0.52 , 1)	0.6 (0.29 , 1)	0.6 (0.29 , 1)	
Average Number NCL Positive	0	5	3	134.66 (134.66 , NA)	1 (1 , 1)	0.8 (0.52 , 1)	0.8 (0.52 , 1)	0.8077
	1	20	15	78.53 (43.92 , NA)	0.8 (0.64 , 1)	0.75 (0.58 , 0.97)	0.55 (0.37 , 0.82)	
	2	29	15	133.18 (42.61 , NA)	0.83 (0.7 , 0.98)	0.68 (0.53 , 0.88)	0.61 (0.46 , 0.82)	
	3	65	36	107.13 (28.58 , NA)	0.71 (0.61 , 0.83)	0.6 (0.48 , 0.73)	0.56 (0.45 , 0.7)	
Average Intensity of NCL	0	5	3	134.66 (134.66 , NA)	1 (1 , 1)	0.8 (0.52 , 1)	0.8 (0.52 , 1)	0.7331
	1	59	34	101.77 (52.14 , NA)	0.79 (0.7 , 0.9)	0.67 (0.56 , 0.8)	0.6 (0.48 , 0.74)	
	2	55	32	67.74 (39.39 , NA)	0.72 (0.61 , 0.85)	0.62 (0.5 , 0.77)	0.54 (0.42 , 0.69)	
Average Intensity of Ki67	1	19	12	49.11 (31.04 , NA)	0.74 (0.56 , 0.96)	0.63 (0.45 , 0.89)	0.47 (0.29 , 0.76)	0.8729
	2	35	22	84 (77.83 , NA)	0.91 (0.82 , 1)	0.82 (0.7 , 0.96)	0.7 (0.56 , 0.87)	
	3	50	26	107.13 (27.1 , NA)	0.71 (0.59 , 0.85)	0.58 (0.46 , 0.74)	0.58 (0.46 , 0.74)	

*Performance status (n=114), Ann Arbor score (n=113), first treatment after biopsy (n=103), and Ki-67 staining (n=104) were not available for all patients. Survival rates at years 1, 3, and 5 along with the 95% confidence intervals and the P-values from the log-rank test (univariable analysis) are provided. ** The difference in OS among the five histology groups was marginally significant (P-value=0.0969). The difference in OS among the 4 performance score groups was significant (P-value=0.0247).*

Table 12: Association between Nucleolin and Ki-67 Markers.

Variable	Levels	Average intensity of Ki67 =1	Average intensity of Ki67 =2	Average intensity of Ki67 =3	p-value
Average Number NCL Positive	0	2(40%)	3(60%)	.(.%)	<.0001
	1	6(33.3%)	9(50%)	3(16.7%)	.
	2	7(29.2%)	10(41.7%)	7(29.2%)	.
	3	4(7%)	13(22.8%)	40(70.2%)	.
Average Intensity of NCL	0	2(40%)	3(60%)	.(.%)	<.0001
	1	12(23.1%)	24(46.2%)	16(30.8%)	.
	2	5(10.6%)	8(17%)	34(72.3%)	.

Fisher's exact test was used to evaluate the association between average intensity of Ki67 and the two values representing NCL staining. The association between average intensity of Ki67 and average number of positive NCL was significant (P-value<0.0001). The association between average intensity of Ki67 and average intensity of NCL was also significant (p-value<0.0001).

Figure 22

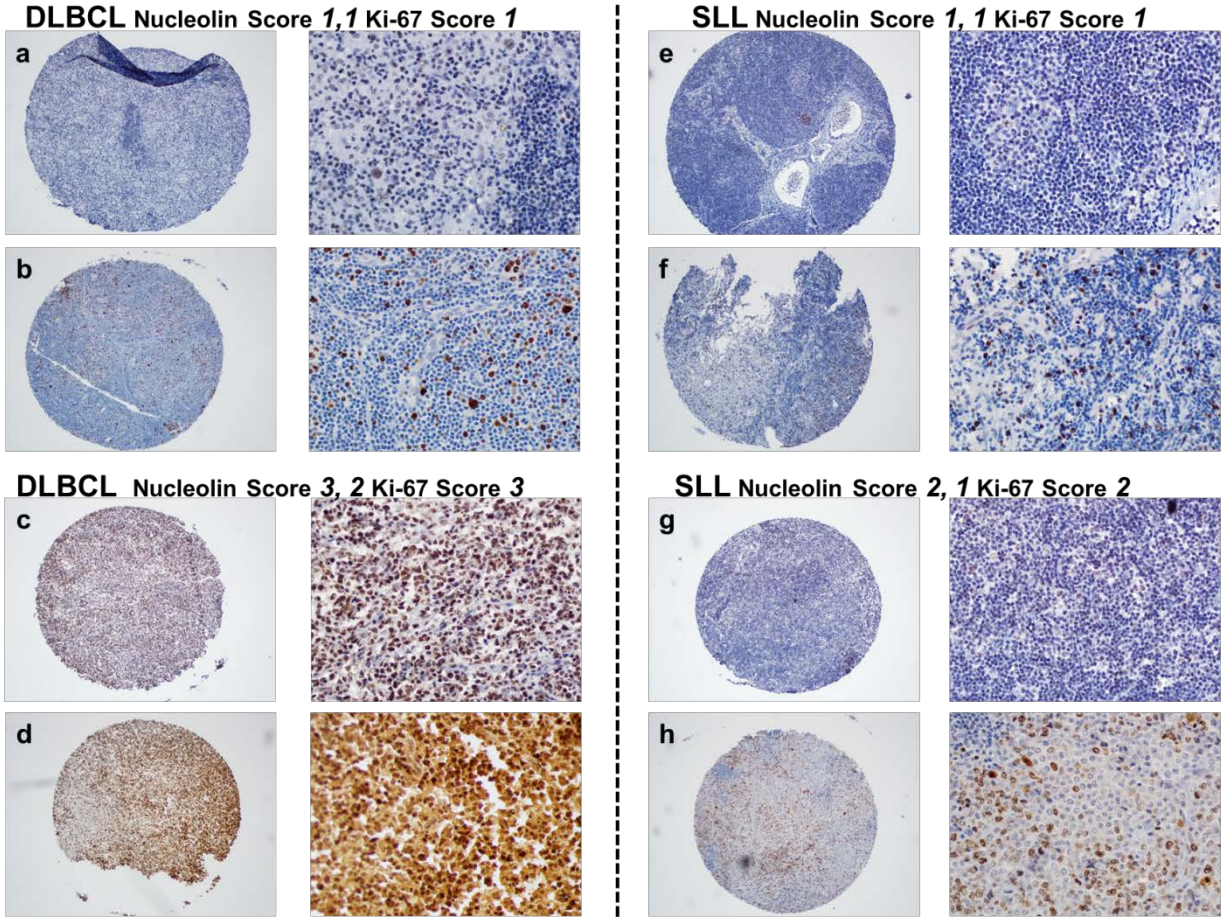

Figure 22: Correlation between Nucleolin and Ki-67 Staining in a DLBCL and SLL.

Representative examples of nucleolin and Ki-67 correlative staining. (a) DLBCL with 1-25% nucleolin-positivity average and low nucleolin intensity score at 10X and 40X, left to right and (b) corresponding low Ki-67 expression at 10X and 40X. (c) DLBCL with <75% nucleolin-positivity average and high nucleolin intensity score at 10X and 40X, left to right; and (d) corresponding high score 3 Ki-67 expression at 10X and 40X. (e) SLL with 1-25% nucleolin-positivity average and low nucleolin intensity score at 10X and 40X, left to right; and (f) corresponding low Ki-67 expression at 10X and 40X. (g) SLL with 25-75% nucleolin-positivity average and low nucleolin intensity score at 10X and 40X, left to right and (h) corresponding intermediate Ki-67 score of 2 at 10X and 40X. The images were captured by the Olympus BX41 microscope system. An Olympus Model DP72 camera and cellSens Standard 1.6 software (Olympus Corporation) was used for acquiring images.

Summary

Our analysis of nucleolin expression revealed that mRNA levels are neither significantly nor consistently upregulated in B-cell lymphomas when compared to healthy individual's B cells. However, as determined by IB, nucleolin protein expression levels were elevated in multiple B-cell lymphoma cell lines, DLBCL and MCL tissues compared to healthy donor isolate B lymphocytes. The fractionation of cytosolic and nuclear proteins from B-cell lymphoma cell lines and healthy donor's B cells revealed increased nucleolin levels in the cytosolic fraction from lymphoma cells. Membrane biotinylation followed by IP of biotin revealed the presence of nucleolin on the cell surface in various B-cell lymphoma cell lines. The preferential nucleolin overexpression and translocation to the cytosol and cell surface indicated deregulation of nucleolin expression in B-cell lymphomas.

We addressed the clinical impact of surface nucleolin by analyzing and comparing healthy individual B cells, cell lines, and MCL, DLBCL, and CLL primary samples by flow cytometry. We found that surface nucleolin was significantly increased in B-cell lymphomas compared to healthy donor B cells. The presence of surface nucleolin was associated with a high risk IPI in patients with B-cell lymphoma. Total nucleolin expression was evaluated by a TMA analysis of a large series of samples from patient with DLBCL, FL, MZL, MCL, and SLL/CLL treated with various chemotherapy regimens. Total nucleolin levels did not show an association with poor clinical outcome, nor with response to chemotherapy as our previous studies on surface nucleolin and Fas had suggested. The 119 TMA patient samples included five different histologic lymphomas, and tissue from naïve as well as relapsed lymphoma which could hinder our assessment of patients. The performance score was highly associated with response status, PFS, OS, and clinical characteristics of our cohort and represented the best single clinical correlative associated with the clinical outcome in this patient population. We found that total nucleolin levels correlated positively with aggressive lymphoma types with the highest nucleolin levels were expressed in DLBCL and lowest levels in CLL/SLL. This relationship may simply be related to the Ki-67 proliferation rates and nucleolin levels. Thus nucleolin levels and Ki-67 levels both indicated a reflection of proliferation levels in these cancers and substantiate the agreement of two prognostic markers in B-cell lymphomas.

Limitations and Future Directions

This report extends the observations of cancer-specific overexpression of nucleolin to B-cell lymphomas, which was not previously characterized. As a retrospective study, there are key elements that could be improved to allow a more robust and comprehensive analysis. The surface

nucleolin was detected in recently collected samples from the MD Anderson Lymphoma Tissue Bank, and therefore follow-up data is limited. Additionally, the Ki-67 staining was not completed on all patients in this cohort, and therefore we were unable to determine if nucleolin's surface expression also correlates with Ki-67 staining scores. It will be beneficial to design a prospective study collecting the follow-up data over time to determine if surface nucleolin is a predictor of outcome.

The surface nucleolin levels were not correlated with the clinical outcome in our TMA, largely because we were unable to distinguish nuclear, cytoplasmic, and surface nucleolin by the employed immunohistochemistry (IHC) method using nucleolin H-6 antibody (Santa Cruz Biotechnologies). Subcellular location of an antigen is a challenge in tissue sections and other staining methods may offer better resolution. This analysis will require a single cell suspension, surface-specific nucleolin antibody or at least a cytoplasmic nucleolin antibody (as both localizations appear to be affected in B-cell lymphomas). It has been reported that nucleolin antibody D3 produces a high surface staining; it may be interesting to determine if we see better extra-nuclear staining by IHC.(178) Moreover, a glycosylated nucleolin specific antibody, gp273, created by Galzio et al. (267), could be utilized to detect surface destined nucleolin, as it has been suggested that newly glycosylated nucleolin is targeted to the surface and cytoplasm.(175) Unfortunately, neither antibody is commercially available. By enriching the TMA with these antibodies, we can better address whether redistribution of nucleolin to the cell surface is a predictor of clinical outcome in B-cell lymphomas, as suggested by correlation of our flow cytometry data with IPI.

Lastly, selection of a group of patients that represents a more homogenous population with fewer variables would strengthen our data. A better group of patients to study would be patients of a single histologic type with all biopsies take prior to treatment start dates which have long follow-up periods. We predict that an SLL cohort may give a significant correlation of nucleolin levels with chemotherapeutic response and outcome, as SLL patients in our cohort had a wide range of Ki-67 and nucleolin marker staining. This would help eliminate most confounding factors caused by the differences in natural history of lymphomas, treatment plans and toxicity profiles.

Chapter 6: Discussion

Fas apoptotic signaling is important for chemotherapy-induced tumor cell elimination. Multiple chemotherapies, including those for lymphomas (doxorubicin, methotrexate, mitoxantrone, bleomycin and rituximab), have been shown to upregulate Fas or/and FasL to promote a more robust tumor elimination potential.(108-111, 113, 115, 143, 308) However, cancers often block Fas signaling through Fas mutagenesis, downregulation of key players in the Fas signaling cascade, and overexpression of apoptosis inhibitors such as c-FLIP and bcl-2 family proteins to achieve chemoresistance.(149, 309) Therefore, it is clear that chemoresistance in cancer has multifactorial origins that converge at Fas signaling.(46, 82, 105, 108, 141) In lymphomas, wild-type Fas is commonly expressed, and overexpression of c-FLIP and bcl-2 family members cannot always explain the observed resistance to Fas-mediated apoptosis.(310) In our investigation into the mechanisms of Fas evasion, we discovered nucleolin as a novel binding partner in activation-resistant Fas in B-cell lymphomas. Nucleolin is a multifunctional protein associated with pro-survival functions in actively dividing cells and its targeting may represent a novel clinical tool for the treatment of B-cell malignancies.

This work revealed that nucleolin-Fas complexes exist on the surface of B-cell lymphomas but not in healthy B cells. We mapped the Fas binding site of nucleolin to the R4-GAR C-terminal domains. We successfully created stable partial nucleolin knockdown cells. Remarkably, nucleolin knockdowns were sensitive to Fas-mediated apoptosis without an increase in Fas surface levels. Further supporting evidence was revealed by evaluation of DISC assembly and caspase activation post-CH-11 challenge of nucleolin partial knockdown cells. We showed an increase in Fas agonist binding to nucleolin in partial knockdowns in comparison with parental and non-silencing BJAB cells. In vivo data confirmed protection against Fas-induced death by nucleolin but not by the nucleolin mutant that did not bind Fas.

Results from previous investigations revealed a correlation with nucleolin and overall survival of pediatric ependymoma, glioma, and melanoma patients.(265, 267, 268) We obtained evidence through flow cytometry that nucleolin surface levels correlate with a worse prognostic risk as determined by the IPI. However, analysis of total nucleolin levels in a TMA of 119 B-cell lymphoma patients did not show an association with nucleolin levels and with progression free survival or overall survival. These results are consistent with surface nucleolin and nucleolin that can bind Fas as the clinically important fraction. We acknowledge there are limitations of the study in that the differences in nucleolin expression as a prognostic and diagnostic marker could be

related to the lack of uniformity among staining techniques. Our assays were performed with a nucleolin antibody different from other studies. Nucleolin levels were associated with diagnosis and performance score and correlated with Ki-67 staining, suggesting total nucleolin as having a proliferative measurement capacity.

We conclude that nucleolin is a novel binding modulator of the Fas death receptor selectively present on the surface of human lymphomas where it effectively blocks Fas signaling as diagramed in Figure 23. Given the common surface expression of nucleolin and the often-impaired Fas signaling in cancer, we predict that nucleolin contributes to chemoresistance and, because of its surface localization, is a viable target for new therapeutic interventions. Therefore, future studies building on the results of this investigation would develop nucleolin-targeting therapeutics with effectiveness in eliminating multiple cancers.

Figure 23:

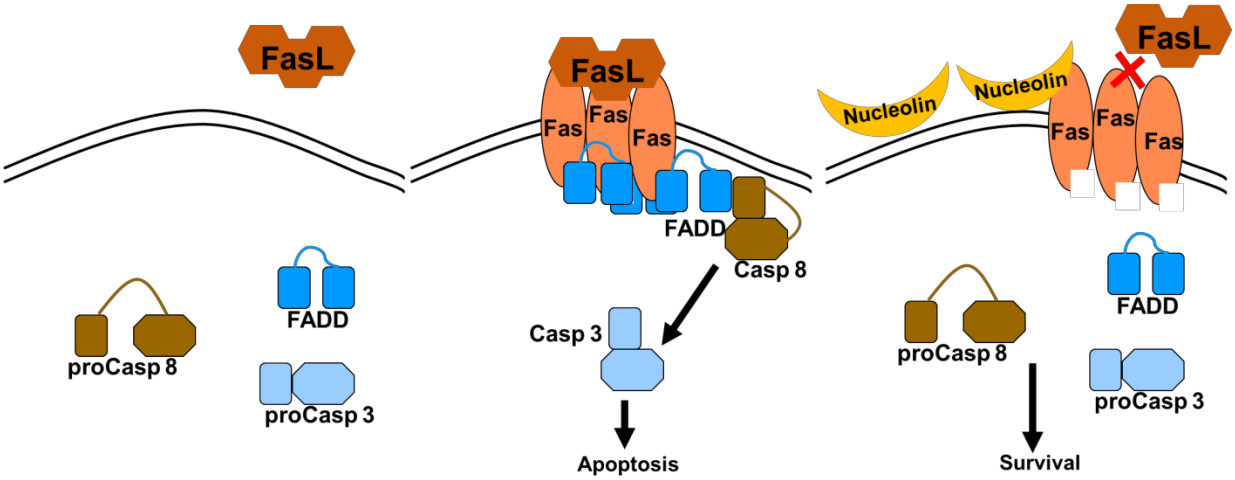

Resting B-cell	Activated/Germinal Center B-cell	B-cell Lymphoma
Low Levels of Nucleolin and Fas	Low Levels of Nucleolin	High Levels of Nucleolin
Cytoplasmic/Nuclear Nucleolin	Cytoplasmic/Nuclear Nucleolin	Surface/Cytoplamic/Nuclear Nucleolin
No Nucleolin-Fas Complex	No Nucleolin-Fas Complex	Nucleolin-Fas Complex Formation

Figure 23: Nucleolin and Fas Regulation in B cells.
Diagram representing our conclusions on nucleolin in B cells and its effects on Fas-mediated apoptotic signaling.

Future Studies

Nucleolin's Effect on Chemotherapy-induced Cell Death

This dissertation clearly demonstrates that nucleolin binds Fas and negatively affects its ability to signal apoptosis. As Fas signaling has been implicated in responses to and the effectiveness of multiple chemotherapy regimens, the next logical extension of our investigation would be to test the sensitivity of nucleolin knockdowns to chemotherapies which have been suggested to utilize Fas, doxorubicin, bleomycin and etoposide. To accomplish these studies, our current stable nucleolin partial knockdown cell lines can be utilized in cell death and cell proliferation assays post-chemotherapy treatment to determine sensitivity. Alternatively, as mentioned previously, a tet-on/off system would allow for a more significant nucleolin decrease and could be utilized in a mouse xenograft tumor growth model in which the effects of doxorubicin, bleomycin, and etoposide could be tested in vivo. These assays would provide further information on levels of nucleolin contributing to chemoresistance, and they could extend to investigations into nucleolin's contribution to chemoresistance in the clinic.

Nucleolin-Fas Complexes and their Dependency on Cell Cycle

Previous studies suggest that nucleolin's modifications, localization and functions have been linked to cell cycle progression, specifically that nucleolin levels rise during G_0-G_1 transition and mitosis.(152, 181) It would be interesting to decipher whether the nucleolin-Fas complex is cell cycle regulated within the context of B cells. For example, does nucleolin bind Fas during or prior to cell division to prevent inadvertent apoptosis at vulnerable phases of the cell cycle or does it constantly protect Fas from FasL stimulation? Specifically, we propose to evaluate nucleolin expression through PCR analysis and Western blotting along with nucleolin-Fas complex formation through coIP following artificial cell cycle synchronization. Cell cycle synchronization can be achieved by several treatments listed in Table 13(311, 312) and can be monitored by flow cytometry analysis of cell cycle in propidium iodide-stained cells.(313) It is important to note that many of the chemical blocks can induce apoptosis and alter Fas-trafficking, therefore it will be important to monitor cell viability and nucleolin function prior to analysis. By performing the proposed analyses we can shed more light on the role of nucleolin-Fas complex regulation in B-cell lymphomas.

Table 13: Potential Cell Cycle Synchronization Methods.

Treatment/Method	Treatment Schedule	Cell Cycle Enrichment Phase
Nocodazole*(312)*	12-16hrs	M Phase
Excess Thymidine*(312)*	10hrs	M Phase
Serum Starvation*(312)*	24-48hrs	G_0 Phase
Isoleucine Depletion*(312)*	36-42hrs	G_0 Phase
Lovastatin*(312)*	24-36hrs	G_1 Phase
Double-Thymidine*(312)* **(Hydroxyurea, Aphidicolin)**	12hrs → release 8hrs → 12hrs	S Phase

Cell synchronizations can be tested with various chemicals and treatments: nocodazole, excess thymidine, serum starvation, isoleucine depletion, lovastatin, and double-thymidine. The treatment time and resulting cell cycle enrichment phase is given for each potential method.(312)

Nucleolin's Role in Apoptosis Regulation throughout B-cell Development

Apoptotic signaling is used throughout every step of B-cell differentiation, and therefore Fas regulatory mechanisms are carefully coordinated throughout the maturation process.(4) The apoptotic and anti-apoptotic molecules that orchestrate the survival or death of cells during B-cell development work in collaboration. Fas and Bcl-2 are two molecules whose expression is finely tuned throughout B-cell development. As B cells proceed through the negative selection processes in the germinal centers of the lymphoid tissue, the anti-apoptotic Bcl-2 molecule is downregulated while apoptosis-mediating Fas molecule is expressed in high levels. In the mantle zones of lymphoid tissues, in which the antigen-dependent humoral response of B cells occurs, Fas expression is lowered while Bcl-2 is inversely upregulated.(102, 149) Therefore, the inverse relationship between Fas and Bcl-2 expression is essential for an effective development and response by B cells (Figure 24). However, disruption of this balance can result in lymphoproliferative disease, lymphoma development and inadequate immune responses. On the basis of our and previous findings that nucleolin participates in the regulation of both molecules, through the stabilization of bcl-2 mRNA and inhibition of Fas signaling, it is an intriguing idea to track nucleolin's expression and function during B-cell development by paying close attention to these two regulatory aspects.

To address the cellular dynamics of nucleolin throughout B-cell development, immunofluorescence, immunohistochemistry and in situ hybridization can be used to analyze various lymphoid compartments to track nucleolin, Fas, and Bcl-2 protein and bcl-2 mRNA levels.(102) Additionally, coIP of the Fas-nucleolin and nucleolin-bcl-2 mRNA complexes can be performed in order to determine if these two nucleolin associations change throughout B-cell development. Our assumption is that nucleolin expression would be low in B cells, except during the proliferative clonal expansion stages (Figure 24). In normal B cells, even when Fas is upregulated, we would not expect to see nucleolin-Fas complexes, as Fas signaling must be active during germinal center selection. However, nucleolin may be utilized to stabilize bcl-2 mRNA in the mantle zone B cells. Due to the deregulation of bcl-2 and Fas in B-cell lymphomas, it would be beneficial to monitor nucleolin's expression levels and its Bcl-2 and Fas regulatory functions in B cell malignancies. Potentially, in malignant B cells nucleolin may bind Fas and bcl-2 mRNA simultaneously as a dual protective effect against cell death. These results may lead to further delineation of nucleolin's role in oncogenesis and its discrepancies from healthy B cells.

Figure 24

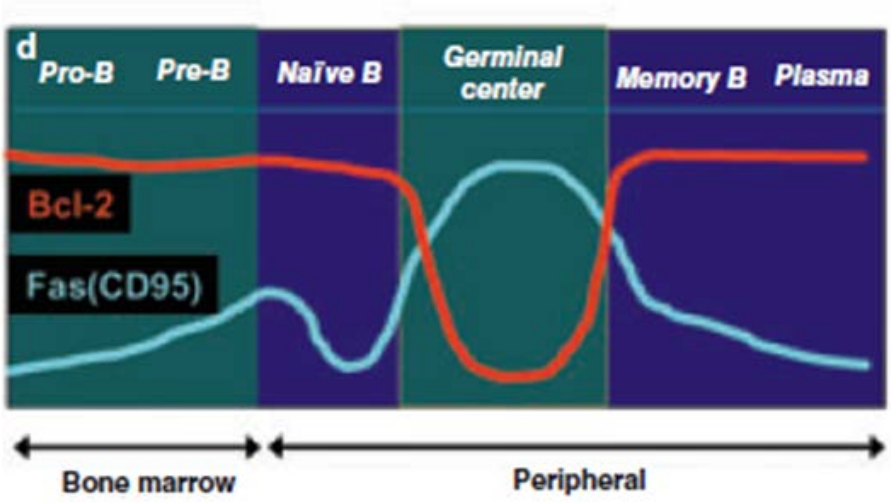

Figure 24: Schematic of Bcl-2 and Fas Levels throughout B-cell Development.

During B-cell differentiation, as represented by colored arrows, Bcl-2 (blue line) and Fas (red line) expression levels fluctuate. Acquired with kind permission from John Wiley and Sons (License 3125510179463). (102) There is potential for nucleolin protein fluctuation throughout B-cell differentiation also.

Expansion of the Characterization of the Nucleolin-Fas Complex

In order to develop targeting agents against the nucleolin-Fas complex, further analysis into the interaction and its kinetics must be carried out. We were able to determine that the extracellular domain of Fas is utilized for complex formation. Further analysis of the interaction should analyze Fas-deletion mutants to identify nucleolin binding site on Fas. The PLAD domain of Fas is essential for these studies. However, the constructs obtained by our laboratory are missing the PLAD domain of Fas, necessary for Fas trimerization, thereby affecting the correct folding and translocation abilities of these Fas mutants. In order to overcome this limitation a new set of Fas mutants with a preserved PLAD domain should be created in order to determine Fas's interaction site with nucleolin.

Additional in depth analysis of the nucleolin R4-GAR domain interaction with Fas through a more detailed mutational analysis on the molecular level would increase our ability to target Fas-nucleolin interaction by peptides or peptidomimetics. This is a potentially very important site for treatment of medical problems mediated via nucleolin overexpression. Logistical issues with mutational analyses arise due to the nature of the GAR domain, essential for nucleolin-Fas complex formation. There is no crystallography data available regarding the GAR domain. However, it is known that the GAR domain has rather high phenylalanine content and is composed predominantly of β-sheets. Mutations of the phenylalanines within this domain would significantly change the hydrophobicity index of nucleolin and potentially cause a loss of β-sheets. Far-UV (190-250nm) circular dichroism (CD) spectroscopy takes advantage of the fact that the polarized light is absorbed differently by alpha-helices, β-sheets and random coils, which allows for quantitation of the relative content of each of those structures within the protein.(314) Therefore CD spectroscopy would be necessary to obtain information about the secondary structure of nucleolin mutants and to compare this information with the wild type nucleolin to determine functionality of the mutant GAR domains.

Additionally, further elucidation of the kinetics of the Fas-nucleolin direct interaction would provide valuable information for targeting the complex. The biacore system, which utilizes immobilization of a protein on a sensor surface, can determine the extent to which different molecules interact, the affinity of binding, the kinetics of complex formation and dissociation.(315, 316) Its use would support and extend our characterizations of the nucleolin-Fas complex formation.

Mechanistic Studies of Nucleolin's Fas-FasL Inhibition

The ability of nucleolin to disrupt the physical interaction between Fas and FasL should be further investigated, as it will provide more extensive insight into the mechanism behind nucleolin-mediated inhibition of Fas. We originally planned to use and expand the validated binding assay described in Figure 8, revealing the interaction of chimeric extracellular Fc:Fas and nucleolin, and add recombinant FasL in order to determine if nucleolin directly competes with FasL for Fas binding. However, our current commercial source of the recombinant nucleolin has been unreliable. Because we have been unable to obtain a validated product for determining interaction, we could not complete the assay. Further collaborations to obtain or create recombinant nucleolin are necessary.

Thus far, there are many unknowns about nucleolin's trafficking and positioning on the cell surface. First, transport of nucleolin to the cell surface was only partially described; it is known to involve a non-classical transport possibly associated with actin cytoskeleton.(178, 216) Second, nucleolin is tethered to the cell surface through an uncharacterized association. Third, extracellular nucleolin is a glycosylated and phosphorylated protein and thus far the recombinant nucleolin available is bacterially produced.(219, 228) There are additional aspects of the nucleolin-Fas model that make it difficult to study nucleolin-Fas interactions. Our unpublished data showed that recombinant nucleolin added to cells does not adhere to the cell surface and does not interfere with the Fas/FasL interaction, underscoring the importance of having an appropriate model with the proper positioning of nucleolin and Fas for complex formation at the plasma membrane. The impact of nucleolin and Fas positioning is further confirmed by our direct interaction data presented in Figure 8. Although, the dose dependent binding of nucleolin confirms a specific direct interaction, only a small fraction of nucleolin bound to Fas even in solution. This suggests that the kinetics of binding may be low or that additional factors not reproduced in the recombinant nucleolin, such as posttranslational modifications and proper folding, affect binding efficiency. Hence, simple addition or secretion of the recombinant R4-GAR mutant to the tissue culture media may not be sufficient for functional assays. It is apparent that further investigations into nucleolin's trafficking and positioning on the cell surface, to identify nucleolin interacting domain(s) required for those processes, are necessary before we can properly study nucleolin on the cell surface. In order to complete mechanistic experiments, future collaborations with protein chemists and pharmacology/kinetic facilities will be necessary.

Targeting Nucleolin-Fas Complexes

By describing the expression of nucleolin in cancer and the role of nucleolin in Fas-mediated apoptosis, we have laid out the basis for the design of novel nucleolin-targeting cancer therapies based on competition; designed molecules targeting the interaction site could cause disassociation of the complex, and thus further enhance killing of tumor cells by increased sensitivity to Fas-mediated apoptosis and combination chemotherapies. It is plausible that by disrupting the nucleolin-Fas complex, by creating small interfering proteins, peptides, or nanobodies derived from or directed to the R4-GAR domain, we could exert a dominant negative or inhibitory effect on the nucleolin-Fas complex. These molecules may by themselves induce apoptosis or sensitize B-cell malignancies to Fas-mediated apoptosis and potentially genotoxic therapies. Once a model of the nucleolin-Fas complex is available, it can be probed with recombinant GAR domain, peptides spanning the R4-GAR domains, and nanobodies targeting the R4-GAR domain.

Monoclonal antibodies targeting nucleolin as a form of treating cancer have been tested. Nucleolin antibodies are already protected by US patents. Nucleolin antibodies are present in systemic lupus erythematosus and allograft failure, suggesting potential unwanted effects that could be mediated by clinical approaches using anti-nucleolin antibodies.(250, 280) Thus, an attractive option is the use of nucleolin with nanobodies containing the variable domain of the heavy chain antibodies from the camelid family.(317) Nanobodies are the smallest fragment of antibodies that are produced naturally to specifically target antigens and therefore their 15kDa size is below the threshold of renal filtration, thereby avoiding renal drug clearance, and their mass production is cheaper than monoclonal antibodies.(318) Nanobodies also display higher affinities, in the nanomolar range, with increased solubility and high thermal stability.(317) Nanobodies are resistant to high pressure, chemical unfolding and various detergents thereby, making them resistant to the harsh conditions within the gastro-intestinal tract. The compact shape and convex binding sites allow for binding in clefts and pockets not normally exposed to larger therapeutics.(318) The compact shape and convex binding site also allows for binding to glycoproteins not accessible to conventional antibodies, due to the large solvent exposed CDR loops.(317) Nanobodies can, similar to conventional antibodies, be humanized and even be created in multimeric forms.(319) Nanobodies are an intriguing option as surface nucleolin targeting nanobodies could be conjugated to toxic chemicals for the delivery of therapeutic agents selectively to tumor cells.(320) Lastly, nanobodies against surface nucleolin conjugated to a labeling reagent could be potentially used as a diagnostic biomarker and prognostic tool for cancers.

In addition, nucleolin-targeting nanobodies can be optimized as diagnostic and imaging tools for enzyme-linked immuno sorbent assay (ELISA) and immunoassays as described below. This experimental plan will allow us to develop therapeutic interventions that may either induce or serve to sensitize cells to Fas-mediated apoptosis when combined with other drugs. Therapies designed against nucleolin may have a competitive edge over current antibodies, such as Rituximab, which targets B-cell markers present on both healthy and cancerous cells. However, nucleolin may have a comparable spectrum of positive and negative effects as nucleolin may be expressed on the surface of normal rapidly proliferating tissues.

Developing Nucleolin as a Diagnostic/Prognostic Tool

Early cancer detection and treatment is known to be an effective plan for the development of a cancer free population. Tumor markers are important for diagnosis, detection, surveillance and management of various malignancies. Currently, there are several tumor-specific markers in clinical practice monitoring lymphomas and leukemias including; beta-2-microglobulin, Philadelphia chromosome, and PML-RARα fusion protein.(321-323) Surface nucleolin has the potential to be used for screening, diagnosis, and prediction of cancer as well as any medical disorders associated with nucleolin dysregulation.(250) In order to determine/develop nucleolin as a potential tumor marker, nucleolin's presence in blood, other bodily fluids and tissues of patients with cancer should be analyzed in more depth.

We determined that total nucleolin in tissue samples correlates with Ki-67 staining, diagnosis and performance score. It is not surprising that nucleolin would have prognostic importance in lymphoma. The aggressiveness of lymphoma across different histologic types is affected by their rate of proliferation. Adverse outcomes have been consistently linked to high rates of proliferation, including proliferation detected by Ki-67.(324-326) In meningioma nucleolin intensity has also been correlated with Ki-67 and cell proliferation.(327) Our results also show that Ki-67 levels correlated with nucleolin staining intensity and number of cells nucleolin-positive cells. In cases where Ki-67 proliferation is used to determine treatment regimens, surface nucleolin levels by single cell suspension may represent a more feasible testing method as tissue biopsies are an invasive test, they do not allow for population screening, and the quantities of the material obtained from a single individual are typically insufficient to run multiple assays.

Therefore, blood and other bodily fluid markers are more practical approaches. Various approaches can be explored to determine nucleolin's potential as a tumor marker including sera testing and potential development of ELISAs against nucleolin, its various cleavage products, and

glycosylated forms. Beyond sera testing, flow cytometry could be utilized as a diagnostic or prognostic method for leukemia and lymphoma by measuring lymphocyte surface levels of nucleolin. Additionally, previous findings using oligomicroarrays indicated that nucleolin expression is upregulated in peripheral blood lymphocytes in early stage cervical cancer, signifying that nucleolin in peripheral blood has already been applied for cancer detection.(270) An ELISA for nucleolin has recently become commercially available and subsequent studies can be done to determine nucleolin levels should the assay be validated for low level detection of nucleolin.

Our studies revealed an increase in nucleolin surface levels in cancers compared to healthy donor B cells that correlated with IPI risk analysis. However, a few healthy donor samples had elevated levels of surface nucleolin. This may be real or false positive result. This finding can be further investigated to clarify the results before using our current staining method and flow cytometry as a clinical tool. Potential explanations for detection of high nucleolin levels in healthy donors include ongoing inflammation/the health status of the donors and assay manipulations which can lead to increased proliferation and membrane permeability, respectively. However, as mentioned earlier, the D3 and gp273 antibodies may be better suited for surface nucleolin staining as a clinical tool.(178, 267) Additional limitations in the use of nucleolin as a tumor marker stems from the fact that various other conditions, including SLE and multiple sclerosis, may produce nucleolin autoantibodies and interfere with nucleolin expression and its levels.(250) However, nucleolin as a potential marker in lymphomas and in cancer can become a tool for use in clinical patient assessment.

Nucleolin as a prognostic/diagnostic tool by immunohistochemistry of B-cell lymphomas will need further investigations. It appears that additional studies in immunohistochemistry will reveal whether this approach has any potential for drawing prognostic information. Our cohort has large variations histological lymphomas and the distribution of scoring among marker level was greatly biased towards a high percentage of cells and intensity. Another contributing factor may have been the various treatment regimens within the cohort. However, our surface nucleolin flow cytometry showed intriguing results that suggest the need for further investigation into nucleolin's role in B-cell lymphoma outcomes using either a larger group of the same cohort of patients with fewer variables or an antibody that is specific for the translocated nucleolin. There are results from other groups that utilize TMA's with uniform histological groups and treatment strategies. This approach may enhance our ability to evaluate nucleolin levels and outcomes. However, it may be nucleolin's translocation that is an important prognostic/diagnostic tool for B-cell lymphomas and therefore repeating the analysis with an antibodies targeting cytoplasmic and surface nucleolin should be performed. Antigen retrieval is a complex procedure particularly when attempts to reach

cell surface in formalin-fixed tissue. Galzio et al demonstrated nucleolin's prognostic role in human gliomas using an anti-glycosylated nucleolin antibody.(267) Previous reports also demonstrate that glycosylated nucleolin is directed to the cytoplasm and surface of cells, and the gp273 antibody developed by Galzio et al was shown to specifically target these locales within glioma cells. Thus, an enrichment of our TMA with the gp273 antibody is warranted to elucidate nucleolin's role in B-cell lymphoma outcome.

Impact and Significance

Cell Surface Nucleolin

Recent studies have identified nucleolin on the cell surface of multiple cancers and cancer-associated endothelial cells and nucleolin is now recognized as a tumor marker.(178, 210, 215, 229, 275, 328) The existence of cell surface nucleolin, although initially surprising, is in accordance with a growing number of studies revealing that under certain conditions nuclear proteins, such as Ku, nucleophosmin, Nopp140, and high mobility group box 1 protein (HMGB1), are present on the cell surface.(190, 329) Membrane localization of HMGB1 and heat shock protein is associated with cytokine signaling in damaged tissues. These two proteins belong to the damage-associated molecular pattern molecules (DAMPs) released during stress, apoptosis, and necrosis. Recently, HMGB1 membrane localization has also been identified during cell growth, suggesting the involvement and a complex role of nuclear proteins in membrane signaling.(330) The surface expression of HGMB1 correlated with a worse prognosis in nasopharyngeal and colon cancers.(331-333) Interestingly, both nucleolin and Nopp140 are proteins phosphorylated by ectokinase, found on the surface of cancer cells.(329) Ku protein expression patterns have been correlated with the prognosis and outcome of melanomas and rectal carcinoma.(334, 335) Similar to nucleolin, autoantibodies for Ku70 have been documented in an autoimmune disease, Graves' disease.(250, 336) The selective expression of nuclear proteins on surface of cancer cell and their correlation with worsening prognosis, points to a new family of prognostic and diagnostic markers to be explored.

Although the surface presence of nucleolin has been observed in multiple disease phenotypes, all of its known surface functions point to it as an indiscriminative docking protein for substrates that support cell survival such as P-selectin, lactoferrin, and hepatocyte growth factor. Nucleolin also acts as a gateway into cells for viruses.(226, 237, 328, 337-341) We confirmed nucleolin's surface localization in lymphomas, and our results reveal that it binds endogenous Fas and promotes survival of lymphoma cells by interfering with Fas apoptotic signaling, thereby

describing a key role of surface nucleolin in cell survival. These cell survival functions may offer additional layers of protection acquired by transformed cells as a novel form of immune protection and chemoresistance.

Recent reports revealed that certain cell surface receptors bind to and block Fas signaling in addition to their own pro-survival signaling functions. Hepatocyte growth factor receptor (HGFR)/c-MET, human herpesvirus-8 K1 and CD44v6/v9 were identified as modulators of Fas signaling through direct interaction with Fas at the cell surface (Table 14).(292-294, 342-346) The presented results add nucleolin to this growing category of Fas regulators. Interestingly, these proteins interact with the extracellular domain of Fas seemingly without a common binding motif. We provide evidence that nucleolin, similar to these receptors, negatively regulates Fas-mediated apoptosis by inhibiting the interaction between Fas and FasL by forming complex with the extracellular domain of Fas on the cell surface. We predict that nucleolin, and these previously identified receptors, bind and lock Fas in an inactive preassembled trimer conformation(347) that prevents FasL ligand access to its binding site or interferes with conformational changes required for efficient FasL binding. Moreover, should this Fas-regulator complex be targeted, we showed that a peptide derived from Fas-binding domain of K1 induces Fas apoptotic signaling, suggesting these receptor-Fas interactions are accessible and amenable to manipulation.(292) A more complete description of how these Fas binding proteins make Fas inaccessible to activation would greatly improve the effectiveness of the numerous lymphoma chemotherapies that depend on Fas signaling for cell elimination.(293-295, 342, 344, 346)

Table 14: New Category of Membrane –Associated Fas Regulators.

	Membrane-associated localization	Pro-survival receptor signaling w/o Fas involvement	Transforming potential	Inhibition of Fas signaling	FasL-Fas disruption	Expression associated with cancer
K1 (293, 294)	+	-	+	+	+	
HGFR/Met (342, 344)	+	+	+	+	+	+
CD44v6/v9 (346)	+	+	enhances	+	?	+
Nucleolin (348)	+	+	+	+	+	+
PML-RARα (295)	+	-	+	+	-	+
CD74	+	+	?	+	?	+

Previously published data has revealed a new category of surface receptors with their own pro-survival signaling capabilities that also bind and interfere with Fas signaling and contribute to the formation of cancer.

Nucleolin as a Prognostic Marker

Studies determining the association of nucleolin expression levels and outcome of patients have shown that nucleolin levels correlate with a progressively worsening cancer phenotype.(265, 268, 297) The identification of nucleolin as a prognostic marker and our determination of nucleolin as an anti-apoptotic protein led us to investigate nucleolin's expression patterns in B-cell lymphomas. The surface expression of nucleolin by flow cytometry correlated to a prognostic value for B-cell lymphomas. However, this was not the case in our TMA analysis studying the correlation of nucleolin levels with survival of B-cell lymphoma patients. Our cohort's outcome could not be explained by differences in total nucleolin levels. However, our demonstration of nucleolin surface level's association with IPI suggests that the prognostic role of nucleolin in B-cell lymphomas is associated with nucleolin translocation abnormalities.

Our results confirm and extend previous findings that nucleolin is associated with distinct pathogeneses of B-cell lymphomas. Moreover, they support findings that nucleolin translocation is a major contributor to nucleolin's correlation with the outcomes of malignancies.

Targeting Nucleolin

Nucleolin is an attractive target for cancer therapy, as it appears to have low off-target effects primarily because of its restrictive expression on the cell surface of cancer cells and cancer

associated cells. Nucleolin serves as a target in pre-clinical trials include F3 peptide, AS1411 aptamer, and LNA-aptamers linked to various drug carriers for delivery of microRNAs, radionuclides and doxorubicin.(277-279, 283, 286, 349) Additionally, anti-nucleolin antibodies in pre-clinical models induce downregulation of bcl-2 mRNA levels and subsequent apoptosis.(350) However, nucleolin antibodies are present in systemic lupus erythematosus and allograft failure, suggesting potential unwanted effects that could be mediated by anti-nucleolin antibodies.(250, 280)

Some agents have advanced to testing in clinical trials. Nucleolin-targeting nucant pseudopeptide (Immupharma) (273) are currently under evaluation in a phase II clinical trial. The nucants predicted mechanisms of action include inhibition of proliferation and angiogenesis and induction of apoptosis. A phase II clinical trial of AS1411 GRO (Antisoma) which destabilizes bcl-2 and induces apoptosis, has shown a 3% partial response rate and 60 % stable disease rate in relapsed renal cell carcinoma.(351, 352) AS1411has also showed a 15% response rate in the treatment of relapsed acute myeloid leukemia.(166, 273, 282, 351, 352)

By defining a novel role for nucleolin as an anti-apoptotic surface protein, we further underscore the potential of these and other nucleolin-targeting therapeutics. Furthermore, our results may explain the variable outcome of nucant pseudopeptide treatments, tested by the Hovanessian group, showing cell death in lymphomas and leukemias and response was restricted to only growth inhibition in other malignant cell types.(229, 273, 274) The differential response by the various malignancies, specifically the apoptotic responses, may be associated with nucleolin's inhibitory effect on Fas-mediated apoptosis. As we only revealed nucleolin-Fas complexes in lymphoid tissues the complex may play prominent role in lymphoid cancers and warrants further investigation. Moreover, given that Fas apoptosis has been linked to the effectiveness of multiple chemotherapies, our discovery that nucleolin regulates Fas-mediated apoptosis indicates that the nucleolin-targeting therapies currently in clinical and pre-clinical trial may benefit from combination with Fas-dependent genotoxic drugs.

The identification and validation of tumor-specific targets for cancer therapy is a primary step in drug discovery and the development process of new therapeutics. The key criterion for target selection includes: overexpression in tumor versus healthy tissues, a pivotal role in the pathogenesis of cancer and the ability to develop small molecules or biologicals targeting its function(s). We conclude that nucleolin not only fits these criteria, but because it functions in multiple hallmarks of cancer: evasion of apoptosis, sustained angiogenesis and limitless replicative potential, nucleolin presents an ideal target for the treatment of cancer. Generation of novel

nucleolin-targeting molecules will be a significant advancement in the elimination of lymphomas and other cancers.

Chapter 7: Materials and Methods

Isolation of Activation-resistant Fas Complexes and Identification of Peptides: BJAB cells and a NHL primary tissue were activated and immunodepleted with the CH-11 anti-Fas antibody (Ig-M subclass; Millipore, Temecula, CA) using anti-IgM agarose beads (Sigma Aldrich, Ayrshire KA). The remaining extracts were immunoprecipitated with agarose beads conjugated with B-10 anti-Fas antibody (Santa Cruz Biotechnology, Santa Cruz, CA). Both fractions were separated by electrophoresis and visualized on silver-stained SDS-PAGE. Any band found exclusively in the B-10 precipitation lane, was excised and digested in-gel using 200 ng of modified sequencing grade trypsin (Promega, Madison, WI) for 18 hours at 37°C. The resulting peptides were extracted for nanoflow liquid chromatography (LC)-mass spectrophotometry (MS)/MS fragmentation with on-line desalting using a Famos autosampler, UltiMate Nano-LC module and Switchos precolumn switching device (Dionex, Sunnyvale, CA). Electrospray ion trap mass spectrophotometry was performed on a linear ion-trap mass spectrophotometer (LTQ Thermo, San Jose, CA). On average, one survey scan was followed by three data-dependent MS/MS scans, using CID to induce fragmentation. Spectra profiles were analyzed for protein matches by database search of the fragment spectra versus the National Center for Biotechnology Information's (NCBI) non-redundant protein database, using the MASCOT search engine (Matrix Science, London, UK).

Cells and Primary B-cell Tissues: Human lymphoma Raji, Jurkat, and BC-3 cell lines were obtained from the NIH AIDS Research & Reference Reagent Program (Pittsburgh, PA) and human BJAB, Daudi, U937, Hela, DB and 293T cell lines were obtained from American Type Culture Collection (ATCC) (Manassas, VA). Jeko and MINO cells were kindly donated by Dr. Eric Davis. Cells were maintained in RPMI 1640 medium (Hyclone Thermo Scientific, Logan, UT) supplemented with 10% fetal bovine serum (FBS) (Atlanta Biologicals, Lawrenceville, GA) in 5% CO_2 atmosphere at 37°C. Cells were passaged at a ratio of one to 4 every 3 days. Cell lines were authenticated by STR analysis (MD Anderson Cancer Center) (10/31/2012) and regularly tested for mycoplasma contamination using mycoALERT mycoplasma detection kit. (Lonza, Rockland, ME). Experiments were performed using early passages of cells obtained from commercial sources.

Peripheral blood B-cells were isolated from healthy donors' blood purchased from Gulf Coast Blood Center (Houston, TX). Isolation was achieved with CD19Pan B Dynabeads, CD19-positive magnetic beads, (Invitrogen Life Technologies, Oslo, Norway). The isolated B-cells were released with the competitive reagent CD19 DETACHaBEAD (Invitrogen Life Technologies, Oslo,

Norway). For confocal PBMC's isolation was achieved by Histopaque-1077 (Sigma Aldrich, Alyshire, KA) gradient centrifugation at 400 g for 30 minutes at RT. Buffy coats were then washed in phosphate-buffered saline (PBS).

Patient cells were collected after written consent from patients at The University of Texas MD Anderson Cancer Center under research protocols LAB08-0190, 2008-0075, and 2005-0656. From these samples, tumor cell enriched buffy coats were isolated by Histopaque-1077 (Sigma Aldrich, Ayrshire, KA) gradient centrifugation at 400 g for 30 minutes at RT. Buffy coats were then washed in PBS supplemented with FBS and aliquoted for storage in RPMI 1640 supplemented with 10% FBS and 5% dimethyl sulfoxide (DMSO) (Fisher, Fairlawn, NJ) at -80°C for further analysis.

For the TMA, 156 cases biopsied between 1993 and 2002 were collected under LAB08-0190. Patients with Hodgkin's lymphoma, T-cell lymphomas, seminomas, and tonsils were excluded from the analysis. Twenty nine patients had missing information on either follow-up or marker expression and were thus excluded from the analysis. One patient had two records and the record labeled as 'L144' was excluded from the analysis. One patient was lost to follow-up right after the biopsy date therefore excluded from the analysis. The final analysis is performed on 119 patients. These cases were analyzed for nucleolin and Ki-67 protein expression. Patients in this study were treated under a variety of drugs and therefore a regimen scheme of CHOP related, Fludarabine related, and Combination therapies was created.

Immunoprecipitation (IP) and Immunoblotting (IB) Analysis: Indicated cells, or homogenized mouse liver tissues were collected by centrifugation, and lysed in lysis buffer (20mM Tris-HCl, 150mM NaCl, 1mM Na2EDTA, 1mM EGTA, 1% Triton, 2.5 mM sodium pyruvate, 1mM β-glycerophosphate, 1 mM Na_3VO_4, 1 μg/mL leupeptin) (Cell Signaling, Danvers, MA) with a phosphatase inhibitor cocktail mix (Roche Diagnostics, Mannheim, Germany) for 1 hour on ice. Whole-cell extracts were clarified by centrifugation at 13,000 rpm for 10 minutes at 4°C. Protein content was quantified using the Bio-Rad protein assay (Bio-Rad Laboratories, Hercules, CA). Lysates were then denatured with SDS loading buffer with dithiothreitol (DTT) (Cell Signaling, Danvers, MA or Boston BioProducts, Ashland, MA) and boiled for 5 minutes prior to loading (25-100μg).

For IP, 3×10^7 cells, 5 mg of homogenized liver protein or primary lymphoma tissue were incubated for 1 hour at 4°C in the cell lysis buffer and the extracts were clarified by centrifugation at 13,000 rpm for 1 minute. Supernatants were incubated with 1-2 μg of the indicated primary antibodies: anti-human Fas (B-10) (Santa Cruz Biotechnologies, Santa Cruz, CA), anti-human Fas

(CH-11) (Millipore, Temecula, CA), anti-TRAIL-R1 HS101 (Axxora, San Diego, CA) and mouse IgG or normal rabbit serum (Invitrogen, Carlsbad, CA) for 1 hour at 4°C with rotation. Where primary antibody agarose conjugates were not available, protein A/G sepharose (Pierce Biotechnology, Rockford, IL), IgM agarose (Sigma Aldrich, Ayrshire KA), or strepavidin agarose (Thermo Scientific, Lafayette, CO) were added to the supernatant pre-incubated with the primary antibody and the mixture was incubated for an additional 1 hour at 4°C.

For recombinant protein assays, a chimeric Fc:Fas (BD Biosciences, San Jose, CA) and recombinant nucleolin-GST (Abnova, Heidelberg, Germany) were resuspended in 300 µl of RIPA buffer (Cell Signaling, Danvers, MA). Fc:Fas was incubated with increasing amount of nucleolin-GST for 1.5 hours at 4°C followed by incubation with protein A agarose for 1 hour at 4°C. Complexes were washed 5 times with co-IP washing buffer (50 mM Tris, pH 8.0, 300 mM NaCl, 0.5% NP-40) containing a protease inhibitor cocktail (Roche Diagnostics, Mannheim, Germany).

The precipitated protein complexes were released from agarose by the addition of 50 µl of SDS with DTT and boiling for 5 minutes prior to being run on 7.5%, 10%, or 15% SDS-PAGE (Bio-Rad Laboratories, Hercules, CA) and transfer to a nitrocellulose membrane at 100V for 1 hour (Schleicher & Schuell, Keene, NH). Proteins were analyzed by IB with 20 µg of antibody: anti-Fas (B-10)-HRP, anti-Fas (N-18), anti-nucleolin MS3-HRP, anti-histone-3, anti-GST (Santa Cruz Biotechnologies, Santa Cruz, CA), anti-Flag (M2)-HRP, anti-β-actin-HRP (Sigma Aldrich, Ayrshire, KA), anti-PARP, mouse specific anti-PARP (D214), anti-cleaved capase-3, anti-caspase-8, mouse specific caspase 8, anti-bcl-2 (Cell Signaling, Danvers, MA), anti-DDK (Origene, Rockville, MD), anti-TRAIL-R1 (Enzo Life Sciences, Farmingdale, NY), anti-p84, anti-GAPDH (Genetex, Irvine, CA). Incubation of membranes with un-conjugated primary antibodies was followed by incubation with corresponding HRP-conjugated secondary antibody. Proteins were visualized by Supersignal West Pico chemiluminescent substrate or Supersignal West Femto chemiluminescent substrate (Thermo Scientific, Rockford, IL) and exposure to film (Bioexpress, Kaysville, UT). Intensity of bands was compared by densitometry using Image J (NIH, http://rsb.info.nih.gov/ij/)

Flow Cytometry Analysis: The degree of apoptosis induced by FasL or CH-11 was evaluated through Annexin V and 7-amino-actinomycin D (7AAD) staining. Cells were washed twice with cold PBS supplemented with 1% FBS, and then resuspended in binding buffer prior to incubation with Annexin V-PE and 7AAD (BD Biosciences, San Jose, CA) for 15 minutes in the dark at RT. Annexin V/7AAD staining was assessed with a BCI XL Analyzer utilizing System II software (Beckman Coulter, Miami, FL).

For detection of surface proteins, cells were washed twice with cold wash buffer PBS supplemented with 1% FBS and subjected 0.25µg/mL of mouse IgG blocking reagent (Invitrogen, Frederick, MD) for 15 minutes at 4°C followed by an additional wash in the wash buffer. The cells were then incubated with the anti-CD95 (UB2)-PE (Beckman Coulter, Marseilles, France) CD19-APC (BD Biosciences, San Jose, CA), C23 (H-6)-AF488 (Santa Cruz Biotechnologies, Santa Cruz, CA) and isotype control mouse IgG_1-PE (BD Biosciences, San Jose, CA), APC Mouse IgG1 kappa (BD Biosciences, San Jose, CA), and A488 Mouse IgG2a (eBioscience, San Diego, CA) antibodies at 4°C for 20 minutes in the dark, washed twice with the wash buffer and resuspended in 200µl of 1% FBS PBS. One microliter of Sytoxblue stain (Invitrogen, Eugene, OR) was added to assess dead cells. Analysis of staining was performed on a LSR Fortessa flow cytometer with Diva software (BD Bioscience, San Jose, CA). Data analysis was performed with FlowJo software (Tree Star Inc, Ashland, OR).

For agonistic antibody and FasL binding and detection, cells were incubated with 7µg of CH-11 or 3µg of FasL (Enzo Life Sciences, Farmingdale, NY) for 20 minutes at 4°C, followed by 2 washes in 1%FBS/PBS. Cells were incubated with 0.25µg/mL of blocking reagent (normal mouse IgG) for 15 minutes at 4°C, followed by an additional wash in 1% FBS/PBS. Subsequently, cells were incubated with APC rat anti-mouse IgM (BD Biosciences, San Jose, CA) and Phycolink anti-FLAG-RPE (Prozyme, Hayward, CA), respectively, at 4°C for 20 minutes in dark, again followed by 2 washes in 1% FBS/PBS. Cells were resuspended in 200µl of wash buffer and analyzed on a LSR Fortessa flow cytometer using Diva software and data analysis was performed using FlowJo software.

Confocal Imaging: BJAB, NHL-derived primary cells, and PBMC's were either stained for surface proteins without fixation or with fixation and permeabilization. Cells were washed in PBS with 1%BSA. For fixation, cells were fixed with 4% paraformaldehyde (Electron Microscopy Sciences, Hatfield, PA) in PBS for 20 minutes at RT and subsequently permeabilized in 0.5% Triton X100 (BioRad, Hercules, CA) in PBS. All cells were then blocked with 1% BSA and 10% goat serum in PBS. Cells were then stained stepwise with the following antibodies in 1%BSA/PBS: anti-Fas antibody (1µg; rabbit anti-CD95; Abcam, Cambridge, MA), alexaflour-647 antibody (1:500; 1%BSA/PBS), anti-nucleolin MS-3 (1µg; 1%BSA/PBS), secondary alexaflour-488 antibody (1:500; 1%BSA/PBS) for 1.5 hrs on ice. Cells were washed twice in 1%BSA/PBS and incubated with WGA alexafluor-555 (Invitrogen, Eugene, OR) for 5 minutes. Cells were washed in PBS followed with 0.1% Tween-20 (Fisher, Fairlawn, NJ) and mounted onto a slides using cytospin and prolong gold antifade reagent with 4',6-diamidino-2-phenylindole, dihydrochloride

DAPI (Invitrogen, Eugene, OR). Images were acquired using a Nikon A1R confocal laser microscope system (Nikon Instruments, Melville, NY). For fluorescent phalloidin-568 staining, BJAB, non-silencing and 906S2 cells were cultured as monolayers on coverslips. Cells were fixed in a 4% formaldehyde solution (Electron Microscopy Sciences, Hatfield, PA) in PBS for 10 minutes at RT and permeabilized with 0.1% Triton X-100 (Bio-Rad, Hercules, CA) in PBS for 5 minutes. Cells were subsequently blocked 1% BSA in PBS (Sigma Aldrich, St. Louis, MO) for 30 minutes. Cells were treated with a dilute 5 µL methanolic stock solution of phalloidin-568 (Invitrogen, Eugene, OR) in 200 µL of PBS containing 1% BSA for 20 minutes at RT and mounted in a prolong gold antifade reagent with DAPI (Invitrogen/Eugene, OR). Images were acquired using a Nikon A1R Confocal Laser Microscope System (Nikon Instruments Inc., Melville, NY).

Plasmids and Transfections: For cell transfections, a plasmid encoding C-terminal myc- and flag-tagged nucleolin, pCMV6-Nucleolin (TrueORF cDNA clones) and the vector control pCMV-ENTRY were used (Origene, Rockville, MD). Partial nucleolin mutants and DNA primers (Sigma Aldrich, St. Louis, MO) (Appendix A) were designed according to the manufacturer's protocol for Quick Change II XL site-directed mutagenesis (Stratagene, Cedar Creek, TX) on pCMV6-Nucleolin. Plasmids were endotoxin-free and sequences were confirmed by GENEWIZ (South Plainfield, NJ). Cells were transfected using Lipofectamine 2000 transfection reagent (Invitrogen, Carlsbad, CA), according to the manufacturer's recommendations, with Opti-Mem Reduced Sera Media (MediaTech, Manassas, VA).

To produce the nucleolin partial knockdowns, 1.2 mg of plasmids encoding shRNAmir30 constructs (OpenBiosystems-ThermoScientific, Lafayette, CO), lentiviral plasmids: pGIPZ-non-silencing, and pGIPZ- GAPDH were transfected into cells using Lipofectamine 2000 transfection reagent (Invitrogen, Carlsbad, CA) according to the manufacturer's recommendations. Transfected cells were selected with 1 µg/mL of puromycin (Sigma Aldrich, St. Louis, MO) for 2 weeks. Cells were subsequently sorted for green fluorescent protein (GFP) expression in an Aria flow activated cell sorter (FACS) (BD Biosciences, San Diego, CA). Single-cell clones were developed through the standard dilution method.

Proliferation Analysis: 0.4% trypan blue cell stain (MP Biomedicals, Solon, OH) was added at a 1:1 ratio of trypan blue to medium containing cells and 10µl was loaded onto a Countess cell counter chamber slide and analyzed for viability and cell number using the Countess automated cell counter (Invitrogen, Oregon). Cell counts were taken every 24 hours for 100 hours.

Transmission Electron Microscopy: Ultrastructural features of BJAB, Non-Silencing, and 906 nucleolin partial knockdowns were obtained and assessed at the High Resolution Electron Microscopy Facility at MD Anderson Cancer Center with Kenneth Dunner. The 1×10^6 cells were washed and fixed in 0.5ml of TEM fixative 2% glutaraldehyde in 0.2 M sodium cacodylate buffer overnight at 4°C. Cells were post-fixed in cacodylate-buffered 1% osmium tetroxide, dehydrated, and embedded in plastic. Thin sections were post-stained with uranyl acetate and lead citrate. Images were obtained using a JEM 1010 transmission electron microscope (JEOL USA Inc, Peabody, MA).

Video Time-Lapse Microscopy: To directly visualize the division patterns of nucleolin partial knockdowns, we used VTLM using the Biostation IM Cell-S1/Cell-S1-P system (Nikon Instruments Inc., Melville, NY). The BJAB, Non-silencing, 906S2, and 906S5 cells at 2×10^4 cells were resuspended in 300µl of fresh media in a Hi-Q4 multi-experiment tissue culture-treated dish (Ibidi, Martinsried, Germany). For tubulin fluorescence, CellLight Tubulin-RFP Bacman 2.0 (Invitrogen, Eugene, OR) was added at 50 PPC (particles per cell) or 20µl per 40,000 cells in 500ul media prior to Hi-Q4 plating. For nuclear staining with VTLM, a nuclear fluorescent dye DRAQ5 (Cell Signaling, Danvers, MA) was added to the media before addition to the Hi-Q4 plate at 1uM concentration. Each image was recorded at 1600x1200 pixels via a 20X objective, using phase contrast and fluorescent channels with an exposure time of 1 minute for 24 hours.

Glycosylation and Sialylation Analysis: 1.5×10^6 BJAB, Non-Silencing control, 906 -P1, -S1, -S2, -S4, and -S5 cells per treatment group were harvested by centrifugation. For sialylation analysis cells were resuspended in 100mU of VCN (Sigma Aldrich, St. Louis, MO) for 1 hr at 37°C. Cells were subsequently washed and collected by centrifugation and lysed in cell SDS/DTT loading buffer (Cell Signaling, Danvers, MA). For glycosylation analysis cells were lysed in RIPA buffer (Cell Signaling, Danvers, MA) for 30 minutes at 4°C. Insoluble material was removed by centrifugation followed by addition of glycoprotein denaturing buffer (New England BioLabs, Ipswich, MA) and incubation for 10 minutes at 100°C. 15uL of 10X reaction buffer, 15uL of NP40 (nonyl phenoxypolyethoxylethanol) and 7.5 uL of PNGaseF (New England BioLabs, Ipswich, MA) were added and incubated at 37°C for 1 hr. Protein levels were analyzed as described in "Immunoprecipitation (IP) and Immunoblot (IB) Analysis"

RNA Isolation and Quantitative Real-Time Polymerase Chain Reaction (PCR): Cells were pelleted at 1×10^6 per tube and stored at -80°C. Thawed pellets were subjected to RNA isolation

using a column centrifuge Qiagen kit (Qiagen Sciences, Germantown, MD) according to the manufacturer's protocol and resuspended in RNAase-free water (Qiagen Sciences, Germantown, MD). RNA levels were measured by spectrophotometry at 260/280nm absorbance using a Victor^{3}V spectrophotometer (PerkinElmer, Waltham, MA).

First-strand cDNA was synthesized using a Superscript™ II reverse transcriptase kit (Invitrogen Life Technologies, Grand Island, NY) according to the manufacturer's protocol. Five hundred nanograms of total RNA was used in a 20µl reaction volume with components oligo (dT) 12-18 (500µg/mL), dNTP mix, and nuclease free water (Invitrogen Life Technologies, Grand Island, NY). The mixture was heated to 65°C for 5 minutes, quickly chilled on ice, and briefly subjected to centrifugation. This step was followed by the addition of First-Strand buffer, 0.1M DTT, and RNaseOUT (40 units/µl) (Invitrogen Life Technologies, Grand Island, NY) and the mixture was further incubated at 42°C for 2 minutes. Finally, 200 units of Superscript™ II reverse transcriptase was added and the total mixture was incubated at 42°C for 50 minutes, followed by heat inactivation at 70°C for 15minutes.

Triplicate samples were analysed on 96-well microtiter plates with the StepOnePlus™ Real-Time PCR Systems (Applied Biosystems, Singapore) using thermocycles of: 95°C for 20 seconds and 60°C for 30 seconds, for 40 cycles. The PCR for bcl-2, nucleolin, fas, GAPDH reaction was performed using TaqMan probes in a 20µl mixture containing a 1:10 volume of cDNA preparation, 10µl of 2X TaqMan Master Mix, and 0.2 µM of each primer (nucleolin, bcl-2 and GAPDH as internal controls) (Applied Biosystems, Foster City, CA) using cycles of 95°C for 15 seconds and 60°C for 1 minute, for 40 cycles.

Surface Biotinylation: To evaluate surface proteins, 15×10^6 cells per cell line were collected and 20×10^6 CD19-positive lymphocytes from healthy donors were used directly after isolation. Cells were washed twice with ice-cold PBS with Ca^{2+} and Mg^{2+} (MediaTech, Manassas, VA) centrifuged at 300 g for 5 minutes to prevent cell breakage, and incubated with 1mg/mL of EZlink sulfo-NHS-biotin (Thermo Scientific, Rockford, IL) in PBS with Ca^{2+} and Mg^{2+} for 40 minutes at 4°C with gentle rotation. After an additional centrifugation at 300 g for 5 minutes, the cells were resuspended in ice-cold serum-free medium, for quenching the reaction and gently rotated for 10 minutes at 4°C. Finally the cells were washed twice in PBS with Ca^{2+} and Mg^{2+}, lysed, and subjected to IP following the protocol described under "Immunoprecipitation (IP) and Immunoblotting (IB) Analysis."

In vivo experiments: Six-8 week old (National Cancer Institute, Bethesda, MD), or 8 week old

(Harlan Laboratories, Indianapolis, Indiana) C57BL/6 mice were transfected with 100 µg of pnuc-myc, PNK-FLAG PSG5, PSG5, nucleolin-PCMVENTRY, NR123-PCMVENTRY, or PCMVENTRY plasmids by rapid tail vein injection in a single bolus dose. At 24 hours after injection, apoptosis was induced by intraperitoneal injection of a lethal dose of of Jo2 agonistic anti-Fas antibody (BD Biosciences, San Jose, CA) (2µg/g or .5µg/g mouse weight for NCI or Harlan mice, respectively). Additional mice were transfected without Jo2 challenge to evaluate the effect of transfection on the livers in the absence of the challenge or were left un-transfected for comparison of normal liver tissue and evaluation of the effect of Jo2 in the absence of rapid tail vein injection. Mice were monitored for 8 hours post-challenge and scored for survival, after which surviving mice were killed by inhalation of 100% CO_2. Liver images were acquired with a Cannon EOS7D with macro lens EF-S 60mm. The livers of all the mice were harvested, divided into 4 sections, and either frozen for homogenization or embedded in paraffin for immunostaining. All procedures were performed in accordance with the guidelines of the Institutional Animal Care and Use Committee at MD Anderson Cancer Center.

Immunostaining: Formalin-fixed, paraffin-embedded liver tissue sections on microscope slides were subjected to deparaffinization, rehydration through a xylene and graded alcohol series, and antigen unmasking (1:1000; Vector Labs, Burlingame, CA). Slides were quenched, blocked to lower nonspecific antibody binding (Vector Labs, Burlingame, CA) and subsequently incubated with primary antibody (1:500) in a humidifier overnight at 4°C. Staining was performed using anti-FLAG M2 (Sigma Aldrich, St Louis, MO) anti-cleaved PARP, and anti-cleaved caspase-3 antibodies (Cell Signaling, Danvers, MA) followed by diluted biotinylated secondary antibody, enhanced with vectastain elite ABC, and developed with a 3,3'-diaminobenzidine (DAB) peroxidase kit (Vector Labs, Burlingame, CA). Sections were then counterstained using an H&E (Vector Labs, Burlingame, CA) and mounted with Permount (Fisher, Fair Lawn, NJ)

TUNEL staining was performed using a DeadEnd™ fluorometric TUNEL kit (Promega, Madison, WI) following the manufacturer's protocol. Stained slides were fixed in prolong gold antifade reagent with DAPI. Staining was performed by Vel-labs (Vel-labs, Missouri City, TX). The images were captured by the Olympus BX41 (Olympus) UPlan FL N 40X/0.75 objective. Images were acquired with DP Controller (Olympus) with a -2 exposure adjustment for TUNEL staining with a FITC filter (Olympus). Adobe Photoshop PS2 was used for further image enhancement of GFP with a +30 brightness for all 4 panels equally.

The TMA was constructed at the MD Anderson Cancer Center McDonnell Morphonomic Core Laboratory under protocol LAB08-0190 using an Advanced Tissue Arrayer ATA-100

(Chemicon International, Temecula, CA). Nucleolin and Ki-67 staining was performed at the MD Anderson Cancer Center Research Histopathology Facility using a Shandon Gemini Stainer (Thermo Scientific, Rockland, IL). The anti-nucleolin H-6 (Santa Cruz, Santa Cruz, CA) antibody was used a concentration of 1:5000. The Ki-67 staining was performed according to standard protocol the of MD Anderson Cancer Center's Core Histology facility. The TMA tissue images were captured by the Olympus BX41 microscope system. An Olympus Model DP72 camera and cellSens Standard 1.6 software (Olympus Corporation) was used for acquiring images.

Immunoreactivity was determined without knowledge of the patients' survival or clinical data. The nucleolin scores were analyzed independently by two hematopathologists. The TMA was stained three times and the average score per case was used for analysis. The classification model was developed prior to staining. No staining of nucleolin was considered a 0 score, a percentage of tumor cell staining 1-25% was considered a 1 score, 25-75% was considered a 2 score, >75% was considered a 3 score. Nucleolin intensity was scored as low or high correlating to the number scale of 1 and 2. Ki-67 intensity was scored as 1, 2 or 3 from lowest to highest.

Apoptosis Induction: To evaluate the sensitivity of cells to Fas-mediated apoptosis, $.5\times10^6$ cells/mL cells were seeded on 24-well plates. For CH-11(Ig-M subclass; Millipore, Temecula, CA) treatment, cells were resuspended in 1mL of serum-free RPMI1640 with the indicated doses of CH-11 and rotated for 1 hour at RT in the dark. Cells were collected by centrifugation at 1000rpm for 5 minutes and resuspended in fresh medium with 10%FBS for overnight incubation at 37°C (18 hours). FasL-mediated cell death was induced by incubating cells with the indicated dose of FasL or superFas (Enzo Life Sciences, Farmingdale, NY) in RPMI 1640 with 10% FBS overnight (18 hours) at 37°C. Cells were stained with AnnexinV and 7AAD and cell death was measured by flow cytometry as described previously under "Flow Cytomety Analysis". For detection of activation of downstream apoptotic targets, 1×10^6 cells were lysed in 50µl of cell lysis buffer (Cell Signaling, Danvers, MA) and subjected to the IB protocol as indicated under the section "Immunoprecipitation (IP) and Immunoblotting (IB) Analysis".

TRAIL treatment was performed on $.5\times10^6$ cells per mL with the indicated doses of TRAIL (Enzo Life Sciences, Farmingdale, NY) (5, 10, or 20 ng) in RPMI1640 supplemented with 10% FBS for approximately 16 hours at 37°C. Cell death was evaluated by DNA content (hypodiploid cells) analysis (353). Briefly, cells were harvested by centrifugation and stained for 4 hours with a hypotonic solution containing propidium iodide (40mg/mL 0.1% sodium citrate, and 0.1% Triton X-100) (Santa Cruz Biotechnology, Santa Cruz, CA) (40 µg/mL in 0.1% sodium citrate (Sigma Aldrich, St. Louis, MO), 0.1% Triton X-100 (BioRad, Hercules, CA). Hypodiploid cells were

quantified by flow cytometry by FACSCalibur (BD Biosciences, San Jose, CA) and analyzed by FlowJo software version 7.6.5 for Microsoft (TreeStar, San Carlos, CA).

Caspase Inhibition: Cells were collected at 0.5×10^6 cells and treated with the indicated dose of caspase 8 inhibitor Z-IETD-FMK (BD Biosciences, San Jose, CA) for 30 minutes in 500µl sera free media RPMI1640 (MediaTech, Manassas, VA) at 37°C. Subsequently, cells were incubated in 500µl of sera free media containing 50ng/ml of CH-11 (Millipore, Temecula, CA) and cells were rotated at RT for 1 hour. Cells were then spun down and resuspended in fresh RPMI1640 supplemented with 10%FBS containing the indicated dose of caspase inhibitor for 16 hours at 37°C. Cell death was measured by Annexin V/7AAD staining as indicated previously.

Cytosolic and Nuclear Fractionation: Cells were collected at 2×10^6 cells or 10×10^6 healthy B cells and fractionated with a Nuclear/Cytosol fractionation kit according to the manufacturers protocol (Biovision, Milpitas, California). Briefly, cells were collected by centrifugation at 600 g for 5 minutes at 4°C. 0.2 ml of buffer 1 (CEB-A Mix containing DTT and Protease Inhibitors) was added for 10 minutes at 4°C.Subsequntly lysates were incubated with 11 µl of ice-cold buffer 2 (Cytosol Extraction Buffer-B) for 1 minute at 4°C. Supernatants were collected after centrifugation for 5 minutes at maximal speed and the remaining pellet was resuspended in 100 µl of buffer 3(Nuclear Extraction Buffer Mix) for a total 40 minutes. Lysates were cleared of insoluble proteins by centrifugation at 16,000 g for 10 minutes.

Statistical Analysis: Experimental data are reported as ±SEM of 3 independent samples, unless otherwise indicated. Differences between groups were calculated using the 2-tailed student's t-test with paired samples (GraphPad Prism, La Jolla, CA). A P value of less than .05 was considered statistically significant.

Patient summary statistics including mean, standard deviation, median, and range for continuous variables (such as age), frequency counts and percentages for categorical variables (such as histology and gender) were reported. The Chi-square test or Fisher's exact test was used to evaluate the association between two categorical. Wilcoxon rank sum test or Kruskal-Wallis test was used to evaluate the difference in a continuous variable between the responders and the non-responders. Kaplan-Meier method was used to estimate time-to-event outcomes including progression free survival, overall survival, and disease specific survival. Median time to event in months with 95% confidence interval was calculated. The log-rank test was used to evaluate the difference in time-to-event outcomes between patient groups. Cox proportional hazards models

were used for the multivariate analyses. Statistical software SAS 9.1.3 (SAS, Cary, NC) and S-Plus 8.0 (TIBCO Software Inc., Palo Alto, CA) were used for all the analyses.

Appendix

A

Figure 26

GAR

Forward GAR-F 5'-CCGCGATCGCCATGGGTGAAGGTGGCTT-3'

Reverse GAR-R 5'-AAGCCACCTTCACCCATGGCGATCGCGG-3'

R4GAR

Forward R4-GAR-F 5'-CGCCGCGATCGCCATGAAAACTCTGTTTGTCAA-3'

Reverse R4-GAR-R 5'-TTGACAAACAGAGTTTTCATGGCGATCGCGGCG-3'

R34GAR

Forward R3,4-GAR-F 5'-CGCCGCGATCGCCATGAAAACTCTGGTTTTAAG-3'

Reverse R3,4-GAR-R 5'-CTTAAAACCAGAGTTTTCATGGCGATCGCGGCG-3'

R234GAR

Forward R2,3,4-GAR-F 5'-CGCCGCGATCGCCATGAGAACACTTTTGGCTA-3'

Reverse R2,3,4-GAR-R 5'-TAGCCAAAAGTGTTCTCATGGCGATCGCGGCG-3'

NR1234

Forward N-R1,2,3,4-F 5'-GACTGGGCCAAACCTAAGACGCGTACGCGG-3’

Reverse N-R1,2,3,4-R 5'-CCGCGTACGCGTCTTAGGTTTGGCCCAGTC-3'

Nterm

Forward N-ter-F 5'-CACAGAACCGACTACGGCTACGCGTACGC-3'

Reverse N-ter-R 5'-GCGTACGCGTAGCCGTAGTCGGTTCTGTG-3'

NR123

Forward NR1,2,3-F 5'-AAGCCAGCCATCCACGCGTACGCGGC-3'

Reverse NR1,2,3-R 5'-GCCGCGTACGCGTGGATGGCTGGCTT-3'

NR12

Forward NR1,2-F 5'-AGCACTTGGAGTGGTGAATCAACGCGTACGCG-3'

Reverse NR1,2-R 5'-CGCGTACGCGTTGATTCACCACTCCAAGTGCT-3'

NR1

Forward NR1-F 5'-AGAGCGAGATGCGACGCGTACGCGGC-3'

Reverse NR1-R 5'-GCCGCGTACGCGTCGCATCTCGCTCT-3'

Figure 25: Primers for the Design of Nucleolin Domain Mutants.

DNA primers were constructed by Sigma Aldrich (St. Louis, MO) and were designed according to the manufacturer’s protocol for Quick Change II XL site-directed mutagenesis (Stratagene, Cedar Creek, TX) on pCMV6-Nucleolin (Origene, Rockville, MD).

Bibliography

1. Arumugam, S., M. C. Miller, J. Maliekal, P. J. Bates, J. O. Trent, and A. N. Lane. 2010. Solution structure of the RBD1,2 domains from human nucleolin. J Biomol NMR 47:79-83.
2. Madej, T., K. J. Addess, J. H. Fong, L. Y. Geer, R. C. Geer, C. J. Lanczycki, C. Liu, S. Lu, A. Marchler-Bauer, A. R. Panchenko, J. Chen, P. A. Thiessen, Y. Wang, D. Zhang, and S. H. Bryant. 2012. MMDB: 3D structures and macromolecular interactions. Nucleic Acids Res 40:D461-464.
3. Kuppers, R. 2005. Mechanisms of B-cell lymphoma pathogenesis. Nat Rev Cancer 5:251-262.
4. Kuppers, R., U. Klein, M. L. Hansmann, and K. Rajewsky. 1999. Cellular origin of human B-cell lymphomas. N Engl J Med 341:1520-1529.
5. Sangle, N. 2011. WHO classification of B-cell lymphoid neoplasms. In Lymphoma-B cell neoplasms. University of Utah and ARUP Laboratories, Pathologyoutlines.com, Inc.
6. Society, L. a. L. 2012. Facts 2012. LLS, National Office 1311 Manaroneck Avenue, Suite 310, White Plains, NY 10605. http://www.lls.org/content/nationalcontent/resourcecenter/freeeducationmaterials/generalcancer/pdf/facts.pdf.
7. Society, A. C. 2012. Cancer Facts and Figures 2012. R. Siegel, editor. American Cancer Society, http://www.cancer.org/acs/groups/content/@epidemiologysurveilance/documents/document/acspc-031941.pdf.
8. Coory, M., and D. Gill. 2008. Decreasing mortality from non-Hodgkin lymphoma in Australia. Intern Med J 38:921-924.
9. Adamson, P., F. Bray, A. S. Costantini, M. H. Tao, E. Weiderpass, and E. Roman. 2007. Time trends in the registration of Hodgkin and non-Hodgkin lymphomas in Europe. Eur J Cancer 43:391-401.
10. Groves, F. D., M. S. Linet, L. B. Travis, and S. S. Devesa. 2000. Cancer surveillance series: non-Hodgkin's lymphoma incidence by histologic subtype in the United States from 1978 through 1995. J Natl Cancer Inst 92:1240-1251.

11. Espey, D. K., X. C. Wu, J. Swan, C. Wiggins, M. A. Jim, E. Ward, P. A. Wingo, H. L. Howe, L. A. Ries, B. A. Miller, A. Jemal, F. Ahmed, N. Cobb, J. S. Kaur, and B. K. Edwards. 2007. Annual report to the nation on the status of cancer, 1975-2004, featuring cancer in American Indians and Alaska Natives. Cancer 110:2119-2152.
12. Ferlay, J., H. R. Shin, F. Bray, D. Forman, C. Mathers, and D. M. Parkin. 2010. Estimates of worldwide burden of cancer in 2008: GLOBOCAN 2008. Int J Cancer 127:2893-2917.
13. Project, T. I. N.-H. s. L. P. F. 1993. A predictive model for aggressive non-Hodgkin's lymphoma. N Engl J Med 329:987-994.
14. Siegel, R., E. Ward, O. Brawley, and A. Jemal. 2011. Cancer statistics, 2011: the impact of eliminating socioeconomic and racial disparities on premature cancer deaths. CA Cancer J Clin 61:212-236.
15. Xu-Monette, Z. Y., L. Wu, C. Visco, Y. C. Tai, A. Tzankov, W. M. Liu, S. Montes-Moreno, K. Dybkaer, A. Chiu, A. Orazi, Y. Zu, G. Bhagat, K. L. Richards, E. D. Hsi, X. F. Zhao, W. W. Choi, X. Zhao, J. H. van Krieken, Q. Huang, J. Huh, W. Ai, M. Ponzoni, A. J. Ferreri, F. Zhou, B. S. Kahl, J. N. Winter, W. Xu, J. Li, R. S. Go, Y. Li, M. A. Piris, M. B. Moller, R. N. Miranda, L. V. Abruzzo, L. J. Medeiros, and K. H. Young. 2012. Mutational profile and prognostic significance of TP53 in diffuse large B-cell lymphoma patients treated with R-CHOP: report from an International DLBCL Rituximab-CHOP Consortium Program Study. Blood 120:3986-3996.
16. Offit, K., F. Lo Coco, D. C. Louie, N. Z. Parsa, D. Leung, C. Portlock, B. H. Ye, F. Lista, D. A. Filippa, A. Rosenbaum, M. Ladanyi, S. Jhanwar, R. Dalla-Favera, and R. S. K. Chaganti. 1994. Rearrangement of the bcl-6 gene as a prognostic marker in diffuse large-cell lymphoma. N Engl J Med 331:74-80.
17. Linch, D. C. 2012. Burkitt lymphoma in adults. Br J Haematol 156:693-703.
18. Dalla-Favera, R., M. Bregni, J. Erikson, D. Patterson, R. C. Gallo, and C. M. Croce. 1982. Human c-*myc onc* gene is located on the region of chromosome 8 that is translocated in Burkitt lymphoma cells. Proc Natl Acad Sci USA 79:7824-7827.
19. Wilson, W. H., K. Dunleavy, S. Pittaluga, U. Hegde, N. Grant, S. M. Steinberg, M. Raffeld, M. Gutierrez, B. A. Chabner, L. Staudt, E. S. Jaffe, and J. E. Janik. 2008. Phase II study of dose-adjusted EPOCH and rituximab in untreated diffuse large B-cell

lymphoma with analysis of germinal center and post-germinal center biomarkers. J Clin Oncol 26:2717-2724.

20. Clodi, K., V. Snell, S. Zhao, F. Cabanillas, M. Andreeff, and A. Younes. 1998. Unbalanced expression of Fas and CD40 in mantle cell lymphoma. Br J Haematol 103:217-219.
21. Jares, P., D. Colomer, and E. Campo. 2012. Molecular pathogenesis of mantle cell lymphoma. J Clin Invest 122:3416-3423.
22. Vandenberghe, E. 1994. Mantle cell lymphoma. Blood Rev 8:79-87.
23. Herrmann, A., E. Hoster, T. Zwingers, G. Brittinger, M. Engelhard, P. Meusers, M. Reiser, R. Forstpointner, B. Metzner, N. Peter, B. Wormann, L. Trumper, M. Pfreundschuh, H. Einsele, W. Hiddemann, M. Unterhalt, and M. Dreyling. 2009. Improvement of overall survival in advanced stage mantle cell lymphoma. J Clin Oncol 27:511-518.
24. Leitch, H. A., R. D. Gascoyne, M. Chhanabhai, N. J. Voss, R. Klasa, and J. M. Connors. 2003. Limited-stage mantle-cell lymphoma. Ann Oncol 14:1555-1561.
25. Gaidano, G., R. Foa, and R. Dalla-Favera. 2012. Molecular pathogenesis of chronic lymphocytic leukemia. J Clin Invest 122:3432-3438.
26. Lehne, G., E. Elonen, M. Baekelandt, T. Skovsgaard, and C. Peterson. 1998. Challenging drug resistance in cancer therapy--review of the First Nordic Conference on Chemoresistance in Cancer Treatment, October 9th and 10th, 1997. Acta Oncol 37:431-439.
27. Wettergren, L., M. Bjorkholm, U. Axdorph, and A. Langius-Eklof. 2004. Determinants of health-related quality of life in long-term survivors of Hodgkin's lymphoma. Qual Life Res 13:1369-1379.
28. Sehn, L. H., J. Donaldson, M. Chhanabhai, C. Fitzgerald, K. Gill, R. Klasa, N. MacPherson, S. O'Reilly, J. J. Spinelli, J. Sutherland, K. S. Wilson, R. D. Gascoyne, and J. M. Connors. 2005. Introduction of combined CHOP plus rituximab therapy dramatically improved outcome of diffuse large B-cell lymphoma in British Columbia. J Clin Oncol 23:5027-5033.
29. Coiffier, B., E. Lepage, J. Briere, R. Herbrecht, H. Tilly, R. Bouabdallah, P. Morel, E. Van Den Neste, G. Salles, P. Gaulard, F. Reyes, P. Lederlin, and C. Gisselbrecht. 2002.

CHOP chemotherapy plus rituximab compared with CHOP alone in elderly patients with diffuse large-B-cell lymphoma. N Engl J Med 346:235-242.

30. Pfreundschuh, M., E. Kuhnt, L. Trumper, A. Osterborg, M. Trneny, L. Shepherd, D. S. Gill, J. Walewski, R. Pettengell, U. Jaeger, P. L. Zinzani, O. Shpilberg, S. Kvaloy, P. de Nully Brown, R. Stahel, N. Milpied, A. Lopez-Guillermo, V. Poeschel, S. Grass, M. Loeffler, N. Murawski, and G. MabThera International Trial. 2011. CHOP-like chemotherapy with or without rituximab in young patients with good-prognosis diffuse large-B-cell lymphoma: 6-year results of an open-label randomised study of the MabThera International Trial (MInT) Group. Lancet Oncol 12:1013-1022.
31. Ng, A. K., A. LaCasce, and L. B. Travis. 2011. Long-term complications of lymphoma and its treatment. J Clin Oncol 29:1885-1892.
32. Baldini, N. 1997. Multidrug resistance--a multiplex phenomenon. Nat Med 3:378-380.
33. Mickisch, G. H., K. Roehrich, J. Koessig, S. Forster, R. K. Tschada, and P. M. Alken. 1990. Mechanisms and modulation of multidrug resistance in primary human renal cell carcinoma. J Urol 144:755-759.
34. Mickisch, G., H. Bier, W. Bergler, M. Bak, R. Tschada, and P. Alken. 1990. P-170 glycoprotein, glutathione and associated enzymes in relation to chemoresistance of primary human renal cell carcinomas. Urol Int 45:170-176.
35. Lai, D., S. Visser-Grieve, and X. Yang. 2012. Tumour suppressor genes in chemotherapeutic drug response. Biosci Rep 32:361-374.
36. Knappskog, S., and P. E. Lonning. 2012. P53 and its molecular basis to chemoresistance in breast cancer. Expert Opin Ther Targets 16 Suppl 1:S23-30.
37. Schulze-Osthoff, K., D. Ferrari, M. Los, S. Wesselborg, and M. E. Peter. 1998. Apoptosis signaling by death receptors. Eur J Biochem 254:439-459.
38. Itoh, N., and S. Nagata. 1993. A novel protein domain required for apoptosis. J Biol Chem 268:10932-10937.
39. Kerr, J. F., A. H. Wyllie, and A. R. Currie. 1972. Apoptosis: a basic biological phenomenon with wide-ranging implications in tissue kinetics. Br J Cancer 26:239-257.
40. Kanduc, D., A. Mittelman, R. Serpico, E. Sinigaglia, A. A. Sinha, C. Natale, R. Santacroce, M. G. Di Corcia, A. Lucchese, L. Dini, P. Pani, S. Santacroce, S. Simone, R. Bucci, and E. Farber. 2002. Cell death: apoptosis versus necrosis (review). International Journal of Oncology 21:165-170.

41. Koopman, G., C. P. Reutelingsperger, G. A. Kuijten, R. M. Keehnen, S. T. Pals, and M. H. van Oers. 1994. Annexin V for flow cytometric detection of phosphatidylserine expression on B cells undergoing apoptosis. Blood 84:1415-1420.
42. Aggarwal, B. B., W. J. Kohr, P. E. Hass, B. Moffat, S. A. Spencer, W. J. Henzel, T. S. Bringman, G. E. Nedwin, D. V. Goeddel, and R. N. Harkins. 1985. Human tumor necrosis factor. J Biol Chem 260:2345-2354.
43. Takahashi, T., M. Tanaka, C. I. Brannan, N. A. Jenkins, N. G. Copeland, T. Suda, and S. Nagata. 1994. Generalized lymphoproliferative disease in mice, caused by a point mutation in the Fas ligand. Cell 76:969-976.
44. Papoff, G., I. Cascino, A. Eramo, G. Starace, D. H. Lynch, and G. Ruberti. 1996. An N-terminal domain shared by Fas/Apo-1 (CD95) soluble variants prevents cell death in vitro. J Immunol 156:4622-4630.
45. Fisher, G. H., F. J. Rosenberg, S. E. Straus, J. K. Dale, L. A. Middleton, A. Y. Lin, W. Strober, M. J. Lenardo, and J. M. Puck. 1995. Dominant interfering Fas gene mutations impair apoptosis in a human autoimmune lymphoproliferative syndrome. Cell 81:935-946.
46. Bewick, M., M. Conlon, A. M. Parissenti, H. Lee, L. Zhang, S. Gluck, and R. M. Lafrenie. 2001. Soluble Fas (CD95) is a prognostic factor in patients with metastatic breast cancer undergoing high-dose chemotherapy and autologous stem cell transplantation. J Hematother Stem Cell Res 10:759-768.
47. Shatnyeva, O. M., A. V. Kubarenko, C. E. Weber, A. Pappa, R. Schwartz-Albiez, A. N. Weber, P. H. Krammer, and I. N. Lavrik. 2011. Modulation of the CD95-induced apoptosis: the role of CD95 N-glycosylation. PLoS One 6:e19927.
48. Albanese, J., S. Meterissian, M. Kontogiannea, C. Dubreuil, A. Hand, S. Sorba, and N. Dainiak. 1998. Biologically active Fas antigen and its cognate ligand are expressed on plasma membrane-derived extracellular vesicles. Blood 91:3862-3874.
49. Keppler, O. T., M. E. Peter, S. Hinderlich, G. Moldenhauer, P. Stehling, I. Schmitz, R. Schwartz-Albiez, W. Reutter, and M. Pawlita. 1999. Differential sialylation of cell surface glycoconjugates in a human B lymphoma cell line regulates susceptibility for CD95 (APO-1/Fas)-mediated apoptosis and for infection by a lymphotropic virus. Glycobiology 9:557-569.

50. Wagner, K. W., E. A. Punnoose, T. Januario, D. A. Lawrence, R. M. Pitti, K. Lancaster, D. Lee, M. von Goetz, S. F. Yee, K. Totpal, L. Huw, V. Katta, G. Cavet, S. G. Hymowitz, L. Amler, and A. Ashkenazi. 2007. Death-receptor O-glycosylation controls tumor-cell sensitivity to the proapoptotic ligand Apo2L/TRAIL. Nat Med 13:1070-1077.

51. Bretz, J. D., P. L. Arscott, A. Myc, and J. R. Baker, Jr. 1999. Inflammatory cytokine regulation of Fas-mediated apoptosis in thyroid follicular cells. J Biol Chem 274:25433-25438.

52. Suda, T., T. Takahashi, P. Golstein, and S. Nagata. 1993. Molecular cloning and expression of the Fas ligand, a novel member of the tumor necrosis factor family. Cell 75:1169-1178.

53. Lee, K. H., C. Feig, V. Tchikov, R. Schickel, C. Hallas, S. Schutze, M. E. Peter, and A. C. Chan. 2006. The role of receptor internalization in CD95 signaling. EMBO J 25:1009-1023.

54. Orlinick, J. R., K. B. Elkon, and M. V. Chao. 1997. Separate domains of the human Fas ligand dictate self-association and receptor binding. J Biol Chem 272:32221-32229.

55. Tartaglia, L. A., T. M. Ayres, G. H. Wong, and D. V. Goeddel. 1993. A novel domain within the 55 kd TNF receptor signals cell death. Cell 74:845-853.

56. Salvesen, G. S., and S. J. Riedl. 2009. Structure of the Fas/FADD complex: a conditional death domain complex mediating signaling by receptor clustering. Cell Cycle 8:2723-2727.

57. Fadeel, B., J. Lindberg, A. Achour, and F. Chiodi. 1998. A three-dimensional model of the Fas/APO-1 molecule: cross-reactivity of anti-Fas antibodies explained by structural mimicry of antigenic sites. Int Immunol 10:131-140.

58. Chinnaiyan, A. M., K. O'Rourke, M. Tewari, and V. M. Dixit. 1995. FADD, a novel death domain-containing protein, interacts with the death domain of Fas and initiates apoptosis. Cell 81:505-512.

59. Boldin, M. P., E. E. Varfolomeev, Z. Pancer, I. L. Mett, J. H. Camonis, and D. Wallach. 1995. A novel protein that interacts with the death domain of Fas/APO1 contains a sequence motif related to the death domain. J Biol Chem 270:7795-7798.

60. Gomez-Angelats, M., and J. A. Cidlowski. 2003. Molecular evidence for the nuclear localization of FADD. Cell Death Differ 10:791-797.

61. Kischkel, F. C., S. Hellbardt, I. Behrmann, M. Germer, M. Pawlita, P. H. Krammer, and M. E. Peter. 1995. Cytotoxicity-dependent APO-1 (Fas/CD95)-associated proteins form a death-inducing signaling complex (DISC) with the receptor. EMBO J 14:5579-5588.
62. Muzio, M., A. M. Chinnaiyan, F. C. Kischkel, K. O'Rourke, A. Shevchenko, J. Ni, C. Scaffidi, J. D. Bretz, M. Zhang, R. Gentz, M. Mann, P. H. Krammer, M. E. Peter, and V. M. Dixit. 1996. FLICE, a novel FADD-homologous ICE/CED-3-like protease, is recruited to the CD95 (Fas/APO-1) death-inducing signaling complex. Cell 85:817-827.
63. Wang, J., H. J. Chun, W. Wong, D. M. Spencer, and M. J. Lenardo. 2001. Caspase-10 is an initiator caspase in death receptor signaling. Proc Natl Acad Sci USA 98:13884-13888.
64. Martin, D. A., R. M. Siegel, L. Zheng, and M. J. Lenardo. 1998. Membrane oligomerization and cleavage activates the caspase-8 (FLICE/MACHalpha1) death signal. J Biol Chem 273:4345-4349.
65. Kischkel, F. C., D. A. Lawrence, A. Tinel, H. LeBlanc, A. Virmani, P. Schow, A. Gazdar, J. Blenis, D. Arnott, and A. Ashkenazi. 2001. Death receptor recruitment of endogenous caspase-10 and apoptosis initiation in the absence of caspase-8. J Biol Chem 276:46639-46646.
66. Barnhart, B. C., E. C. Alappat, and M. E. Peter. 2003. The CD95 type I/type II model. Semin Immunol 15:185-193.
67. Fulda, S., E. Meyer, C. Friesen, S. A. Susin, G. Kroemer, and K. M. Debatin. 2001. Cell type specific involvement of death receptor and mitochondrial pathways in drug-induced apoptosis. Oncogene 20:1063-1075.
68. Cohen, G. M. 1997. Caspases: the executioners of apoptosis. Biochem J 326 (Pt 1):1-16.
69. Sabol, S. L., R. Li, T. Y. Lee, and R. Abdul-Khalek. 1998. Inhibition of apoptosis-associated DNA fragmentation activity in nonapoptotic cells: the role of DNA fragmentation factor-45 (DFF45/ICAD). Biochem Biophys Res Commun 253:151-158.
70. Kaufmann, T., A. Strasser, and P. J. Jost. 2012. Fas death receptor signalling: roles of Bid and XIAP. Cell Death Differ 19:42-50.
71. Pop, C., J. Timmer, S. Sperandio, and G. S. Salvesen. 2006. The apoptosome activates caspase-9 by dimerization. Mol Cell 22:269-275.

72. Riedl, S. J., and G. S. Salvesen. 2007. The apoptosome: signalling platform of cell death. Nat Rev Mol Cell Biol 8:405-413.
73. Jayaraman, S. 2005. Flow cytometric determination of mitochondrial membrane potential changes during apoptosis of T lymphocytic and pancreatic beta cell lines: comparison of tetramethylrhodamineethylester (TMRE), chloromethyl-X-rosamine (H2-CMX-Ros) and MitoTracker Red 580 (MTR580). J Immunol Methods 306:68-79.
74. Algeciras-Schimnich, A., E. M. Pietras, B. C. Barnhart, P. Legembre, S. Vijayan, S. L. Holbeck, and M. E. Peter. 2003. Two CD95 tumor classes with different sensitivities to antitumor drugs. Proc Natl Acad Sci U S A 100:11445-11450.
75. Tanaka, T., and N. Umesaki. 2003. Fas antigen (CD95) mediates cell survival signals to regulate functional cellular subpopulations in normal human endometrial stromal cells. Int J Mol Med 11:757-762.
76. Green, D. R. 2010. Cancer: A wolf in wolf's clothing. Nature 465:433.
77. Watanabe-Fukunaga, R., C. I. Brannan, N. G. Copeland, N. A. Jenkins, and S. Nagata. 1992. Lymphoproliferation disorder in mice explained by defects in Fas antigen that mediates apoptosis. Nature 356:314-317.
78. Lynch, D. H., M. L. Watson, M. R. Alderson, P. R. Baum, R. E. Miller, T. Tough, M. Gibson, T. Davis-Smith, C. A. Smith, K. Hunter, D. Bhat, W. Din, R. G. Goodwin, and M. F. Seldin. 1994. The mouse Fas-ligand gene is mutated in gld mice and is part of a TNF family gene cluster. Immunity 1:131-136.
79. Teachey, D. T., A. E. Seif, and S. A. Grupp. 2010. Advances in the management and understanding of autoimmune lymphoproliferative syndrome (ALPS). Br J Haematol 148:205-216.
80. Rieux-Laucat, F., F. Le Deist, C. Hivroz, I. A. Roberts, K. M. Debatin, A. Fischer, and J. P. de Villartay. 1995. Mutations in Fas associated with human lymphoproliferative syndrome and autoimmunity. Science 268:1347-1349.
81. Takahashi, H., F. Feuerhake, J. L. Kutok, S. Monti, P. Dal Cin, D. Neuberg, J. C. Aster, and M. A. Shipp. 2006. FAS death domain deletions and cellular FADD-like interleukin 1beta converting enzyme inhibitory protein (long) overexpression: alternative mechanisms for deregulating the extrinsic apoptotic pathway in diffuse large B-cell lymphoma subtypes. Clin Cancer Res 12:3265-3271.

82. Friesen, C., S. Fulda, and K. M. Debatin. 1999. Induction of CD95 ligand and apoptosis by doxorubicin is modulated by the redox state in chemosensitive- and drug-resistant tumor cells. Cell Death Differ 6:471-480.

83. Hanahan, D., and R. A. Weinberg. 2000. The hallmarks of cancer. Cell 100:57-70.

84. Oue, F. G., V. A. Phan, V. H. Phan, N. F. LaRusso, and G. J. Gores. 1998. Alterations in Fas and Fas ligand expression in cholangiocarcinoma: A mechanism of escape from immunosurveillance. Gastroenterology 114:A1325-A1325.

85. Knipping, E., K. M. Debatin, K. Stricker, B. Heilig, A. Eder, and P. H. Krammer. 1995. Identification of soluble APO-1 in supernatants of human B- and T-cell lines and increased serum levels in B- and T-cell leukemias. Blood 85:1562-1569.

86. Niitsu, N., K. Sasaki, and M. Umeda. 1999. A high serum soluble Fas/APO-1 level is associated with a poor outcome of aggressive non-Hodgkin's lymphoma. Leukemia 13:1434-1440.

87. Cheng, J., T. Zhou, C. Liu, J. P. Shapiro, M. J. Brauer, M. C. Kiefer, P. J. Barr, and J. D. Mountz. 1994. Protection from Fas-mediated apoptosis by a soluble form of the Fas molecule. Science 263:1759-1762.

88. Pitti, R. M., S. A. Marsters, D. A. Lawrence, M. Roy, F. C. Kischkel, P. Dowd, A. Huang, C. J. Donahue, S. W. Sherwood, D. T. Baldwin, P. J. Godowski, W. I. Wood, A. L. Gurney, K. J. Hillan, R. L. Cohen, A. D. Goddard, D. Botstein, and A. Ashkenazi. 1998. Genomic amplification of a decoy receptor for Fas ligand in lung and colon cancer. Nature 396:699-703.

89. Yu, K. Y., B. Kwon, J. Ni, Y. Zhai, R. Ebner, and B. S. Kwon. 1999. A newly identified member of tumor necrosis factor receptor superfamily (TR6) suppresses LIGHT-mediated apoptosis. J Biol Chem 274:13733-13736.

90. Chang, P. M. H., P. M. Chen, S. L. Hsieh, C. H. Tzeng, J. H. Liu, T. J. Chiou, W. S. Wang, C. C. Yen, J. P. Gau, and M. H. Yang. 2008. Expression of a soluble decoy receptor 3 in patients with diffuse large B-cell lymphoma predicts clinical outcome. International Journal of Oncology 33:549-554.

91. Ohshima, K., S. Haraoka, M. Sugihara, J. Suzumiya, C. Kawasaki, M. Kanda, and M. Kikuchi. 2000. Amplification and expression of a decoy receptor for Fas ligand (DcR3) in virus (EBV or HTLV-I) associated lymphomas. Cancer Lett 160:89-97.

92. Sato, T., S. Irie, S. Kitada, and J. C. Reed. 1995. FAP-1: a protein tyrosine phosphatase that associates with Fas. Science 268:411-415.
93. Irmler, M., M. Thome, M. Hahne, P. Schneider, K. Hofmann, V. Steiner, J. L. Bodmer, M. Schroter, K. Burns, C. Mattmann, D. Rimoldi, L. E. French, and J. Tschopp. 1997. Inhibition of death receptor signals by cellular FLIP. Nature 388:190-195.
94. Himeji, D., T. Horiuchi, H. Tsukamoto, K. Hayashi, T. Watanabe, and M. Harada. 2002. Characterization of caspase-8L: a novel isoform of caspase-8 that behaves as an inhibitor of the caspase cascade. Blood 99:4070-4078.
95. Fiory, F., P. Formisano, G. Perruolo, and F. Beguinot. 2009. Frontiers: PED/PEA-15, a multifunctional protein controlling cell survival and glucose metabolism. Am J Physiol Endocrinol Metab 297:e592-601.
96. Condorelli, G., G. Vigliotta, A. Cafieri, A. Trencia, P. Andalo, F. Oriente, C. Miele, M. Caruso, P. Formisano, and F. Beguinot. 1999. PED/PEA-15: an anti-apoptotic molecule that regulates FAS/TNFR1-induced apoptosis. Oncogene 18:4409-4415.
97. Ruiz-Ruiz, M. C., M. Izquierdo, G. de Murcia, and A. Lopez-Rivas. 1997. Activation of protein kinase C attenuates early signals in Fas-mediated apoptosis. Eur J Immunol 27:1442-1450.
98. Okura, T., L. Gong, T. Kamitani, T. Wada, I. Okura, C. F. Wei, H. M. Chang, and E. T. Yeh. 1996. Protection against Fas/APO-1- and tumor necrosis factor-mediated cell death by a novel protein, sentrin. J Immunol 157:4277-4281.
99. Jung, Y. S., K. S. Kim, K. D. Kim, J. S. Lim, J. W. Kim, and E. Kim. 2001. Apoptosis-linked gene 2 binds to the death domain of Fas and dissociates from Fas during Fas-mediated apoptosis in Jurkat cells. Biochem Biophys Res Commun 288:420-426.
100. Ola, M. S., M. Nawaz, and H. Ahsan. 2011. Role of Bcl-2 family proteins and caspases in the regulation of apoptosis. Mol Cell Biochem 351:41-58.
101. Timmer, T., E. G. de Vries, and S. de Jong. 2002. Fas receptor-mediated apoptosis: a clinical application? J Pathol 196:125-134.
102. Kondo, E., and T. Yoshino. 2007. Expression of apoptosis regulators in germinal centers and germinal center-derived B-cell lymphomas: insight into B-cell lymphomagenesis. Pathol Int 57:391-397.

103. Smolewski, P., and T. Robak. 2011. Inhibitors of apoptosis proteins (IAPs) as potential molecular targets for therapy of hematological malignancies. Curr Mol Med 11:633-649.
104. Xerri, L., F. Palmerini, E. Devilard, T. Defrance, R. Bouabdallah, J. Hassoun, and F. Birg. 2000. Frequent nuclear localization of ICAD and cytoplasmic co-expression of caspase-8 and caspase-3 in human lymphomas. J Pathol 192:194-202.
105. Eichhorst, S. T., S. Muerkoster, M. A. Weigand, and P. H. Krammer. 2001. The chemotherapeutic drug 5-fluorouracil induces apoptosis in mouse thymocytes in vivo via activation of the CD95(APO-1/Fas) system. Cancer Res 61:243-248.
106. Yoshimoto, Y., M. Kawada, D. Ikeda, and M. Ishizuka. 2005. Involvement of doxorubicin-induced Fas expression in the antitumor effect of doxorubicin on Lewis lung carcinoma in vivo. Int Immunopharmacol 5:281-288.
107. Fulda, S., C. Friesen, and K. M. Debatin. 1998. Molecular determinants of apoptosis induced by cytotoxic drugs. Klin Padiatr 210:148-152.
108. Friesen, C., I. Herr, P. H. Krammer, and K. M. Debatin. 1996. Involvement of the CD95 (APO-1/Fas) receptor/ligand system in drug-induced apoptosis in leukemia cells. Nat Med 2:574-577.
109. Muller, M., S. Strand, H. Hug, E. M. Heinemann, H. Walczak, W. J. Hofmann, W. Stremmel, P. H. Krammer, and P. R. Galle. 1997. Drug-induced apoptosis in hepatoma cells is mediated by the CD95 (APO-1/Fas) receptor/ligand system and involves activation of wild-type p53. J Clin Invest 99:403-413.
110. Herr, I., D. Wilhelm, T. Bohler, P. Angel, and K. M. Debatin. 1997. Activation of CD95 (APO-1/Fas) signaling by ceramide mediates cancer therapy-induced apoptosis. EMBO J 16:6200-6208.
111. Friesen, C., S. Fulda, and K. M. Debatin. 1997. Deficient activation of the CD95 (APO-1/Fas) system in drug-resistant cells. Leukemia 11:1833-1841.
112. Hannun, Y. A. 1997. Apoptosis and the dilemma of cancer chemotherapy. Blood 89:1845-1853.
113. Muller, M., S. Wilder, D. Bannasch, D. Israeli, K. Lehlbach, M. Li-Weber, S. L. Friedman, P. R. Galle, W. Stremmel, M. Oren, and P. H. Krammer. 1998. p53 activates the CD95 (APO-1/Fas) gene in response to DNA damage by anticancer drugs. J Exp Med 188:2033-2045.

114. Poulaki, V., C. S. Mitsiades, and N. Mitsiades. 2001. The role of Fas and FasL as mediators of anticancer chemotherapy. Drug Resist Updat 4:233-242.
115. Amoroso, A., S. Hafsi, L. Militello, A. E. Russo, Z. Soua, M. C. Mazzarino, F. Stivala, and M. Libra. 2011. Understanding rituximab function and resistance: implications for tailored therapy. Front Biosci 16:770-782.
116. Owen-Schaub, L. B., W. Zhang, J. C. Cusack, L. S. Angelo, S. M. Santee, T. Fujiwara, J. A. Roth, A. B. Deisseroth, W. W. Zhang, E. Kruzel, and et al. 1995. Wild-type human p53 and a temperature-sensitive mutant induce Fas/APO-1 expression. Mol Cell Biol 15:3032-3040.
117. Muller, M., C. A. Scaffidi, P. R. Galle, W. Stremmel, and P. H. Krammer. 1998. The role of p53 and the CD95 (APO-1/Fas) death system in chemotherapy-induced apoptosis. Eur Cytokine Netw 9:685-686.
118. Dimberg, L. Y., A. I. Dimberg, K. Ivarsson, T. Stromberg, A. Osterborg, K. Nilsson, F. Oberg, and H. Jernberg Wiklund. 2005. Ectopic and IFN-induced expression of Fas overcomes resistance to Fas-mediated apoptosis in multiple myeloma cells. Blood 106:1346-1354.
119. Crescenzi, E., F. Pacifico, A. Lavorgna, R. De Palma, E. D'Aiuto, G. Palumbo, S. Formisano, and A. Leonardi. 2011. NF-kappaB-dependent cytokine secretion controls Fas expression on chemotherapy-induced premature senescent tumor cells. Oncogene 30:2707-2717.
120. Wilson, A. J., A. C. Chueh, L. Togel, G. A. Corner, N. Ahmed, S. Goel, D. S. Byun, S. Nasser, M. A. Houston, M. Jhawer, H. J. Smartt, L. B. Murray, C. Nicholas, B. G. Heerdt, D. Arango, L. H. Augenlicht, and J. M. Mariadason. 2010. Apoptotic sensitivity of colon cancer cells to histone deacetylase inhibitors is mediated by an Sp1/Sp3-activated transcriptional program involving immediate-early gene induction. Cancer Res 70:609-620.
121. Pang, H., K. Miranda, and A. Fine. 1998. Sp3 regulates fas expression in lung epithelial cells. Biochem J 333 (Pt 1):209-213.
122. Lasham, A., E. Lindridge, F. Rudert, R. Onrust, and J. Watson. 2000. Regulation of the human fas promoter by YB-1, Puralpha and AP-1 transcription factors. Gene 252:1-13.
123. Mo, Y. Y., and W. T. Beck. 1999. DNA damage signals induction of Fas ligand in tumor cells. Mol Pharmacol 55:216-222.

124. Muzio, M., B. R. Stockwell, H. R. Stennicke, G. S. Salvesen, and V. M. Dixit. 1998. An induced proximity model for caspase-8 activation. J Biol Chem 273:2926-2930.
125. Houghton, J. A., F. G. Harwood, and D. M. Tillman. 1997. Thymineless death in colon carcinoma cells is mediated via Fas signaling. Proc Natl Acad Sci USA 94:8144-8149.
126. Kasibhatla, S., T. Brunner, L. Genestier, F. Echeverri, A. Mahboubi, and D. R. Green. 1998. DNA damaging agents induce expression of Fas ligand and subsequent apoptosis in T lymphocytes via the activation of NF-kappa B and AP-1. Mol Cell 1:543-551.
127. Reap, E. A., K. Roof, K. Maynor, M. Borrero, J. Booker, and P. L. Cohen. 1997. Radiation and stress-induced apoptosis: a role for Fas/Fas ligand interactions. Proc Natl Acad Sci USA 94:5750-5755.
128. Mahmood, Z., and Y. Shukla. 2010. Death receptors: targets for cancer therapy. Exp Cell Res 316:887-899.
129. Raghavendra, P. B., N. Pathak, and S. K. Manna. 2009. Novel role of thiadiazolidine derivatives in inducing cell death through Myc-Max, Akt, FKHR, and FasL pathway. Biochem Pharmacol 78:495-503.
130. Heikaus, S., K. S. Matuszek, C. V. Suschek, U. Ramp, P. Reinecke, E. Grinstein, J. Haremza, H. E. Gabbert, and C. Mahotka. 2008. Paclitaxel (Taxol)-induced apoptosis in human epithelioid sarcoma cell lines is enhanced by upregulation of CD95 ligand (FasL/Apo-1L). J Cancer Res Clin Oncol 134:689-695.
131. Volpert, O. V., T. Zaichuk, W. Zhou, F. Reiher, T. A. Ferguson, P. M. Stuart, M. Amin, and N. P. Bouck. 2002. Inducer-stimulated Fas targets activated endothelium for destruction by anti-angiogenic thrombospondin-1 and pigment epithelium-derived factor. Nat Med 8:349-357.
132. Yao, P. L., Y. C. Lin, P. Sawhney, and J. H. Richburg. 2007. Transcriptional regulation of FasL expression and participation of sTNF-alpha in response to sertoli cell injury. J Biol Chem 282:5420-5431.
133. Micheau, O., A. Hammann, E. Solary, and M. T. Dimanche-Boitrel. 1999. STAT-1-independent upregulation of FADD and procaspase-3 and -8 in cancer cells treated with cytotoxic drugs. Biochem Biophys Res Commun 256:603-607.
134. Lahiry, L., B. Saha, J. Chakraborty, A. Adhikary, S. Mohanty, D. M. Hossain, S. Banerjee, K. Das, G. Sa, and T. Das. 2010. Theaflavins target Fas/caspase-8 and

Akt/pBad pathways to induce apoptosis in p53-mutated human breast cancer cells. Carcinogenesis 31:259-268.

135. Bush, J. A., K. J. Cheung, Jr., and G. Li. 2001. Curcumin induces apoptosis in human melanoma cells through a Fas receptor/caspase-8 pathway independent of p53. Exp Cell Res 271:305-314.

136. Eischen, C. M., T. J. Kottke, L. M. Martins, G. S. Basi, J. S. Tung, W. C. Earnshaw, P. J. Leibson, and S. H. Kaufmann. 1997. Comparison of apoptosis in wild-type and Fas-resistant cells: chemotherapy-induced apoptosis is not dependent on Fas/Fas ligand interactions. Blood 90:935-943.

137. Villunger, A., A. Egle, M. Kos, B. L. Hartmann, S. Geley, R. Kofler, and R. Greil. 1997. Drug-induced apoptosis is associated with enhanced Fas (APO-1/CD95) ligand expression but occurs independently of Fas (APO-1/CD95) signaling in human T-acute lymphatic leukemia cells. Cancer Res 57:3331-3334.

138. McGahon, A. J., A. P. Costa Pereira, L. Daly, and T. G. Cotter. 1998. Chemotherapeutic drug-induced apoptosis in human leukaemic cells is independent of the Fas (APO-1/CD95) receptor/ligand system. Br J Haematol 101:539-547.

139. Ferrari, D., A. Stepczynska, M. Los, S. Wesselborg, and K. Schulze-Osthoff. 1998. Differential regulation and ATP requirement for caspase-8 and caspase-3 activation during CD95- and anticancer drug-induced apoptosis. J Exp Med 188:979-984.

140. Newton, K., and A. Strasser. 2000. Ionizing radiation and chemotherapeutic drugs induce apoptosis in lymphocytes in the absence of Fas or FADD/MORT1 signaling. J Exp Med 191:195-200.

141. Li, S., Y. Zhou, Y. Dong, and C. Ip. 2007. Doxorubicin and selenium cooperatively induce Fas signaling in the absence of Fas/Fas ligand interaction. Anticancer Res 27:3075-3082.

142. Alas, S., C. P. Ng, and B. Bonavida. 2002. Rituximab modifies the cisplatin-mitochondrial signaling pathway, resulting in apoptosis in cisplatin-resistant non-Hodgkin's lymphoma. Clin Cancer Res 8:836-845.

143. Friesen, C., S. Fulda, and K. M. Debatin. 1999. Cytotoxic drugs and the CD95 pathway. Leukemia 13:1854-1858.

144. Posovszky, C., C. Friesen, I. Herr, and K. M. Debatin. 1999. Chemotherapeutic drugs sensitize pre-B ALL cells for CD95- and cytotoxic T-lymphocyte-mediated apoptosis. Leukemia 13:400-409.

145. Strand, S., W. J. Hofmann, H. Hug, M. Muller, G. Otto, D. Strand, S. M. Mariani, W. Stremmel, P. H. Krammer, and P. R. Galle. 1996. Lymphocyte apoptosis induced by CD95 (APO-1/Fas) ligand-expressing tumor cells--a mechanism of immune evasion? Nat Med 2:1361-1366.

146. Los, M., I. Herr, C. Friesen, S. Fulda, K. Schulze-Osthoff, and K. M. Debatin. 1997. Cross-resistance of CD95- and drug-induced apoptosis as a consequence of deficient activation of caspases (ICE/Ced-3 proteases). Blood 90:3118-3129.

147. Petak, I., D. M. Tillman, F. G. Harwood, R. Mihalik, and J. A. Houghton. 2000. Fas-dependent and -independent mechanisms of cell death following DNA damage in human colon carcinoma cells. Cancer Res 60:2643-2650.

148. Plumas, J., M. C. Jacob, L. Chaperot, J. P. Molens, J. J. Sotto, and J. C. Bensa. 1998. Tumor B cells from non-Hodgkin's lymphoma are resistant to CD95 (Fas/Apo-1)-mediated apoptosis. Blood 91:2875-2885.

149. Kondo, E., T. Yoshino, I. Yamadori, Y. Matsuo, N. Kawasaki, J. Minowada, and T. Akagi. 1994. Expression of Bcl-2 protein and Fas antigen in non-Hodgkin's lymphomas. Am J Pathol 145:330-337.

150. Hofmann, W. K., S. de Vos, K. Tsukasaki, W. Wachsman, G. S. Pinkus, J. W. Said, and H. P. Koeffler. 2001. Altered apoptosis pathways in mantle cell lymphoma detected by oligonucleotide microarray. Blood 98:787-794.

151. Ginisty, H., H. Sicard, B. Roger, and P. Bouvet. 1999. Structure and functions of nucleolin. J Cell Sci 112 (Pt 6):761-772.

152. Srivastava, M., and H. B. Pollard. 1999. Molecular dissection of nucleolin's role in growth and cell proliferation: new insights. FASEB J 13:1911-1922.

153. Srivastava, M., O. W. McBride, P. J. Fleming, H. B. Pollard, and A. L. Burns. 1990. Genomic organization and chromosomal localization of the human nucleolin gene. J Biol Chem 265:14922-14931.

154. Nicoloso, M., M. Caizergues-Ferrer, B. Michot, M. C. Azum, and J. P. Bachellerie. 1994. U20, a novel small nucleolar RNA, is encoded in an intron of the nucleolin gene in mammals. Mol Cell Biol 14:5766-5776.

155. Rebane, A., and A. Metspalu. 1999. U82, a novel snoRNA identified from the fifth intron of human and mouse nucleolin gene. Biochim Biophys Acta 1446:426-430.
156. Farin, K., A. Di Segni, A. Mor, and R. Pinkas-Kramarski. 2009. Structure-function analysis of nucleolin and ErbB receptors interactions. PLoS One 4:e6128.
157. Daniely, Y., D. D. Dimitrova, and J. A. Borowiec. 2002. Stress-dependent nucleolin mobilization mediated by p53-nucleolin complex formation. Mol Cell Biol 22:6014-6022.
158. Heine, M. A., M. L. Rankin, and P. J. DiMario. 1993. The Gly/Arg-rich (GAR) domain of Xenopus nucleolin facilitates in vitro nucleic acid binding and in vivo nucleolar localization. Mol Biol Cell 4:1189-1204.
159. Storck, S., M. Thiry, and P. Bouvet. 2009. Conditional knockout of nucleolin in DT40 cells reveals the functional redundancy of its RNA-binding domains. Biol Cell 101:153-167.
160. Ghisolfi, L., G. Joseph, F. Amalric, and M. Erard. 1992. The glycine-rich domain of nucleolin has an unusual supersecondary structure responsible for its RNA-helix-destabilizing properties. J Biol Chem 267:2955-2959.
161. Stepanova, V., T. Lebedeva, A. Kuo, S. Yarovoi, S. Tkachuk, S. Zaitsev, K. Bdeir, I. Dumler, M. S. Marks, Y. Parfyonova, V. A. Tkachuk, A. A. Higazi, and D. B. Cines. 2008. Nuclear translocation of urokinase-type plasminogen activator. Blood 112:100-110.
162. Hanakahi, L. A., Z. Bu, and N. Maizels. 2000. The C-terminal domain of nucleolin accelerates nucleic acid annealing. Biochemistry 39:15493-15499.
163. Bouvet, P., J. J. Diaz, K. Kindbeiter, J. J. Madjar, and F. Amalric. 1998. Nucleolin interacts with several ribosomal proteins through its RGG domain. J Biol Chem 273:19025-19029.
164. Nisole, S., E. A. Said, C. Mische, M. C. Prevost, B. Krust, P. Bouvet, A. Bianco, J. P. Briand, and A. G. Hovanessian. 2002. The anti-HIV pentameric pseudopeptide HB-19 binds the C-terminal end of nucleolin and prevents anchorage of virus particles in the plasma membrane of target cells. J Biol Chem 277:20877-20886.
165. Khurts, S., K. Masutomi, L. Delgermaa, K. Arai, N. Oishi, H. Mizuno, N. Hayashi, W. C. Hahn, and S. Murakami. 2004. Nucleolin interacts with telomerase. J Biol Chem 279:51508-51515.

166. Teng, Y., A. C. Girvan, L. K. Casson, W. M. Pierce, Jr., M. Qian, S. D. Thomas, and P. J. Bates. 2007. AS1411 alters the localization of a complex containing protein arginine methyltransferase 5 and nucleolin. Cancer Res 67:10491-10500.

167. Allain, F. H., D. E. Gilbert, P. Bouvet, and J. Feigon. 2000. Solution structure of the two N-terminal RNA-binding domains of nucleolin and NMR study of the interaction with its RNA target. J Mol Biol 303:227-241.

168. Bhatt, P., C. d'Avout, N. S. Kane, J. A. Borowiec, and A. Saxena. 2012. Specific domains of nucleolin interact with Hdm2 and antagonize Hdm2-mediated p53 ubiquitination. FEBS J 279:370-383.

169. Shen, E. C., M. F. Henry, V. H. Weiss, S. R. Valentini, P. A. Silver, and M. S. Lee. 1998. Arginine methylation facilitates the nuclear export of hnRNP proteins. Genes Dev 12:679-691.

170. Tuteja, N., N. W. Huang, D. Skopac, R. Tuteja, S. Hrvatic, J. Zhang, S. Pongor, G. Joseph, C. Faucher, F. Amalric, and et al. 1995. Human DNA helicase IV is nucleolin, an RNA helicase modulated by phosphorylation. Gene 160:143-148.

171. Dumler, I., V. Stepanova, U. Jerke, O. A. Mayboroda, F. Vogel, P. Bouvet, V. Tkachuk, H. Haller, and D. C. Gulba. 1999. Urokinase-induced mitogenesis is mediated by casein kinase 2 and nucleolin. Curr Biol 9:1468-1476.

172. Mi, Y., S. D. Thomas, X. Xu, L. K. Casson, D. M. Miller, and P. J. Bates. 2003. Apoptosis in leukemia cells is accompanied by alterations in the levels and localization of nucleolin. J Biol Chem 278:8572-8579.

173. Belenguer, P., M. Caizergues-Ferrer, J. C. Labbe, M. Doree, and F. Amalric. 1990. Mitosis-specific phosphorylation of nucleolin by p34cdc2 protein kinase. Mol Cell Biol 10:3607-3618.

174. Hoja-Lukowicz, D., M. Przybylo, E. Pochec, A. Drabik, J. Silberring, M. Kremser, D. Schadendorf, P. Laidler, and A. Litynska. 2009. The new face of nucleolin in human melanoma. Cancer Immunol Immunother 58:1471-1480.

175. Carpentier, M., W. Morelle, B. Coddeville, A. Pons, M. Masson, J. Mazurier, and D. Legrand. 2005. Nucleolin undergoes partial N- and O-glycosylations in the extranuclear cell compartment. Biochemistry 44:5804-5815.

176. Fang, S. H., and N. H. Yeh. 1993. The self-cleaving activity of nucleolin determines its molecular dynamics in relation to cell proliferation. Exp Cell Res 208:48-53.

177. Bugler, B., M. Caizergues-Ferrer, G. Bouche, H. Bourbon, and F. Amalric. 1982. Detection and localization of a class of proteins immunologically related to a 100-kDa nucleolar protein. Eur J Biochem 128:475-480.
178. Hovanessian, A. G., F. Puvion-Dutilleul, S. Nisole, J. Svab, E. Perret, J. S. Deng, and B. Krust. 2000. The cell-surface-expressed nucleolin is associated with the actin cytoskeleton. Exp Cell Res 261:312-328.
179. Chen, C. M., S. Y. Chiang, and N. H. Yeh. 1991. Increased stability of nucleolin in proliferating cells by inhibition of its self-cleaving activity. J Biol Chem 266:7754-7758.
180. Bouche, G., M. Caizergues-Ferrer, B. Bugler, and F. Amalric. 1984. Interrelations between the maturation of a 100 kDa nucleolar protein and pre rRNA synthesis in CHO cells. Nucleic Acids Res 12:3025-3035.
181. Derenzini, M., V. Sirri, D. Trere, and R. L. Ochs. 1995. The quantity of nucleolar proteins nucleolin and protein B23 is related to cell doubling time in human cancer cells. Lab Invest 73:497-502.
182. Hoffmann, J., and G. Schwoch. 1989. Co-ordinated changes in the cyclic AMP signalling system and the phosphorylation of two nuclear proteins of Mr 130,000 and 110,000 during proliferative stimulation of the rat parotid gland by isoprenaline. . Biochem J 263:785-793.
183. Zhou, G., M. L. Seibenhener, and M. W. Wooten. 1997. Nucleolin is a protein kinase C-zeta substrate. J Biol Chem 272:31130-31137.
184. Schneider, H. R., G. H. Reichert, and O. G. Issinger. 1986. Enhanced casein kinase II activity during mouse embryogenesis. Eur J Biochem 161:733-738.
185. Caizergues-Ferrer, M., P. Mariottini, C. Curie, B. Lapeyre, N. Gas, F. Amalric, and F. Amaldi. 1989. Nucleolin from Xenopus laevis: cDNA cloning and expression during development. Genes Dev 3:324-333.
186. Dickinson, L. A., and T. Kohwi-Shigematsu. 1995. Nucleolin is a matrix attachment region DNA-binding protein that specifically recognizes a region with high base-unpairing potential. Mol Cell Biol 15:456-465.
187. Pickering, B. F., D. Yu, and M. W. Van Dyke. 2011. Nucleolin protein interacts with microprocessor complex to affect biogenesis of microRNAs 15a and 16. J Biol Chem 286:44095-44103.

188. Erard, M. S., P. Belenguer, M. Caizergues-Ferrer, A. Pantaloni, and F. Amalric. 1988. A major nucleolar protein, nucleolin, induces chromatin decondensation by binding to histone H1. Eur J Biochem 175:525-530.
189. Kobayashi, J., H. Fujimoto, J. Sato, I. Hayashi, S. Burma, S. Matsuura, D. J. Chen, and K. Komatsu. 2012. Nucleolin participates in DNA double-strand break-induced damage response through MDC1-dependent pathway. PLoS One 7:e49245.
190. Storck, S., M. Shukla, S. Dimitrov, and P. Bouvet. 2007. Functions of the histone chaperone nucleolin in diseases. Subcell Biochem 41:125-144.
191. Yang, T. H., W. H. Tsai, Y. M. Lee, H. Y. Lei, M. Y. Lai, D. S. Chen, N. H. Yeh, and S. C. Lee. 1994. Purification and characterization of nucleolin and its identification as a transcription repressor. Mol Cell Biol 14:6068-6074.
192. Zaidi, S. H., and J. S. Malter. 1995. Nucleolin and heterogeneous nuclear ribonucleoprotein C proteins specifically interact with the 3'-untranslated region of amyloid protein precursor mRNA. J Biol Chem 270:17292-17298.
193. Chen, J., K. Guo, and M. B. Kastan. 2012. Interactions of nucleolin and ribosomal protein L26 (RPL26) in translational control of human p53 mRNA. J Biol Chem 287:16467-16476.
194. Ying, G. G., P. Proost, J. van Damme, M. Bruschi, M. Introna, and J. Golay. 2000. Nucleolin, a novel partner for the Myb transcription factor family that regulates their activity. J Biol Chem 275:4152-4158.
195. Takagi, M., M. J. Absalon, K. G. McLure, and M. B. Kastan. 2005. Regulation of p53 translation and induction after DNA damage by ribosomal protein L26 and nucleolin. Cell 123:49-63.
196. Daniely, Y., and J. A. Borowiec. 2000. Formation of a complex between nucleolin and replication protein A after cell stress prevents initiation of DNA replication. J Cell Biol 149:799-810.
197. De, A., S. L. Donahue, A. Tabah, N. E. Castro, N. Mraz, J. L. Cruise, and C. Campbell. 2006. A novel interaction of nucleolin with Rad51. Biochem Biophys Res Commun 344:206-213.
198. Gaudreault, I., D. Guay, and M. Lebel. 2004. YB-1 promotes strand separation in vitro of duplex DNA containing either mispaired bases or cisplatin modifications, exhibits

endonucleolytic activities and binds several DNA repair proteins. Nucleic Acids Res 32:316-327.

199. Wang, Y., J. Guan, H. Wang, Y. Wang, D. Leeper, and G. Iliakis. 2001. Regulation of DNA replication after heat shock by replication protein a-nucleolin interactions. J Biol Chem 276:20579-20588.

200. Yang, C., M. S. Kim, D. Chakravarty, F. E. Indig, and F. Carrier. 2009. Nucleolin Binds to the Proliferating Cell Nuclear Antigen and Inhibits Nucleotide Excision Repair. Mol Cell Pharmacol 1:130-137.

201. Hanakahi, L. A., L. A. Dempsey, M. J. Li, and N. Maizels. 1997. Nucleolin is one component of the B cell-specific transcription factor and switch region binding protein, LR1. Proc Natl Acad Sci USA 94:3605-3610.

202. Borggrefe, T., M. Wabl, A. T. Akhmedov, and R. Jessberger. 1998. A B-cell-specific DNA recombination complex. J Biol Chem 273:17025-17035.

203. Schmidt-Zachmann, M. S., C. Dargemont, L. C. Kuhn, and E. A. Nigg. 1993. Nuclear export of proteins: the role of nuclear retention. Cell 74:493-504.

204. Morimoto, H., A. Ozaki, H. Okamura, K. Yoshida, B. R. Amorim, H. Tanaka, S. Kitamura, and T. Haneji. 2007. Differential expression of protein phosphatase type 1 isotypes and nucleolin during cell cycle arrest. Cell Biochem Funct 25:369-375.

205. Konishi, T., Y. Karasaki, M. Nomoto, H. Ohmori, K. Shibata, T. Abe, K. Shimizu, H. Itoh, and K. Higashi. 1995. Induction of heat shock protein 70 and nucleolin and their intracellular distribution during early stage of liver regeneration. J Biochem 117:1170-1177.

206. Gas, N., M. L. Escande, and B. J. Stevens. 1985. Immunolocalization of the 100 kDa nucleolar protein during the mitotic cycle in CHO cells. Biol Cell 53:209-218.

207. Zhu, Y., D. Lu, and P. DiMario. 1999. Nucleolin, defective for MPF phosphorylation, localizes normally during mitosis and nucleologenesis. Histochem Cell Biol 111:477-487.

208. Turck, N., O. Lefebvre, I. Gross, P. Gendry, M. Kedinger, P. Simon-Assmann, and J. F. Launay. 2006. Effect of laminin-1 on intestinal cell differentiation involves inhibition of nuclear nucleolin. J Cell Physiol 206:545-555.

209. Xu, X., F. Hamhouyia, S. D. Thomas, T. J. Burke, A. C. Girvan, W. G. McGregor, J. O. Trent, D. M. Miller, and P. J. Bates. 2001. Inhibition of DNA replication and induction of S phase cell cycle arrest by G-rich oligonucleotides. J Biol Chem 276:43221-43230.

210. Hovanessian, A. G., C. Soundaramourty, D. El Khoury, I. Nondier, J. Svab, and B. Krust. 2010. Surface expressed nucleolin is constantly induced in tumor cells to mediate calcium-dependent ligand internalization. PLoS One 5:e15787.

211. Martelli, A. M., I. Robuffo, R. Bortul, R. L. Ochs, F. Luchetti, L. Cocco, M. Zweyer, R. Bareggi, and E. Falcieri. 2000. Behavior of nucleolar proteins during the course of apoptosis in camptothecin-treated HL60 cells. J Cell Biochem 78:264-277.

212. Drygin, D., A. Siddiqui-Jain, S. O'Brien, M. Schwaebe, A. Lin, J. Bliesath, C. B. Ho, C. Proffitt, K. Trent, J. P. Whitten, J. K. Lim, D. Von Hoff, K. Anderes, and W. G. Rice. 2009. Anticancer activity of CX-3543: a direct inhibitor of rRNA biogenesis. Cancer Res 69:7653-7661.

213. Bonnet, H., O. Filhol, I. Truchet, P. Brethenou, C. Cochet, F. Amalric, and G. Bouche. 1996. Fibroblast growth factor-2 binds to the regulatory beta subunit of CK2 and directly stimulates CK2 activity toward nucleolin. J Biol Chem 271:24781-24787.

214. Koutsioumpa, M., C. Polytarchou, J. Courty, Y. Zhang, N. Kieffer, C. Mikelis, S. S. Skandalis, U. Hellman, D. Iliopoulos, and E. Papadimitriou. 2013. Interplay between alphavbeta3 integrin and nucleolin regulates human endothelial and glioma cell migration. J Biol Chem 288:343-354.

215. Said, E. A., J. Courty, J. Svab, J. Delbe, B. Krust, and A. G. Hovanessian. 2005. Pleiotrophin inhibits HIV infection by binding the cell surface-expressed nucleolin. FEBS J 272:4646-4659.

216. Huang, Y., H. Shi, H. Zhou, X. Song, S. Yuan, and Y. Luo. 2006. The angiogenic function of nucleolin is mediated by vascular endothelial growth factor and nonmuscle myosin. Blood 107:3564-3571.

217. Kim, S. K., and M. Srivastava. 2003. Stability of Nucleolin protein as the basis for the differential expression of Nucleolin mRNA and protein during serum starvation. DNA Cell Biol 22:171-178.

218. Shibata, Y., T. Muramatsu, M. Hirai, T. Inui, T. Kimura, H. Saito, L. M. McCormick, G. Bu, and K. Kadomatsu. 2002. Nuclear targeting by the growth factor midkine. Mol Cell Biol 22:6788-6796.

219. Losfeld, M. E., D. E. Khoury, P. Mariot, M. Carpentier, B. Krust, J. P. Briand, J. Mazurier, A. G. Hovanessian, and D. Legrand. 2009. The cell surface expressed nucleolin is a glycoprotein that triggers calcium entry into mammalian cells. Exp Cell Res 315:357-369.

220. Zhang, J., G. Tsaprailis, and G. T. Bowden. 2008. Nucleolin stabilizes Bcl-XL messenger RNA in response to UVA irradiation. Cancer Res 68:1046-1054.

221. Chen, C. Y., R. Gherzi, J. S. Andersen, G. Gaietta, K. Jurchott, H. D. Royer, M. Mann, and M. Karin. 2000. Nucleolin and YB-1 are required for JNK-mediated interleukin-2 mRNA stabilization during T-cell activation. Genes Dev 14:1236-1248.

222. Herblot, S., P. Chastagner, L. Samady, J. L. Moreau, C. Demaison, P. Froussard, X. Liu, J. Bonnet, and J. Theze. 1999. IL-2-dependent expression of genes involved in cytoskeleton organization, oncogene regulation, and transcriptional control. J Immunol 162:3280-3288.

223. Meyuhas, O., V. Baldin, G. Bouche, and F. Amalric. 1990. Glucocorticoids repress ribosome biosynthesis in lymphosarcoma cells by affecting gene expression at the level of transcription, posttranscription and translation. Biochim Biophys Acta 1049:38-44.

224. Tu, X., R. Baffa, S. Luke, M. Prisco, and R. Baserga. 2003. Intracellular redistribution of nuclear and nucleolar proteins during differentiation of 32D murine hemopoietic cells. Exp Cell Res 288:119-130.

225. Borer, R. A., C. F. Lehner, H. M. Eppenberger, and E. A. Nigg. 1989. Major nucleolar proteins shuttle between nucleus and cytoplasm. Cell 56:379-390.

226. Chandra, M., S. Zang, H. Li, L. J. Zimmerman, J. Champer, A. Tsuyada, A. Chow, W. Zhou, Y. Yu, H. Gao, X. Ren, R. J. Lin, and S. E. Wang. 2012. Nuclear translocation of type I transforming growth factor beta receptor confers a novel function in RNA processing. Mol Cell Biol 32:2183-2195.

227. Sengupta, T. K., S. Bandyopadhyay, D. J. Fernandes, and E. K. Spicer. 2004. Identification of nucleolin as an AU-rich element binding protein involved in bcl-2 mRNA stabilization. J Biol Chem 279:10855-10863.

228. Losfeld, M. E., A. Leroy, B. Coddeville, M. Carpentier, J. Mazurier, and D. Legrand. 2011. N-Glycosylation influences the structure and self-association abilities of recombinant nucleolin. FEBS J 278:2552-2564.

229. Destouches, D., D. El Khoury, Y. Hamma-Kourbali, B. Krust, P. Albanese, P. Katsoris, G. Guichard, J. P. Briand, J. Courty, and A. G. Hovanessian. 2008. Suppression of tumor growth and angiogenesis by a specific antagonist of the cell-surface expressed nucleolin. PLoS One 3:e2518.

230. Larrucea, S., R. Cambronero, C. Gonzalez-Rubio, B. Fraile, C. Gamallo, G. Fontan, and M. Lopez-Trascasa. 1999. Internalization of Factor J and cellular signalization after Factor J-cell interaction. Biochem Biophys Res Commun 266:51-57.

231. Qiu, J., and K. E. Brown. 1999. A 110-kDa nuclear shuttle protein, nucleolin, specifically binds to adeno-associated virus type 2 (AAV-2) capsid. Virology 257:373-382.

232. Koutsioumpa, M., G. Drosou, C. Mikelis, K. Theochari, D. Vourtsis, P. Katsoris, E. Giannopoulou, J. Courty, C. Petrou, V. Magafa, P. Cordopatis, and E. Papadimitriou. 2012. Pleiotrophin expression and role in physiological angiogenesis in vivo: potential involvement of nucleolin. Vasc Cell 4:4.

233. Kleinman, H. K., B. S. Weeks, F. B. Cannon, T. M. Sweeney, G. C. Sephel, B. Clement, M. Zain, M. O. Olson, M. Jucker, and B. A. Burrous. 1991. Identification of a 110-kDa nonintegrin cell surface laminin-binding protein which recognizes an A chain neurite-promoting peptide. Arch Biochem Biophys 290:320-325.

234. Kibbey, M. C., B. Johnson, R. Petryshyn, M. Jucker, and H. K. Kleinman. 1995. A 110-kD nuclear shuttling protein, nucleolin, binds to the neurite-promoting IKVAV site of laminin-1. J Neurosci Res 42:314-322.

235. Watanabe, T., H. Tsuge, T. Imagawa, D. Kise, K. Hirano, M. Beppu, A. Takahashi, K. Yamaguchi, H. Fujiki, and M. Suganuma. 2010. Nucleolin as cell surface receptor for tumor necrosis factor-alpha inducing protein: a carcinogenic factor of Helicobacter pylori. J Cancer Res Clin Oncol 136:911-921.

236. Fu, Y., Y. Chen, X. Luo, Y. Liang, H. Shi, L. Gao, S. Zhan, D. Zhou, and Y. Luo. 2009. The heparin binding motif of endostatin mediates its interaction with receptor nucleolin. Biochemistry 48:11655-11663.

237. Shi, H., Y. Huang, H. Zhou, X. Song, S. Yuan, Y. Fu, and Y. Luo. 2007. Nucleolin is a receptor that mediates antiangiogenic and antitumor activity of endostatin. Blood 110:2899-2906.

238. Burks, D. J., J. Wang, H. Towery, O. Ishibashi, D. Lowe, H. Riedel, and M. F. White. 1998. IRS pleckstrin homology domains bind to acidic motifs in proteins. J Biol Chem 273:31061-31067.

239. Harms, G., R. Kraft, G. Grelle, B. Volz, J. Dernedde, and R. Tauber. 2001. Identification of nucleolin as a new L-selectin ligand. Biochem J 360:531-538.

240. Di Segni, A., K. Farin, and R. Pinkas-Kramarski. 2008. Identification of nucleolin as new ErbB receptors- interacting protein. PLoS One 3:e2310.

241. Take, M., J. Tsutsui, H. Obama, M. Ozawa, T. Nakayama, I. Maruyama, T. Arima, and T. Muramatsu. 1994. Identification of nucleolin as a binding protein for midkine (MK) and heparin-binding growth associated molecule (HB-GAM). J Biochem 116:1063-1068.

242. Uribe, D. J., K. Guo, Y. J. Shin, and D. Sun. 2011. Heterogeneous nuclear ribonucleoprotein K and nucleolin as transcriptional activators of the vascular endothelial growth factor promoter through interaction with secondary DNA structures. Biochemistry 50:3796-3806.

243. Huddleson, J. P., N. Ahmad, and J. B. Lingrel. 2006. Up-regulation of the KLF2 transcription factor by fluid shear stress requires nucleolin. J Biol Chem 281:15121-15128.

244. Fahling, M., A. Steege, A. Perlewitz, B. Nafz, R. Mrowka, P. B. Persson, and B. J. Thiele. 2005. Role of nucleolin in posttranscriptional control of MMP-9 expression. Biochim Biophys Acta 1731:32-40.

245. Otake, Y., S. Soundararajan, T. K. Sengupta, E. A. Kio, J. C. Smith, M. Pineda-Roman, R. K. Stuart, E. K. Spicer, and D. J. Fernandes. 2007. Overexpression of nucleolin in chronic lymphocytic leukemia cells induces stabilization of bcl2 mRNA. Blood 109:3069-3075.

246. Grinstein, E., P. Wernet, P. J. Snijders, F. Rosl, I. Weinert, W. Jia, R. Kraft, C. Schewe, M. Schwabe, S. Hauptmann, M. Dietel, C. J. Meijer, and H. D. Royer. 2002. Nucleolin as activator of human papillomavirus type 18 oncogene transcription in cervical cancer. J Exp Med 196:1067-1078.

247. Grinstein, E., Y. Shan, L. Karawajew, P. J. Snijders, C. J. Meijer, H. D. Royer, and P. Wernet. 2006. Cell cycle-controlled interaction of nucleolin with the retinoblastoma protein and cancerous cell transformation. J Biol Chem 281:22223-22235.

248. Fu, Z., and C. Fenselau. 2005. Proteomic evidence for roles for nucleolin and poly[ADP-ribosyl] transferase in drug resistance. J Proteome Res 4:1583-1591.
249. Martelli, A. M., M. Zweyer, R. L. Ochs, P. L. Tazzari, G. Tabellini, P. Narducci, and R. Bortul. 2001. Nuclear apoptotic changes: an overview. J Cell Biochem 82:634-646.
250. Minota, S., W. N. Jarjour, N. Suzuki, Y. Nojima, R. A. Roubey, T. Mimura, A. Yamada, T. Hosoya, F. Takaku, and J. B. Winfield. 1991. Autoantibodies to nucleolin in systemic lupus erythematosus and other diseases. J Immunol 146:2249-2252.
251. Hirata, D., M. Iwamoto, T. Yoshio, H. Okazaki, J. Masuyama, A. Mimori, and S. Minota. 2000. Nucleolin as the earliest target molecule of autoantibodies produced in MRL/lpr lupus-prone mice. Clin Immunol 97:50-58.
252. Liu, J., L. Yin, H. Dong, E. Xu, L. Zhang, Y. Qiao, Y. Liu, L. Li, and J. Jia. 2012. Decreased serum levels of nucleolin protein fragment, as analyzed by bead-based proteomic technology, in multiple sclerosis patients compared to controls. J Neuroimmunol 250:71-76.
253. Brockstedt, E., A. Rickers, S. Kostka, A. Laubersheimer, B. Dorken, B. Wittmann-Liebold, K. Bommert, and A. Otto. 1998. Identification of apoptosis-associated proteins in a human Burkitt lymphoma cell line. . J Biol Chem 273:28057-28064.
254. Pasternack, M. S., K. J. Bleier, and T. N. McInerney. 1991. Granzyme A binding to target cell proteins. J Biol Chem 266:14703-14708.
255. Yang, C., D. A. Maiguel, and F. Carrier. 2002. Identification of nucleolin and nucleophosmin as genotoxic stress-responsive RNA-binding proteins. Nucleic Acids Res 30:2251-2260.
256. Hirano, K., Y. Miki, Y. Hirai, R. Sato, T. Itoh, A. Hayashi, M. Yamanaka, S. Eda, and M. Beppu. 2005. A multifunctional shuttling protein nucleolin is a macrophage receptor for apoptotic cells. J Biol Chem 280:39284-39293.
257. Larrucea, S., C. Gonzalez-Rubio, R. Cambronero, B. Ballou, P. Bonay, E. Lopez-Granados, P. Bouvet, G. Fontan, M. Fresno, and M. Lopez-Trascasa. 1998. Cellular adhesion mediated by Factor J, a complement inhibitor. J Biol Chem 273:31718-31725.
258. Ishimaru, D., L. Zuraw, S. Ramalingam, T. K. Sengupta, S. Bandyopadhyay, A. Reuben, D. J. Fernandes, and E. K. Spicer. 2010. Mechanism of regulation of bcl-2 mRNA by nucleolin and A+U-rich element-binding factor 1 (AUF1). J Biol Chem 285:27182-27191.

259. Suganuma, M., T. Watanabe, K. Yamaguchi, A. Takahashi, and H. Fujiki. 2012. Human gastric cancer development with TNF-alpha-inducing protein secreted from Helicobacter pylori. Cancer Lett 322:133-138.

260. Hirano, M., S. Kaneko, T. Yamashita, H. Luo, W. Qin, Y. Shirota, T. Nomura, K. Kobayashi, and S. Murakami. 2003. Direct interaction between nucleolin and hepatitis C virus NS5B. J Biol Chem 278:5109-5115.

261. Callebaut, C., S. Nisole, J. P. Briand, B. Krust, and A. G. Hovanessian. 2001. Inhibition of HIV infection by the cytokine midkine. Virology 281:248-264.

262. Tate, A., S. Isotani, M. J. Bradley, R. A. Sikes, R. Davis, L. W. Chung, and M. Edlund. 2006. Met-Independent Hepatocyte Growth Factor-mediated regulation of cell adhesion in human prostate cancer cells. BMC Cancer 6:197.

263. Semenkovich, C. F., R. E. Ostlund, Jr., M. O. Olson, and J. W. Yang. 1990. A protein partially expressed on the surface of HepG2 cells that binds lipoproteins specifically is nucleolin. Biochemistry 29:9708-9713.

264. Saxena, A., C. J. Rorie, D. Dimitrova, Y. Daniely, and J. A. Borowiec. 2006. Nucleolin inhibits Hdm2 by multiple pathways leading to p53 stabilization. Oncogene 25:7274-7288.

265. Ridley, L., R. Rahman, M. A. Brundler, D. Ellison, J. Lowe, K. Robson, E. Prebble, I. Luckett, R. J. Gilbertson, S. Parkes, V. Rand, B. Coyle, R. G. Grundy, C. Children's, and C. Leukaemia Group Biological Studies. 2008. Multifactorial analysis of predictors of outcome in pediatric intracranial ependymoma. Neuro Oncol 10:675-689.

266. Modena, P., F. R. Buttarelli, R. Miceli, E. Piccinin, C. Baldi, M. Antonelli, I. Morra, L. Lauriola, C. Di Rocco, M. L. Garre, I. Sardi, L. Genitori, R. Maestro, L. Gandola, F. Facchinetti, P. Collini, G. Sozzi, F. Giangaspero, and M. Massimino. 2012. Predictors of outcome in an AIEOP series of childhood ependymomas: a multifactorial analysis. Neuro Oncol 14:1346-1356.

267. Galzio, R., F. Rosati, E. Benedetti, L. Cristiano, S. Aldi, S. Mei, B. D'Angelo, R. Gentile, G. Laurenti, M. G. Cifone, A. Giordano, and A. Cimini. 2012. Glycosilated nucleolin as marker for human gliomas. J Cell Biochem 113:571-579.

268. Mourmouras, V., G. Cevenini, E. Cosci, M. C. Epistolato, M. Biagioli, L. Barbagli, P. Luzi, S. Mannucci, and C. Miracco. 2009. Nucleolin protein expression in cutaneous melanocytic lesions. J Cutan Pathol 36:637-646.

269. Peng, L., J. Liang, H. Wang, X. Song, A. Rashid, H. F. Gomez, L. J. Corley, J. L. Abbruzzese, J. B. Fleming, D. B. Evans, and H. Wang. 2010. High levels of nucleolar expression of nucleolin are associated with better prognosis in patients with stage II pancreatic ductal adenocarcinoma. Clin Cancer Res 16:3734-3742.

270. Sheng, J., and W. Y. Zhang. 2010. Identification of biomarkers for cervical cancer in peripheral blood lymphocytes by oligonucleotide microarrays. Zhonghua Yi Xue Za Zhi 90:2611-2615.

271. Suzuki, N., T. Saito, and T. Hosoya. 1987. In vivo effects of dexamethasone and cycloheximide on the phosphorylation of 110-kDa proteins and the protein kinase activities of rat liver nucleoli. J Biol Chem 262:4696-4700.

272. Drygin, D., A. Lin, J. Bliesath, C. B. Ho, S. E. O'Brien, C. Proffitt, M. Omori, M. Haddach, M. K. Schwaebe, A. Siddiqui-Jain, N. Streiner, J. E. Quin, E. Sanij, M. J. Bywater, R. D. Hannan, D. Ryckman, K. Anderes, and W. G. Rice. 2011. Targeting RNA polymerase I with an oral small molecule CX-5461 inhibits ribosomal RNA synthesis and solid tumor growth. Cancer Res 71:1418-1430.

273. Krust, B., D. El Khoury, I. Nondier, C. Soundaramourty, and A. G. Hovanessian. 2011. Targeting surface nucleolin with multivalent HB-19 and related Nucant pseudopeptides results in distinct inhibitory mechanisms depending on the malignant tumor cell type. BMC Cancer 11:333.

274. El Khoury, D., D. Destouches, R. Lengagne, B. Krust, Y. Hamma-Kourbali, M. Garcette, S. Niro, M. Kato, J. P. Briand, J. Courty, A. G. Hovanessian, and A. Prevost-Blondel. 2010. Targeting surface nucleolin with a multivalent pseudopeptide delays development of spontaneous melanoma in RET transgenic mice. BMC Cancer 10:325.

275. Christian, S., J. Pilch, M. E. Akerman, K. Porkka, P. Laakkonen, and E. Ruoslahti. 2003. Nucleolin expressed at the cell surface is a marker of endothelial cells in angiogenic blood vessels. J Cell Biol 163:871-878.

276. Moura, V., M. Lacerda, P. Figueiredo, M. L. Corvo, M. E. Cruz, R. Soares, M. C. de Lima, S. Simoes, and J. N. Moreira. 2012. Targeted and intracellular triggered delivery of therapeutics to cancer cells and the tumor microenvironment: impact on the treatment of breast cancer. Breast Cancer Res Treat 133:61-73.

277. Prickett, W. M., B. D. Van Rite, D. E. Resasco, and R. G. Harrison. 2011. Vascular targeted single-walled carbon nanotubes for near-infrared light therapy of cancer. Nanotechnology 22:455101.

278. Drecoll, E., F. C. Gaertner, M. Miederer, B. Blechert, M. Vallon, J. M. Muller, A. Alke, C. Seidl, F. Bruchertseifer, A. Morgenstern, R. Senekowitsch-Schmidtke, and M. Essler. 2009. Treatment of peritoneal carcinomatosis by targeted delivery of the radio-labeled tumor homing peptide bi-DTPA-[F3]2 into the nucleus of tumor cells. PLoS One 4:e5715.

279. Hu, Q., G. Gu, Z. Liu, M. Jiang, T. Kang, D. Miao, Y. Tu, Z. Pang, Q. Song, L. Yao, H. Xia, H. Chen, X. Jiang, X. Gao, and J. Chen. 2013. F3 peptide-functionalized PEG-PLA nanoparticles co-administrated with tLyp-1 peptide for anti-glioma drug delivery. Biomaterials 34:1135-1145.

280. Qin, Z., B. Lavingia, Y. Zou, and P. Stastny. 2011. Antibodies against nucleolin in recipients of organ transplants. Transplantation 92:829-835.

281. Bates, P. J., D. A. Laber, D. M. Miller, S. D. Thomas, and J. O. Trent. 2009. Discovery and development of the G-rich oligonucleotide AS1411 as a novel treatment for cancer. Exp Mol Pathol 86:151-164.

282. Soundararajan, S., W. Chen, E. K. Spicer, N. Courtenay-Luck, and D. J. Fernandes. 2008. The nucleolin targeting aptamer AS1411 destabilizes Bcl-2 messenger RNA in human breast cancer cells. Cancer Res 68:2358-2365.

283. Kim, J. K., K. J. Choi, M. Lee, M. H. Jo, and S. Kim. 2012. Molecular imaging of a cancer-targeting theragnostics probe using a nucleolin aptamer- and microRNA-221 molecular beacon-conjugated nanoparticle. Biomaterials 33:207-217.

284. Ye, M., J. Hu, M. Peng, J. Liu, J. Liu, H. Liu, X. Zhao, and W. Tan. 2012. Generating Aptamers by Cell-SELEX for Applications in Molecular Medicine. Int J Mol Sci 13:3341-3353.

285. Gupta, A. K., and M. Gupta. 2005. Synthesis and surface engineering of iron oxide nanoparticles for biomedical applications. Biomaterials 26:3995-4021.

286. Kanwar, J. R., K. Roy, and R. K. Kanwar. 2011. Chimeric aptamers in cancer cell-targeted drug delivery. Crit Rev Biochem Mol Biol 46:459-477.

287. Curtin, J. F., and T. G. Cotter. 2003. Live and let die: regulatory mechanisms in Fas-mediated apoptosis. Cell Signal 15:983-992.

288. Owen-Schaub, L. 2001. Soluble Fas and cancer. Clin Cancer Res 7:1108-1109.
289. Kamei, T., M. Inui, M. Nakase, S. Nakamura, K. Okumura, K. Hiramoto, and T. Tagawa. 2005. Experimental therapy using interferon-gamma and anti-Fas antibody against oral malignant melanoma cells. Melanoma Res 15:393-400.
290. Tillman, D. M., I. Petak, and J. A. Houghton. 1999. A Fas-dependent component in 5-fluorouracil/leucovorin-induced cytotoxicity in colon carcinoma cells. Clin Cancer Res 5:425-430.
291. Otten, H. G., W. G. van Ginkel, A. Hagenbeek, and E. J. Petersen. 2004. Prevalence and clinical significance of resistance to perforin- and FAS-mediated cell death in leukemia. Leukemia 18:1401-1405.
292. Daniluk, U., C. Kerros, R. H. Tao, J. F. Wise, X. Ao, Z. Berkova, and F. Samaniego. 2012. The peptide derived from the Ig-like domain of human herpesvirus 8 K1 protein induces death in hematological cancer cells. J Exp Clin Cancer Res 31:69.
293. Berkova, Z., S. Wang, J. F. Wise, H. Maeng, Y. Ji, and F. Samaniego. 2009. Mechanism of Fas signaling regulation by human herpesvirus 8 K1 oncoprotein. J Natl Cancer Inst 101:399-411.
294. Wang, S., S. Wang, H. Maeng, D. P. Young, O. Prakash, L. E. Fayad, A. Younes, and F. Samaniego. 2007. K1 protein of human herpesvirus 8 suppresses lymphoma cell Fas-mediated apoptosis. Blood 109:2174-2182.
295. Tao, R. H., Z. Berkova, J. F. Wise, A. H. Rezaeian, U. Daniluk, X. Ao, D. H. Hawke, J. E. Karp, H. K. Lin, J. J. Molldrem, and F. Samaniego. 2011. PMLRARalpha binds to Fas and suppresses Fas-mediated apoptosis through recruiting c-FLIP in vivo. Blood 118:3107-3118.
296. Lapeyre, B., H. Bourbon, and F. Amalric. 1987. Nucleolin, the major nucleolar protein of growing eukaryotic cells: an unusual protein structure revealed by the nucleotide sequence. Proc Natl Acad Sci USA 84:1472-1476.
297. Hu, J., M. Lin, T. Liu, J. Li, B. Chen, and Y. Chen. 2011. DIGE-based proteomic analysis identifies nucleophosmin/B23 and nucleolin C23 as over-expressed proteins in relapsed/refractory acute leukemia. Leuk Res 35:1087-1092.
298. Lin, Z., D. K. Crockett, M. S. Lim, and K. S. Elenitoba-Johnson. 2003. High-throughput analysis of protein/peptide complexes by immunoprecipitation and automated LC-MS/MS. J Biomol Tech 14:149-155.

299. Bennett, M., K. Macdonald, S. W. Chan, J. P. Luzio, R. Simari, and P. Weissberg. 1998. Cell surface trafficking of Fas: a rapid mechanism of p53-mediated apoptosis. Science 282:290-293.

300. Finke, J., R. Fritzen, P. Ternes, P. Trivedi, K. J. Bross, W. Lange, R. Mertelsmann, and G. Dolken. 1992. Expression of bcl-2 in Burkitt's lymphoma cell lines: induction by latent Epstein-Barr virus genes. Blood 80:459-469.

301. Ugrinova, I., K. Monier, C. Ivaldi, M. Thiry, S. Storck, F. Mongelard, and P. Bouvet. 2007. Inactivation of nucleolin leads to nucleolar disruption, cell cycle arrest and defects in centrosome duplication. BMC Mol Biol 8:66.

302. Liu, F., Y. Song, and D. Liu. 1999. Hydrodynamics-based transfection in animals by systemic administration of plasmid DNA. Gene Ther 6:1258-1266.

303. Schuchmann, M., E. E. Varfolomeev, F. Hermann, F. Rueckert, D. Strand, H. Koehler, S. Strand, A. W. Lohse, D. Wallach, and P. R. Galle. 2003. Dominant negative MORT1/FADD rescues mice from CD95 and TNF-induced liver failure. Hepatology 37:129-135.

304. Szulc, J., M. Wiznerowicz, M. O. Sauvain, D. Trono, and P. Aebischer. 2006. A versatile tool for conditional gene expression and knockdown. Nat Methods 3:109-116.

305. Zhang, M. Z., Z. C. Sun, X. R. Fu, F. F. Nan, Q. X. Fan, X. A. Wu, L. Geng, W. Ma, and R. L. Wang. 2009. Analysis of serum proteome profiles of non-Hodgkin lymphoma for biomarker identification. J Proteomics 72:952-959.

306. Watanabe, T., K. Hirano, A. Takahashi, K. Yamaguchi, M. Beppu, H. Fujiki, and M. Suganuma. 2010. Nucleolin on the cell surface as a new molecular target for gastric cancer treatment. Biol Pharm Bull 33:796-803.

307. Hoster, E., M. Dreyling, W. Klapper, C. Gisselbrecht, A. van Hoof, H. C. Kluin-Nelemans, M. Pfreundschuh, M. Reiser, B. Metzner, H. Einsele, N. Peter, W. Jung, B. Wormann, W. D. Ludwig, U. Duhrsen, H. Eimermacher, H. Wandt, J. Hasford, W. Hiddemann, M. Unterhalt, G. German Low Grade Lymphoma Study, and N. European Mantle Cell Lymphoma. 2008. A new prognostic index (MIPI) for patients with advanced-stage mantle cell lymphoma. Blood 111:558-565.

308. Stel, A. J., B. Ten Cate, S. Jacobs, J. W. Kok, D. C. Spierings, M. Dondorff, W. Helfrich, H. C. Kluin-Nelemans, L. F. de Leij, S. Withoff, and B. J. Kroesen. 2007. Fas receptor clustering and involvement of the death receptor pathway in rituximab-

mediated apoptosis with concomitant sensitization of lymphoma B cells to Fas-induced apoptosis. J Immunol 178:2287-2295.

309. Bullani, R. R., B. Huard, I. Viard-Leveugle, H. R. Byers, M. Irmler, J. H. Saurat, J. Tschopp, and L. E. French. 2001. Selective expression of FLIP in malignant melanocytic skin lesions. J Invest Dermatol 117:360-364.

310. Sunter, N. J., K. Scott, R. Hills, D. Grimwade, S. Taylor, L. J. Worrillow, S. E. Fordham, V. J. Forster, G. Jackson, S. Bomken, G. Jones, and J. M. Allan. 2012. A functional variant in the core promoter of the CD95 cell death receptor gene predicts prognosis in acute promyelocytic leukemia. Blood 119:196-205.

311. Krek, W., and J. A. DeCaprio. 1995. Cell synchronization. Methods Enzymol 254:114-124.

312. Jackman, J., and P. M. O'Connor. 2001. Methods for synchronizing cells at specific stages of the cell cycle. Curr Protoc Cell Biol Chapter 8:Unit 8 3.

313. Fried, J., A. G. Perez, and B. D. Clarkson. 1976. Flow cytofluorometric analysis of cell cycle distributions using propidium iodide. Properties of the method and mathematical analysis of the data. J Cell Biol 71:172-181.

314. Whitmore, L., and B. A. Wallace. 2008. Protein secondary structure analyses from circular dichroism spectroscopy: methods and reference databases. Biopolymers 89:392-400.

315. Jason-Moller, L., M. Murphy, and J. Bruno. 2006. Overview of Biacore systems and their applications. Curr Protoc Protein Sci Chapter 19:Unit 19 13.

316. Majka, J., and C. Speck. 2007. Analysis of protein-DNA interactions using surface plasmon resonance. Adv Biochem Eng Biotechnol 104:13-36.

317. Muyldermans, S., T. N. Baral, V. C. Retamozzo, P. De Baetselier, E. De Genst, J. Kinne, H. Leonhardt, S. Magez, V. K. Nguyen, H. Revets, U. Rothbauer, B. Stijlemans, S. Tillib, U. Wernery, L. Wyns, G. Hassanzadeh-Ghassabeh, and D. Saerens. 2009. Camelid immunoglobulins and nanobody technology. Vet Immunol Immunopathol 128:178-183.

318. Bell, A., Z. J. Wang, M. Arbabi-Ghahroudi, T. A. Chang, Y. Durocher, U. Trojahn, J. Baardsnes, M. L. Jaramillo, S. Li, T. N. Baral, M. O'Connor-McCourt, R. Mackenzie, and J. Zhang. 2010. Differential tumor-targeting abilities of three single-domain antibody formats. Cancer Lett 289:81-90.

319. Vincke, C., R. Loris, D. Saerens, S. Martinez-Rodriguez, S. Muyldermans, and K. Conrath. 2009. General strategy to humanize a camelid single-domain antibody and identification of a universal humanized nanobody scaffold. J Biol Chem 284:3273-3284.

320. Revets, H., P. De Baetselier, and S. Muyldermans. 2005. Nanobodies as novel agents for cancer therapy. Expert Opin Biol Ther 5:111-124.

321. Kurzrock, R., J. U. Gutterman, and M. Talpaz. 1988. The molecular genetics of Philadelphia chromosome-positive leukemias. N Engl J Med 319:990-998.

322. Cooper, E. H., and T. Plesner. 1980. Beta-2-microglobulin review: its relevance in clinical oncology. Med Pediatr Oncol 8:323-334.

323. Miller, W. H., Jr., K. Levine, A. DeBlasio, S. R. Frankel, E. Dmitrovsky, and R. P. Warrell, Jr. 1993. Detection of minimal residual disease in acute promyelocytic leukemia by a reverse transcription polymerase chain reaction assay for the PML/RAR-alpha fusion mRNA. Blood 82:1689-1694.

324. Determann, O., E. Hoster, G. Ott, H. Wolfram Bernd, C. Loddenkemper, M. Leo Hansmann, T. E. Barth, M. Unterhalt, W. Hiddemann, M. Dreyling, W. Klapper, N. European Mantle Cell Lymphoma, and G. the German Low Grade Lymphoma Study. 2008. Ki-67 predicts outcome in advanced-stage mantle cell lymphoma patients treated with anti-CD20 immunochemotherapy: results from randomized trials of the European MCL Network and the German Low Grade Lymphoma Study Group. Blood 111:2385-2387.

325. Szczuraszek, K., G. Mazur, M. Jelen, P. Dziegiel, P. Surowiak, and M. Zabel. 2008. Prognostic significance of Ki-67 antigen expression in non-Hodgkin's lymphomas. Anticancer Res 28:1113-1118.

326. Nicolaides, C., S. Dimou, and N. Pavlidisa. 1998. Prognostic factors in aggressive non-Hodgkin's lymphomas. Oncologist 3:189-197.

327. Ohkoudo, M., H. Sawa, Y. Shiina, H. Sato, K. Kamata, J. Iijima, H. Yamamoto, M. Fujii, and I. Saito. 1996. Morphometrical analysis of nucleolin immunohistochemistry in meningiomas. Acta Neuropathol 92:1-7.

328. Nisole, S., B. Krust, C. Callebaut, G. Guichard, S. Muller, J. P. Briand, and A. G. Hovanessian. 1999. The anti-HIV pseudopeptide HB-19 forms a complex with the cell-

surface-expressed nucleolin independent of heparan sulfate proteoglycans. J Biol Chem 274:27875-27884.

329. Kubler, D. 2001. Ecto-protein kinase substrate p120 revealed as the cell-surface-expressed nucleolar phosphoprotein Nopp140: a candidate protein for extracellular Ca2+-sensing. Biochem J 360:579-587.

330. Lotze, M. T., and K. J. Tracey. 2005. High-mobility group box 1 protein (HMGB1): nuclear weapon in the immune arsenal. Nat Rev Immunol 5:331-342.

331. Wu, D., Y. Ding, S. Wang, Q. Zhang, and L. Liu. 2008. Increased expression of high mobility group box 1 (HMGB1) is associated with progression and poor prognosis in human nasopharyngeal carcinoma. J Pathol 216:167-175.

332. Peng, R. Q., X. J. Wu, Y. Ding, C. Y. Li, X. J. Yu, X. Zhang, Z. Z. Pan, D. S. Wan, L. M. Zheng, Y. X. Zeng, and X. S. Zhang. 2010. Co-expression of nuclear and cytoplasmic HMGB1 is inversely associated with infiltration of CD45RO+ T cells and prognosis in patients with stage IIIB colon cancer. BMC Cancer 10:496.

333. Shen, X., L. Hong, H. Sun, M. Shi, and Y. Song. 2009. The expression of high-mobility group protein box 1 correlates with the progression of non-small cell lung cancer. Oncol Rep 22:535-539.

334. Korabiowska, M., M. Tscherny, J. Stachura, H. Berger, C. Cordon-Cardo, and U. Brinck. 2002. Differential expression of DNA nonhomologous end-joining proteins Ku70 and Ku80 in melanoma progression. Mod Pathol 15:426-433.

335. Komuro, Y., T. Watanabe, Y. Hosoi, Y. Matsumoto, K. Nakagawa, N. Tsuno, S. Kazama, J. Kitayama, N. Suzuki, and H. Nagawa. 2002. The expression pattern of Ku correlates with tumor radiosensitivity and disease free survival in patients with rectal carcinoma. Cancer 95:1199-1205.

336. Prabhakar, B. S., G. P. Allaway, J. Srinivasappa, and A. L. Notkins. 1990. Cell surface expression of the 70-kD component of Ku, a DNA-binding nuclear autoantigen. J Clin Invest 86:1301-1305.

337. Reyes-Reyes, E. M., and S. K. Akiyama. 2008. Cell-surface nucleolin is a signal transducing P-selectin binding protein for human colon carcinoma cells. Exp Cell Res 314:2212-2223.

338. Legrand, D., K. Vigie, E. A. Said, E. Elass, M. Masson, M. C. Slomianny, M. Carpentier, J. P. Briand, J. Mazurier, and A. G. Hovanessian. 2004. Surface nucleolin

participates in both the binding and endocytosis of lactoferrin in target cells. Eur J Biochem 271:303-317.

339. Shimakami, T., M. Honda, T. Kusakawa, T. Murata, K. Shimotohno, S. Kaneko, and S. Murakami. 2006. Effect of hepatitis C virus (HCV) NS5B-nucleolin interaction on HCV replication with HCV subgenomic replicon. J Virol 80:3332-3340.

340. Tayyari, F., D. Marchant, T. J. Moraes, W. Duan, P. Mastrangelo, and R. G. Hegele. 2011. Identification of nucleolin as a cellular receptor for human respiratory syncytial virus. Nat Med 17:1132-1135.

341. Waggoner, S., and P. Sarnow. 1998. Viral ribonucleoprotein complex formation and nucleolar-cytoplasmic relocalization of nucleolin in poliovirus-infected cells. J Virol 72:6699-6709.

342. Accordi, B., S. Pillozzi, M. C. Dell'Orto, G. Cazzaniga, A. Arcangeli, G. T. Kronnie, and G. Basso. 2007. Hepatocyte growth factor receptor c-MET is associated with FAS and when activated enhances drug-induced apoptosis in pediatric B acute lymphoblastic leukemia with TEL-AML1 translocation. J Biol Chem 282:29384-29393.

343. Moumen, A., A. Ieraci, S. Patane, C. Sole, J. X. Comella, R. Dono, and F. Maina. 2007. Met signals hepatocyte survival by preventing Fas-triggered FLIP degradation in a PI3k-Akt-dependent manner. Hepatology 45:1210-1217.

344. Wang, X., M. C. DeFrances, Y. Dai, P. Pediaditakis, C. Johnson, A. Bell, G. K. Michalopoulos, and R. Zarnegar. 2002. A mechanism of cell survival: sequestration of Fas by the HGF receptor Met. Mol Cell 9:411-421.

345. Mielgo, A., V. Brondani, L. Landmann, A. Glaser-Ruhm, P. Erb, D. Stupack, and U. Gunthert. 2007. The CD44 standard/ezrin complex regulates Fas-mediated apoptosis in Jurkat cells. Apoptosis 12:2051-2061.

346. Mielgo, A., M. van Driel, A. Bloem, L. Landmann, and U. Gunthert. 2006. A novel antiapoptotic mechanism based on interference of Fas signaling by CD44 variant isoforms. Cell Death Differ 13:465-477.

347. Edmond, V., B. Ghali, A. Penna, J. L. Taupin, S. Daburon, J. F. Moreau, and P. Legembre. 2012. Precise mapping of the CD95 pre-ligand assembly domain. PLoS One 7:e46236.

348. Samaniego, F., J. F. Wise, T. R., H. Zhu, X. Ao, Z. Chen, W. Zhuang, F. K. Braun, R. Mathur, J. E. Romaguera, L. Fayad, M. Wang, P. McLaughlin, T. McDonnell, K. P.

Patel, S. S. Neelapu, L. W. Kwak, and B. Z. 2012. Regulation of Fas-mediated apoptosis in B-cell lymphomas by nucleolin ASH Abstracts:2406.

349. Fang, X., and W. Tan. 2010. Aptamers generated from cell-SELEX for molecular medicine: a chemical biology approach. Acc Chem Res 43:48-57.

350. Fogal, V., K. N. Sugahara, E. Ruoslahti, and S. Christian. 2009. Cell surface nucleolin antagonist causes endothelial cell apoptosis and normalization of tumor vasculature. Angiogenesis 12:91-100.

351. Rosenberg, J. E., H. A. Drabkin, P. Lara, A. L. Harzstark, R. A. Figlin, G. W. Smith, F. Erlandsson, and D. A. Laber. 2010. A phase II, single-arm study of AS1411 in metastatic renal cell carcinoma. In Journal of Clinical Oncology. suppl; abstr 4590.

352. Rizzieri, D., K. Stockerl-Goldstein, A. Wei, R. H. Herzig, F. Erlandsson, and R. K. Stuart. 2010. Long-term outcomes of responders in a randomized, controlled phase II trial of aptamer AS1411 in AML. In Journal of Clinical Oncology. suppl; abstr 6557.

353. Riccardi, C., and I. Nicoletti. 2006. Analysis of apoptosis by propidium iodide staining and flow cytometry. Nat Protoc 1:1458-1461.

Vita

Jillian Wise was raised in Foxborough Massachusetts along with her siblings Stephanie Wise, Sara Campbell, and Shannon Collins by their parents David and Diane Wise. During her attendance at Worcester Polytechnic Institute during the pursuit of her Bachelor of Sciences, Jillian completed three theses while studying in London UK, Namibian Africa, and at MD Anderson Cancer Center Orlando. During the completion of her major qualifying project at MD Anderson Cancer Center Orlando, Jillian worked under the supervision of Dr. Cheryl Baker focusing on the relationship between chemotherapeutic sensitivity and radiation treatment schedules in pancreatic cancer. In August 2007, Jillian joined the University of Texas Health Science Center Graduate School of Biomedical Sciences and University of Texas MD Anderson Cancer Center. Jillian carried out her dissertation in the Department of Lymphoma/Myeloma at the University of Texas MD Anderson Cancer Center under the guidance of Dr. Felipe Samaniego. Jillian was awarded the American Legion Auxiliary Fellowship in Cancer Research, the NIH T32 Trainee Fellowship with the Center for Clinical and Translational Sciences, the Vivian L. Smith Young Immunologist of the Year, and the Ralph M. Steinman Award for Basic Immunology Research.